



University of HUDDERSFIELD

University of Huddersfield Repository

Pillutla, Girish Sarma

Design and Development of Stand-Alone Water Filled Radiator System for Built Environment Applications

Original Citation

Pillutla, Girish Sarma (2017) Design and Development of Stand-Alone Water Filled Radiator System for Built Environment Applications. Doctoral thesis, University of Huddersfield.

This version is available at <http://eprints.hud.ac.uk/id/eprint/34349/>

The University Repository is a digital collection of the research output of the University, available on Open Access. Copyright and Moral Rights for the items on this site are retained by the individual author and/or other copyright owners. Users may access full items free of charge; copies of full text items generally can be reproduced, displayed or performed and given to third parties in any format or medium for personal research or study, educational or not-for-profit purposes without prior permission or charge, provided:

- The authors, title and full bibliographic details is credited in any copy;
- A hyperlink and/or URL is included for the original metadata page; and
- The content is not changed in any way.

For more information, including our policy and submission procedure, please contact the Repository Team at: E.mailbox@hud.ac.uk.

<http://eprints.hud.ac.uk/>

DESIGN AND DEVELOPMENT
OF STAND-ALONE WATER
FILLED RADIATOR SYSTEM
FOR BUILT ENVIRONMENT
APPLICATIONS

Girish Sarma Pillutla

BEng Mechanical Engineering, University of Pune

MSc. Automotive Systems Design and Analysis, University of Huddersfield

Director of Studies: Prof. Rakesh Mishra

A thesis submitted to the University of Huddersfield in partial fulfilment of the
requirements for the degree of Doctor of Philosophy

University of Huddersfield

June 2017

Abstract

On an average the temperatures in the UK are low and drive the need for space heating, to maintain thermal comfort in built environments. As per the climate change act of 2008, by year 2050 UK committed to reducing its GHG (Green House Gases) emissions by 80% from a baseline of 1990 [4] with an intermediate goal for year 2020 to reducing emissions from homes by 29% from a baseline of 2008 [5]. There have been significant developments in legislation, energy efficiency of building innovation in insulation but it is important to investigate the trends and improvements in the heating systems themselves.

The losses in central heating systems are due to intermittent heating – accounting for approximately 10%, distribution losses – accounting for approximately 5% and losses due to separate hot water storage requirements to meet hot water demands from the same boiler-approximately 2kW. Another significant loss factor is heat loss from the network of pipes carrying hot water to the radiators.

Stand-alone radiators have presented themselves as a viable alternative to central heating systems by providing, modularity, flexibility and controllability. Although there are several systems commercially available there is no product or research available on water filled stand-alone radiator systems.

A systematic study on viability of water filled stand-alone radiator is undertaken and a new stand-alone water filled radiator has been developed which offers the benefit of a central heating radiator system without the complexity of plumbing, installation and maintenance. In the new product development process, both mechanical and hydraulic considerations have been accounted for to ensure a safe, robust and commercially viable product is developed.

Detailed experimental evaluations of radiators under different flow configurations and flow rates for two radiator sizes have been carried out. The results obtained from the investigation have been quantified and graphically represented. Two key parameters to quantify pressure loss and pressure variations in a radiator have been developed. Relationship of pressure drop to flow velocity has been developed and a non-dimensional parameter, loss co-efficient K for radiators has been developed.

Detailed CFD based analysis to quantify the effect of radiator size and the port diameter under different flow configurations and flow rates has been carried out. The results obtained from the investigation have been quantified and graphically represented. A non-dimensional geometric factor has been developed to account for the effect of radiator size on performance parameters. A unique relationship has been established between loss co-efficient and port diameter to quantify the influence of inlet and out port diameters.

A detailed investigation of the various costs involved in heating a room using a stand-alone radiator system has been carried out and a radiator sizing and cost estimation process has been developed for stand-alone radiator. A methodological approach to predict cost for water filled stand-alone system has been developed which accounts for manufacturing cost and operation cost. A cost comparative study of central heating system and a stand-alone has been conducted to quantify cost benefit of one system to the other.

Copyright Statement

1. The author of this thesis (including any appendices and/or schedules to this thesis) owns any copyright in it (the “Copyright”) and he has given The University of Huddersfield the right to use such Copyright for any administrative, promotional, educational and/or teaching purposes.
2. Copies of this thesis, either in full or in extracts, may be made only in accordance with the regulations of the University Library. Details of these regulations may be obtained from the Librarian. This page must form part of any such copies made.
3. The ownership of any patents, designs, trademarks and any and all other intellectual property rights except for the Copyright (the “Intellectual Property Rights”) and any reproductions of copyright works, for example graphs and tables (“Reproductions”), which may be described in this thesis, may not be owned by the author and may be owned by third parties. Such Intellectual Property Rights and Reproductions cannot and must not be made available for use without the prior written permission of the owner(s) of the relevant Intellectual Property Rights and/or Reproductions.

Acknowledgements

During the thesis journey, many individuals have helped me and without their support this journey would not have been possible.

First and foremost I would like to express my gratitude to my supervisor Prof. Rakesh Mishra for his guidance, support and encouragement to complete my work. His knowledge and expertise in flow analysis and diagnostics were inspirational. His feedback on the work undertaken through the development and analysis phase has helped me collate the work in a logical manner.

I would like to thank Dr. Simon Barrans my co –supervisor whose support and contribution during the product development phase was critical and he helped successfully deliver the KTP program. Experimental work on the radiators would not have been possible with the contribution of Dr. Suman Pradhan who helped me run the experiments on weekends and evening. I am very thankful to Dr. Simon Fletcher and Dr. Naeem Mian who allowed me to use their temperature controlled room and thermal imaging system. Dr Vihar Malviya, Dr. Taimoor Asim and Dr. Ibad Kureshi for their help and support in CFD software and on using high performance computing systems.

When one does research part-time there are people who are not directly associated with the research but play a critical role. My colleagues and management at RLE International have been very supportive and always encouraged me to continue my studies and complete my thesis especially Dr. D Gowland and Mr M Gillett. I would also like to thank Mr John Barrans at Height UK Ltd (industry partner) for the opportunity and for giving me one of the most valuable and practical advise which helped me become a good engineer.

Last but not the least I would like to thank my family, my wife Rajeswari and son Meirav for their love, support and patience while I stayed away from home to pursue my degree. My parents and sister Deepa, who supported me emotionally and had faith in me.

Abbreviations

Various abbreviations and terms used in this text are listed below

EU European Union

TRV Temperature Regulation Valve

IDHEE Institute of Domestic Heating & Environmental Engineers

SWOT Strength, Weakness, Opportunity and Threats

BBOE Bottom Bottom Opposite Ends

BTOE Bottom Top Opposite Ends

HCP Hydraulic Capsules in Pipe

lpm litres per minute

CONTENTS

1	INTRODUCTION	23
1.1	BACKGROUND.....	23
1.1.1	<i>Characteristics of heating systems in built environment.....</i>	<i>28</i>
1.1.1.1	Central Heating systems.....	30
1.1.1.2	Individual/ Standalone systems.....	30
1.1.2	<i>Design and performance considerations for central heating systems.....</i>	<i>31</i>
1.2	MOTIVATION OF PRESENT WORK.....	34
1.3	RESEARCH AIM.....	37
1.4	OUTLINE OF THESIS.....	38
2	LITERATURE REVIEW	40
2.1	STAND-ALONE WATER FILLED RADIATORS: PRODUCT DEVELOPMENT PROCESS....	41
2.1.1	<i>Summary of literature regarding current stand-alone heating systems.....</i>	<i>50</i>
2.2	LITERATURE REVIEW ON FACTORS INFLUENCING THE PERFORMANCE OF RADIATORS.....	51
2.2.1	<i>Summary of literature regarding performance parameters of radiators</i>	<i>55</i>
2.3	CFD BASED QUANTITATIVE FLOW ANALYSIS IN RADIATORS	57
2.3.1	<i>Summary of literature regarding quantitative flow analysis in radiators....</i>	<i>58</i>
2.4	COST MODEL AND OPTIMISATION OF RADIATORS	60
2.4.1	<i>Summary of literature regarding optimisation of radiators.....</i>	<i>63</i>
2.5	SCOPE OF WORK	64
2.6	SPECIFIC RESEARCH OBJECTIVES	65
3	EXPERIMENTAL AND NUMERICAL SETUP	66
3.1	INTRODUCTION.....	66
3.2	EXPERIMENTAL APPROACH.....	67
3.2.1	<i>Initial Experimental setup</i>	<i>68</i>
3.2.2	<i>Test procedure.....</i>	<i>70</i>
3.2.3	<i>Range of parameters</i>	<i>71</i>
3.2.4	<i>Experimental setup.....</i>	<i>72</i>
3.3	NUMERICAL SETUP.....	73
3.3.1	<i>Governing equations of fluid.....</i>	<i>75</i>
3.3.2	<i>Mass Conservation in 3D.....</i>	<i>76</i>
3.3.3	<i>Momentum Equations in 3D.....</i>	<i>76</i>

3.3.4	<i>Energy Equation in 3D</i>	78
3.3.5	<i>Pre- Processing</i>	79
3.3.5.1	Geometry.....	79
3.3.5.2	Meshing.....	80
3.3.6	<i>Solver Setting</i>	81
3.3.7	<i>Mesh independent analysis</i>	83
3.3.8	<i>Post processing</i>	83
3.3.9	<i>Summary</i>	84

4 DEVELOPMENT OF A NOVEL STAND-ALONE WATER FILLED RADIATOR..... 85

4.1	BESPOKE PRODUCT DEVELOPMENT PROCESS.....	86
4.1.1	<i>Overview of existing product development process</i>	86
4.1.1.1	Generic product development process.....	87
4.1.1.2	Spiral product development process.....	88
4.1.1.3	Complex system development process.....	89
4.1.1.4	Summary of stage based NPD process.....	91
4.1.2	<i>Development of a bespoke product development process for stand-alone radiator system</i>	92
4.1.2.1	Constraints for the new development process for stand-alone radiator.....	92
4.1.2.2	Development process framework for stand-alone radiator.....	93
4.1.2.3	Bespoke new product development process.....	94
4.1.3	<i>Summary of bespoke product development process</i>	99
4.2	CONCEPT DEVELOPMENT OF A STAND-ALONE RADIATOR.....	100
4.2.1	<i>Project Ideation</i>	101
4.2.2	<i>Program definition and market review</i>	102
4.2.3	<i>Product attributes and benchmarking</i>	103
4.2.4	<i>Feature list and innovation</i>	104
4.2.5	<i>Product architecture, layout and feasibility</i>	106
4.2.6	<i>Business case analysis</i>	113
4.2.7	<i>Summary of concept phase</i>	114
4.3	STAND-ALONE WATER FILLED RADIATOR DEVELOPMENT.....	115
4.3.1	<i>Concept maturation</i>	115
4.3.2	<i>Hydraulic Design</i>	115
4.3.3	<i>Mechanical design - Component design and selection</i>	122
4.3.3.1	Radiator Panels.....	122
4.3.3.2	Heater system.....	126
4.3.3.3	Pumps.....	129
4.3.3.4	Control system.....	132

4.3.3.5	Operating fluid	133
4.3.4	<i>Design for Manufacture and Assembly (DFMA)</i>	136
4.3.5	<i>DFMEA (Design Failure Mode Effect and Analysis)</i>	138
4.4	STAND-ALONE WATER FILLED RADIATOR MANUFACTURING	140
4.4.1	<i>Sub-Assembly process and Quality assessment</i>	140
4.4.2	<i>Final assembly and testing</i>	142
4.4.3	<i>Product performance evaluation</i>	145
4.5	SUMMARY.....	148
5	CRITICAL PERFORMANCE ANALYSIS OF STAND-ALONE WATER FILLED RADIATORS	150
5.1	TEMPERATURE DISTRIBUTION ANALYSIS OF DOUBLE AND SINGLE PANEL RADIATORS WITH TWO FLOW CONFIGURATIONS	151
5.1.1	<i>Double Panel BBOE Configuration</i>	151
5.1.2	<i>Single Panel BBOE Configuration</i>	152
5.1.3	<i>Double Panel BTOE Configuration</i>	154
5.1.4	<i>Single Panel BTOE Configuration</i>	154
5.1.5	<i>Summary of temperature distribution in double and single panel radiator</i> 156	
5.2	TEMPERATURE DISTRIBUTION ANALYSIS TO QUANTIFY THE EFFECT OF TEMPERATURE AND FLOW RATE	157
5.2.1	<i>Summary of temperature distribution at different flow rates</i>	166
5.3	PRESSURE DROP ACROSS THE RADIATOR	166
5.3.1	<i>Pressure drop analysis in a 3060 radiator</i>	168
5.3.2	<i>Loss Co-efficient analysis in a 3060 radiator</i>	170
5.3.3	<i>Pressure drop analysis in a 6100 radiator</i>	173
5.3.4	<i>Loss Co-efficient analysis in a 6100 radiator</i>	174
5.3.5	<i>Summary of pressure drop across radiator</i>	176
5.4	PRESSURE VARIATION ANALYSIS IN A RADIATOR	177
5.4.1	<i>Pressure variation analysis in a 3060 radiator</i>	178
5.4.2	<i>Pressure variation analysis in a 6100 radiator</i>	186
5.4.3	<i>Summary of pressure variation in a radiator</i>	193
5.5	SUMMARY.....	194
6	QUANTITATIVE ANALYSIS OF GEOMETRIC PARAMETERS IN RADIATORS	195
6.1	INTRODUCTION.....	195

6.2	VALIDATION AND COMPARISON OF COMPUTATIONAL AND EXPERIMENTAL ANALYSIS	196
6.2.1	<i>Comparative study of pressure drop in BBOE configuration</i>	<i>196</i>
6.2.2	<i>Comparative study of pressure drop in BTOE configuration</i>	<i>197</i>
6.2.3	<i>Comparative study of Pressure distribution ratio Co-efficient in BBOE configuration</i>	<i>198</i>
6.2.4	<i>Comparative study of Pressure distribution ratio Co-efficient in BBOE configuration</i>	<i>199</i>
6.2.5	<i>Key observation</i>	<i>199</i>
6.3	QUANTITATIVE ANALYSIS OF RADIATOR SIZE ON INTERNAL FLOW PARAMETERS	200
6.3.1	<i>Introduction</i>	<i>200</i>
6.3.2	<i>Pressure drop in BBOE configuration</i>	<i>201</i>
6.3.3	<i>Pressure drop in BTOE configuration</i>	<i>202</i>
6.3.4	<i>Loss coefficient in BBOE configuration</i>	<i>203</i>
6.3.5	<i>Loss co-efficient in BTOE configuration</i>	<i>204</i>
6.3.6	<i>Loss co-efficient as a function of radiator size</i>	<i>205</i>
6.3.7	<i>Analysis of radiator size on pressure distribution</i>	<i>210</i>
6.3.8	<i>Qualitative analysis of velocity variation</i>	<i>216</i>
6.3.8.1	X- Velocity profiles across the radiator- 8mm	218
6.3.8.2	Y- Velocity profiles across the radiator- 8mm	221
6.3.8.3	Z- Velocity profiles across the radiator - 8mm	224
6.3.8.4	Y- Velocity distribution in the central plane – 8mm	227
6.3.8.5	Velocity magnitude contours – 8mm	231
6.4	QUANTIFYING THE EFFECT OF INLET AND OUTLET PORT DIAMETER	234
6.4.1	<i>Geometry of the ports</i>	<i>235</i>
6.4.2	<i>Analysis of port diameter on pressure drop in a system</i>	<i>237</i>
6.4.3	<i>Analysis of port diameter on pressure distribution</i>	<i>241</i>
6.5	SUMMARY	243
7	DEVELOPMENT OF COST MODEL AND OPTIMISED STAND-ALONE WATER FILLED RADIATOR FOR BUILT ENVIORNMENT	244
7.1	OPTIMISATION OF RADIATORS	245
7.2	COST OF RADIATOR	246
7.3	COST OF HEATER	247
7.4	FIXED COST	248
7.5	TOTAL MANUFACTURING COST	249
7.6	OPERATING COST	250

7.6.1	<i>Pumping cost</i>	250
7.6.2	<i>Heating cost</i>	250
7.7	EFFECT OF DIAMETER ON PUMPING COST	252
7.8	COST OF OWNERSHIP	254
7.9	COMPUTING HEATING COST FOR A ROOM	257
7.10	DESIGN EXAMPLE FOR HEATING A ROOM	258
7.11	OPTIMISATION OF TOTAL HEAT COST PER DAY BY VARYING RADIATOR SIZE	260
7.12	COMPARATIVE STUDY OF STAND-ALONE RADIATOR TO A CENTRAL HEATING SYSTEM	264
7.13	SUMMARY	267
8	CONCLUSION	268
8.1	RESEARCH PROBLEM SYNOPSIS	269
8.2	AIM AND MAIN ACHIEVEMENTS.....	270
8.3	THESIS CONCLUSIONS	274
8.4	THESIS CONTRIBUTIONS.....	282
8.5	RECOMMENDATIONS FOR FUTURE WORK.....	284
9	REFERENCES	286
10	APPENDIX I	293
10.1	FLOW SENSOR DATA SHEETS	294
10.2	PRESSURE SENSOR DATA SHEET	296
10.3	DATA LOGGER DATA SHEET	300
10.4	THERMAL CAMERA DATASHEET	305
10.5	K-TYPE THERMOCOUPLE DATASHEET.....	307
10.6	METROLOGICAL REPORT FOR RADIATOR INTERNAL SURFACE	308
10.6.1	<i>Introduction</i>	308
10.6.2	<i>Methodology</i>	308
10.6.3	<i>Results</i>	309
10.6.4	<i>Screen Shot Images</i>	309
10.6.5	<i>Conclusions</i>	310

LIST OF FIGURES

Figure 1-1 Mean temperature - Winter average in United Kingdom [1]	23
Figure 1-2 Mean temperature - Annual average in United Kingdom [1]	23
Figure 1-3 ASRAE comfort zone chart [2].....	24
Figure 1-4 Example of EPC certificate (By Drawn by User: Gralo - Self-created, Public Domain) [7].....	25
Figure 1-5 Flow chart for main calculation steps using EN ISO 13790 [10]	27
Figure 1-6 Hypocaust system introduced by Romans [14].....	28
Figure 1-7 Schematic of central heating system [9]	29
Figure 1-8 Heat loss from a pipe in central heating [15]	34
Figure 2-1 Performance of old TRV using different boiler controls Liao [17].....	41
Figure 2-2 Comparison of unbalanced, remedied and fully balanced heat distribution system [18]	43
Figure 2-3 Types of product innovation [23].....	47
Figure 2-4 Discontinuous product development [24].....	48
Figure 2-5 Generic product development process [25].....	48
Figure 2-6 Typical variation of heat emission with water connection [35].....	52
Figure 2-7 Output diagram for BBOE double panel radiator [38].....	54
Figure 2-8 Friction heads of various radiators and convectors - experimental work by Giesecke [39].....	55
Figure 2-9 Fuel charges for gas based heating system over a year [60].....	62
Figure 2-10 Heater size for a room heating [61].....	62
Figure 3-1 Isometric illustrative view of stand-alone water filled radiator.....	68
Figure 3-2 Radiator panel configuration [60]	68
Figure 3-3 Initial Experimental setup.....	69
Figure 3-4 Front View of experimental setup	72
Figure 3-5 Overview of CFD model	73
Figure 3-6 Geometry for CFD model	79
Figure 3-7 Mesh model for 3060 radiator.....	81
Figure 3-8 Reference planes in CFD model	84
Figure 4-1 Generic product development process [24].....	87
Figure 4-2 Spiral product development process	88
Figure 4-3 Complex system development process	89
Figure 4-6 Concept Development	100
Figure 4-7 Schematic layout A - based on key components of a central heating system	107
Figure 4-8 Schematic layout B - based on key components of a stand-alone (oil-filled) system	107
Figure 4-9 Architecture of the new heating system.....	109
Figure 4-10 Panel configuration in domestic radiator [60].....	116
Figure 4-11 Design intent package and layout for stand-alone heating system.	121
Figure 4-12 K2 radiator mounted on a wall [64]	122

Figure 4-13 Heater with straight element	126
Figure 4-14 Heater with U shaped element.....	127
Figure 4-15 Heater with coil element and increase flow volume.....	127
Figure 4-16 Exploded view of Laing pump [68].....	131
Figure 4-17 Technical specification for a PCB used in a stand-alone system.....	132
Figure 4-18 Isometric illustrative view of stand-alone water filled radiator.....	133
Figure 4-19 Fernox Anti freeze and anti rust [70].....	134
Figure 4-20 Fernox biocide [71]	135
Figure 4-21 Pump and heater jig	141
Figure 4-22 Test Bench for Sub Units.....	142
Figure 4-23 Filling jig for radiators	143
Figure 4-24: Stand-Alone water filled radiators [72]	144
Figure 4-25 Test room BS EN 442 [50]	146
Figure 5-1 Temperature profile double panel radiator - °C (BBOE) [59].....	151
Figure 5-2 Temperature profile in s single panel radiator - °C (BBOE) [59]	152
Figure 5-3: Normalised temperature Variance with respect to inlet - double panel (BBOE) [59].....	153
Figure 5-4: Normalised temperature Variance with respect to inlet single panel (BBOE) [59].....	153
Figure 5-5 Temperature profile on a double panel - °C (BTOE).....	154
Figure 5-6 Temperature profile in a Single panel - °C (BTOE)	155
Figure 5-7: Normalised temperature Variance with respect to inlet (double BTOE)	155
Figure 5-8: Normalised temperature variance with respect to inlet (single BTOE).....	156
Figure 5-9: Variation of the non-dimensional parameter with respect to different radiator combination.	156
Figure 5-10: Schematic of panel layout	158
Figure 5-11: Temperature Distribution on Panel [Flow rate 0.32 m/s, 70 °C].....	159
Figure 5-12: Temperature Distribution on the panel [Flow rate: 0.25 m/s, 70 °C]	160
Figure 5-13: Temperature distribution on the panel [Flow rate: 0.32m/s, 60 °C].....	161
Figure 5-14: Temperature Distribution on the panel [Flow rate: 0.25m/s, 60 °C]	162
Figure 5-15: Temperature distribution on the panel [Flow rate: 0.32m/s, 50 °C].....	163
Figure 5-16: Temperature distribution on the panel [Flow rate : 0.25m/s, 50 °C].....	164
Figure 5-17 Variation of pressure differential with velocity (300 x 600 mm radiator)	168
Figure 5-18 Variation of Loss co-efficient with change in velocity (300 x 600 mm radiator).....	170
Figure 5-19 Variation of Loss co-efficient with the change in Reynolds Number (300 x 600 mm radiator)	171
Figure 5-20 Variation of pressure differential with velocity (600 x 1000 mm radiator)	173
Figure 5-21 Variation of Loss co-efficient with change in velocity (600 x 1000 mm radiator).....	174
Figure 5-22 Variation of Loss co-efficient with change in Reynolds number (600 x 1000 mm radiator)	175
Figure 5-23 Radiator setup for pressure distribution.....	177
Figure 5-24 Normalised pressure variation in 3060 radiator - Flow 1	178
Figure 5-25 Normalised pressure variation in 3060 radiator - Flow 2	179
Figure 5-26 Normalised pressure variation in 3060 radiator - Flow 3	180
Figure 5-27 Normalised pressure variation in 3060 radiator - Flow 4	181

Figure 5-28- Normalised pressure variation in 3060 radiator - Flow 5	182
Figure 5-29 Pressure distribution ratio co-efficient vs velocity (300 mm x 600 mm radiator).....	185
Figure 5-30 Normalised pressure variation in 6100 radiator - Flow 1	186
Figure 5-31 Normalised pressure variation in 6100 radiator - Flow 2	187
Figure 5-32 Normalised pressure variation in 6100 radiator - Flow 3	188
Figure 5-33 Normalised pressure variation in 6100 radiator - Flow 4	189
Figure 5-34 Normalised pressure variation in 6100 radiator – Flow 5	190
Figure 5-35 Pressure distribution ratio co-efficient vs velocity (600mm x 1000mm radiator).....	192
Figure 6-1 Experimental to CFD comparison- Pressure loss against velocity - Base model BBOE	196
Figure 6-2 Experiment to CFD comparison- Pressure loss against velocity - Base model –BTOE.....	197
Figure 6-3 Experiment to CFD comparison- Pressure distribution ratio- Base- BBOE.....	198
Figure 6-4 Experiment to CFD comparison- Pressure distribution ratio- Base- BTOE	199
Figure 6-5 Comparison of pressure drop in 3 radiators of varying sizes - BBOE	201
Figure 6-6 Comparison of pressure drop in 3 radiators of varying sizes - BTOE	202
Figure 6-7 Comparison of Loss Co-efficient in 3 radiators of varying sizes – BBOE	203
Figure 6-8 Comparison of Loss Co-efficient in 3 radiators of varying sizes – BTOE.....	204
Figure 6-9 Loss co-efficient as a function of geometric factor – BBOE	207
Figure 6-10 Loss co-efficient as a function of geometric factor – BTOE	207
Figure 6-11 Loss co-efficient vs Geometric factor for both configurations	208
Figure 6-12 Normalised pressure variation in 3060 radiator.....	211
Figure 6-13 Normalised pressure variation in 4070 radiator.....	212
Figure 6-14 Normalised pressure variation analysis in 6100 radiator	213
Figure 6-15 Pressure distribution co-efficient vs flow velocity for 3 radiators- BBOE.....	214
Figure 6-16 Pressure distribution co-efficient vs flow velocity for 3 radiators - BTOE	214
Figure 6-17 Pressure distribution ratio co-efficient as function of flow velocity independent of radiator size and flow configuration	215
Figure 6-18 X - Velocity profiles in a 3060 radiator	218
Figure 6-19 X- Velocity profiles in 4070 radiator	219
Figure 6-20 X velocity profiles in a radiator	220
Figure 6-21 Y- Velocity profiles in 3060 radiator	221
Figure 6-22 Y - Velocity profiles in 4070 radiator	222
Figure 6-23 Y velocity profiles in 6100 radiator	223
Figure 6-24 Z - Velocity profiles in 3060 radiator.....	224
Figure 6-25 Z -Velocity profiles in 4070 radiator	225
Figure 6-26 Z velocity profiles in 6100 radiator	226
Figure 6-27 Y Velocity distribution along the central plane in 3060 radiator	227
Figure 6-28 Y velocity distribution along central plane in 4070 radiator.....	228
Figure 6-29 Y velocity distribution along central plane in 6100 radiator.....	229
Figure 6-30 Velocity magnitude contours in 3060 radiator.....	231
Figure 6-31 Velocity Magnitude contours in 4070 radiator.....	232

Figure 6-32 Velocity magnitude contours in a 6100 radiator 233

Figure 6-33 6mm port diameter 235

Figure 6-34 8 mm port diameter -CFD 235

Figure 6-35 12mm port diameter -CFD 236

Figure 6-36 Pressure drop across radiator vs flow rate with change in port diameter 237

Figure 6-37 Effect of port diameter on loss co-efficient in a radiator 238

Figure 6-38 Normalised loss co-efficient vs Reynolds number 239

Figure 6-39 Loss Co-efficient vs Loss co-efficient for 6mm port diameter 239

Figure 6-40 Pressure distribution ratio as function of flow rate for different inlet and outlet port diameter – BBOE 241

Figure 6-41 Pressure distribution ratio as a function flow rate for different inlet and outlet port diameter - BTOE 242

Figure 7-1 Pressure drop vs flow rate for three port diameters 252

Figure 7-2 Pump operating cost for three port diameters over range of flow rates 253

Figure 7-3 Variation of power and pressure loss with geometric factor 255

Figure 7-4 Variation of ownership cost and operation cost with geometric factor 256

Figure 7-5 Variation of power input and output with weight of radiator 260

Figure 7-6 Power input and output variation with geometric factor 261

Figure 7-7 Variation of Total heat cost per day with weight 261

Figure 7-8 Variation of total heat cost per day with geometric factor 262

Figure 7-9 Variation of ownership cost and operation cost with weight 263

Figure 7-10 Total heat cost per day comparison (GCH to Stand-alone) for various built environment 266

LIST OF TABLES

<i>Table 2-1 Summary of radiator burns - review by Harper [22]</i>	45
<i>Table 3-1 variables for consideration in investigation of radiators</i>	67
<i>Table 3-2 Range of parameters</i>	72
<i>Table 3-3 Meshing parameters for CFD model</i>	80
<i>Table 3-4 Mesh independence - pressure criterion</i>	83
<i>Table 4-1 SWOT Analysis for new heating system development process</i>	101
<i>Table 4-2 Product attribute based on customer requirements</i>	103
<i>Table 4-3 Product benchmarking against attributes</i>	104
<i>Table 4-4 Product feature list</i>	105
<i>Table 4-5 Decision analysis matrix for schematic layout</i>	108
<i>Table 4-6 Concept Design Failure Mode Effect and Analysis for stand-alone radiator</i>	112
<i>Table 4-7 Initial Bill of Materials</i>	113
<i>Table 4-8 Volume of water per radiator [60]</i>	116
<i>Table 4-9 Range of volume of water in stand-alone radiator</i>	118
<i>Table 4-10 Concept Maturation - new layout</i>	120
<i>Table 4-11 Revised parts list for a stand-alone radiator</i>	121
<i>Table 4-12 System specification based on design intent layout</i>	122
<i>Table 4-13 Comparison of radiator panel manufacturing process</i>	123
<i>Table 4-14 Technical specification of radiator panel [64]</i>	125
<i>Table 4-15 Comparison of heater for stand-alone radiators</i>	128
<i>Table 4-16 Comparison of common central heating pumps</i>	131
<i>Table 4-17 Manufacturing BoM for stand-alone radiator</i>	137
<i>Table 4-18 DFMEA on completed stand-alone radiator</i>	139
<i>Table 4-19 Thermal output of stand-alone radiators as per BS EN 442 test</i>	148
<i>Table 5-1 description of parameters</i>	157
<i>Table 5-2: Summary of key factors</i>	165
<i>Table 5-3 Loss co-efficient 300 x600 radiator</i>	172
<i>Table 5-4 Loss co-efficient for 600 x1000 mm radiator</i>	176
<i>Table 5-5 Normalised pressure distribution in a 300 x 600 mm radiator</i>	184
<i>Table 5-6 Pressure distribution ratio co-efficient for BBOE and BTOE (300mm x 600mm radiator)</i>	185
<i>Table 5-7 Normalised pressure distribution in 600mm x 1000mm radiator</i>	191
<i>Table 5-8 Pressure distribution ratio co-efficient for BBOE and BTOE (600mm x 1000mm radiator)</i>	192
<i>Table 6-1 Stand-alone radiator sizes</i>	200
<i>Table 6-2 Geometric factor based on radiator size</i>	206
<i>Table 6-3 Geometric factors and loss-co-efficient for stand-alone radiators</i>	209
<i>Table 6-4 Pressure distribution ratio in three radiators</i>	210

<i>Table 6-5 Peak Reynolds number in vertical channels.....</i>	<i>230</i>
<i>Table 7-1 Weight per unit length of radiator [60]</i>	<i>246</i>
<i>Table 7-2 Max heat output from K1 radiator [60]</i>	<i>247</i>
<i>Table 7-3 Common components contributing towards fixed cost</i>	<i>249</i>
<i>Table 7-4 Pump operating cost with three port diameters and range of flow rates</i>	<i>253</i>
<i>Table 7-5 Geometry and cost for radiator with height 0.6 m</i>	<i>258</i>
<i>Table 7-6 Floor area of test built environments</i>	<i>264</i>
<i>Table 7-7 Heat demand and total heat cost per day for gas central heating.....</i>	<i>264</i>
<i>Table 7-8 Total heat cost per day for gas central heating including investment and installation.....</i>	<i>265</i>
<i>Table 7-9 Total heat cost per day for stand-alone radiator system.....</i>	<i>265</i>
<i>Table 8-1 Thermal output of stand-alone radiators as per BS EN 442 test.....</i>	<i>275</i>

LIST OF EQUATIONS

<i>Equation 1-1 Heat transfer from radiator</i>	<i>32</i>
<i>Equation 1-2 Energy demand on the boiler</i>	<i>33</i>
<i>Equation 2-1 Head loss in a radiator [39].....</i>	<i>54</i>
<i>Equation 4-1 Volume of water in a radiator</i>	<i>116</i>
<i>Equation 4-2 Volume of water in flow circuit in a stand-alone system</i>	<i>117</i>
<i>Equation 4-3 Co-efficient of thermal expansion</i>	<i>120</i>
<i>Equation 4-4 Potential difference as a function of current and resistance.....</i>	<i>128</i>
<i>Equation 4-5 Power as a function of potential difference and current.....</i>	<i>128</i>
<i>Equation 4-6 Power as a function of Current and resistance.....</i>	<i>129</i>
<i>Equation 4-7 mass flow rate of water in a stand-alone system</i>	<i>130</i>
<i>Equation 4-8 Characteristic equation of radiator BS EN 442</i>	<i>146</i>
<i>Equation 4-9 Km- characteristics equation of radiator BS EN 442</i>	<i>146</i>
<i>Equation 4-10 n characteristic equation of radiator BS EN 442</i>	<i>147</i>
<i>Equation 4-11 Factor based on EN 442</i>	<i>147</i>
<i>Equation 4-12 Factor based on EN 442</i>	<i>147</i>
<i>Equation 4-13 Heat output from a single panel radiator</i>	<i>147</i>
<i>Equation 4-14 Heat output from a double panel radiator.....</i>	<i>147</i>
<i>Equation 5-1 Head loss in a pipe.....</i>	<i>166</i>
<i>Equation 5-2 Loss co-efficient as a function of friction and hydraulic diameter.....</i>	<i>166</i>
<i>Equation 5-3 Loss co-efficient as function of head loss</i>	<i>167</i>
<i>Equation 5-4 Reynolds number.....</i>	<i>167</i>
<i>Equation 5-5 Hydraulic diameter of pipe.....</i>	<i>167</i>
<i>Equation 5-6 Friction loss as function of Reynolds number.....</i>	<i>171</i>
<i>Equation 5-7 Loss co-efficient for 3060 radiator – BBOE Exp</i>	<i>171</i>
<i>Equation 5-8 Loss co-efficient for 3060 radiator – BTOE Exp</i>	<i>172</i>
<i>Equation 5-9 Loss co-efficient for 6100 radiator – BBOE Exp</i>	<i>175</i>
<i>Equation 5-10 Loss co-efficient for 6100 radiator – BTOE Exp</i>	<i>175</i>
<i>Equation 6-1 Number of channels in the radiator</i>	<i>205</i>
<i>Equation 6-2 Diagonal length of the radiator.....</i>	<i>205</i>
<i>Equation 6-3 Volume of fluid in the radiator</i>	<i>205</i>
<i>Equation 6-4 Geometric factor</i>	<i>206</i>
<i>Equation 6-5 Geometric factor as a function radiator dimensions.....</i>	<i>206</i>
<i>Equation 6-6 Equation to determine Loss co-efficient.....</i>	<i>208</i>
<i>Equation 6-7 Loss co-efficient of 8mm port dia as function of loss co-efficient of 6mm port dia.....</i>	<i>240</i>
<i>Equation 6-8 Loss co-efficient of 12mm port dia as function of loss co-efficient of 6mm port dia.....</i>	<i>240</i>
<i>Equation 7-1 Total cost for stand-alone radiator</i>	<i>245</i>

<i>Equation 7-2 Total cost of radiator (detailed)</i>	<i>245</i>
<i>Equation 7-3 Weight of radiator as a function of length and height.....</i>	<i>246</i>
<i>Equation 7-4 Cost of radiator as a function of radiator weight.....</i>	<i>246</i>
<i>Equation 7-5 Cost of radiator as a function of radiator length and height</i>	<i>246</i>
<i>Equation 7-6 Cost of heater as a function of wattage.....</i>	<i>247</i>
<i>Equation 7-7 Fixed cost of radiator</i>	<i>249</i>
<i>Equation 7-8 Total manufacturing cost</i>	<i>249</i>
<i>Equation 7-9 Cost for pumping the fluid in radiator.....</i>	<i>250</i>
<i>Equation 7-10 Power consumption of pump</i>	<i>250</i>
<i>Equation 7-11 Cost of pumping the fluid in radiator as function of pressure drop and flow rate</i>	<i>250</i>
<i>Equation 7-12 Power consumption cost for heating</i>	<i>250</i>
<i>Equation 7-13 Power consumption for heating.....</i>	<i>251</i>
<i>Equation 7-14 Power consumption cost for heating</i>	<i>251</i>
<i>Equation 7-15 Total operating cost</i>	<i>251</i>
<i>Equation 7-16 Total cost of ownership per day.....</i>	<i>254</i>
<i>Equation 7-17 Total cost of operation per day.....</i>	<i>254</i>
<i>Equation 7-18 Total heating cost per day.....</i>	<i>255</i>

NOMENCLATURE

a	Cross-sectional Area of the Pipe (m^2)
D	Diameter of Pipe (m)
f	Darcy Friction Factor
g	Acceleration due to gravity (m/sec^2)
H	Height of radiator (m)
H_f	Head loss (m)
K	Loss Coefficient
L	Length of radiator (m)
n	Number of Channels
ΔP	Pressure Drop (Pa)
V_w	Flow Rate (m^3/sec)
Re	Reynolds Number
s	Specific Gravity
u	Local Flow Velocity in X direction (m/sec)
V	Flow Velocity (m/sec)
C_{Total}	Total cost for stand-alone water filled radiator (£)
$C_{\text{Manufacturing}}$	Manufacturing cost of stand-alone water filled radiator (£)
$C_{\text{Operation}}$	Running cost of stand-alone water filled radiator (£)
C_{radiator}	Cost of radiator panel (£)
C_{heater}	Cost of heater unit (£)

C_{fixed}	Fixed manufacturing cost (£)
$C_{\text{power-pump}}$	Cost of power consumption in pump (£)
$C_{\text{power-heater}}$	Cost of power consumption in heater (£)
C_1	Cost per unit weight of radiator panel (£/kg)
C_2	Cost of heater unit per unit Watt (£/W)
C_3	Fixed cost of components (£)
C_4	Fixed cost of components (£)
C_5	Cost of power consumption per unit Watt (pump) (£/W)
C_6	Cost of power consumption per unit Watt (heater) (£/W)
$C_{\text{ownership/day}}$	Cost of ownership per day (£/day)
$C_{\text{operation/day}}$	Cost of operation per day (£/day)
$C_{\text{total heat/day}}$	Total heat cost of operation per day (£/day)
C_{pw}	Specific heat capacity

SYMBOLS

α	Function of Reynolds Number
ρ	Density (Kg/m ³)
μ	Dynamic Viscosity (Pa-sec)
Υ	Specific Weight (N/m ³)
η_{pump}	Efficiency of the Pump (%)
η_{heater}	Efficiency of the Heater (%)
ε	Roughness Height of the Pipe (m)
π	Pi
i	Specific Internal Energy (J/Kg)
σ	Normal Stress (Pa)
τ_{pump}	Utility factor for pump (%)
τ_{heater}	Utility factor for heater (%)
ξ	Pressure distribution co-efficient
Φ	Thermal output

SUBSCRIPTS

av Average

i Inlet

h Horizontal

v Vertical

w Water

R Radiator

fc fluid circuit

P_{3B_Exp} experimental pressure loss co-efficient for 3060 radiators in BBOE configuration

P_{3T_Exp} experimental pressure loss co-efficient for 3060 radiators in BTOE configuration

P_{6B_Exp} experimental pressure loss co-efficient for 6100 radiators in BBOE configuration

P_{6T_Exp} experimental pressure loss co-efficient for 6100 radiators in BTOE configuration

P_{3B_CFD} numerical pressure loss co-efficient for 3060 radiators in BBOE configuration

P_{3T_CFD} numerical pressure loss co-efficient for 3060 radiators in BTOE configuration

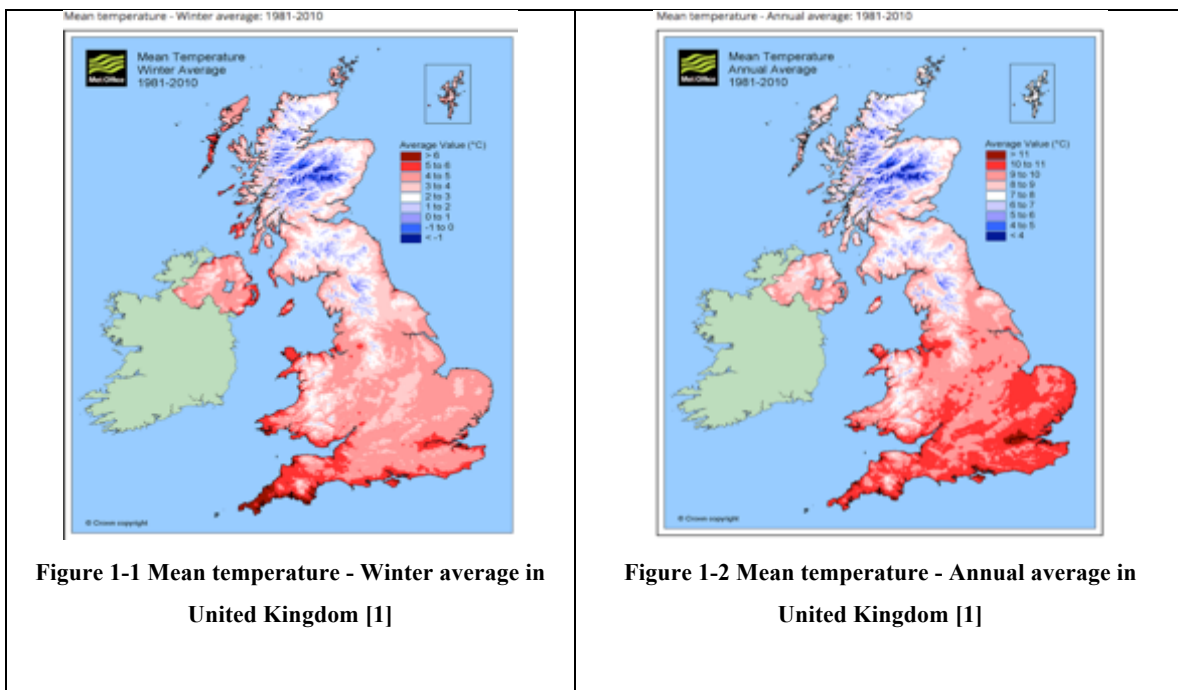
P_{6B_CFD} numerical pressure loss co-efficient for 6100 radiators in BBOE configuration

P_{6T_CFD} numerical pressure loss co-efficient for 6100 radiators in BTOE configuration

1 INTRODUCTION

1.1 Background

Solar radiation is the primary natural heat source, which changes with the time of the year, latitude, elevation and proximity to water bodies. Global temperatures vary significantly where certain regions in Middle East go above 50°C and regions in Russia reach temperatures below -60°C. As shown in Figure 1-1 and Figure 1-2, according to Met office official statistics [1], in the UK, mean temperature during winter months ranges from -1°C and 6°C, while the annual mean temperature ranges between 4°C and 11°C. On an average the temperatures in the UK are low and drive the need for space heating, to maintain thermal comfort.



Studies have shown that thermal comfort depends on air temperature, radiant temperature, relative humidity, air velocity, activity and clothing. The ASHRAE (American Society of Heating, Refrigeration and Air-Conditioning engineers) comfort zone chart [2] shows that optimum temperature is between 18°C and 22°C with the relative humidity between 50% and 70 %. With low temperature outside it is vital to have an effective space heating.

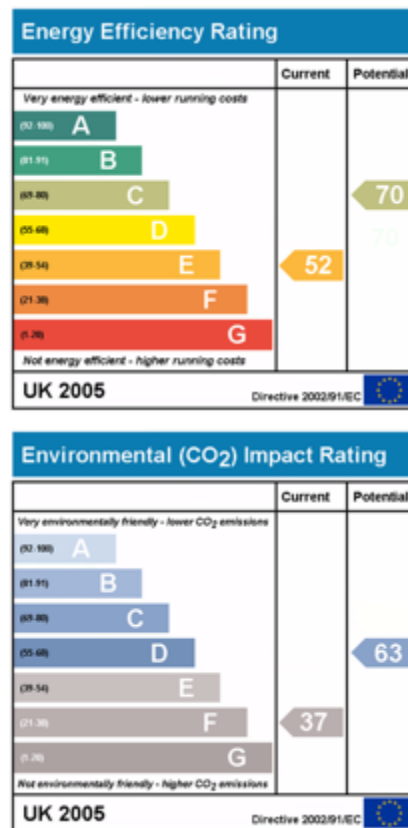


Figure 1-4 Example of EPC certificate (By Drawn by User: Gralo - Self-created, Public Domain) [7]

There are number of factors that influence the efficiency of the building and affect the perceived comfort for the occupant. These are

- a) Room temperature – Actual temperature of the room relative to outside weather conditions
- b) Temperatures on the surface of the rooms – Surface temperature is significant for perceived comfort as a cold surface (like window) would act as heat sink for the occupant in the vicinity and cause discomfort
- c) Draught – Cold surfaces like windows or poorly insulated walls cause heat loss from adjacent air causing the downward flow of air. The movement of cold air causes discomfort to the occupants.
- d) Ventilation – Ample ventilation is key to ensure stale air is removed from buildings and fresh air is introduced. Poor ventilation can cause air leaks and loss of heat
- e) Wind influences – External wind influences the airflow in the property by causing pressure variation. Structures in exposed areas require considerably more insulation and secondary features to retain heat in the property.

- f) Distribution of heat – Constant temperature and even distribution of heat in the room helps perceived comfort. A combination of adequate heating and ample insulation helps deliver good heat distribution.
- g) Heat losses – As mentioned above heat losses in a building are mainly due to
 - a. Transmission – Thermal transmittance can be controlled by insulation
 - b. Ventilation – Can be controlled by providing exhaust fans, ventilations ducts

Co-efficient of thermal transmittance also known as U- value is very important in estimating heating retention in a building. Since 1965 [8] there have been significant changes in legislation to reduce the U-values, where in 1965 the U -values was 1.7 for walls and 1.4 for roofs and in 2002 the U-values are 0.35 for walls and 0.25 for roofs. Insulating the houses improves heat retention and the trend in insulation thickness has seen a 1000% increase in insulation thickness between 1965 and 2002. Most new built properties in the UK now have an energy rating of B or C.

BS EN ISO 13790 [10] standard for energy performance of buildings details the calculating methodology for calculating annual energy use for space heating and cooling of residential and non-residential buildings. Figure 1-5 [10] illustrates the flow chart for main steps used to calculate the annual energy needs of the buildings.

G.M. Huebner et al. [3] have compared national survey statistics with the model suggested by BS EN ISO 13790 and found that the average demand temperature in English houses is 20.58 C and the average temperature when the heating was operational was 19.52 C. It has been observed that the standard assumes the set point temperature not to vary more than 4 K (Kelvin). In practice the variation is much larger. Similar standard for heating systems in buildings is BS EN 15316 [11], which gives methods for calculation of system energy requirements and system efficiencies. This mainly covers Space heating generation systems and heat pump systems.

In summary there have been significant developments in legislation, energy efficiency of building innovation in insulation but it is also important to investigate the trends and improvements in the heating systems themselves.

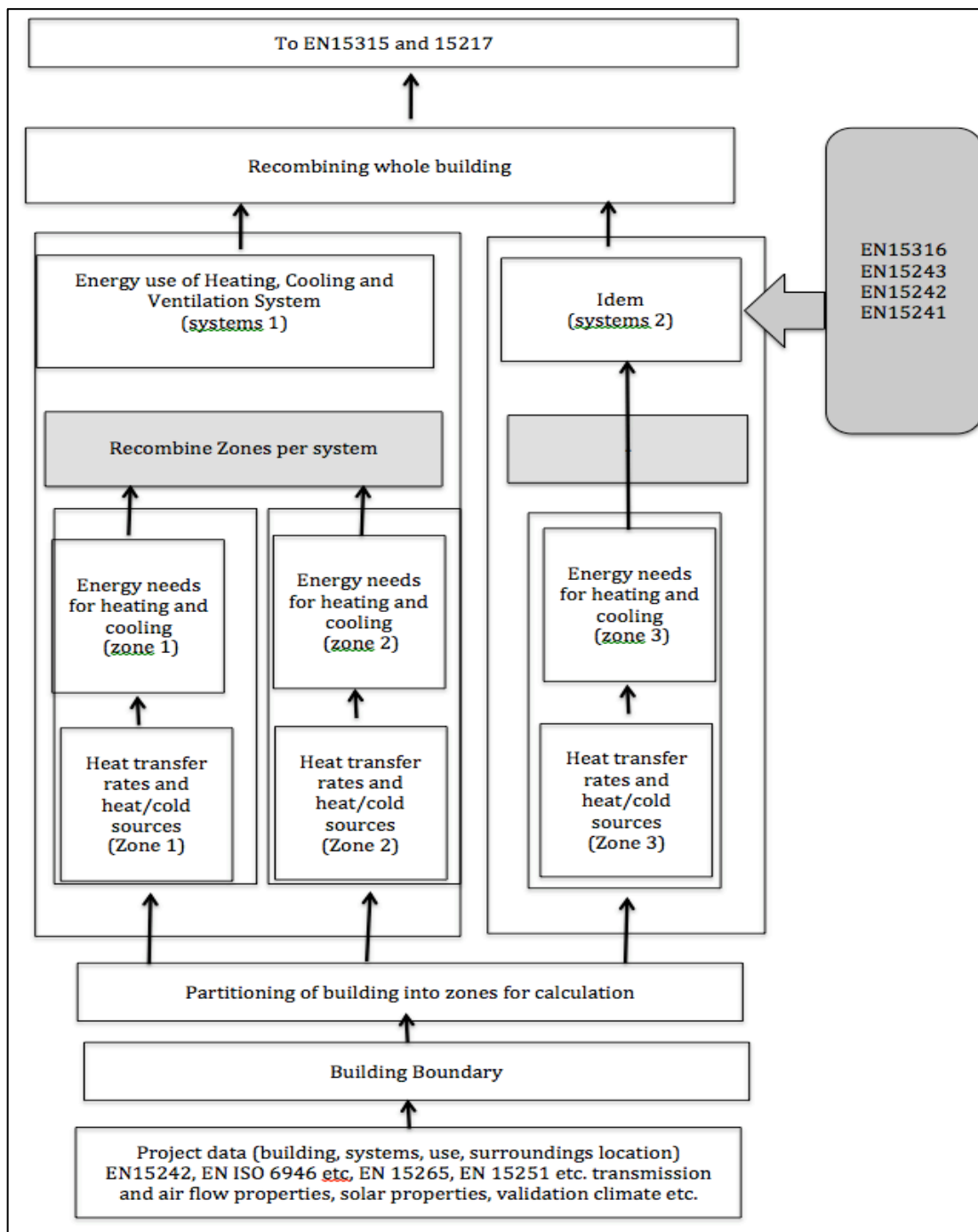


Figure 1-5 Flow chart for main calculation steps using EN ISO 13790 [10]

1.1.1 Characteristics of heating systems in built environment

Since the time of cavemen, open fires have been used to keep warm in cold climates. It was in AD43 when the Romans who introduced central space heating in the UK. The system was called Hypocaust (which is derived from Latin “*hypocaustum*” (hypo- under, caustum-burn / heat). The system is comprised of a hollow space under the floor of the building, which is heated by centrally generated hot air. Figure 1-6 is an example of the hypocaust system found during an archaeological survey.



Figure 1-6 Hypocaust system introduced by Romans [14]

In 1807, William Strutt and Charles Sylvester invented a hot air ventilated system where fresh air from outside was heated in a central furnace and circulated through the building via large central ducts. The application of the system was limited for cost constraints. Later in 1857 a Russian businessman Franz San Galli founded column radiators. The system comprised of larger columns of steel with water channels inside allowing water to flow. The heated column in turn would heat the surrounding air. Even this system was not widely used due to high cost. Despite of these early inventions until early 20th open wood fires were the dominant sources of space heating. Electric fires were commercially available shortly after 1908. In 1930's cast iron column radiators in Britain were available for heating but were very heavy and required over 20 litres of water, which was heated in a separate boiler. As time progressed, design of the heating system evolved and in 1960's the first panel radiators was available which improved the both size and the thermal performance. The boiler

systems, which heat the water for central heating, have improved efficiency, but the general layout and operation has been the same.

Since early 20th century central heating systems have proven to be more efficient, clean and cost effective. A central heating system converts chemical, mechanical and electrical energy into useable thermal energy. The thermal energy generated from the device is used to heat a primary medium, which in turn heats the air in the room. Figure 1-7 shows a typical installation of central heating system.

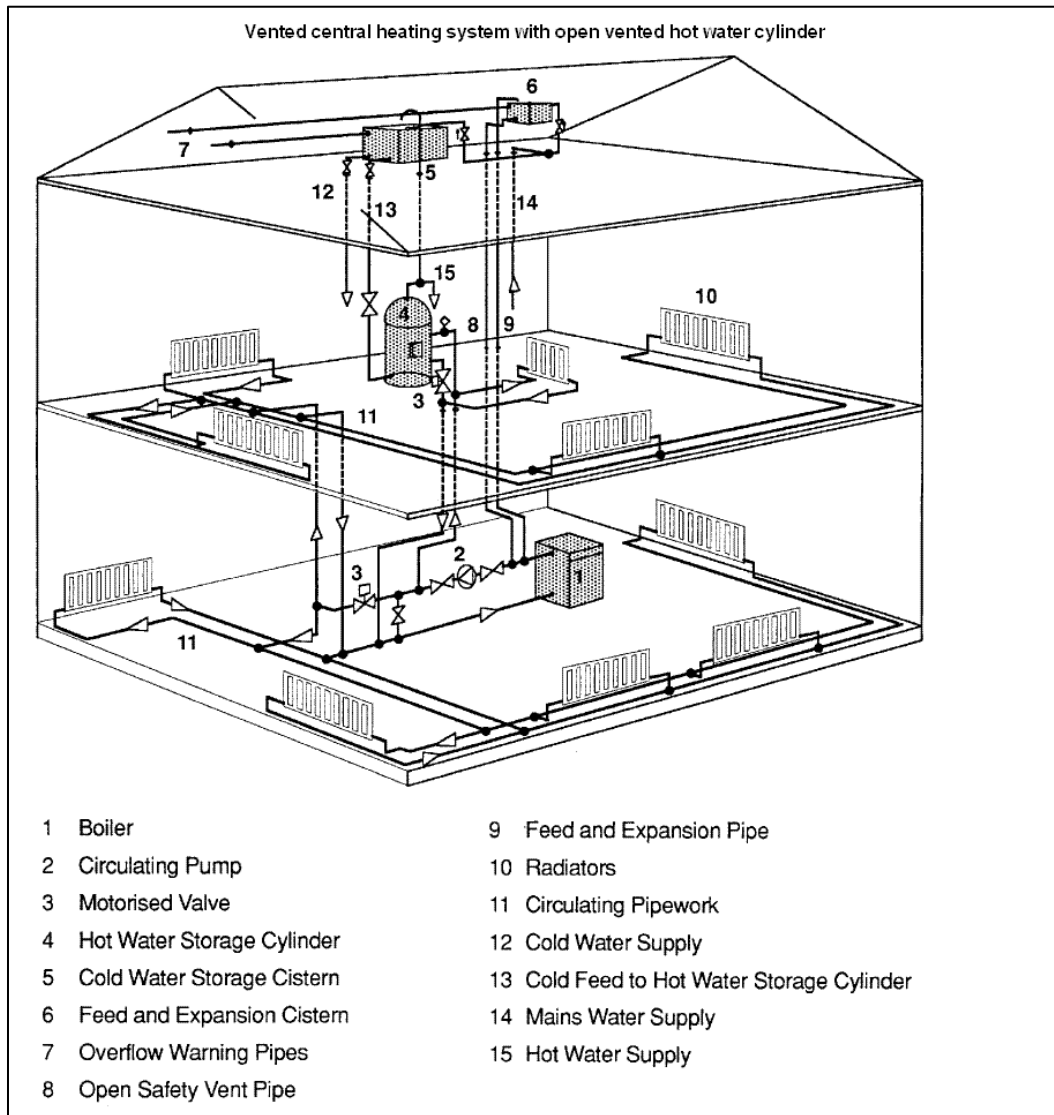


Figure 1-7 Schematic of central heating system [9]

1.1.1.1 Central Heating systems

There are a number of different types of central heating systems. These have been classified based on the type of fuel used in the primary heating device

- Wood or Coal furnace -- This system has a furnace where wood or coal is used as fuel to heat water. This heated water can be used as the primary fluid, where it is circulated to a heat exchanger through a network of pipes. Alternatively, the heated water is used to heat air, which is then delivered to the required space through a ventilation system. The system has similar problems to the open fire systems described earlier.
- Gas fired — Gas fired central heating systems use compressed natural gas (CNG) or liquid petroleum gas (LPG) as fuel. Unlike wood or coal based system described earlier. Water is heated in an enclosed, compact unit and then pumped through the pipe work. The entire system can be either vented or pressurised closed system. A vented system requires more frequent maintenance compared to a closed system.
- Electric Boiler—An electric boiler uses electricity as the energy source. An immersed element heats the water that is circulated through the central heating system. The electric system has been proven to be most economical to run and maintain.
- Solar/ Geothermal - In some systems solar or geothermal energy is used to heat the water for the central heating. Such systems rely only on renewable energy source to heat the primary fluid.

1.1.1.2 Individual/ Standalone systems

Individual or standalone systems are singular units, which heat the vicinity when powered. Most of the standalone systems are self-contained. They provide flexibility and help target heat in a specific area when required. Similar to central heating systems, they are mainly classified based on primary fuel. A summary of the various systems is given below: -

- Wood burning – This is metal or ceramic casing mounted on an insulated stand. The casing is filled with wood or coal and ignited. The combustion generates heat, which is used for space heating.
- Gas – Bottled natural gas or LPG (Liquefied Petroleum Gas), is fixed to a burner. Heat is generated by combustion of the gas.
- Electric -- Electric standalone systems are the most common systems available in the market. A heating element converts electric energy into thermal energy. These are

mainly classified based on the method used to draw the heat away from the element and heat the surrounding space.

- Free Convection based electric heater- these system have a naked heating element or a hot surface enclosed in an electrically insulated casing. The system relies, on convective heat transfer due to temperature difference between ambient air and the element. The heated air then rises and circulates in the surroundings.
- Forced Convection based electric heater- the construction of this heater is similar to a free convection system with an addition of a fan. Instead of free convective heat transfer, the fan forces the air over the element and expels hot air from the vents.

Similar to central heating systems, standalone electric systems also can be classified based on the primary heating fluid. In these systems an electric element is used to heat the primary fluid within a radiator, which in turn heats the panel. The heated panel acts as a heat exchanger and heats the ambient air.

Oil filled radiators—These radiators are filled with synthetic oil. Once heated, the oil retains the energy due to high specific heat capacity. The oil transfers the energy to the panel through convection and the heated panel transfer the energy to the ambient air. These radiators do not require a pump to circulate the oil.

It can be seen from the above discussion that there are a number of different systems, which can be used of space heating. There are however design and performance considerations which affect the efficiency of the radiator and the perceived comfort. These have been discussed in Section 1.1.2.

1.1.2 Design and performance considerations for central heating systems

With the development in engineering, central heating systems have been used for space heating since early twentieth century. A central heating system as the name suggests, has a central node that heats a primary fluid, which is circulated through heat exchangers located in the space to be heated. The heat exchangers in turn heat the ambient air in the room. There are a number of different types of central heating systems. They can be mainly be classified based on the primary heat source. These systems can be further classified based on the primary fluid used.

Significant amount of material is available from EST (Energy Saving Trust) [15] and IDHEE (Institute of Domestic Heating & Environmental Engineers) [12] to design and calculate the size of the boiler for the whole house and the size of heat emitter for each

room. The sizing is based on the following factors whilst allowing for losses, which are inherent to central heating systems

- a) Room size (length, width and height)
- b) Number of exposed and internal walls
- c) Heat transmittance (U –values) for the surfaces (floors, walls, windows, roof)
- d) Number of air changes (ventilation)

The losses in central heating systems are

- a) Losses due to intermittent heating – accounting for approximately 10%
- b) Distribution losses – accounting for approximately 5%
- c) Losses due to separate hot water storage requirements to meet hot water demands from the same boiler- approximately 2kW

Significant contributing factor for central heating system losses is intermittent heating. As the hot water circulates through the system it losses heat through the radiators to the cold air in the room. Heat transfer from the radiator system is made up of convective heat transfer and radiative heat transfer. Equation 1-1 represents the heat output from a radiator.

$$Q_{radiator} = [hA(T_{radiator} - T_{air})] + [\sigma \times \epsilon \times A \times (T_{radiator}^4 - T_{air}^4)]$$

Equation 1-1 Heat transfer from radiator

$Q_{radiator}$ - Heat output of radiator in Watts

h – convective heat transfer co-efficient

A – area of the radiator panel exposed to air

$T_{radiator}$ - Temperature of radiator in Kelvin

T_{air} - Temperature of surrounding air in Kelvin

It can be seen from the equation that, higher the temperature differential between the air and the surface of the radiator, higher the heat transfer, but as the water in the system cools heat transfer rate goes down dropping the efficiency of the system. As the water circulates back to the storage tank/boiler it is relatively cold. Higher the temperatures difference between the outlet and inlet of the boiler higher the demand.

$$Q_{Boiler} = m \cdot C_p (T_{outlet} - T_{inlet})$$

Equation 1-2 Energy demand on the boiler

Q_{Boiler} - Heat demand on boiler in Watts

m - mass flow rate in m/s

T_{outlet} - Temperature of water at the outlet of boiler

T_{inlet} - Temperature of water at the inlet of boiler

As seen from above equation the temperature drop should be minimised to reduce the power demand on the boiler. This can be achieved by circulating the water at an optimum flow rate. The flow rate is directly proportional to the net volume of water required to be circulated in the system. The volume of water is a function of property size, number of radiator and the length of pipe network. If a pump with sufficient head and flow rate is selected it will support the system. As the flow rate increases frictional losses in the system increase, which in turn increases the demand on the pump. Frictional loss in pipes further increases with the reduction in pipe diameter.

Another significant loss factor is heat loss from the network of pipes carrying hot water to the radiators. Fuel efficiency booklet [15] has accurately accounted for losses per meter of pipe and also quantified the effect of insulation. Heat loss from pipes carrying hot water at 75 C is given by Figure 1-8.

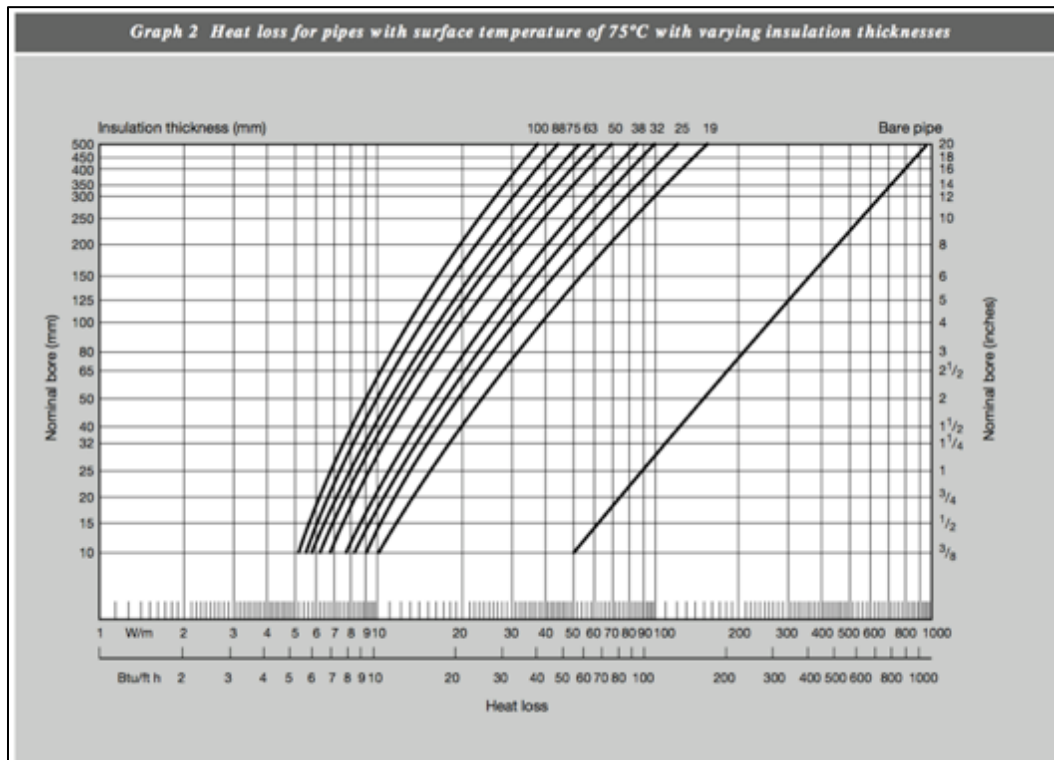


Figure 1-8 Heat loss from a pipe in central heating [15]

A bare pipe of 12mm bore (common central heating pipe) losses up to 50 W/m which can go down to 10 W/m if insulated by a 19mm thick insulation. This suggests that insulation of central heating pipes can significantly reduce the heat loss but will add to the installation cost. In summary, there are a number of factors, which influence the performance of central heating systems.

1.2 Motivation of present work

To meet challenging targets of carbon emission from domestic heating, major developments and innovations in improving the thermal efficiency of buildings have taken place in the last two decades. There have also been developments in the heating systems, which have become efficient but it was found necessary to review currently used central heating systems. A systematic study of the effectiveness and limitations of these systems is required to identify better heating systems to reduce energy consumption and improve effectiveness of the heating systems.

Of the various proposals available to improve the efficiency of central heating systems, operating the central heating system at low temperature seems to be the most restrictive as the power output from individual radiators in the system goes down and the time to comfort temperature increases. TRV (Temperature Regulation Valve) on each radiator coupled with

room thermostats are the most desired means to manage demands and control energy consumption. However these have some limitations. For instance if in a three bedroom house the TRV in two rooms is set to low but there is a higher demand from the third room, the large boiler and pump unit in the central heating system will still have to operate to heat and circulate the water through the entire system. The system would require very complex and expensive plumbing to mitigate this problem, which may not be an option in all building environments. Some stand-alone systems do offer the flexibility to heat individual rooms but compromise comfort and air quality (humidity). Hence a novel method for reducing domestic heating energy consumption is required. New systems found this way would be expected to improve thermal characteristics of radiators, whilst providing good control, scalability, ease of installation and economic benefit over central heating and conventional stand-alone systems.

Stand-alone radiators have existed for the past 20 years and presented themselves as a viable alternative to central heating systems by providing, modularity, flexibility and controllability. Although there are several systems commercially available there is no product or research available on water filled stand-alone systems. A systematic study on viability of water filled stand-alone systems is required. A detailed new product development approach has to be utilised to develop a radiator systems that offers the comfort and function of central heating system and flexibility and controllability of stand-alone systems. The product developed has to be commercially viable, easy to manufacture, meet customer requirements at right cost and above all offer efficient clean heating system alternative.

Product development of such a system would involve component and system testing, physical and numerical performance evaluation to calculate thermal output of stand-alone radiator systems. A robust methodology is required which would cater to the exacting requirements of a novel stand –alone radiator system. Existing research and methodologies for predicting performance of radiators are specific to central heating system radiators, which are limited to lower flow velocities. Hence a methodology to bridge this gap has to be formulated to predict the thermal and hydrodynamic performance of stand-alone water filled radiator system. This will enable accurate component selection to achieve maximum output from a self-contained system. Product development process will use modern manufacturing process to optimise cost of the components and the end product without compromising function.

The effect of modifying key components like heat source, pump and pipe layout in a radiator has an impact on flow parameters in a radiator which in turn affect pressure drop and flow distribution in the radiator. Hence it is required to understand the influence of such systems on internal flow characteristics and overall performance of radiators. A robust method for predicting pressure losses and pressure distribution needs to be devised. Such an approach would require thorough analysis of the effect of geometric parameters over a range of flow rates and configurations. The findings from this numerical investigation have to be used to optimise the stand-alone radiator design and validated with physical testing. The study could also be extended to quantify losses in individual radiators in a central heating system.

1.3 Research Aim

Motivation for research has given specific aims for the research activity discussed in this thesis. Detailed sub-objectives of the study will be discussed after a thorough literature review in the next chapter. Main research aim and the four broad research sub-objectives have been formulated for this work as given below

Aim

Design and development of a cost effective stand-alone water filled radiator for built environment applications

High-level objectives

1. New product development process and development of a state of the art stand-alone water filled radiator
2. Critical performance analysis of stand-alone water filled radiators
3. CFD based quantitative flow analyses in a stand-alone water filled radiator
4. Development of cost model and optimal design for a stand-alone water filled radiator

The research aim along with high-level objectives will provide a framework for finding solution to most of the practical problems encountered in the real world problems associated with space heating using stand-alone water filled radiators and flow parameters in the radiators that affect the performance. These can be considered satisfactory for this study. Detailed literature review is presented in the next chapter, which focuses on the research aims and identify knowledge gaps that will be addressed in consequent chapters.

1.4 Outline of Thesis

Based on the review of the emission targets, improvements in the building efficiency and current trend of the heating systems, the thesis presents the body of work, which has been carried out in the current research study.

Chapter 1 provides an overview of emissions due to heating, current targets and improvements in building regulations, efficiency of buildings and current trends in heating systems. From this overview, the motivation for carrying out this research work is described, which identifies the key research area, which will be reviewed in chapter 2.

Chapter 2 consists of a detailed review of the products and research carried out in the field of heating systems. It includes review of current heating systems and methods of new product development. Furthermore a review of factors influencing the performance of radiators has been discussed. Review of the factors influencing internal flow in radiators and optimisations techniques to improve cost and performance have also been discussed. Details of the scope of research and specific research aims and objectives have been outlined.

Chapter 3 documents rational for experimental process and details of the setup and procedure have been discussed. The fundamentals of computational fluid dynamics that come into affect to evaluate fluid flow in a radiator are discussed. Meshing techniques that have been used for the flow domain, along with CFD modelling of the radiators, including solver settings and boundary conditions that have been specified to solve the flow domain have also been discussed.

Chapter 4 consists of detailed design and development of a novel stand-alone water filled radiator, using bespoke new product development process. Methodical, concept development has been undertaken to develop a robust product specification to meet the business case. The developed concept has been matured into a product that can be manufactured. Detailed component design and selection has been discussed. Test procedures to evaluate product performance and the results thereof have also been discussed.

Chapter 5 includes temperature distribution and temperature drop in a stand-alone water filled radiator and these have been quantitatively evaluated. The pressure and flow distribution in the radiator have been experimentally analysed in detail. Effect of point of entry and radiator size on the pressure loss and distribution have been analysed at various flow velocities.

Chapter 6 presents detailed CFD based investigation of geometric parameters in a radiator that influence the flow and pressure. Effect of size of radiator has been analysed using three radiator sizes, two flow configurations and 5 flow velocities. A semi-empirical model for prediction of loss co-efficient in a radiator has been developed which is independent of radiator size. Likewise, effect of port diameter in a radiator has been analysed under various flow configurations and flow velocities, leading to develop another semi-empirical model for prediction of loss –co-efficient independent of port diameter.

Chapter 7 develops a cost model to calculate the cost of ownership and optimisation for radiators based on least cost principle. The cost model uses thermal requirements for a room as input and predicts the manufacturing and running cost for the stand-alone water filled radiator. A cost comparison study has been undertaken to outline the economies of stand-alone system to a central heating system.

Chapter 8 concludes the findings of this study; outlines the research goals and additions to the knowledge in heating system, in terms of new product design, development, and flow evaluations within the radiator. Recommendations for future work have also been included.

2 LITERATURE REVIEW

After reviewing the need to reduce the emissions from building and studying the improvements in the efficiency of building in the previous chapter, a detailed literature review has been presented in this chapter which will highlight the need for development of stand-alone water filled radiator and the knowledge gap in the existing literature. It includes published works regarding current trends in heating systems and new product development, standard performance evaluation, parameters influencing performance, internal flow and pressure distribution in the radiators and optimisation methodologies for radiators. Based on the knowledge gap found in the literature review, scope of research has been defined and research objectives of this study have been formulated.

2.1 Stand-alone water filled radiators: product development process

As discussed in chapter one there are several designs of heating systems. The most common design is a central heating system. As discussed in chapter 1, central heating system has a central node where the fluid is heated before being circulated through the pipe network to exchange heat with the surrounding space through radiators [16]. Liao [17] et al. have investigated the control features available in a central heating system. The survey conducted in their research has shown that the boiler and heat emitter controls in the UK are resulting in poor performance of the systems. Poor control leads to undesirable temperatures in the buildings, which in turn results in occupant discomfort and higher fuel costs

Incorporating one or combination of the following systems generally achieves control in central heating.

- a) Boiler control
- b) TRV (temperature regulation valves) on individual emitters (radiators)
- c) Central motorised valves to control flow to the emitters

In the following some specific examples of these effects are shown.

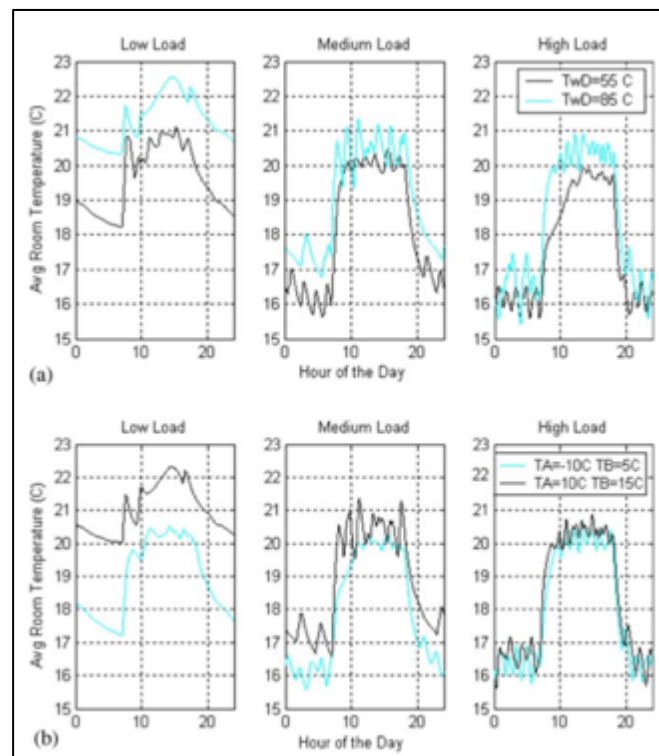


Figure 2-1 Performance of old TRV using different boiler controls Liao [17]

Liao [17] as shown in Figure 2-1, also found that in general TRV's are not set appropriately and TRV older than 2 years did not function as per design specification where the comfort ratio dropped by approximately 5%. Central heating boiler is generally over specified hence consuming more energy.

Ahren et al. [18] have shown that using energy balancing, the heat energy savings can be achieved in the range from 1% to 19% depending on dwelling type, age, location and initial specific heat energy consumption across EU (European Union). They predict total potential savings across the sector amount to 22.6 Mtoe, a reduction of 7.3%; 53% of these come from reduction in pumping power required by heating distribution systems and 47% of these come from reduction in the heat energy consumed by heating systems. The study has also suggested that large central heating / district heating systems have an unbalanced hydraulic system which results in the radiators closest to the pump to receive oversupply of hot water and greater than desired heat output, while remote radiators receive water below the design temperature resulting in lower heat output. This can be seen by the illustration in Figure 2-2.

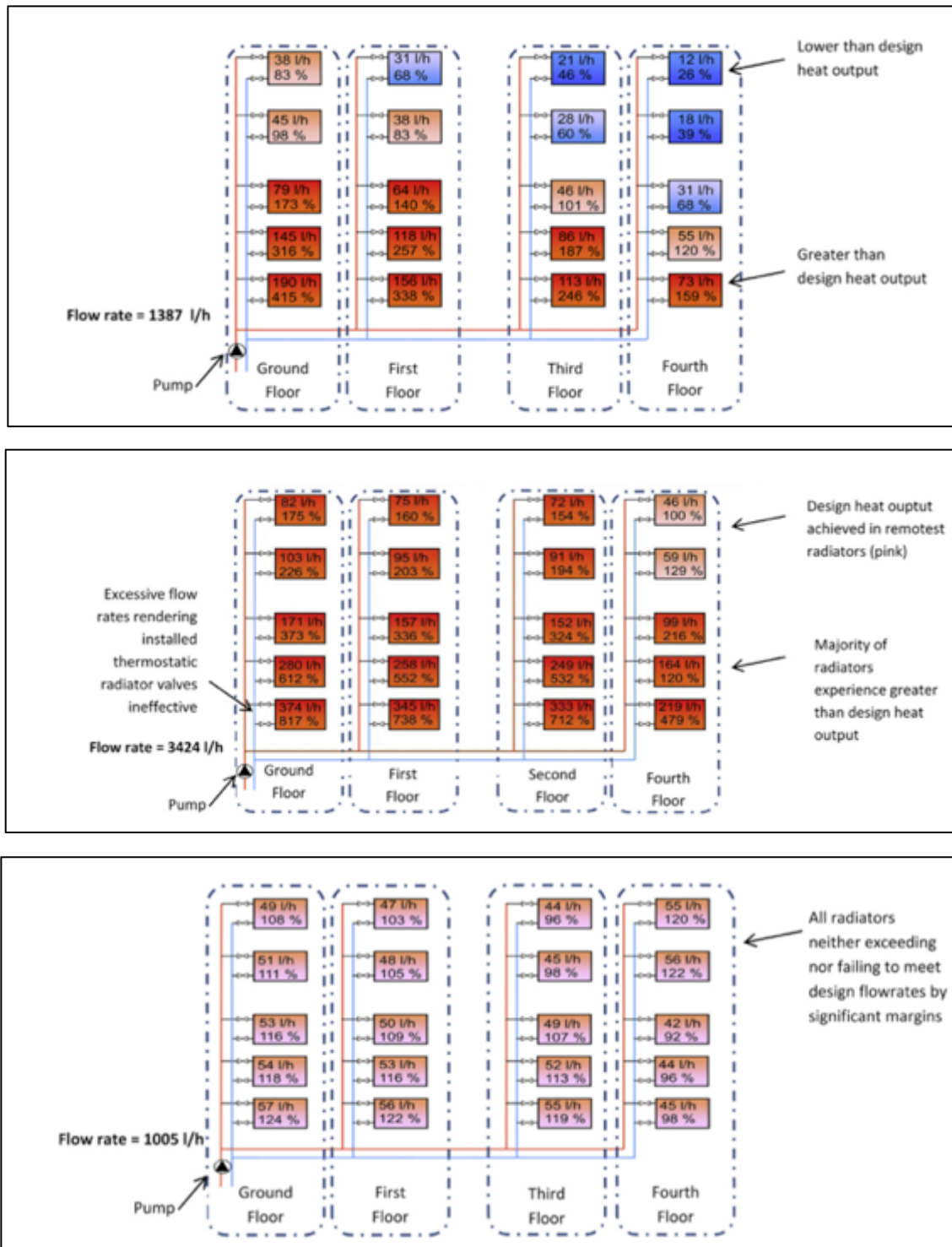


Figure 2-2 Comparison of unbalanced, remedied and fully balanced heat distribution system [18]

It can be seen that significantly higher flow rates are required to achieve operational temperatures in all radiators in a modified system, which still results in losses with wasted heat in hotter radiators. A finely tuned balanced system can be achieved with thermostatic radiator valves but this has cost implication and relies on careful adjustment from the users. As

mentioned above, review from Liao [17] has shown most users do not adjust the TRV system optimally.

In addition to lack of control, the losses in the system are prevalent due to long pipe networks. As discussed in chapter 1, a 12mm diameter pipe can lose up to 50W/m if it is not insulated. Insulation for the pipes can reduce the losses but add to the overall cost of the system.

Beck et. Al, [19, 20] have carried out extensive investigation to analyse the working of radiator panels in a central heating system. They have reported that optimizing the location of the radiators within the room can increase the output of radiators. Also decreasing the height above the ground and by increasing their spacing from the wall from the standard installation would improve the airflow characteristics over the radiator. The attachment of convector fins to panel radiators increases the surface area and hence the convective heat transfer. They also concluded that different combinations of fluid entry and exit positions could affect radiator performance.

Several aspects of radiator design affect their output. Some are based on their position,

1. The output of radiators can be slightly increased by decreasing their height above the ground and by increasing their spacing from the wall [19].
2. The attachment of fins to panel radiators increases the convection heat transfer [19].
3. Different connection positions can affect the performance. The most common installation being with both connectors at the bottom (BBOE). However introducing the flow at the top (BTOE) can improve the temperature distribution within the radiator and is used in the standard.
4. Facing the wall adjacent to the radiator with insulated reflector can lower the heat loss through the wall by 70% [20]. This will however lower the heat output from the radiator [20] as the heated wall acts as another convecting surface.
5. It is well known that fouling can dramatically lower the heat output from radiators that rely on convection.

The use of metallic paint finishes can reduce the radiant component of radiator heat outputs by up to 10% [19].

Central heating system is robust and reliable but offers little controllability, it is expensive to maintain and is not flexible if the layout has to change in a built environment. In addition to

losses and lack of flexibility central heating systems also have some safety concerns. Harper et al [21, 22] have published finding of their analysis of burns admitted to Welsh regional Burns and Plastics Unit. In one study conducted in 1995 they have extrapolated that if a radiator is operating with a surface temperature between 70°C and 80°C a partial thickness burn would be produced in less than 0.2 seconds. Further their investigation in 1996 has consolidated the incidence of radiator contact burns from various sources, which is shown in Table 2-1. It can be seen that significant number of radiator burn injuries are recorded. The study also revealed during the course of the survey of the 50 patients who sustained burn injury the mean TBSA (total body surface area) burned was 1.58% and half of the injuries were full depth burns.

Reference	Radiator burns	Overall injury
Datubo	4	47 (childhood contact burns)
HASS	87	827 (radiator injuries)
HALAR	9	43 (adult contact burns)
	2	56(childhood contact burns)
Hampton	19	51 (burns secondary to epilepsy)

Table 2-1 Summary of radiator burns - review by Harper [22]

Health guide notes from BS EN 442 [13] indicate that the surface temperature of the radiator around vulnerable occupants (patients in care homes, hospitals etc.) should not exceed 43°C. This is achieved either by running radiators at lower temperatures or adding covers on top of standard central heating radiators, Both approaches reduce the effectiveness of the radiator significantly.

Stand-alone systems as the name suggest are independent and in most cases are small mobile units, which can be easily relocated. Stand-alone heating systems are commercially available and as discussed in chapter 1 there are many designs that can be classified based either on primary heating source or type of fluid used.

General perception is that the stand-alone systems are not efficient. As dictated by law of conservation of energy “ energy can neither be created nor be destroyed, but can only change from one form of energy to another.” Hence all stand-alone heating systems convert 100% of electric energy to heat energy to the surrounding space, but each system operates differently.

One of the major drawbacks of each of the current hot element convector stand-alone system is the ability to control the air temperature similar to a central heating system without

loosing air quality (humidity). The heating elements in the convector style heaters can exceed 100° C which dehumidifies the air and can cause discomfort to the occupant. Oil filled radiators overcome the problem as the maximum surface temperature is limited to 75°C, but due to high specific heat capacity of oil the system takes a long time to reach operating temperature which contributes to customer annoyance. Water has lower specific heat capacity compared to oil and hence can reach the operating temperature faster. It can operate at 75° C without the risk of boiling.

Collaborative work between University of Huddersfield and a local company, a new product development program was undertaken to develop water filled stand-alone radiator. Market research revealed that only two companies in the UK manufactured water filled stand-alone systems, which were acquired by the parent company that collaborated with UoH, with a view to capture a large market share and to develop a range of wet flow radiators compliant with regulations and economically competitive to other brands all over the world. This acquisition resulted in availability of four main types of products. Each of the four radiators had different operating systems (control systems and heating elements for maintaining the temperature).

The manufacture of wide ranging products with little commonality has made the overall technical management as well as marketing process extremely complicated. To optimise the manufacturing process, a product has been envisaged which could function as any of the above as well as provided economy of scale in manufacturing operation. New product development of a single radiator model, which will be flexible enough to function as any of the four models mentioned above and offering huge savings in manufacturing efforts as well as product marketing efforts. Also increase the market share. Thus the requirement of developing a product with improved modularity, functionality and flexibility was established. In the following review of literature has been carried out to identify suitable product development processes that could be adapted for the development of stand-alone water filled radiator.

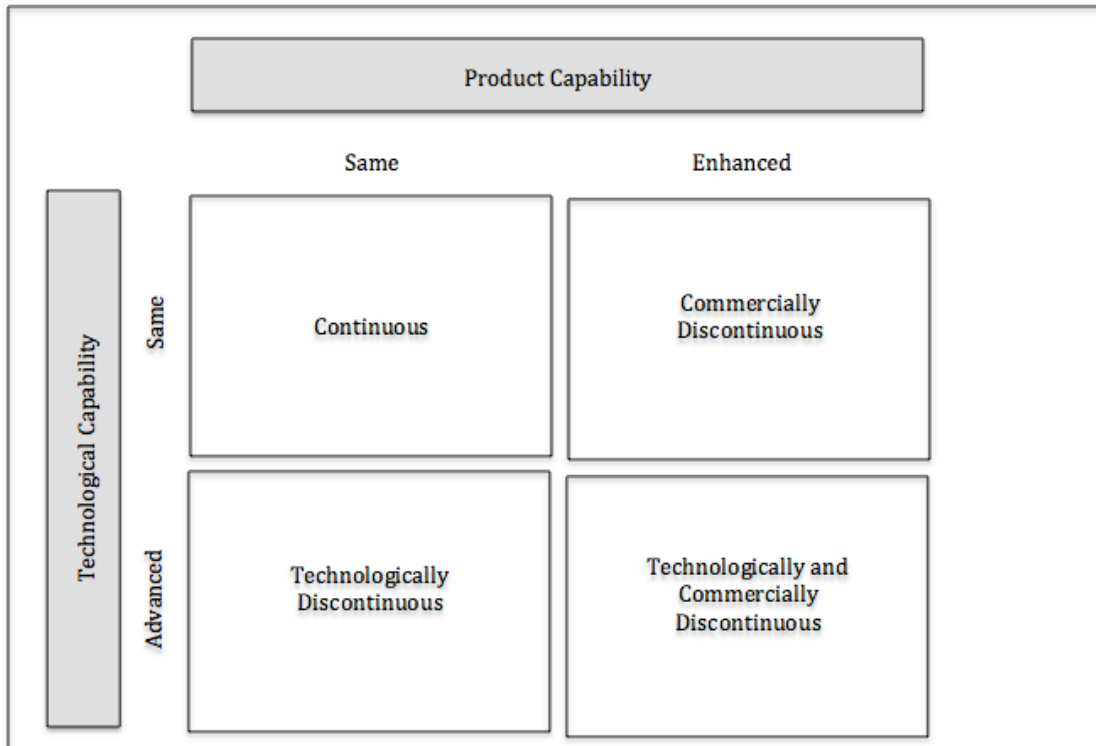


Figure 2-3 Types of product innovation [23]

In order to achieve a profitable product, robust methodologies and process have to be followed. Discontinuous innovation and new product development process discussed by Veryzer [23] in Figure 2-3 shows that innovation can be introduced in a product where the technology changes can be introduced without noticeable difference to the end customer, such innovation are classified as technologically discontinuous. Alternatively, innovation can be introduced where the product capability is enhanced and noticeable by the customer such innovation is called commercially discontinuous innovation. When both product and technical capability of the product are enhanced commercially and technologically discontinuous product is developed. Discontinuous innovation involves a high degree of technological uncertainty and long development times. The discontinuous product development process shown in Figure 2-4 includes multiple prototype phases, which will be both time consuming and expensive.

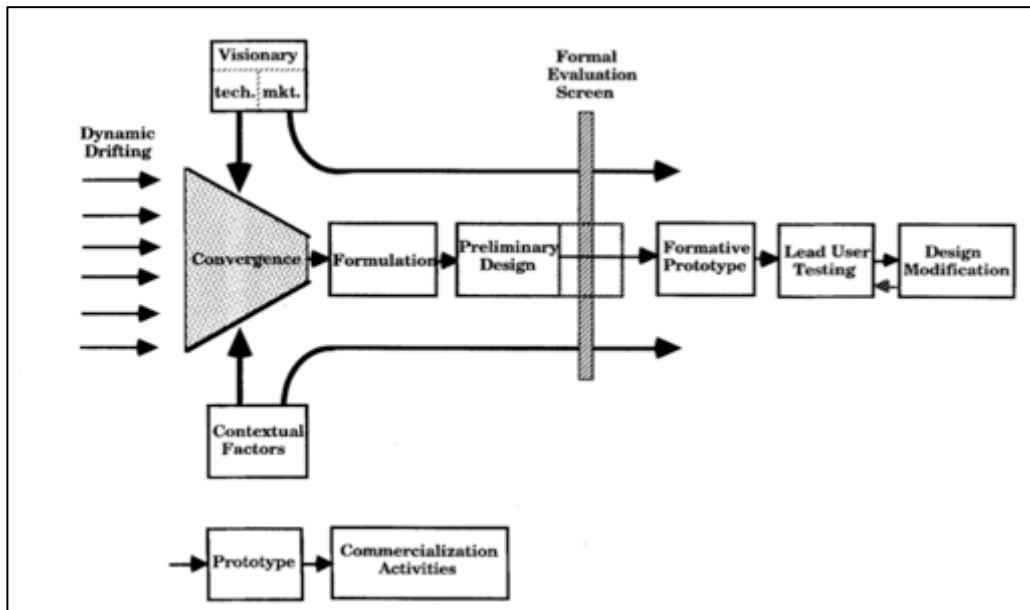


Figure 2-4 Discontinuous product development [24]

This being a fixed time project, requiring the product to be in the market as early as possible necessitated the development of a purpose built process for product development.

New product development methodologies discussed by Ulrich [24], outlines the 5 key stages of product development.

- 1) Planning
- 2) Concept development
- 3) System level design
- 4) Detailed design
- 5) Test and refinement
- 6) Production ramp up

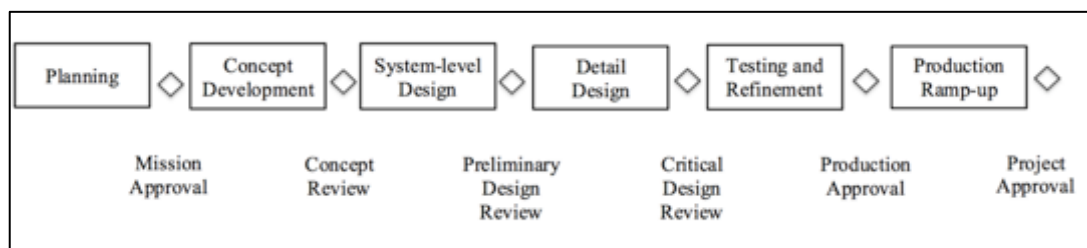


Figure 2-5 Generic product development process [25]

Ulrich further emphasised the importance of adapting the generic product development process based on innovation, market requirements, and number of variants developed for a product and intended production process. This generic product development process will

require extensive modifications, if used for new stand-alone water filled radiator development. Ulrich has further mentioned application of other product development processes such as spiral and complex product development process. These processes will also need extensive modifications for application into stand-alone radiator development.

Review from Ohio University [25] has highlighted the reason for new product failures. Some of the reasons are over estimation of market size, poor design, high price, high development cost and competition. It is required to avoid the reasons mentioned in the process to be developed for stand-alone radiator development.

Research carried out by [26-28] has shown that it is important to develop the product that can react to the change in market and customer requirements. The design and manufacturing methodology employed should be able to reconfigure to deal with such changes.

Product manufacturers have converted their product catalogues to product portfolios to be competitive and manufacture the product with a view to mass customisation [29-32]. Portfolio approach commonly applies to products, which share components, manufacturing processes and are based on a common platform [33]. Automotive industry is a prime example of mass customisation using a common vehicle platform. I aim to utilise this approach in developing a customised process for product design of stand-alone radiator system.

Mesa et. al. [34] have developed an interesting methodology to define reconfigurable system architecture for a compact heat exchanger assembly machine. The study suggests that according to manufacturing experts, a new generation of manufacturing system that is adaptable and flexible while responding to market dynamics is required and called reconfigurable manufacturing system (RMS). The literature focuses mainly in system reconfiguration at machine level through modifying modules from the family of product reconfiguration variables. The study highlights the importance of modular approach to reconfigure the product but the algorithm used is suitable for a very dynamic system where requirements and demand changes on regular basis. The approach may not be directly suitable for low to mid volume manual manufacturing process where a wide range of thermal outputs are required. This approach is not suitable for product development as it focuses on improving functionality and modularity of existing product family. It also does not take into account the manufacturing quality control as well as the performance testing.

2.1.1 Summary of literature regarding current stand-alone heating systems

Based on the literature review presented above for central heating systems it can be summarised that the published literature clearly highlights the drawback of existing central heating system. The literature emphasis that the central heating systems has lack of control and the proposed methods to reduce losses in the system are expensive, require regulatory changes and maintenance. Last but not the least central heating system does not offer flexibility for extensions and modifications.

A stand-alone system aims to solve the above concerns but the current systems that are commercially available, either cause occupant discomfort or annoyance. Hence there is a need to develop stand-alone water filled radiator that can overcome the concerns raised.

Literature review on new product development process has been carried out. Although it offers an in-depth guide for generic approach in some instances and a very bespoke process for semi/highly automated product-manufacturing process, there is little than can be used directly to develop new water filled stand-alone radiators. There is also limited literature on quality assurance process in the product development and manufacturing phase.

Development of a new stand-alone radiator to consolidate the product range, optimise manufacturing process and deliver customer expectations would require careful consideration and a robust design and development process. In addition due to the short delivery time it is imperative that the proposed development process can deliver robust quality. A bespoke product development approach has to developed that is unique for the domestic heating system which will cater to a wider consumer market and produced at competitive cost with a manual manufacturing process. The developed product will then need to be tested over a wide range of operating conditions to ensure its suitability.

2.2 Literature review on factors influencing the performance of radiators

In the previous section detailed literature review has been conducted on central heating systems and their concerns. A detailed review of new product development methodologies has been carried out. In this section factors affecting performance of radiators are investigated, with an aim to identify the knowledge gaps and develop research scope research for experimental investigation on radiators.

Peach [35], has found that the ratio of actual surface area A_c and projected area A_r is defined as stretch ratio A_c/A_r ratio and it has an effect on heat transfer from the radiator. Heat output is given by the equation

$$Q = h_r \cdot A_r \cdot \Delta t + h_c \cdot A_c \cdot \Delta t$$

Q Heat output from radiator

h_r Convective heat transfer co-efficient – projected surface area

A_r Projected surface area

h_c Convective heat transfer co-efficient – actual surface area

A_c Actual surface area

Based on this formulation, Peach [35] has approximated the proportion of total emission for single and double panel radiators. A single panel has 50:50 heat emissions in radiation and convection. The split changes to 30:70 for a double panel radiator. The investigation also discusses effect of fin and tube geometry and effect of surface coating on heat transfer rate. Emissivity of the surface affects the performance and studies recommend an oxidized metallic surface for best performance. Another geometric feature, which affects the heat output, is the height of the radiator. As the height increases the motive force causing the air to circulate through the emitter gets larger. A very significant parameter investigated is the effects of flow and return connection position. The study reveals that the top entry of water in a radiator offers highest emission and at high water flow rates forced flow effect gets dominant.

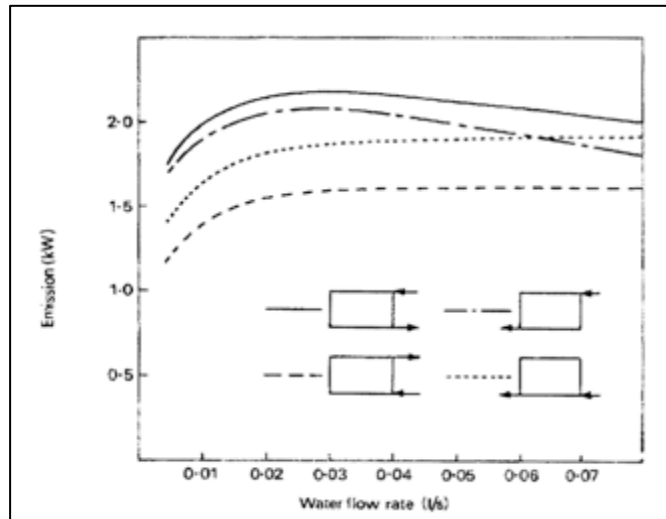


Figure 2-6 Typical variation of heat emission with water connection [35]

Water flow rate has an influence on heat transfer. Equation for heat transfer is given by

$$Q = \frac{h_o h_i}{h_i + r h_o} A_o \Delta t$$

Where

h = heat transfer co-efficient ($\text{W}/\text{m}^2 \text{ } ^\circ\text{C}$)

A = Area (m^2)

r = ration A_o/A_i

Δt = temperature difference between heating and heated fluid ($^\circ\text{C}$)

$h_i v^{0.8}$

v = fluid velocity (m/s)

Based on the above equations Peach [35] has concluded that even if the velocity is doubled heat emitted from the radiator (Q) increase only by a 25%.

Walter and Fine [36] have documented performance of radiators and convectors using medium temperature water and found that all the appliances tested follow the following form

$$Q = \text{constant} \times (\Delta t)^n$$

Where

Q = heat emission

Δt = Temperature difference between means water temperature and mean air temperature (° C)

McIntyre [37] in his was work has identified that the heat output from conventional hot water radiator falls as the return temperature is reduced, showing much lower heat output from a pressed steel radiator that that calculated using conventional formula. Similar to Ward [38] power output is given by the formula

$$P = B(\Delta T_m)^n$$

Where

(ΔT_m) - arithmetic mean temperature difference between radiator and room air temperature

n= 1.3 based on experimental work carried out by McIntyre [37]

Ward [38] has a carried out similar investigation to McIntyre and also found that heat output from conventional radiators falls as the return temperature and the mass flow rate are reduced. The standard conditions for test are inlet water temperature at 90° C and the return is 70°C with the room temperature at 20° C. Ward similar to McIntyre has found that as the flow rate is reduced the residence time of water in the radiator is increased and thus the return temperature falls. Resulting output from radiator is substantially different from the expected standard equation due to mixing of incoming water with the water within the radiator.

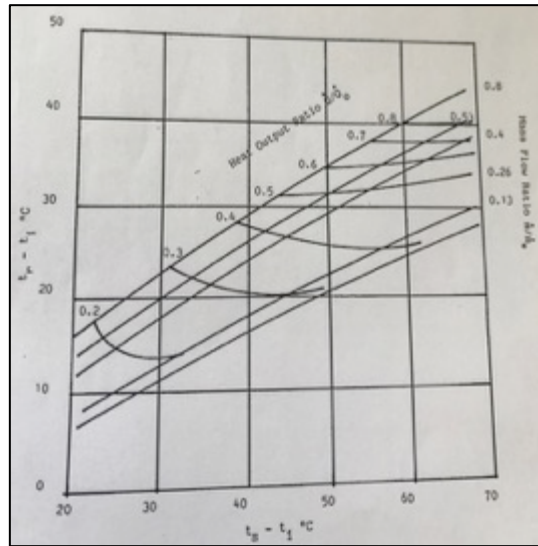


Figure 2-7 Output diagram for BBOE double panel radiator [38]

Giesecke [39] has found that design of the radiator system has implication on the thermal output of the system. The flow rate in a given system influences its heat output and hence a suitable pump should be selected to meet the pumping demand for maximum heat output whilst accounting for the head loss in the system. A combination of flow rate, temperature drop and mixing of fluid in the radiator make it difficult to predict the output of the radiator in practice particularly in conjunction with thermostatic control valves. Giesecke [39] also found that in a central heating radiator frictional head loss increases with the increase in flow rate. Experimental investigation of column radiators at various flow rates has given the following general equation, which accounts for the length of radiator and flow rate. The investigation was carried out at only 3 flow rates 437, 905 and 1814 lb. per hour.

$$H_f = 0.000395P^{2.18} + 0.001125P^{1.54}$$

Equation 2-1 Head loss in a radiator [39]

Where

H_f = friction head in milli inches of water

P = rate of flow in lb. of water per hr.

S = number of sections in a radiator.

A summary of his investigation is also given below in Figure 2-8. Cast iron radiators are shown by curve I, II and III where I has 7 sections, II has 15 and III has 22 sections. Curve III

has the highest head loss for a given flow rate, suggesting that the increase in the length of radiator increases head loss

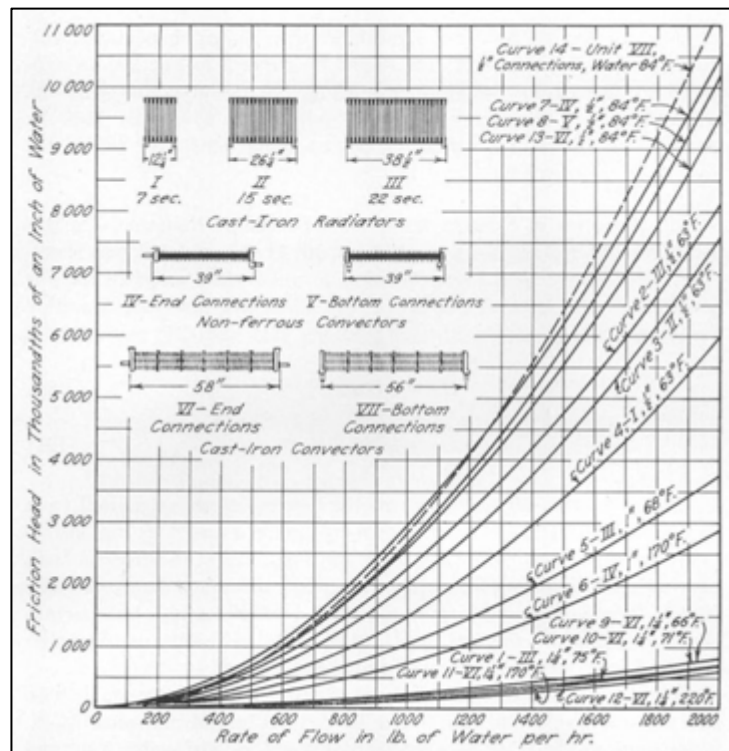


Figure 2-8 Friction heads of various radiators and convectors - experimental work by Giesecke [39]

Giesecke [39] has concluded the following:

1. Friction head produced by the water flowing through a radiator or convector may be divided into three parts,
 - a. Friction head at inlet – has the largest contribution
 - b. Friction head at outlet – medium contribution, and
 - c. Friction head within the unit itself- lowest contribution
2. For a given flow of water the size of connection has an important influence on the friction head at inlet and outlet and therefore also on overall friction head
3. It also found that the within the range of velocities observed in practice the heat emission of cast iron convectors is apparently independent of the velocity of water flowing through the convector.

2.2.1 Summary of literature regarding performance parameters of radiators

Based on the literature review presented above, for the factors that influence the performance of radiators, it can be summarised that the published literature is severely limited

to central heating applications and the flow rates typically observed in the central heating system. Temperature drop across has been investigated for central heating system but pressure drop across the radiator and temperature and pressure distribution has not been investigated. Flow configuration for a stand-alone radiator cannot be accurately designed for practical purposes. Hence, there is a need of better understanding of the flow structure within radiator system. Furthermore, a wider range of investigations are required in order to built-up an adequate database for accurate analysis of geometric parameters in radiators.

For head loss in radiators and pipelines, it can be summarised that the published literature is severely limited in terms of the range of flow velocities, radiator size, influence of height and length, pressure drop considerations and detailed analysis of the flow parameters within the radiators, such as the pressure variations and the velocity distributions. Based on the equations summarised here, demand on pump and pump sizing cannot be accurately designed for practical purposes. Hence, there is a need of better understanding of the flow structure within stand-alone radiators.

2.3 CFD based quantitative flow analysis in radiators

In the previous section detailed literature review has been conducted on performance prediction of radiators/ heat exchangers with an aim to identify the knowledge gaps and develop scope research for experimental investigation on radiators. In this section detailed literature review has been conducted with an aim to establish the knowledge gaps in the area of effect of local flow features on performance of radiators/ heat exchangers. Unfortunately, the information available on internal flow characteristics within a radiator is very limited. In the following available work on radiators along side flow characteristics within geometries similar to stand-alone radiators have also been reviewed, with a view to establish analytical methodology.

Etemad [40] has developed general equations for fully developed laminar flows in complex geometries. The equations are obtained by developing equivalent diameters for complex duct shapes. The process involves creating N circles with perimeter P and area A . Equivalent diameter is then given by

$$D_e = 4A/P$$

But different duct shapes can have the same equivalent diameter but different pressure drop across them. In order to mitigate this a non-dimensional diameter has been suggested by Shah [51]

$$D^* = D_e / D_{\max}$$

D^* and N are non-dimensional numbers which help define the shape of the cross section of the duct.

Dehdakhel et. al. [41] carried out CFD investigations on thermo-siphons and obtained temperature field at various fill ratios. Sato et. al. [42] evaluated the effects of the duct geometry on the temperature field within a thermal system. Subramanian et. al. [43] used different size of the ducts to evaluate thermal performance and obtained that non-uniform flows in the tubes affects thermal performance considerably. Iordanou et. al. [44] investigated effect of placing inserts on the performance of thermal systems and they obtained that placing additional metal mass increases the thermal retention capability. Combination of the research work presented by [41], [42], [43] and [44] has provided a very good insight into the geometric

parameters that influence the performance of thermo-siphon system, which in some respects is a similar heat exchanger to a stand-alone water filled radiator.

Freegah et. al. [45] carried out investigation on a closed thermo-siphon hot water solar system, with a view to analyse internal flow characteristics with the help of computational fluid dynamics software. They found that CFD can be effectively utilized for deciphering the inter flow mechanics with reasonable ease. They could compute velocity and temperature variations within the fluid carrying ducts. This information is not available for stand-alone radiators and we hope to decipher the complex flow mechanics within such systems through the use of CFD.

Freegah et. al. [46] has presented an interesting numerical study on establishing effect of header pipe dimension on flow characteristics within flow distributing tubes of a thermal system. It has been found that the header pipe dimension affects the flow distribution in the ducts considerably and should be optimised for optimum performance.

El. Din [47] investigated the effect of shape of the flow ducts on the heat transfer characteristics. They uniquely established the affect of various diameter ratios on the heat transfer characteristics, indicating that geometric dimensions used must be carefully chosen for optimum performance.

Freegah et. al. [48] carried out another interesting investigation on affect of shape of flow distributing pipes within a thermal system on the performance of the system. They investigated, a straight pipe and helical pipe with different number of turns. They found that increasing number of turns considerably affects the temperature of a thermal system.

Freegah et. al. [49] carried out carried detailed investigation on the flow characteristics within distributing ducts within thermal system. They obtained that the velocity profiles within the duct depend on the thermal loading and the temperature profile of the working fluid also depends on the thermal loading of the system. They clearly highlighted that under working conditions the system operates under transient mode.

2.3.1 Summary of literature regarding quantitative flow analysis in radiators

Based on the literature review presented earlier, it can be seen that the flow distribution within radiator geometry may affect its overall performance. The research works reviewed have clearly indicated that the flow distribution within the main duct and the distributing duct depends on geometries of these ducts as well as restrictions present in these ducts.

In a typical stand-alone radiator, there are a number of geometrical features, for example, inlet connection, port size flow path length as well as distribution of the channels that may affect the pressure drop across the system. It is an important area of investigation for flow system mapping and hence considerable effort will be directed towards this.

2.4 Cost model and optimisation of radiators

Kowalski [74] has described an optimum design method of a two-column radiator used in central heating. In the study radiator heating capacity per unit mass, building depth and heating capacity have been assumed. Based on this the radiator heating capacity per unit mass is expressed as

$$\vec{p}_{Qm} = \vec{p} = (\rho, g_1, p', u, \alpha, p_{Ql})$$

Where the parameter vector for radiator heating capacity per unit length is

$$\vec{p}_{QL} = \vec{p} = (C_0, D_h \wedge D_e \wedge D_s, g, g_2, g_3, t_w, \gamma_P, C_P, \beta^*, \xi_m, \lambda, \epsilon, \sigma)$$

Where

ρ is mass density of radiator material,

t_w is air temperature

γ_P is specific gravity of air

C_P specific heat of air

β^* co-efficient of cubical expansion,

ξ_m co-efficient of local resistance

λ co-efficient of frictional resistance by flow of air flux

ϵ degree of emissivity

σ Boltzmann constant

Using the above relationship and structural relationships amongst the constraints the quantity model for the radiator has been formulated. The triple-objective design optimisation of the radiator has increased the solution quality compared with a single objective optimisation.

Bojic [75], has used a linear programming approach to optimise the heat distribution in a district heating system by adjusting values and retrofitting a resized substation heat exchanger. Overheating of some building and under heating of some buildings leads to thermal comfort issues. Hydraulic equations and the energy balance equations are developed to account for heat

input and thermal comfort. The objective of the approach has been to minimise loss of thermal comfort in the heated building. The approach addresses the concerns with changes in the flow circuit that affect the characteristic of the design of the heating system. The approach has suggested using valves to adjust the flow rate and introducing a new heat exchanger to adjust the heat input to the substation.

Arslanturk [76] has used an approximate analytical model to evaluate the optimum dimension of a central heating radiator. The approach has accounted for the geometrical constraints associated with production techniques and thermal constraints to maximise the heat transfer rate for a given radiator. The radiator volume fraction is expressed as a ratio of frontal area of radiator and total frontal area in square meters.

For three different ambient fluid temperatures, the variation of maximum heat transfer rate and optimum tube radius as a function of volume fraction has shown that the curves reach an asymptotic value of heat transfer rate at larger values of volume fraction.

In this study geometric parameters have been developed which have been optimised for maximum heat output. Asim [77] has developed an optimisation model for HCPs (hydraulic capsules in a pipe) based on hydraulic design. The model makes use of least cost principle, which states the total cost of the system is minimum, where the total cost refers to sum of operating cost and manufacturing cost. The approach has considered hydraulic parameters like, pressure drop, hydraulic diameter of the pipe, density of the fluid and the capsules, shape of the of capsule and orientation of the pipe in the cost model and then optimised for least cost. This approach is valuable to ascertain cost of operation, cost of manufacture and possibly cost of ownership.

Arup [78] in a CIBSE symposium in 2015 have identified energy, operational, maintenance and repair cost for a central heating system using a gas boiler. Figure 2-9, graphically represents the findings. It can be seen that the standing charge, boiler maintenance cost and boiler replacement cost are constant irrespective of the property size.

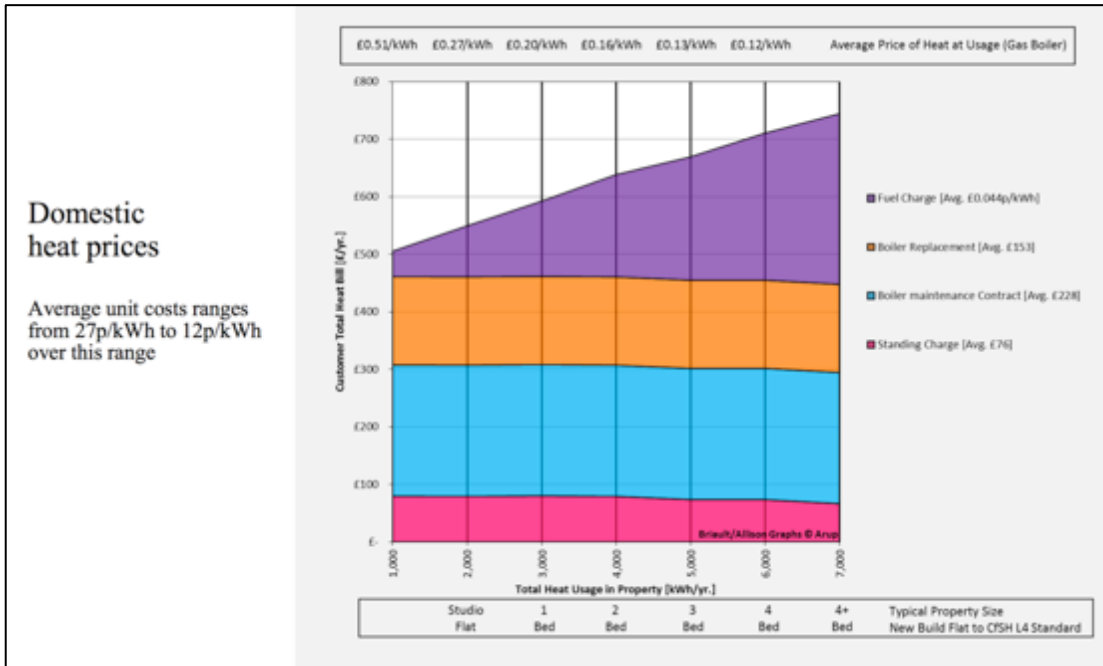


Figure 2-9 Fuel charges for gas based heating system over a year [60]

The variable is the fuel charge, which is dependent on the size of the property. The standard cost gets amortised and have relatively lower impact on the larger properties. The average unit cost per unit ranges from £0.12/kWh to £0.27/kWh. The study assumes standard usage and maintenance but does not account for the initial purchase cost of the heating system and the installation cost, which can be significant.

Room Size (Sq Ft with 8 foot ceiling)	Watts (Poor insulation)	Watts (Avg. insulation)	Watts (Full insulation)
20 sq ft	250	250	250
40 sq ft	500	500	500
60 sq ft	750	750	450
80 sq ft	1000	1000	750
100 sq ft	1250	1000	750
120 sq ft	1500	1250	1000
140 sq ft	1750	1500	1250
160 sq ft	2000	1750	1250
180 sq ft	2250	2000	1500
200 sq ft	2500	2000	1500
220 sq ft	2750	2250	1750
240 sq ft	3000	2400	2000

Figure 2-10 Heater size for a room heating [61]

The literature [61] recommends that a typical room needs 12.5 W/ft^2 for a room with poor insulation. Similarly it recommends 10 W/ft^2 and 7.5 W/ft^2 for an average and well-insulated room. The recommendations are based on a roof height of 8 ft. Converting in SI units heat requirements are 134.55 W/m^2 , 107.64 W/m^2 and 80.73 W/m^2 for a room with poor, average and good insulation.

2.4.1 Summary of literature regarding optimisation of radiators

Based on the literature review presented above, on optimisation techniques used in central heating and radiators, it can be summarised that the published literature is severely limited in terms of optimisation techniques for operational and manufacturing cost of radiator system. The literature does give an insight into cost model techniques and approach but, there is limited literature or tool available to estimate the manufacturing cost, operation cost, total heat cost/day. Due to the unique nature of the stand-alone radiator a customised and bespoke methodology has to be developed for the stand-alone radiator application. Further a study has to be undertaken to compare cost of heating between a central heating system and a stand-alone system to quantify the difference.

2.5 Scope of work

As discussed in the literature review central heating system has several drawbacks due to high initial cost, thermal losses in the system, lack of control, cost of maintenance and very limited flexibility in terms of control and modularity. A stand-alone radiator will aim to overcome these limitations and provide an effective heating alternative. The new product development techniques discussed in the literature have outlined aspects of new product development process and highlighted the importance of product specification, concept and product architecture. There is a need to modify the generic process to develop a bespoke process for a stand-alone radiator and account for quality assurance process.

The literature published thus far focuses mainly on the macro parameters influencing the performance of radiators in a central heating system. Work carried out, as reported in the literature focuses on improving the performance of radiators by increasing the effective convective and radiative area of the radiators. There is little work done on quantitative evaluation of relationship between flow and temperature distribution and the macro performance parameters. The published literature is focused on central heating system and not directly applicable to stand-alone system. Hence, a key area to focus is experimental investigation of affect of point of fluid entry on flow and thermal performance of a stand-alone heating radiator. Furthermore, the published work does not take into consideration wide range of flow rates and their affect on the pressure drop across the system. These changes have a significant effect on the performance of a standalone system. Evaluation of pressure loss and detailed understanding of flow variables will provide important information to develop a parametric model to predict performance of a standalone system. This work aims to study key parameters within a radiator to get least pressure drop and maximum flow distribution.

Key performance characteristics of the radiator to be evaluated are

1. Effect of point of entry
2. Pressure drop across a radiator
3. Pressure distribution across the radiator
4. Flow distribution

The optimisation work published is limited to a finned tube system and does not account for variation in flow, cold spots and pressure drop. An optimisation model will aim to minimise cost whilst providing adequate heating for a room. Also the literature discussed above is

limited to performance of domestic radiators in a central heating system. The literature thus far does not account for the internal flow characteristics of panel radiators.

2.6 Specific research objectives

1. Develop a bespoke new product development process for stand-alone radiators
2. Identify product design specifications for a new standalone water filled radiators
3. Design and development of a novel stand-alone water filled radiator
4. Performance evaluation of stand-alone water filled radiators
5. To analyse temperature distribution in a stand-alone water filled radiator
6. To analyse the effect of point of entry and flow rate on pressure drop in a radiator
7. To analyse the effect of point of entry and flow rate on pressure distribution in a radiator
8. To formulate the effect of radiator size on pressure drop and pressure distribution in a radiator
9. To formulate the effect of port diameter on pressure drop and pressure distribution in a radiator
10. Development of robust cost model for stand-alone radiators
11. Optimisation of radiator cost and comparative study of stand-alone radiator to a central heating system

3 EXPERIMENTAL AND NUMERICAL SETUP

3.1 Introduction

The aims and the subsequent objectives detailed in chapter 1 require detailed experimental and numerical investigation. A robust experimental methodology is required to investigate the flow in and across the radiator. Like wise detailed CFD based quantitative flow analyses is required to ascertain local performance in a stand-alone radiator. In this chapter details of the experimental and numerical setup have been discussed.

The experiments carried out during the development of the stand-alone radiators have been carried out in accordance with BS EN 442 (1997). The tests are very robust to evaluate heat output of a radiator in a temperature-controlled environment but did not quantify any operational parameters. Experimental evaluation of the performance characteristics of radiators is key for this investigation. As highlighted in the literature review to characterise flow and temperature distribution in a stand lone radiator one has to evaluate the effect of point of entry, operational pressure, flow and temperature.

3.2 Experimental Approach

As shown in Figure 3-1 and Figure 3-2 stand-alone water filled radiators are constructed normally using K2 (double panel) type radiators with the control unit assembled between the two panels. The panels and the construction of the stand-alone water filled radiator are explained in chapter 4. The general construction is the same as standard central heating radiators with the exception of fin configuration and orientation of T joints (detailed in chapter 4). Each stand-alone radiator has a dedicated boiler, pump and control unit. This has a significant influence on the performance of radiators. Stand-alone systems operate at a maximum flow rate of 0.3 m/s, which is significantly lower, compared to a central heating system, which operates between 0.9 to 1.8 m/s. As a result the pressure drops in the system and flow characteristics are very different. Unlike central heating system temperature control on stand-alone system (each radiator) is better. Wards [3], McIntyre [5] and Giesecke [7] have shown that flow rate and temperature have a direct influence on heat output of a radiator in a central heating system. As mentioned above stand-alone radiators have a different range of operational parameters and hence a detailed investigation is warranted to quantify the effect of each parameter. A setup has been designed to help investigate performance with the following variables.

Flow configuration	BBOE, BTOE, TTOE and BTSE
Flow rates	0 lpm to 11 lpm (step of 0.5)
Radiator size	3060 (300 x 600 mm) to 6100 (600 x 1000 mm)
Radiator type	K1 and K2 radiator

Table 3-1 variables for consideration in investigation of radiators

Above variables result in 22 flow rates, 4 flow configurations, and four radiators. To test all combinations of these variables would involve a large experimental program resulting in a total of 352 experiments. A typical run takes an average of 3 hours, equating to 1056 hours of experiments. This approach would be expensive and time consuming.

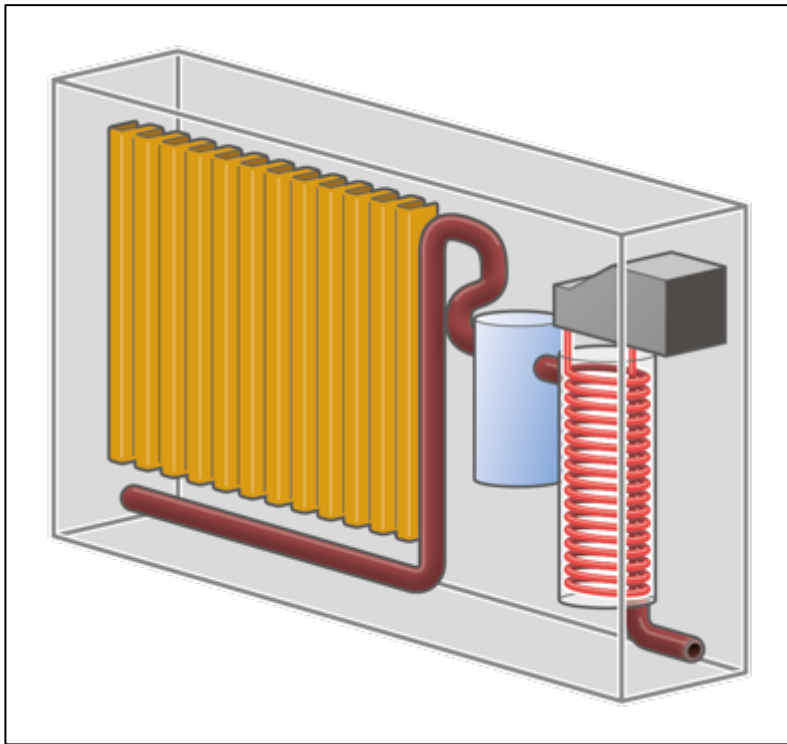


Figure 3-1 Isometric illustrative view of stand-alone water filled radiator



Figure 3-2 Radiator panel configuration [60]

To rationalise the range of parameters an initial set of experiments were carried out to quantify the influence and focus the research in the critical range of parameters.

3.2.1 Initial Experimental setup

Initially a double panel radiator and single panel radiator with a combination of point of fluid entries have been used as a stand-alone system. Both the radiators are 300mm X 600mm [height x length] sourced from a single supplier to eliminate the effect of material grade, profile, end connector size and shape. Table 3-1 shows various parameters that have been measured or computed in the present investigation. Figure 3-3 shows the schematic diagram of the experimental setup. The diagram shows (1) control unit comprising heater element control electronics and a circulating pump. The outlet of the pump is connected to the bottom left of the radiator (4), this point would be referred to as the inlet point and is common for both the

layouts. For the first configuration (BBOE) the outlet of the radiator is at the bottom right of the radiator. Water is filled using the top left entry point. The top right point is fitted with an air bleed valve to ensure the radiator is completely filled with water. For a BTOE system the outlet is at the top right of the radiator with the bleed valve located at the top left. The water is filled at bottom right for BTOE layout. To evaluate the flow performances digital pressure gauges (3) and (5) have been used at inlet and outlet. A needle valve is used to control the flow rate of water in the system. A flow meter (7) is used between the outlet of the pump and the inlet of the radiator to determine the flow rate. To evaluate the thermal performance, K-type thermocouples (2) and (6) have been used to measure the inlet and outlet temperatures of water. The experiments have been conducted in a temperature-controlled environment to ensure maximum thermal load on the system.

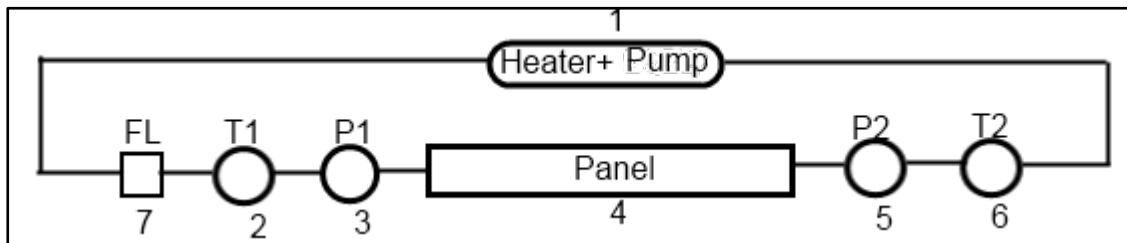


Figure 3-3 Initial Experimental setup

The flow meter and pressure sensors have been connected to the computer via the data logger. The flow is regulated using a needle valve.

For the purpose of these experiments a FLIR S65HSV thermal camera has been used along with ‘ThermaCAM Researcher Pro 2.7’ software. The camera is mounted on a tripod with fixed height and viewing angle to maintain consistency in the results. The tripod is positioned in front of the radiator panel such that the distance between the panel and camera lens is at a fixed distance of 2 m. This distance is recorded in the camera. The emissivity of the radiator paint (RAL 9016) is obtained from the manufacturer and recorded in to the system (0.96). As mentioned the tests have been carried out in a temperature-controlled environment with known emissivity (0.8) of the walls and ensuring that no additional heat sources are present in the room. The camera is set to capture an image every 10 seconds to match the sample rate of the pressure and temperature data logger. Before starting the experiments due care is taken to calibrate and ensure accuracy. Temperature reading near the inlet of the radiator panel has been recorded using a K-Type thermocouple and the camera. The thermocouple have a sensitivity of $41\mu\text{V}/^\circ\text{C}$ and accuracy of $2.2\text{ }^\circ\text{C}$ at 0°C . The position, camera angle and focus have been fine-tuned till the two reading were within 1/1000 of a degree. The images are used

to quantify the radiator surface temperature and help visualize the fluid path. Although care is taken to minimise errors, the accuracy of the thermal imaging system and the thermocouples add to variations from one set of experiments to the other. In order to mitigate this where possible local temperature readings are normalised to the inlet water temperature. Normalised results help eliminate the uncertainty and will not influence the outcome.

Detailed specifications and datasheets of the thermocouple and the camera have been provided in appendix 1.

3.2.2 Test procedure

To start the experiment the rig was setup for the required configuration (BBOE or BTOE). The operating temperature of the radiator was the temperature corresponding to the temperature of water within the heater placed upstream of the inlet of the radiator. This temperature was programmed using a wireless controller provided by the radiator manufacturer. Following steps were carried out to set the temperature of the radiator: -

- a. Press advance and holiday together until new window is visible in the controller.
- b. Scroll down to Surf and press select
- c. Scroll to desire temperature
- d. When press ok Light in the radiator flashes at this point
- e. Press clear
- f. Press boost to operate radiator

For steady state experiments, the system is run for at least 60 mins to allow the flow to stabilise. The data logger software has been set to capture the readings at 50 Hz.

Rationalisation of Flow Configuration

Literature review has suggested that the TBOE (Top Bottom Opposite End) and BBOE (Bottom Bottom Opposite End) are common flow configurations with TBOE layout offering maximum temperature drop across the radiator. Package constraints discussed in chapter 4, have suggested that the only two configurations possible in a stand-alone system are BBOE and BTOE. Hence it is suggested that for the current investigation flow configurations are limited to BBOE and BTOE.

Rationalisation of Flow range

Selection of the pump is discussed in detail in chapter 4 as part of the design and development of a stand-alone radiator. The pump selected for the system has a max flow rate of 11 lpm and

does not have an electronic control for the for flow rate. As stated above, flow is controlled using a needle valve. It has been observed that a quarter turn (90°) of the needle valve corresponds to approximately 1 lpm. In addition during the thermal evaluation of the radiator, the flow rate could not be reduced below 5 lpm, as the fluid around the boiler would start boiling. This resulted in reducing the initial range discussed in Table 3-1 to 6 lpm to 11 lpm with 5 increments.

Rationalisation of Radiator configuration

A stand-alone system is constructed using a K2 (double panel) radiator. Panel configuration from different manufacturers is different. In some the two panels in a K2 system are in series and in some they are in parallel. The one in series would have higher pressure drop compared to the radiators with the panels in parallel. In the stand-alone radiators the panels are in parallel configuration. Previous work from Akin [34] has shown that the flow in the two panels is similar. In order to compare numerical analysis work carried out in CFD with the experimental work, a single panel radiator would offer a lower mesh size and hence reduce the computing time and power. Comparative study between K1- Single panel radiator and K2- Double panel radiator has been undertaken in chapter 5 but for the reasons mentioned, flow investigation has been conducted on a single panel radiator.

Rationalisation of Radiator size

Stand-alone radiators are made in a range of sizes as tabulated in Table 6-1. Experimental investigation is limited to the smallest and the largest radiator. This allows investigation to capture the effect of length and height over the entire range.

By Rationalising the flow configuration, flow rate, and radiator configuration and size, the experimental work has reduced to a manageable size, without compromising the quality and scope of information. The ranges of parameters are tabulated in the following section.

3.2.3 Range of parameters

Flow configuration	BBOE, BTOE
--------------------	------------

Flow rates	6 lpm (litres per minute) to 11 lpm (step of 1)
Radiator size	3060 (300 x 600 mm) and 6100 (600 x 1000 mm)
Radiator type	K1 radiator

Table 3-2 Range of parameters

3.2.4 Experimental setup

In the present investigation a number of studies have been carried out experimentally. For this purpose two standalone radiators have been used with different combinations of radiator panel and point of fluid entries. Figure 3-4 shows the schematic diagram of the experimental setup and shows control unit comprising heater element control electronics and a circulating pump. The outlet of the pump is connected to the bottom left of the radiator; this point would be referred to as the inlet point. For the first configuration (BBOE) the outlet of the radiator is at the bottom right of the radiator. Similarly, for second configuration (BTOE) the outlet is at the top right of the radiator. At each outlet, isolation valve is placed to ensure the radiator can be operated in BBOE and BTOE configuration one at a time.

The water is filled using the bottom left entry point. The top left point is fitted with an air bleed valve to ensure the radiator is completely filled with water.

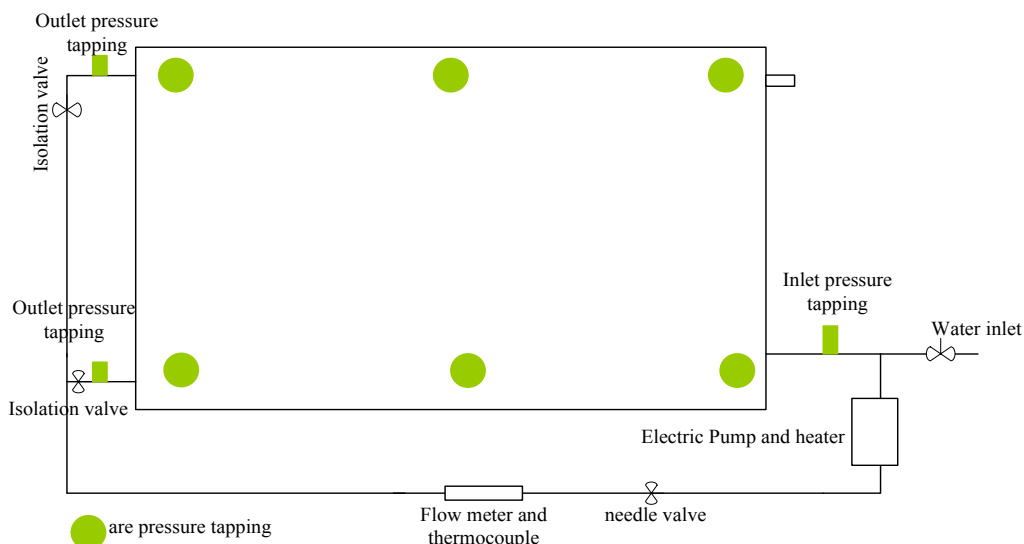


Figure 3-4 Front View of experimental setup

Pressure gauges are placed at inlet, outlet and at six different position in the radiator to evaluate the pressure drop at the corresponding points. A needle valve is used to control the flow rate of water in the system. A flow meter is placed between the outlet of the radiator and the inlet of

the radiator to determine the flow rate. A 16 channel ‘MC DAQ’ is used to log the information at the sampling rate of 50Hz. For each flow rate and the data has been logged for 10 minutes. Results from the experimental work have been discussed in detail in chapter 5.

3.3 Numerical setup

The numerical investigation of this study has been undertaken using Computational Fluid Dynamics (CFD) based tools that uses complex algorithms and iteratively solves the numerical equations governing the fluid flow in systems dictated by specified boundary conditions.

This section will focus and elaborate on the working principles of using CFD; the governing equations relative to this project; pre-processing involving the geometry and meshing of the radiator designs; and the solver execution stating the boundary conditions and numerical parameters setup for the models.

CFD Codes: -

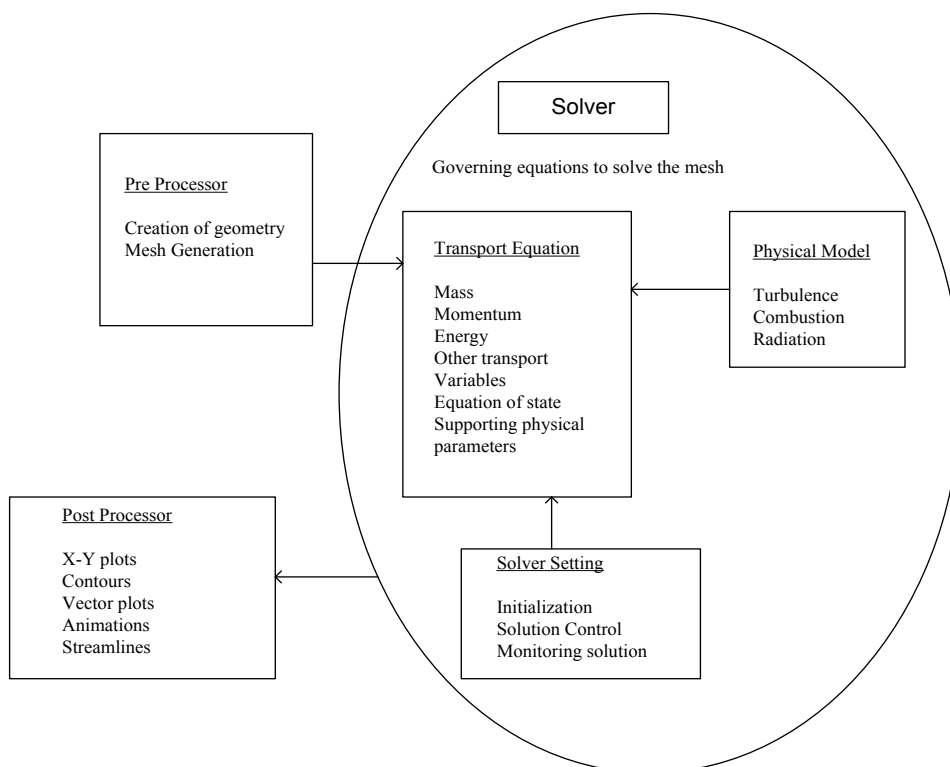


Figure 3-5 Overview of CFD model

CFD codes are structured around a robust numerical algorithm that can tackle fluid-flow problems. A user-friendly graphical user interface (GUI) applications and environments are used to input the problem parameters and examine the computed results. The codes provide

complete CFD analysis, comprises of three main elements, (i) a pre-processor, (ii) a solver and (iii) a post-processor. The functions of these elements are briefly explained in the next paragraphs. Figure 3-5 presents a framework that illustrates the interconnectivity of the three aforementioned elements within the CFD elements.

The pre-processing consists of the input of a flow problem to a CFD program by means of an operator friendly interface and the subsequent transformations of this input into a form suitable for the use by the solver. The user activities at the pre-processing stage involve the definition of the geometry of the region of interest, grid generation – the sub-division of the domain into a number of smaller, non-overlapping sub-domains known as grid or mesh of cells and selection of physical and chemical phenomena that need to be modelled. The stage also includes specifications of fluid properties and definition of appropriate boundary conditions at cells that coincide with or touch the domain boundary.

The solver primarily consists of setting up the numerical model and the computation/monitoring of the solution. The setting up of the numerical model includes the following:

- Selection of appropriate physical models - turbulence, combustion, multiphase or radiation etc.
- Defining material properties like the fluid, solid, mixture etc.
- Prescribing operating conditions
- Prescribing boundary conditions
- Prescribing solver setting
- Prescribing initial solution
- Setting up convergence monitors

The computation of the solution includes:

1. The discretised conservation equations are solved iteratively. A number of iterations are required to reach a converged solution.
2. Convergence is reached when a change in solution variables from the first iteration to the next is negligible. Residuals provide a mechanism to help monitor this trend.
3. The accuracy of the converged solution is dependent upon problem setup, grid resolution, grid independence, appropriateness and accuracy of the physical model.

Post processing comprises the examination of the results obtained and revision of the model based on these results. The results can be viewed as contours, vector plots or specific values at specific region.

3.3.1 Governing equations of fluid

The CFD tools are based on the fundamental governing equations of fluid dynamics – the continuity, momentum and energy equations. They are the mathematical statements of three fundamental physical principles upon which the fluid dynamics is based:

- Mass is conserved.
- Newton's second law, $F = ma$.
- Energy is conserved.

There are various ways that the aforementioned governing principles can be applied to a fluid, including the system approach and the control volume approach. By definition, a system is a collection of matter of fixed identity (same fluid particles), which may move, flow, and interact with its surroundings. A control volume, on the other hand, is a volume in space independent of mass through which fluid may flow.

3.3.2 Mass Conservation in 3D

The first step in the derivation of the mass conservation equation is to write down a mass balance equation for the fluid element [35]:

$$\begin{array}{l} \text{Rate of increase of mass in fluid} \\ \text{element} \end{array} = \begin{array}{l} \text{Net rate of flow of mass into} \\ \text{fluid element} \end{array}$$

For liquids, as the density is constant, the mass conservation equation is:

$$\text{Div } \mathbf{u} = 0$$

This equation describes the net flow of mass out of the element across its boundaries. The above equation in longhand notation can be written as:

$$\frac{\partial u}{\partial x} + \frac{\partial v}{\partial y} + \frac{\partial w}{\partial z} = 0$$

3.3.3 Momentum Equations in 3D

Newton's second law states that the rate of change of momentum of a fluid particle equals the sum of the forces on the particle:

$$\begin{array}{l} \text{Rate of increase of Momentum of} \\ \text{fluid particle} \end{array} = \begin{array}{l} \text{Sum of flow of forces on fluid} \\ \text{particle} \end{array}$$

There are two types of forces on fluid particles. These are surface forces and the body forces. Surface forces include pressure, viscous and gravity forces while body forces include centrifugal and electromagnetic forces. It is a common practice to highlight the contributions due to the surface forces as separate terms in the momentum equations and to include the effects of body forces as source terms.

The x-component [54] of the momentum equation is found by setting the rate of change of x- momentum of the fluid particle equal to the total force in the x – direction on the element due to surface stresses, plus the rate of increase of x – momentum due to sources.

$$\rho \frac{Du}{Dt} = \frac{\partial(-p + \tau_{xx})}{\partial x} + \frac{\partial\tau_{yx}}{\partial y} + \frac{\partial\tau_{zx}}{\partial z} + S_{Mx}$$

Similarly y and z – component of momentum equation are given by:

$$\rho \frac{Dv}{Dt} = \frac{\partial\tau_{xy}}{\partial x} + \frac{\partial(-p + \tau_{yy})}{\partial y} + \frac{\partial\tau_{zy}}{\partial z} + S_{My}$$

$$\rho \frac{Dw}{Dt} = \frac{\partial\tau_{xz}}{\partial x} + \frac{\partial\tau_{yz}}{\partial y} + \frac{\partial(-p + \tau_{zz})}{\partial z} + S_{Mz}$$

The sign associated with pressure is opposite to that associated with normal viscous stresses, because the usual sign convention takes a tensile stress to be positive normal stress so that the pressure, which is by definition a compressive normal force, has a minus sign with it. The effects of surface stresses are accounted for explicitly; source terms S_{Mx} , S_{My} and S_{Mz} in above equations include contributions due to body forces only.

3.3.4 Energy Equation in 3D

The energy equation is derived from the first law of thermodynamics, which stated that the rate of change of energy of a fluid particle is equal to the rate of heat addition to the fluid particle plus the rate of work done on the particle:

$$\begin{array}{l} \text{Rate of increase} \\ \text{of energy of fluid} \\ \text{particle} \end{array} = \begin{array}{l} \text{Net rate of} \\ \text{heat added to} \\ \text{fluid particle} \end{array} + \begin{array}{l} \text{Net rate of} \\ \text{work done on} \\ \text{fluid particle} \end{array}$$

Conservation of energy of the fluid particle is ensured by equating the rate of change of energy of the fluid particle to the sum of the net rate of work done on the fluid particle, the net rate of heat addition to the fluid and the rate of increase of energy due to sources. The energy equation is (Versteeg and Malalasekera 2007) [53]

$$\begin{aligned} \rho \frac{DE}{Dt} = & -\text{div}(pu) \\ & + \left[\frac{\partial(u\tau_{xx})}{\partial x} + \frac{\partial(u\tau_{yx})}{\partial y} + \frac{\partial(u\tau_{zx})}{\partial z} + \frac{\partial(v\tau_{xy})}{\partial x} + \frac{\partial(v\tau_{yy})}{\partial y} + \frac{\partial(v\tau_{zy})}{\partial z} \right. \\ & \left. + \frac{\partial(w\tau_{xz})}{\partial x} + \frac{\partial(w\tau_{yz})}{\partial y} + \frac{\partial(w\tau_{zz})}{\partial z} \right] + \text{div}(k \text{ grad } T) + S_E \end{aligned}$$

3.3.5 Pre- Processing

This section provides the details of the numerical modelling that has been used in the present study. The CFD package that has been used in this study is ANSYS Workbench [55]. The pre-processing is categorised into two sub-sections: (i) creation of geometry and (ii) creation of meshing. This section provides the details of geometric modelling and the meshing of the radiator in question.

3.3.5.1 Geometry

Three-dimensional geometry of the radiator has been numerically modelled in ANSYS work bench. Geometry consists of two zones, fluid zone and solid zone.

Fluid zone is a three dimensional geometry where the water flow occurs within the radiator as shown in Figure 3-6. Length and width of the radiator is 600mm and 300 mm respectively. Inlet of the radiator was placed at the bottom of the right corner of the radiator while outlet was placed at the top and bottom of the left side of the radiator to simulate BTOE and BBOE configuration. Both, inlet and outlet are made 6 mm. As shown in the figure radiator consists of two rows and 18 columns. Each row is of 25 mm and columns are 10 mm. Geometry for the computational model was developed to represent physical parts. Each feature, component and system was measured for reference. Internal flow surface was measured under an infinite focus microscope (IFM) giving accurate surface roughness to be incorporated in the computational model.

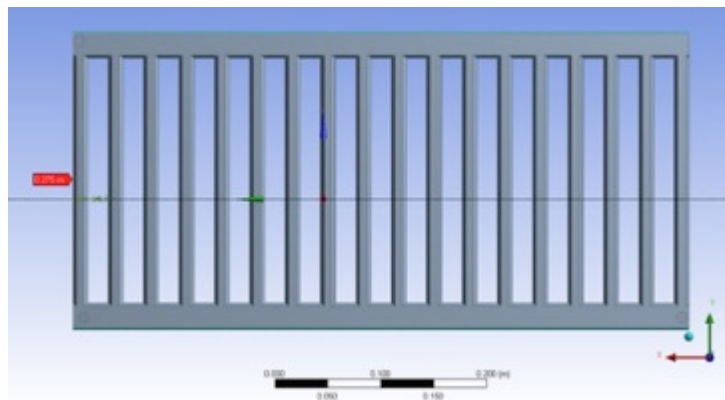


Figure 3-6 Geometry for CFD model

3.3.5.2 Meshing

To analyse the modelled radiator in the FLUENT® solver, it requires creating a mesh structure. The mesh structure specifies the resolution at which FLUENT® analyses the model. This section provides details of the meshing parameters used for this simulation.

Min mesh size	0.008 mm
Max mesh size	2 mm
Use automatic inflation	Program controlled
Inflation option	First layer thickness
First layer height	0.1 mm
Max layer	5
Growth rate	1.2
Mesh Element	1999680

Table 3-3 Meshing parameters for CFD model

Table 3-3 depicts the mesh condition the maximum mesh size is 2mm, the minimum mesh size is .008 mm. in order to make sure that the mesh is distributed symmetrically automatic inflation with the program controlled has been used with first layer thickness of .5mm and maximum layer of 5. The mesh element was 1999680 with growth rate of 1.2. Figure 3-7 shows the mesh generated with the above specification.

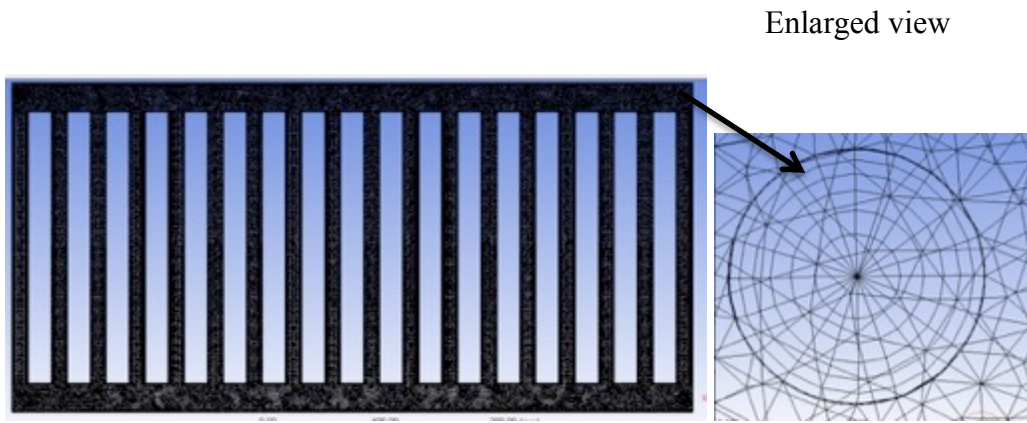


Figure 3-7 Mesh model for 3060 radiator

Three meshes have been chosen for Mesh Independence Test. The first mesh has 1 million mesh elements whereas the second mesh has 3 million mesh elements and the third mesh has 5 million elements. The results for the Mesh Independence testing are discussed in section 3.3.9.

3.3.6 Solver Setting

The solver used in the present study is called FLUENT, which is an integral part of CFD package ANSYS 15. The analysis has been carried out in steady state, with working fluid water.

Selection of Model: -

Since the compressibility of the flow within the radiator can be neglected, a pressure-based solver has been nominated for the flow diagnosis within the radiator. In this model, the density of the fluid remains constant and the primary fluid flow parameter that is being solved iteratively is the pressure within the flow domain.

In addition to the aforementioned settings, there is a need to model the turbulence in the flow as well. This is because the investigations carried out in the present study focuses on the turbulent flow in the pipelines within the radiator. The criteria for internal flows to be turbulent is that the Reynolds number of the flow should be higher than 4000. Furthermore, in practise the velocity of the flow normally ranges from 0.6m/sec to 2m/sec. These velocities correspond to Reynolds number of 6500 to 22000 for the radiator under consideration. Hence, the flow is turbulent in the radiator and a turbulence model is required to predict the parameters of turbulence in the pipeline with reasonable accuracy. Standard turbulent model K- ϵ has been implemented for this analysis.

In the present study, the investigations have been carried out in a radiator with the working fluid as water. The properties of water within the radiator have been defined as liquid-water with a density of 998.2Kg/m^3 and dynamic viscosity of 0.001003Kg/m-sec .

Following Boundary conditions have been implemented in this study.

A) Inlet Boundary conditions

1. Mass flow inlet of 0.012 kg/s
2. Turbulent intensity 5%
3. Hydraulic diameter $.006\text{m}$ (calculated based on measurement of inlet and outlet port diameter)

B) Outlet Boundary conditions

1. Pressure outlet of 0 Gauge Pa
2. Turbulent intensity 5%
3. Hydraulic diameter $.006\text{m}$ (calculated based on measurement of inlet and outlet port diameter)

C) Wall Boundary conditions

1. Stationary wall
2. Wall roughness 0.00007 (measured from a radiator sample details in appendix)

Convergence Criteria: -

Getting to a converged solution is often necessary. A converged solution indicates that the solution has reached a stable state and the variations in the flow parameters, with respect to the iterative process of the solver, have concluded. Hence, only a converged solution can be treated as one that predicts the solution of the flow problem with reasonable accuracy.

The default convergence criterion for the continuity, velocities in three dimensions and the turbulence parameters in ANSYS 15 is 0.001 . This means that when the change in the continuity, velocities and turbulence parameters drops down to the fourth place after decimal, the solution is treated as a converged solution. However, in many practical applications, the default criterion does not necessarily indicate that the changes in the solution parameters have died out. Hence, it is often better to monitor the convergence rather than relying on the default convergence criteria.

In the present study, static pressure on the inlet and outlet faces of the Test section has been monitored throughout the iterative process. The solution has been considered converged once the static pressure at both these faces has become stable. Here a stable solution can be either one in which the pressure fluctuations have died out completely or have become cyclic having same amplitude in each cycle.

After numerically simulating the flow of radiator, various results have been gathered from CFD tool. Detailed discussions on these results are presented in chapter 6.

3.3.7 Mesh independent analysis

As discussed earlier, three different meshes with one million, 3 million and 5 million mesh elements have been chosen for mesh independence testing. The results obtained, shown in Table 3-4, depict that the difference in the pressure drop between 1 million and 3 million is 8.6% and between 3 and 5 million is 0.0002%. It can therefore be concluded that the mesh with three million elements is capable of accurately predicting the flow features and hence has been chosen for further analysis of radiator in question.

Mesh Size	Pressure drop across radiator (PA)	% variation 1 million to 3million	% variation 3 million to 5 million
1million	1061914.00	8.6622	0.0002
3million	109904.25		
5million	109882.02		

Table 3-4 Mesh independence - pressure criterion

3.3.8 Post processing

Numerical simulations have been processed in Microsoft Excel and ANSYS. As shown the CFD model is setup with a velocity inlet and a pressure outlet. Primary reference planes have been created to capture X, Y and Z velocity profile. XY plane also helps visualise the velocity vector and magnitude across the radiator. A further reference plane has been developed to in XZ plane across the mid height of the radiator to review the velocity in individual vertical channels of the radiator.

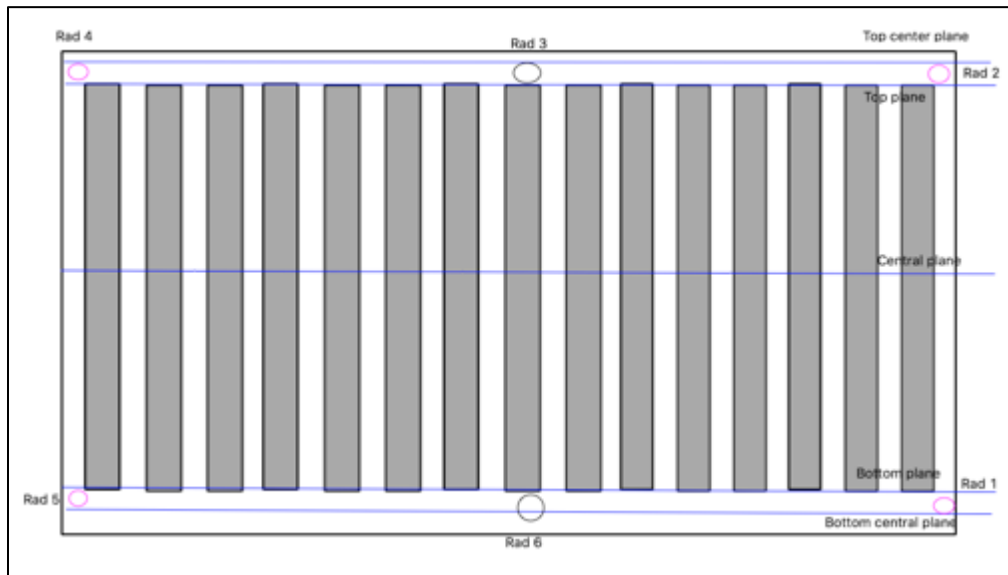


Figure 3-8 Reference planes in CFD model

Numerical analysis carried out based on the above setup have been discussed in detail in chapter 6.

3.3.9 Summary

Experimental and numerical setups have been discussed, in this chapter .The experimental set up has been used to evaluate global pressure loss, pressure distribution and temperature distribution over a range of flow velocities, which will be discussed in chapter 5. The numerical setup has been used to evaluate global as well as local flow parameters in chapter 6.

4 DEVELOPMENT OF A NOVEL STAND-ALONE WATER FILLED RADIATOR

It has been discussed in Chapter 1 that space heating in domestic built environment is a significant contributor towards carbon emissions and improving efficiency of heating systems and building structures alike is significantly important to reduce the demand on energy resources. Literature review in chapter 2 has shown a significant amount of work that is directed towards improving thermal performance of buildings by using modern insulation materials and techniques. Review of developments in heating systems over the past decade has shown that central heating is the most widely used system for domestic heating but the system comes at high installation cost, is difficult to control and offers no flexibility. This has presented an opportunity to develop a system, which overcomes these shortcomings whilst improving effectiveness and thermal comfort over existing stand-alone systems in the market. The literature on existing new product development process is exhaustive but needs significant adaptation to be used for stand-alone radiator development process. In this chapter development of a bespoke product development process that is customised for stand-alone radiators is presented. Further the application of the process to deliver stand-alone water filled radiator has also been included, which would ensure the product has significant innovation whilst providing commercial success.

Stand-alone water filled radiator system was developed as part of a collaborative work between UoH (university of Huddersfield) and a local company. The project proposal was to develop an innovative new stand-alone radiator and launch it in shortest possible time.

4.1 Bespoke product development process

As discussed in chapter 2 at present there are a few designs for stand-alone radiators but none of them are water based. Limited reference for water based stand-alone systems meant that a new product had to be developed. As stated in [24] a new product development refers to original product, product modifications, product improvements and brands developed from research and development. The proposed, water filled stand-alone radiators aims to provide all the flexibility and controllability of a stand-alone system combined with comfort and effectiveness of a central heating system. NPD (New Product Development) has been regarded as effective ways to deal with competitive environment, in order to integrate knowledge, accelerate the process of product innovation to improve profitability.

4.1.1 Overview of existing product development process

This section provides an overview of the existing NPD (new product development) models/process. A critical review of these processes in light of constraints for stand-alone radiator development is carried out where weakness of these processes is highlighted. The NPD process [24] discussed in chapter 2 outlines a framework and details 3 product development process flows.

- 1) Generic product development process
- 2) Spiral development process and
- 3) Complex development process

4.1.1.1 Generic product development process

This process is used to develop products when there is a market demand and technology available to fulfil the demand. It is process and platform intensive, where the product is customised as per changing market requirements. Due to the high-risk nature of the product and unique requirements of the market this process is sequential. As it can be seen in Figure 4-1 each phase is followed by a review/milestone to confirm product and project feasibility.

Detailed planning is required to establish the market demands, assess the capabilities of the company undertaking the task, and establish a fairly robust product specification before major financial and resource commitment. The plan along with a sound business case is reviewed in the mission approval milestone before progressing to concept development. Single concept, compatible with the product specification is developed. In this stage parameters that influence the product performance are identified and established. At the end of the concept phase concept review is conducted. If the concept is not approved the process is repeated. System level design is carried out on the approved concept. In this stage, all aspects of the product delivery (e.g. design, finance, manufacturing and marketing) form a cross-functional team to develop the product. System level design outlines the specifications for the sub-systems and components for detail design. Preliminary design review milestone reviews the product against the target and the project against the business plan. Further investment and commitment to the project is made at this milestone.

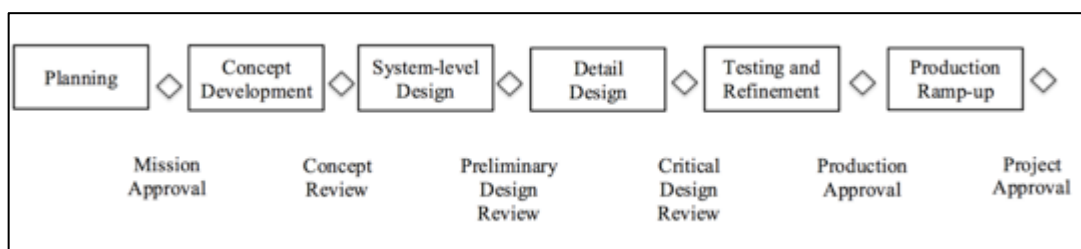


Figure 4-1 Generic product development process [24]

On approval detail design is carried out on the product before it is presented for critical design review. Approved design is tested to meet product specification and concerns identified in the testing phase are addressed by the design modifications. Testing the product late in the development phase can significantly impact project timing and have a financial impact, increasing overall risk. A successful testing would ensure production approval, which would lead to production ramp-up.

In summary a Generic product development process will deliver a robust product but would require long development time and cost due to the sequential stage-block process. This process is not suitable for products where design, development, validation and launch have to be carried out in very short time.

4.1.1.2 Spiral product development process

Spiral product development process is suitable for products that require quick launch and are very time sensitive. These are mostly suitable for products that are modifications of existing products or next generation of the products already in market. As it can be seen in Figure 4-2, the early stages in spiral development process are similar to the generic process where planning, concept development and system level design are carried out in a sequential manner. As the products are iterations or upgrades of the existing products, the preliminary stages are relatively shorter compared to the generic process. After the first three stages, instead of a preliminary design review a cycle plan review is conducted to ascertain the product position and targeted to the market. Hence unlike a generic process in this process there is a market push and minimal technology advancement.

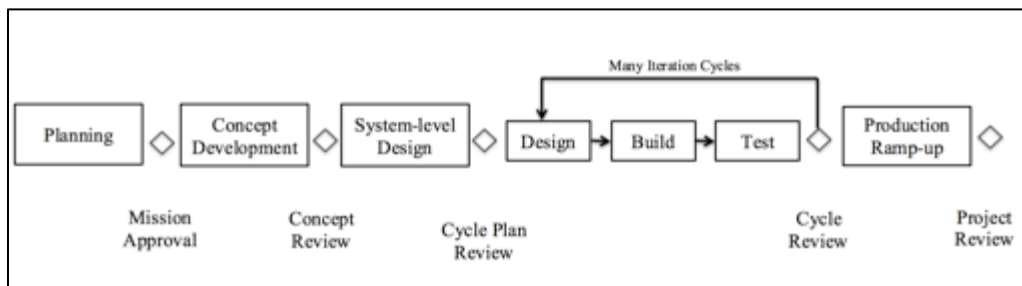


Figure 4-2 Spiral product development process

Upon defining the market position, an iterative cycle comprising of design, build and testing is undertaken to develop a product suitable for the target market identified in mission approval and cycle plan review. In a cycle review milestone “design-build-test” iteration is reviewed to progress into production ramp-up. Once a suitable product is developed, production ramp-up is initiated.

In summary a Spiral product development process is suitable for quick-build products where design-build-test activities are repeated in relatively less time. Nevertheless multiple iterations can be expensive and not suitable for products where system, components and testing cost are very high. Additionally this process does not analyse the sub-systems/ components individually, which can be a significant issue in case of radiator development.

4.1.1.3 Complex system development process

This process is used to develop large-scale products such as automobiles and airplanes, where the complexity is very high with multiple system interactions. This process is a modification of the Generic process and addresses system level issues. It is process and platform intensive, where the product has multiple variants. Due to high complexity nature of the product system level design phase becomes critical. As it can be seen in Figure 4-3 first two stages are similar to generic product development process.

Due to significantly complex systems, large investment cost and long development and testing, in this process there is huge emphasis on detailed planning. It is required to establish the market demands, and establish a robust product specification before major financial and resource commitment. A detailed plan along with a sound business case including, product specification, manufacturing concept, launch timing and market forecast is reviewed in the mission approval milestone before progressing to concept development. Concept development phase considers the architecture of the entire system. Unlike generic product development process, development of multiple architectures is encouraged in the concept phase. A few concepts are developed in parallel that are compatible with the product specification. In this stage global parameters that influence the product performance are identified and established as constraints.

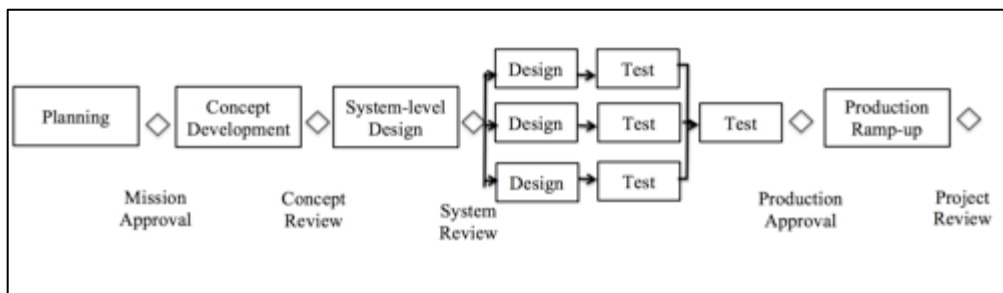


Figure 4-3 Complex system development process

At the end of the concept phase various concepts are reviewed and one selected to be developed further. System level design is critical in the complex product development process, where detailed development is carried out on sub-system and component. This activity is done in parallel using cross-functional teams to address product, process and quality aspects of the system. System review milestone reviews the product against the target and the project against the business plan.

Detail design and test on all the sub-system and components is carried out in parallel to reduce the development time. This approach heavily relies on good integration across all

aspects of the product and requires dedicated resource for product and project management. A successful testing would ensure production approval, which would lead to production ramp-up.

In summary a Complex product development process is designed to deliver a robust and complex product but would require long development time and large resource. This can increase the development cost and will not be suitable for products where finances and resource are limited.

4.1.1.4 Summary of stage based NPD process

Stage based process analysed thus far offer a very methodical process but need considerable modifications when used in practice. The NPD process parameters change significantly depending on the product and manufacturing process being developed. Another key aspect that influences the NPD process is the overall capabilities, strength and weakness of the organisation leading the activity. The process is also heavily influenced by management control, which can reduce the progress, be over prescriptive and the decision making may not always be objective.

Another criticism of the standard process is that the process is mainly sequential and offers little flexibility to overlap stages. The decisions are focused around the milestones deliverables, which are set upfront in the NPD process which are not compatible with actual dynamic processes in small and mid scale manufacturing environment that heavily influence the product definition. This approach makes it difficult to manage with the staged approach.

These processes also need to take into account the functionality; modularity and flexibility aspects of product usage that may result in wider market reach and better return of investment for the company.

4.1.2 Development of a bespoke product development process for stand-alone radiator system

In the previous section stage-based NPD processes have been critically analysed. In the absence of a product development process that can be applied to stand-alone radiator system with the constraints of the organisation a bespoke product development process has to be developed.

4.1.2.1 Constraints for the new development process for stand-alone radiator

In order to develop a bespoke development process, it is important to understand the constraints of the organisation, product attributes, variants and timing.

Due to the limited size of the organisation limited manpower was allocated to the project. As discussed in previous section available time for the project was limited. There are significant financial constraints, which limited the ability to test multiple concepts. Radiators are manufactured and sold in a wide range of sizes, which have different heat outputs. This increases manufacturing complexity and possibility of assembly errors in the production process. Existing manufacturing processes is labour intensive that leads to reduced production and loss in revenue. Furthermore, warranty issues with the existing product impact customer perception and expensive repairs.

It is envisaged that the new product improves functionality, reduces complexity, has lean manufacturing process and addresses warranty concerns by introducing quality assurance process with the constraints discussed earlier.

Any individual stage-based process discussed earlier does not provide solution with the constraints for the stand-alone radiator.

4.1.2.2 Development process framework for stand-alone radiator

A framework has to be established for the process that will address the constraints discussed in previous section. Mitigation actions for the constraints and modification to the above process have been carried out in this section.

Due to availability of two design of water filled stand-alone radiator, one would be inclined to think that a spiral product development system would a logical option. Nevertheless, the concerns highlighted regarding, design complexity of the two radiators, manufacturing issues and quality concerns leading to warranty claims, warrant a need to approach the design of the stand-alone radiator as a new product and revisit market requirements, product concept and possibly develop a common platform architecture with modularity at sub-system and component level.

A complex system is suitable for large-scale products that are customised for individual applications. Emphasis on a robust concept phase can provide a stable platform for design and development and in addition parallel design and test regime proposed in this process is very beneficial for simultaneous development of sub-systems and components. Nevertheless the complex process is inherently, time intensive and expensive due to significant design and testing done downstream of the system level design. A failure at later stages of the development process can lead to wasted effort and delay in product launch.

With these arguments, it is logical to approach the development of stand-alone by modifying the three staged processes to deliver a bespoke process. As an outline the new process requires a detailed product ideation phase followed by a robust concept phase that incorporates product attributes, testing requirements and manufacturing feasibility. In order to minimise failures further downstream in the process a concept-virtual validation activity is suggested. This is similar to the design-test activity in critical product development process but carried out ahead of detail system design. Virtual validation process eliminates the need of expensive physical test and using engineering tools like DFMEA highlights any concerns in the concept.

Upon completion of the concept phase the new process, introduces concept maturation and detail design phase. It is important to have an overlap the two to reduce the resource allocation. In the stage multiple sub-systems are matured, designed and validated. As discussed in the previous section, a significant challenge with stand-alone radiators is to reduce complexity and increase modularity. Staged development processes reviewed in 4.1.1 do not offer any functionality to address this. Hence it is envisaged that the

reconfigurable manufacturing system (RMS) proposed by Mesa [34] is incorporated in the bespoke development process for stand-alone radiators

It is also proposed that virtual and physical performance validation and manufacturing assessments are carried out in parallel. This will allow a simultaneous product, process and performance development. Use of advanced engineering validation tools would also help identify potential quality issues in both product and process. A quality assurance stage is also incorporated in the process to control product, manufacturing process and performance quality. This stage is overlapping with the product testing and manufacturing trials to optimise the overall development time of the product. Addition of the quality assurance stage will enable design of quality checkpoints throughout the product manufacturing and delivery phase. This is followed by launch preparation and to ensure production processes are operating to the expected quality standard and production rates. Lastly the product is launched with upon successful completion of the development process.

4.1.2.3 Bespoke new product development process

Based on the above discussion a bespoke new product development process for stand-alone radiators is shown in figure 4-4. The new process has incorporated stages and activities from a generic and complex product development process.

Similar to the staged processes, the new process also has a planning stage, but additional inputs from benchmarking of existing products and competitive set is taken along with market research.

Unlike the concept stage in generic and complex process the concept stage in the new process has multiple parallel activities to develop system and sub-system level concepts line with product specification and each concept is virtually validated to eliminate design and quality concerns down stream. This enables delivery of a very robust concept phase.

After the concept phase the new process is significantly different to the three staged processes as it has concept maturation and detail design combined in one stage to reduce development time and operate with lower resource. The concept of sub-systems and components are segregated into three functions. The functions are hydraulic, mechanical and system. Hydraulic activity matures the concept of the pump and fluid circuit and develops individual components. Similarly, mechanical concept and design activity matures the development of systems like radiator, heater and exterior panels. System level activity integrates the two with inputs from performance validation and manufacturing validation. It

is important to note that unlike any of the staged processes, there is significant overlap between stages and parallel stages to optimise time and cost. In this stage RMS (reconfigurable manufacturing system) is also incorporated to methodically reduce complexity and improve manufacturability based on a common platform.

An additional stage is introduced to review quality of product design, manufacturing process and product performance. This delivers a robust development process. This is followed by a dedicated stage to launch preparation where focus is on achieving design and production intent quality and production volume. This is a very important stage for products where the production process is labour intensive that can lead to quality issues. Launch preparation is followed by production ramp-up.

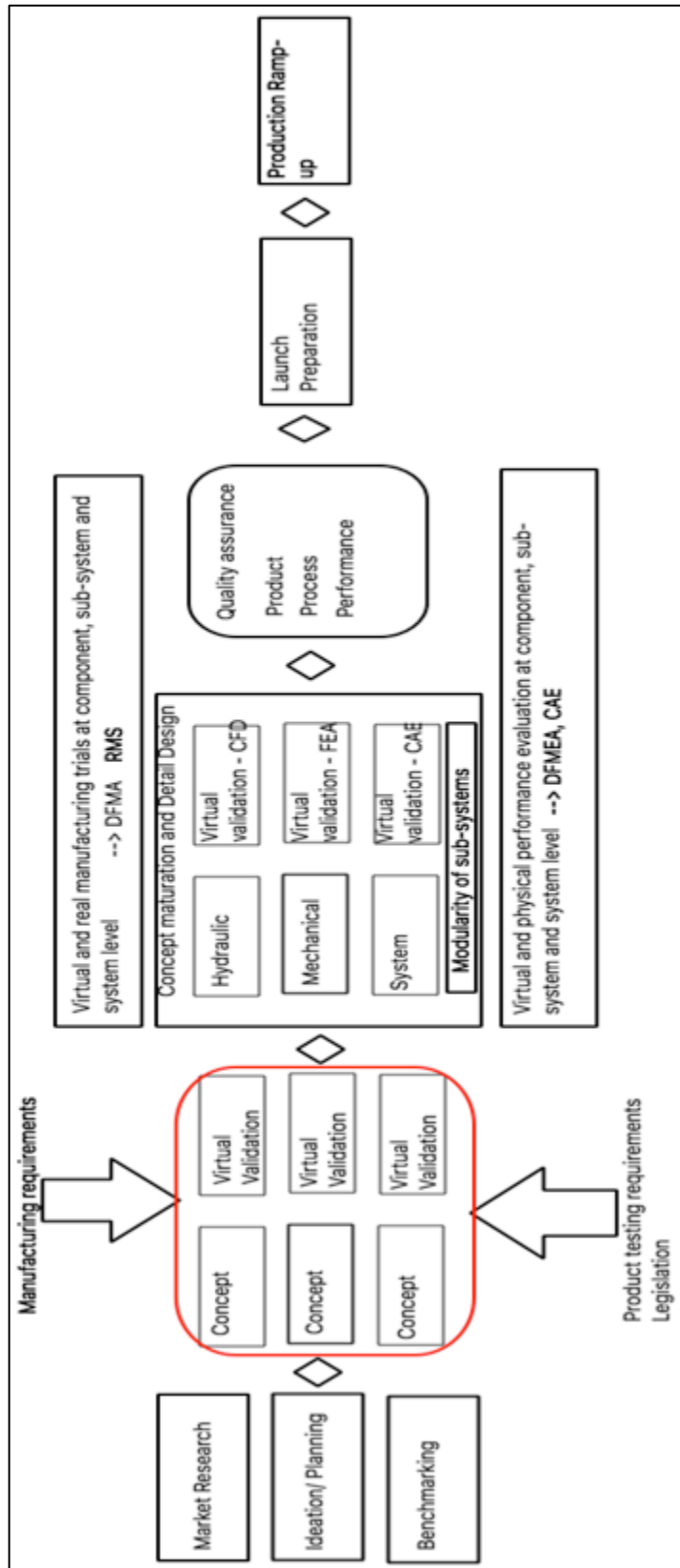


Figure 4-4 Bespoke new product development process for stand-alone system

Figure4-5 illustrates flow and interconnectivity envisaged in the bespoke new product development process for stand-alone radiator. In this it can be seen that the process is very complex with multiple stages and activities running in parallel. Large circles represent the key stages and the smaller circles represent the activities that feed into the main stage. Interconnectivity of each of these main stages and some sub-activities is key to achieve a robust product. The block diagram shown in figure 4-4 does not easily allow incorporation of some key sub stages and activities. It is worth noting that affective sourcing with competitive and cost effective supplier base is key for a stand-alone system. This helps reduce development time by sourcing off the shelf components with validated test and performance criterion to deliver system and product level requirements.

Although best efforts are made to deliver a high quality and cost effective product, in some instances there is scope to improve cost, quality or both. Hence it can be said that product development does not stop at product ramp-up or launch. It is important to incorporate TVM (total value management) engineering to enable continuous improvements. This process enables critically evaluate the developed products and find opportunities to improve quality, reduce cost to increase profitability or reduce cost of ownership for the end customer by improving the design.

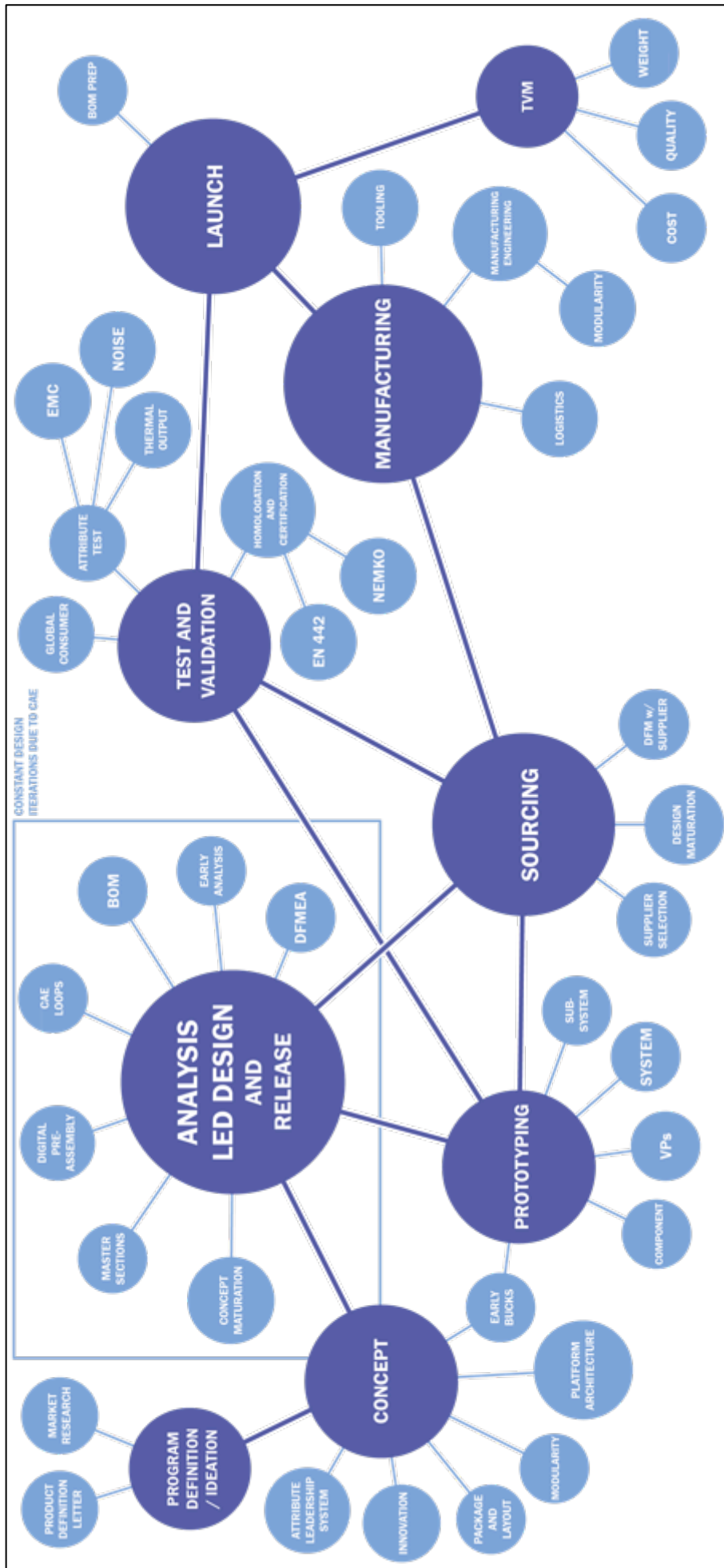


Figure 4-5 Illustration of the bespoke product development process for stand-alone radiators

4.1.3 Summary of bespoke product development process

Figure 4-4 and figure 4-5 show a bespoke new product development approach that combines approach of existing staged product development process and commercial demands to the organisation to industrialise novel water filled stand-alone radiator. It can be seen that a number of activities have to be undertaken simultaneously to successfully launch a product. Key activities are concept, analysis led design, prototyping, test and validation, manufacturing and launch. The approach also highlights the organic nature of new product development for a stand-alone radiator, where some of the supporting activities are interlinked and influence the outcome of the following activity. This bespoke process will be deployed to the design and development of the product, manufacturing process to deliver the product and last but not the least to critically evaluate the product design to identify opportunities to optimise the cost of ownership.

4.2 Concept Development of a stand-alone radiator

As discussed in the bespoke product development process in 4.1.2, for a successful product development a robust concept phase is key, as it helps define the strategy, design parameters, market position, timing, costs and manufacturing methodology. Concept development is comprised of project ideation, product definition, market review, product attributes/parameters, benchmarking, features list and innovation, product architecture and layout, early product feasibility and business analysis

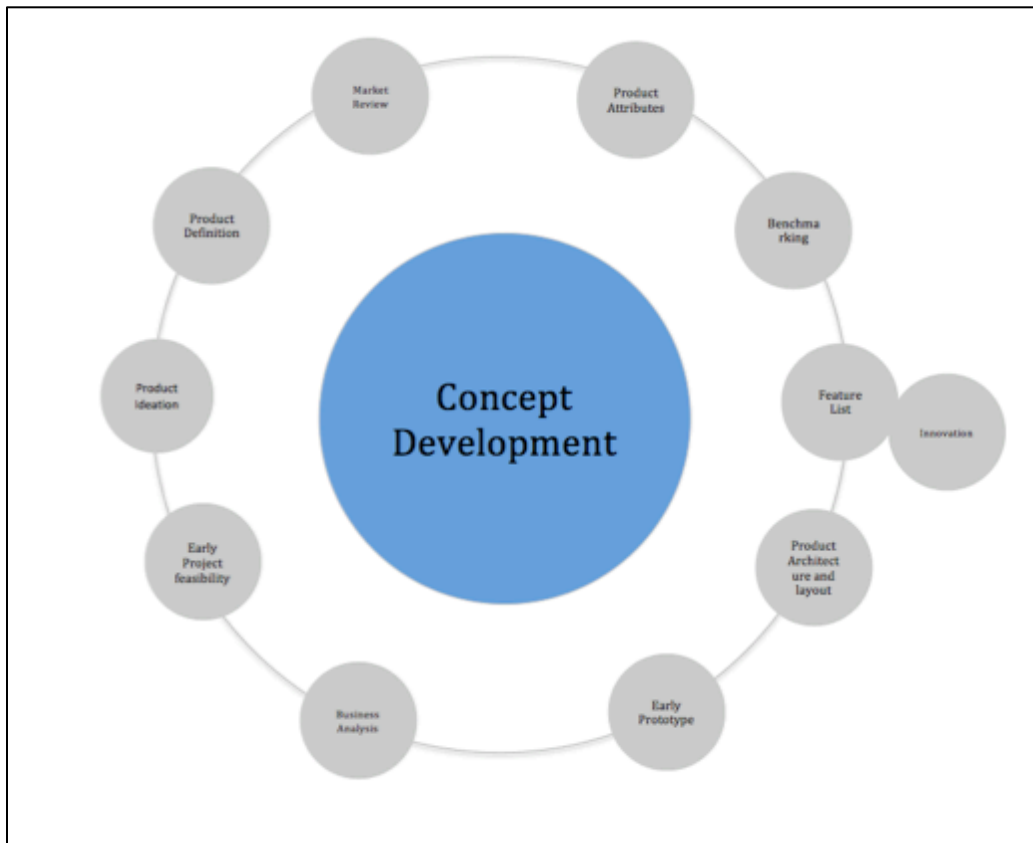


Figure 4-6 Concept Development

4.2.1 Project Ideation

Project ideation starts with basic internal and external SWOT (Strength Weakness, Opportunity and Threat) analysis to identify the scope of the product, define expected performance of the product and capture that in a product definition letter. SWOT analysis for stand-alone heating systems is shown in Table 4-1.

	<i>Helpful</i>	<i>Harmful</i>
Internal	<p>Strengths</p> <ul style="list-style-type: none"> • Knowledge of key components like heating elements and pumps • Wide supplier base including low cost countries • Infrastructure (factory space and equipment) is secure • Government sponsored project • Research based robust product 	<p>Weakness</p> <ul style="list-style-type: none"> • Never developed heating system for domestic application • Knowledge of legal and performance requirement not known • If dedicated design and development team not available • If development process does not meet time scales government funding will lapse
External	<p>Opportunities</p> <ul style="list-style-type: none"> • Demand for stand-alone heating systems for new builds and extensions is high • No competition in the UK – no water filled systems • Low installation cost • Potential to partner with new home builder • Potential to export the product • Water filled radiator gives comfort of central heating and flexibility of stand alone system 	<p>Threats</p> <ul style="list-style-type: none"> • If product is not developed within given timescales there would be competition • If the product is not protected (by copyright/ patents) similar products manufactured in low cost countries can offer the product at lower costs • As the product is new, product certification and approval is not clear

Table 4-1 SWOT Analysis for new heating system development process

The SWOT analysis undertaken at the early stages of the project has been very valuable to identify the threats and weakness and put mitigation actions in place. To ensure dedicated

resource is available to develop the radiator who could be take ownership of the task a research team along with an associate with relevant knowledge and experience was appointed. Likewise the strengths and opportunities identified were exploited to maximise the benefit. The analysis and following mitigation actions enable the team to define the objective of the 2 year product development phase.

4.2.2 Program definition and market review

Once the objective had been established a PDL (product definition letter) was put in place. A PDL is a document, which captures the design theme and expected performance criteria for the radiators. At this stage only a rough outline of the radiator is in place (e.g.- stand-alone radiator which should be different to the existing products in the market). With the PDL in place a market review was undertaken to ascertain the trends, demands and expectations from the customer the end user. The study conducted by the partner company at the “Home and Building design show “ revealed that the customer expectation was to have a heating system that had the following features

- 1) Easy and in-expensive to install
- 2) Low cost of operation
- 3) Safe – heating system which could be left un attended without the fear of overheating
- 4) Controllability – easy to control
- 5) Comfortable – heating system which does not make the surrounding dry and uncomfortable
- 6) Low noise
- 7) Compatible with existing design,

As it can be seen, the outcomes from the market review are a combination of objective and subjective requirements. In order to translate the market requirements to objective (measurable) attributes, product parameters have to be defined which would deliver the performance defined by each of these attributes. In the Table 4-2 below a measurable attribute has been assigned to each requirement.

Customer requirements	Product attribute
Easy and in-expensive to install	Plug and Play system
Low operation cost	High efficiency and effectiveness
Safe	Failsafe systems to prevent hazard in all environments
Controllability	Digital temperature control
Comfortable	Operation at safe temperatures
Low noise	Fan-less operation
Compatibility with existing design	Neutral design

Table 4-2 Product attribute based on customer requirements

4.2.3 Product attributes and benchmarking

As shown in the figure4-5, for bespoke product development process for stand-alone radiators, ALS (Attribute leadership Strategy) and benchmarking is an important aspect of concept development. Once the key product attributes are identified, review of similar, existing and competitive products in the market is undertaken to ascertain market position, USP (unique selling points) and earmark any innovation in the product. To develop ALS the product description letter for the new radiator is compared to

- 1) Central heating systems – most widely used heating system
- 2) Electric Oil filled radiator system (stand-alone)
- 3) Electric fan heater (stand-alone)
- 4) Electric hot element heater (heater)

Performance and features of each of the benchmarked system has been objectively compared against the product attributes identified in Table 4-2. Outcome of the analysis is detailed in Table 4-3. The analysis shows that the only the stand-alone systems are plug and play. All systems are efficient but there is lag in oil filled radiator to attain operating temperature due to high specific heat capacity of primary fluid. Fail-safe systems for central heating and oil filled radiators are good but in spite of a thermostat, electric fan heaters and hot element heaters can pose a risk if covered. Most systems except for the electric fan heater rely on natural convection. All systems have some form of thermostat but controllability is limited in central heating system. In summary based on the ALS analysis it is recommended that the new stand-alone system would out should incorporate the best features for safety, effectiveness and operability.

	Central heating system	Electric oil filled radiator	Electric fan heater	Electric hot element heater
Plug and Play system		Yes	Yes	Yes
High efficiency and effectiveness	Yes	Efficient but has thermal lag	Efficient	Efficient
Failsafe systems to prevent hazard in all environments	No heating elements near occupants – no fire hazard	No heating elements near occupants – no fire hazard but can over heat if covered	Heating element enclosed but known to be dangerous if covered	Heating element enclosed but known to be dangerous if covered
Digital temperature control	No – Individual TRV on radiators	Mechanical thermostat – no remote operation	Mechanical thermostat – no remote operation	Mechanical thermostat – no remote operation
Operation at safe temperatures	Yes	Yes	Can over heat and cause burns	Can over heat and cause burns
Fan-less operation	Yes	Yes	No	Yes
Neutral design	Conventional and most common design-discrete	Various designs, generally on a portable stand	Very small and portable	Various designs, generally wall mounted and discrete

Table 4-3 Product benchmarking against attributes

4.2.4 Feature list and innovation

Benchmarking exercise enabled us to identify key features and design language for the new heating system. A feature list for the new heating system has been developed which would deliver customer expectations and create a unique position for the product in the market. Feature list will then be compared to current and known technology within the company and in the competitor products to identify USPs (unique selling points) and innovation. Feature list for the new heating system is developed to be equal or better than the benchmarked systems. Feature list for the new heating system is given in Table 4-4

	Benchmarked Central heating	Benchmarked Stand – alone systems	New radiator
Power range	0.9kW to 3kW	0.5 kW to 2kW	0.5kW to 2kW
Performance	~85% conversion of energy to usable heat for Central heating systems	>97% for stand alone systems	>97% efficient
Design	Fixed for Central heating	Modular and portable	Modular, modern and neutral design
Installation	Plumbed, complex and expensive for central heating system	Plug and play – no installation	Minimal or no installation required
Comfort	Comfortable, does not impact humidity	Most stand-alone systems produce dry air causing discomfort	Comfortable, should not impact humidity
Safety	Safe operating temperatures, with fail safe systems in the central boiler	Hot element systems are prone to fire hazards and there are limited fail safe features	No exposed heating elements. The system should have adequate fail safe systems
Accreditation	All central heating systems have to installed by qualified personnel and require safety certification.	Stand-alone systems do not require specialist knowledge and safety certification is not mandatory	The system should not require specialist knowledge but provide safety certification to improve product perception

Table 4-4 Product feature list

As per [56], feature list for the proposed heating systems will define fit, form and function of the product and determine the product specification. Hence it is very important to ensure the feature list is extensive at the concept development phase. Once the concept is approved, feature list will be re-visited to align with the development of the detail design.

Such a system with all the above listed features did not exist in the market; hence a novel design was required to make the system

- 1) Self contained radiator – No external plumbing
- 2) Maintenance free – once installed does not require annual maintenance

- 3) Modular (single unit or multiple units to control the heating of the house) – RF (radio frequency) controlled system
- 4) Effective and efficient- ensure the system gets to operating temperature quick and converts more than 97% electrical energy into usable heat.

4.2.5 Product architecture, layout and feasibility

In order to deliver the feature list, stand-alone water filled radiator had to be developed which provided the comfort, ease of a central heating system and modularity, flexibility, ease of installation of a stand-alone system.

Product attribute and feature list provided a good blueprint to create a layout for the proposed heating system. It is important to do a product architecture and layout study ahead of detail design. In the concept phase a few options for the layout are put in place and an initial DFMEA (Design Failure Mode Effect and Analysis) study is undertaken to address any potential design and manufacturing problems.

To develop stand-alone heating system that encompasses all the benefits of a central heating system a detailed review of the central heating system is required. From the literature review conducted in chapter 2 and Figure 1-7, it can be seen that the key components in a typical modern central heating are 1) boiler 2) pump, 3) vent cistern 4) pipes 5) valves and 6) radiators. Likewise a in a stand-alone system key components are 1) Heating element (similar to boiler), 2) electrical control unit, 3) thermostat, 4) external casing and 5) primary fluid (in oil filled radiators).

Based on the two systems two schematic layouts have been created as shown in Figure 4-7 and Figure 4-8.

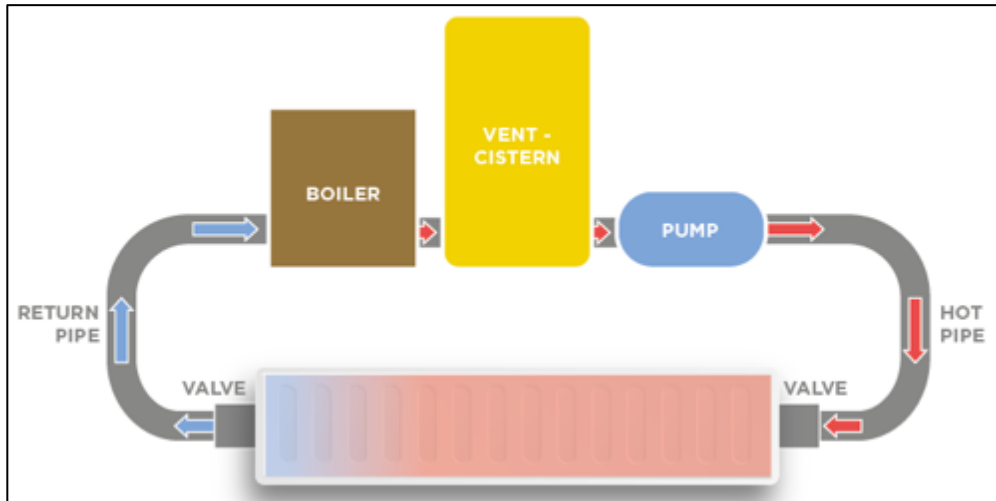


Figure 4-7 Schematic layout A - based on key components of a central heating system

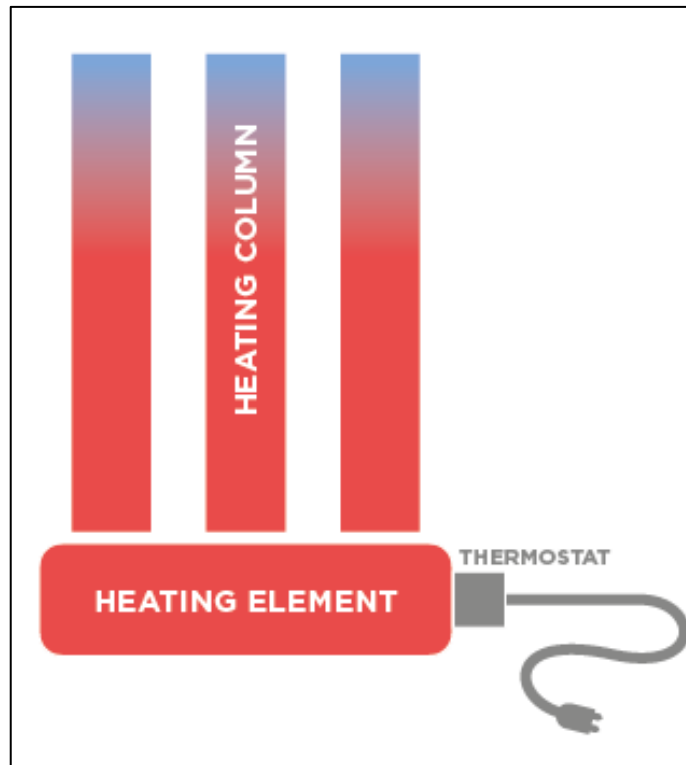


Figure 4-8 Schematic layout B - based on key components of a stand-alone (oil-filled) system

Based on the two schematic layouts an object decision analysis matrix has been developed to ascertain primary architecture of the new heating system and ensure the product meets the product attributes. Findings from the analysis are shown in Table 4-5. The decision matrix uses a RAG (Red Amber Green) indicator where each colour indicates a status against expected performance /product attribute.

Red → Fails to meet product attribute

Amber → Meets product attribute but needs assessment

Green → Meets product attribute

	Power range	Design	Installation	Comfort	Performance	Safety
Layout A	The layout allows usage of dedicated boiler which would cover the range of outputs	Complex design in many components - needs separate package for components	Complex layout would need installation of various components	Temperature of the radiator can be maintained at constant temperature by tuning the boiler. Max temperature can be controlled	Radiator has a large surface area allowing better heat transfer to the surrounding air but potential to lose heat from pipe work	Remote boiler keeps high temperature elements away from user. Dedicated vent and cistern relieve the pressure
Layout B	Heating element in the system heats the fluid directly hence power is restricted	Very compact	Self contained system with the need to connect to mains supply	Built in thermostat gives good control and helps maintain comfortable temperature	Low surface area would not deliver comparable heat transfer to the surroundings	Although the system has a thermostat there are no secondary safety features

Table 4-5 Decision analysis matrix for schematic layout

Based on the objective evaluation, architecture for the new system was developed to incorporate the best features of the two schemes and at the same time eliminate the shortcomings of individual systems. The requirements for the architecture of the new heating system have been outlined in Figure 4-9

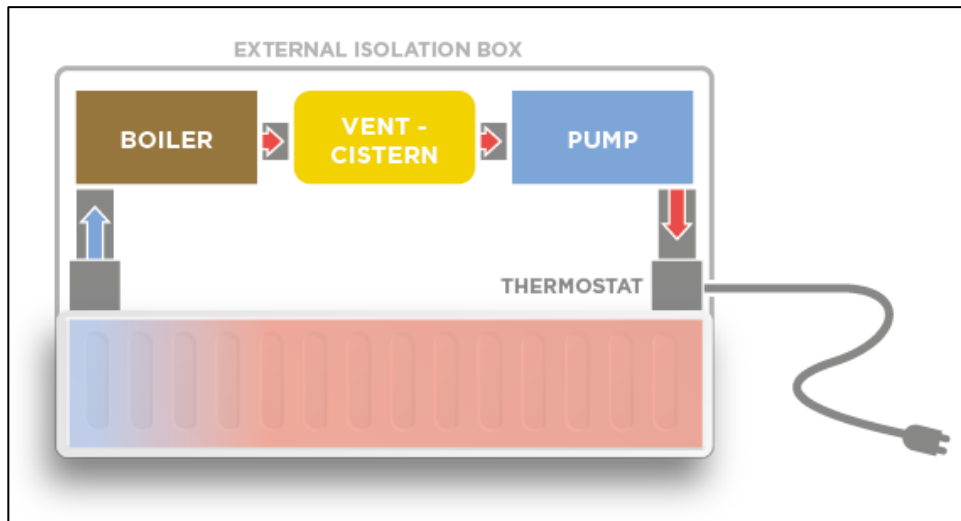


Figure 4-9 Architecture of the new heating system

Upon developing the concept architecture a DFMEA for the system has been developed. DFMEA [38] is an analytical tool that uses inductive reasoning for failure analysis to address quality, reliability and safety of the design. DFMEA also identifies potential failure modes and helps establish a mitigation action against each failure mode. Once a potential failure mode is identified a design / concept review is carried out to determine

- a) Cause of failure - Inductive reasoning based
- b) Severity of failure - Score of 1-10 with 1 being not relevant and 10 being catastrophic
- c) Probability - Score of 1-10 with 1 being not likely and 10 being frequent
- d) Effect of failure - Consequence of failure
- e) Detection - Method by which failure is detected: as the current DFMEA is for the concept, here Detection is used to determine if the concept has accounted for such an event/failure
- f) Detection score - Score of 1-10 with 1 being certain detection and 10 being undetected
- g) RPN (Risk Priority Number) – Severity, probability and detection scores are used to calculate the impact of the failure

$$\text{RPN} = \text{Severity} \times \text{Probability} \times \text{Detection}$$
- h) Mitigation /Recommendations – Actions recommended to take corrective action in the design/ concept to reduce overall risk.

Although FMEA was used in specialised disciplines dealing with safety critical systems and/or industries involving mass production, it has been deemed important for the

development of this heating system as it has a potential to cause harm to occupants in the vicinity of the system. There are many DFMEA software commercially available in the market but for cost optimisation and the nature of the product a bespoke DFMEA tool has been developed. Table 4-6 shows the DFMEA carried out on the initial heating system architecture shown in Figure 4-9.

Function	Potential failure mode	Potential failure effect	Severity	Potential Cause of failure	Probability	Current Design detection	Detection Score	RPN Score	Recommendations
Stand-alone system to effectively and efficiently heat the surrounding air	System does not expel adequate heat	Poor performance	8	Surface area of heated surface is not enough to expel the heat generated by the boiler unit	10	Inherent to the architecture	2	160	Maximise the surface area of the heated surface
		Customer dissatisfaction							
	Air circulation around the radiator is restricted	Poor performance		Isolation box restricts air flow behind and under the radiator	10	Inherent to architecture	2	160	Ensure clear air flow paths around the radiator
		Customer dissatisfaction							
	System has hot and cold spots	Poor performance		Pump in the system is not circulating water adequately	5	Difficult to detect unless full diagnosis is done	8	320	Ensure pump is operational all times
		Customer dissatisfaction							
Stand-alone system should operate safely	System is over pressurised	Occupants in vicinity exposed to hot water and burnt	10	Pressure relief not incorporated	10	Fault undetected	8	800	Ensure system has pressure relief
	System has hot spots/ areas which could cause burns	Occupants in vicinity exposed to hot surface and burnt	10	Occupant able to access the heating element inside the enclosure	2	Heating element is in enclosure and hot water is pumped	9	180	Ensure occupant cannot access the heating element
Installation time and cost are high	Does not provide any benefit over current systems	Customer dissatisfaction and loss of sales	9	Enclosure + radiator assembly bulky	10	Current architecture requires installation	1	90	Modify architecture to reduce/ eliminate installation

System requires maintenance	Does provide any benefit over current systems	Customer dissatisfaction and loss of sales	9	Enclosure + radiator assembly	10	Current architecture requires maintenance	1	90	Modify architecture to reduce/eliminate maintenance
-----------------------------	---	--	---	-------------------------------	----	---	---	----	---

Table 4-6 Concept Design Failure Mode Effect and Analysis for stand-alone radiator

Based on the DFMEA carried out on the concept architecture the following are observed

- Using a conventional radiator provides large surface area compared to oil filled radiators but the isolation box reduces the overall surface area of the system
- The radiator system has lower surface temperatures (compared to heating elements) ensuring the surrounding air is not dry.
- Using water-based system over oil-based systems reduces the lag and hence increases effectiveness.
- Enclosing the secondary components with potentially high temperature makes the system safe but introduces installation and maintenance problems
- Radiator with enclosure is still bulky compared to conventional stand-alone systems making it not suitable for all domestic applications.
- Vent and cistern system restricts the portability of the system

Following actions/design specifications were investigated to mitigate the risks

- 1) Design the boiler and pump so as to reduce the overall dimension of the enclosure to
 - a. Improve the exposed surface area of the radiator.
 - b. Reduce the overall size to improve installation and handling
 - c. Improve airflow around the radiator
- 2) Design the system with fail-safe systems to control high pressures and temperature (incorporate power isolation thermostats)
- 3) Develop a self-contained no loss system to ensure no maintenance is required.

Product definition, product attribute, feature list and the findings from DFMEA are used to create technical specifications for stand-alone water filled radiator system.

4.2.6 Business case analysis

A research-based approach is very valuable for developing a product but it is extremely important to ensure the heating system proposed is commercially feasible. The project spend in the concept phase is typically less than 2% of the overall project budget [25]. Before further spending is approved project investment cost and piece cost has to be evaluated to ensure required funding is available and the expected sales price of the heating system will deliver the expected profit. The technical specification gives a good guide to determine product, system and component specification. Using the system specification an initial BoM (bill of materials) is created. As most of the major components from the proposed heating system were similar to traditional central heating system, fairly accurate system cost have been used to track costs the system.

	Description	Qty	Price	Sub Total	Total
1	Radiator	1	£10 - £58	£10 - £58	£119.5 - £229.5
2	Pump	1	£12	£12	
3	Heater	1	£30- £67	£30	
4	Electronic control unit	1	£40	£40	
5	Valves	4	£5	£5	
6	Exterior panels	1 set	£6 - £25	£6 - £25	
7	Pipes	1 set	£3 -£6	£3 -£6	
8	Labour	0.9 hr	15/hr	£13.5	

Table 4-7 Initial Bill of Materials

(NB- cost figures shown are not accurate and values have been rounded off to protect commercial agreements)

Initial manufacturing cost for each stand-alone system ranges between £120 and £230 depending on the radiator size and power output. The BoM cost for these systems is benchmarked against the sales price of the existing competitor products to arrive at the target sales price. Sales price analysis has not been covered to protect commercial agreements. The predicted sales price has then been used in conjunction with the sales projection to determine turnover and profit form the product. As mentioned in the SWOT analysis (Table 4-1), a significant advantage of developing the heating system in the company is to ensure negligible investment in infrastructure for the assembly line and manufacturing. This has led to a sound business case to pursue further development.

4.2.7 Summary of concept phase

Literature review in chapter 2 has provided a good foundation to generate system requirements, ideation and innovation, which have been compared against customer, needs and market demands. Product definition has been used to develop concepts, which enabled us to create a DFMEA (Design Failure Mode Effect and Analysis) to do early assessment of concept. System architecture has been developed based on validated concepts, which were assessed for product cost and project investment estimates. The cost estimates enabled detailed business analysis and market feasibility for the product. A robust concept has been developed and detailed development of all components, systems and processes have been discussed in section 4.2. Manufacturing and performance challenges encountered during the development process have been addressed in section 4.3.

4.3 Stand-alone water filled radiator development

Concept phase laid a good foundation by providing a feature list, attributes and initial BoM. DFMEA process undertaken has provided early feasibility, but a detailed evaluation of the system is required to progress the design. In this section we will review concept maturation, detailed component design, develop a DVP (design verification process) to validate the performance of the design and do a manufacturing feasibility study.

4.3.1 Concept maturation

To further develop the concept we have to investigate components that can deliver the attributes and be safe in operation. Health and safety requirements of the radiator system heavily influence the design and selection of components. Heating systems have to comply with legislative requirements mentioned in chapter 2. In addition a water filled radiator system has to comply to BS EN ISO 9001:2000 for quality control [57], BS 7593 [58] for corrosion mitigation, BS EN 442 [13] for manufacturing and testing standards and not exceed 8 bar of pressure during operation. Components shown in the architecture in Figure 4-9 and bill of materials in Table 4-7 have to meet quality, pressure and manufacturing criteria.

4.3.2 Hydraulic Design

The most critical aspect of the proposed architecture is the fluid circuit. It is important to understand how the water is heated, circulated and maintained to get maximum performance from the system. The pump takes hot water from the vented cistern and circulates it to the radiator. As the hot water circulates in the radiator heats the radiator surface, which in turn losses heat to the surrounding through convection and radiation. As a consequence water leaving the radiator is cooler. The water then enters the boiler where it is re-heated and stored in the cistern.

The radiator plays a critical role for heat emission, hence it is important to first determine the type of radiator used in the system. Water filled panel radiators in central heating systems come in many sizes and panel configurations. The panels vary in length and height. A further variation is the number of panels in a radiator. The most common ones are K1 - single panel radiator and K2 - double panel radiators. Very rarely one can find more than 2 panels in a radiator.

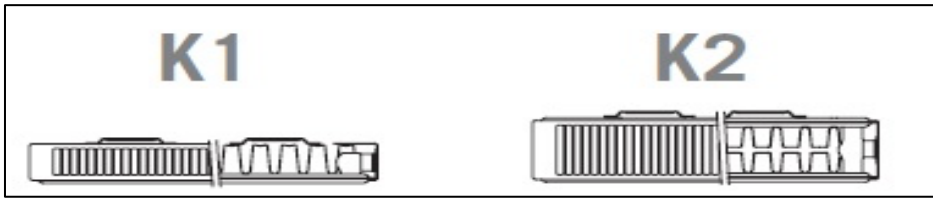


Figure 4-10 Panel configuration in domestic radiator [60]

An important aspect of the radiator system is the exposed surface area, which is proportional to heat output. To maximise the heat output from a radiator fins are added to the panels. In order to maximise the output for a given volume of space occupied by the unit K2 (type 22) radiators have been selected for the design. The design may also provide some package benefit, which will be evaluated when supporting components are selected.

As the intended radiator is similar to the ones used in central heating, we can use the same design criteria to determine the amount of fluid required in the system, flow rate and heating demand from the boiler. Table 4-8 gives volume of water used per unit length of radiator for a given height.

Height	300	400	500	600	700
Litres/meter length of radiator	3.6	4.47	5.33	6.2	7.07

Table 4-8 Volume of water per radiator [60]

Quinn radiators [60] have quantified the amount of water required per unit length of radiator for a given radiator height. This allows installers to calculate the net volume of water required for the central heating system. In the present case this information could help determine the component size and specification. It can be seen that for every 100 mm increase in height volume of water increases by 0.87 litres per unit length of radiator. Also the smallest radiator manufactured is a 300 mm high radiator. Using the two we can formulate that the volume of water in a radiator is given by Equation 4-1.

$$Volume\ of\ water\ in\ radiator\ (Q_R) = L \times \left\{ 3.6 + \left(\frac{\Delta H \times 0.87}{0.1} \right) \right\}$$

Equation 4-1 Volume of water in a radiator

Where

Q_R – Volume of water in radiator (litres)

L – Length of radiator (m)

ΔH – Incremental increase in height of radiator from a 0.3 m radiator (m)

Assumption from the concept architecture is to use a standard 15mm copper pipe to connect all the units and the pump used for circulation would be a standard off the shelf central heating pump. For initial calculations, it is assumed that volume of water in the flow circuit (pipes, pump and boiler) would be equal to the volume of water in a 15mm pipe with the same length as that of the radiator. Hence the volume of water in the flow circuit is given by Equation 4-2

$$\text{Volume of water in flow circuit } (Q_{fc}) = \left(\frac{\pi \times d^2}{4} \right) \times L$$

Equation 4-2 Volume of water in flow circuit in a stand-alone system

Where

Q_{fc} - Volume of water in the flow circuit of a stand-alone radiator

d- internal diameter of the pipe (0.012m for current study) (m)

L – length of radiator (m)

Power range for the new heating system is 0.5kW to 2kW. As per the Quinn data sheet [60], the shortest type 22 radiator with 300mm height, which can deliver 0.5kW, is 500 mm and the longest type 22 radiator with 600mm height, which can deliver 2kW output, is 1000 mm long. In addition there will be an amount of water in the pipe, the boiler and the cistern. The cistern, which is carrying hot water, should have the same volume of all other systems combined to ensure the system operates seamlessly and the pump does not run dry. Using the dimensions and Equation 4-1 and Equation 4-2 the volume of water required in the stand-alone radiator system is calculated. Range of volumes is given in Table 4-9.

	Minimum (litres)	Maximum (litres)
Volume of water for radiator (a)	1.8	6.2
Volume of water in pipes and pump (b)	0.05652	0.113
Volume of water in cistern (c=a+b)	1.85652	6.313
Total Volume (2c)	3.713	12.626

Table 4-9 Range of volume of water in stand-alone radiator

Above analysis has helped determine dimensions of the following key systems

- a) Radiator type
- b) Radiator size (max and min sizes)
- c) Net volume of water in the system (max and min volume)
- d) Cistern size (max and min size)

On establishing the dimensions a package and layout study has been undertaken to optimise the product size and ensure the system is modular. Objective evaluations of the proposed layouts have been review in Table 4-10. It can be seen from layout 1 and 2, packaging a 6.5 litre cistern makes the system bulky. In order to optimise the package, concept has been modified to eliminate the cistern and use the radiator to store the water and make an unvented closed loop fluid circuit. Layout 3, 4 and 5 show three options for the revised concept. Advantages and dis-advantages of each layout have been presented in Table 4-10.

Layout		Description	Issues
1	 <p>A top-down view of a radiator. The radiator is a long, white, ribbed rectangular unit. To its right, there are four colored boxes representing components: a brown box labeled 'BOILER' with a blue arrow pointing up, a yellow box labeled 'CISTERN', a blue box labeled 'PUMP' with a red arrow pointing down, and a vertical orange box labeled 'CONTROL BOX'.</p>	<p>Top View- Boiler, pump and control unit are placed behind radiator with the control box</p>	<p>Mounting brackets for radiators are at the back. This layout does not allow easy mounting</p>
2	 <p>A top-down view of a radiator. The radiator is a long, white, ribbed rectangular unit. To its left, there are three colored boxes representing components: a vertical orange box labeled 'CONTROL BOX', a blue box labeled 'PUMP' with a red arrow pointing right, and a yellow box labeled 'CISTERN' with a blue arrow pointing left. Below the cistern is a brown box labeled 'BOILER'.</p>	<p>Top View- Boiler, pump and control unit are placed as a separate unit</p>	<p>Layout allows mounting but is bulky and requires complex installation</p>
3	 <p>An elevation view of a radiator. The radiator is a large, white, ribbed rectangular unit. To its right, there are three colored boxes representing components: a brown box labeled 'BOILER' with a blue arrow pointing left, a blue box labeled 'PUMP' with a red arrow pointing right, and a vertical orange box labeled 'CONTROL BOX'.</p>	<p>Elevation view- Boiler, pump and control unit are placed on the side of the radiator with the control box</p>	

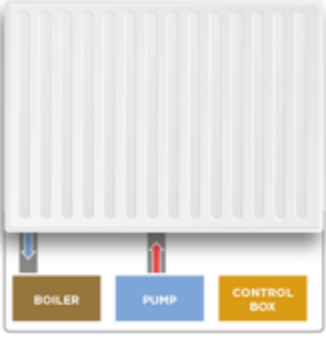
4		Elevation view- Boiler, pump and control unit are placed under the radiator with the control box	
---	---	---	--

Table 4-10 Concept Maturation - new layout

Although this approach helps eliminate the cistern it introduced a major challenge. Water expands when heated. Co-efficient of thermal expansion of water is given by Equation 4-3. The co-efficient for water at 20°C is 0.000207/°C and at 70°C is 0.000582/°C [61]. Temperature differential of 50°C, causes volume increase of 1.88%. This results in an increase of 3.33 x10⁻⁵ m³ and 11.3 x10⁻⁵ m³ in the smallest and the largest radiator respectively.

$$\alpha_v = \frac{1}{V} \left(\frac{dV}{dT} \right)$$

Equation 4-3 Co-efficient of thermal expansion

Although the metal radiator and pipes expand when heated, the increase in volume is less than the volume increase of the water. This increases the operating pressure greater than 0.5 bar, which changes the legislative requirements for the heating system. As per BS EN ISO 60335-2 [63], if heating system has liquid and is pressurised, it should be able to withstand twice the highest pressure measured during the test conditions in BS EN 442. In order to comply with the requirements, design specifications of the components have been modified.

Off the shelf central heating components operate at maximum 2-3 bar of pressure. Having a closed loop stand-alone system requires a bespoke design to meet the system targets.

Package layout 3 and 4 in Table 4-10, show that the system is compact but the pump, control box and the boiler (heating element) are exposed, which cause safety concerns, where the electrical circuit can be damaged and the occupant get burnt by getting in contact with the hot components. To eliminate this concern the concept is further matured into a design intent layout. The layout is shown in Figure 4-11 and the description of the components is given in Table 4-11.

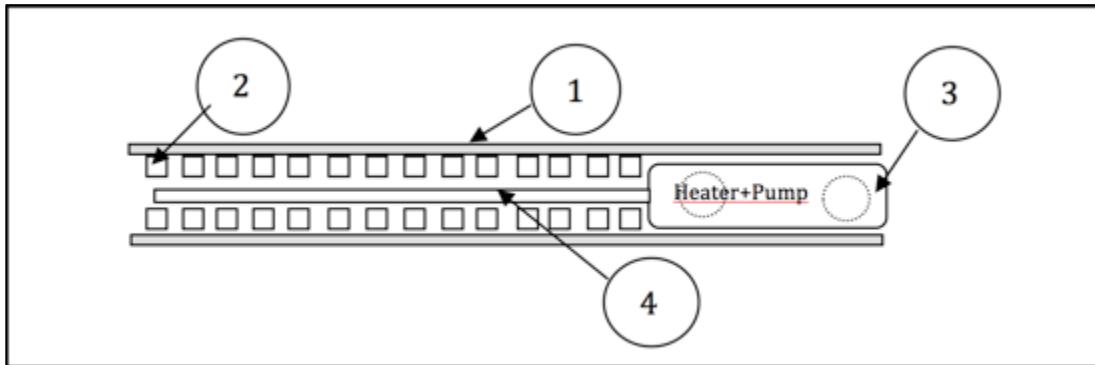


Figure 4-11 Design intent package and layout for stand-alone heating system.

1	Radiator
2	Radiator Fins
3	Control unit (Heater, pump and electronic circuit board)
4	Copper pipe

Table 4-11 Revised parts list for a stand-alone radiator

System specification - Table 4-12 details specification for the key systems used in the stand-alone radiator. Range of size (dimension) operating specification and description of the system are given for radiator, heater, pump and control box. The specifications have been developed to meet the product attribute and deliver the feature list. Detailed component level design activity will be undertaken in 4.2.3 to deliver this specification.

	System	Size	Specification	Description
1	Radiator	300x500 to 600 x1000	Modified, K2 (type 22) radiator with thermal output range of 0.5kW - 2kW Should withstand 8 bar	Standard radiator installation with out plumbing. Needs modification to package heater, pump and control unit assembly
2	Boiler/heater	Max dimension 60 mm diameter	0.9 kW to 2 kW heating capacity Should withstand 8 bar	Diameter restricted to ensure package between the radiator panels
3	Pump	Max dimension 60 mm diameter	Flow rate 10 lpm Should withstand 8 bar	Diameter restricted to ensure package between the radiator panels

4	Control box	Max width 60 mm	IP 45 to mitigate water ingress and ensure no mechanical damage is done as per 60335 test requirements	High water ingress protection ensures the system can be installed in bathrooms in zone 2, 3 and 4.
---	-------------	-----------------	--	--

Table 4-12 System specification based on design intent layout

4.3.3 Mechanical design - Component design and selection

Based on the system specification in Table 4-12, stand-alone radiator comprises a modified double panel radiator with reduced fins to accommodate a control unit. A control unit is made up of an electronic circuit board enclosed in an IP (ingress protection) [62] rated plastic box, a heating element and a pump to complete the hydraulic circuit.

The process involved a few manufacturing challenges to ensure the control system fit between panels whilst accommodating the panel tolerance. The design constraints were

- 1) To fit the control unit between radiators panels,
- 2) Maximise the number of fins
- 3) A control system with a common design to be used in different radiator

4.3.3.1 Radiator Panels

Panel radiators have been around for the past 4 decades. There have been some improvements [14] as discussed in chapter 2 but the design is fairly similar across all manufacturers, as they are manufactured in accordance with the BS EN 442 standards. As shown in Figure 4-10, most common configurations for panel radiators are K1 and K2, which are a single panel and double panel. For the current application K2 radiator is selected to maximise the heat output for given projection of the radiator.

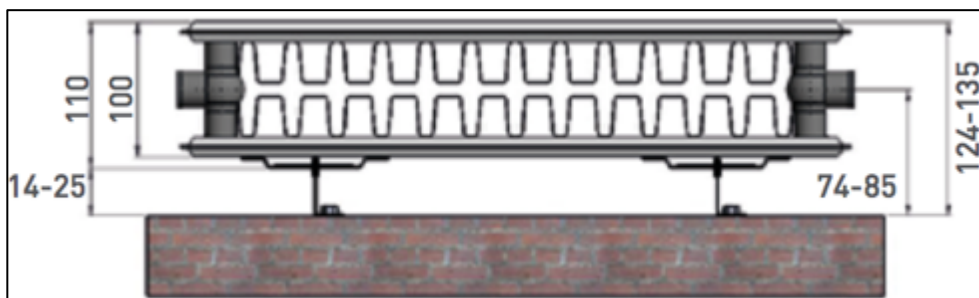


Figure 4-12 K2 radiator mounted on a wall [64]

A panel of the radiator can be made in following two methods.

- 1) Two single sheet press formed and then welded all along the edge of the panels
- 2) A large single sheet press formed, folded and then welded along three edges.

Each method has its advantages. It is important to understand these to ensure the most suitable process is selected for the stand-alone system. The two have been compared in Table 4-13. It can be seen that the two sheet radiator provides a better flow path but poorer finish and is more expensive.

	Two sheet press formed	Single sheet press formed and folded
Advantages	<ul style="list-style-type: none"> • Improves manufacturing tolerance • Smaller tool size • Provides a larger flow channel, hence reducing friction losses in the system 	<ul style="list-style-type: none"> • Improves manufacturing time • Provides a cleaner finish at the leading edge, giving better perception of quality
Disadvantages	<ul style="list-style-type: none"> • Higher manufacturing time hence higher cost • Rough finish on leading edge requiring additional finisher panel to cover the edge 	<ul style="list-style-type: none"> • Large tool size • Higher tolerances • Smaller flow channels

Table 4-13 Comparison of radiator panel manufacturing process

Initial assessments have been made on both designs and the difference in performance has been marginal, leading to select the single sheet press formed and folded radiator that provided a cost benefit by 10%. Although the type (K2) and manufacturing process has been selected, radiator is not suitable for packaging the heater, pump and control unit as shown in Figure 4-11. In order to meet package requirements following modifications are required.

- 1) Reduce the fins in the standard radiator by 240 mm
- 2) Change the orientation of the T-joint connectors to face in (standard central heating radiator has the T-joint connectors facing out). This modification increases in the manufacturing cost of the radiator panel and hence has an impact on the manufacturing cost.

The two mandatory modifications meant that the radiator is not standard built and would require non-standard production process, making the radiators more expensive than the original estimates. In order to get a competitive price a bespoke technical specification and tender for quotation has been sent to multiple radiator manufacturers. An illustration of the technical specification is shown in Table 4-14, which details Type, materials, geometric parameters, surface treatments, colour and compliance.

Type	K2- Type 22 Double panel
Panel material	Cold rolled steel conforming to EN 10130, thickness 1.20+/- 0.09 mm, pitch for channels 33.33mm
Panel spacing	Distance between the two panels 70mm +/- 3mm
Fin material	Cold rolled steel conforming to EN 10130, thickness 0.45+/- 0.05 mm
Fin spacing	33.33mm pitch with no fins for 240mm measured from right hand side of the radiator
Cover material	Cold rolled steel conforming to EN 10130, thickness 0.75+/- 0.09 mm
T-joints	G ½” x 4 with 2 bottom T-joints facing inside
Pressure	Pressure tested to min 8 bar
Surface treatment	Surface treatment in accordance with DIN 55900-1
Colour	Final paint colour RAL 9016 for panels, fins and covers
Compliance	Meet BS EN 442 and ISO 9001

Table 4-14 Technical specification of radiator panel [64]

Quotation from suppliers detailed their technical capability, compliance with standards, price and value proposition. A decision analysis matrix has been created to objectively compare and choose the best supplier. For commercial reasons the details of the quotations and the decision analysis have not been disclosed. Upon evaluation Termoteknik radiators [64], manufactured in Turkey gave best price and quality for the modified radiators. An important element of the technical specification is to minimise the variation between the two panels of the K2 radiators.

In summary a modified K2 radiator panel has been designed and developed to meet the package requirements by maintaining a 70 mm +/- 3 mm gap between the two panels and

the reduced fins allow room for the sub unit. Also two T- joint connectors have also been modified to allow concealed connections.

4.3.3.2 Heater system

Heater is the most critical system to generate hot water for the radiators to emit heat. The power range for the heater must be marginally higher than the power range of the radiator, in order to account for losses in the system. It is important to minimise the number of heaters without compromising the performance of the radiator. This will allow a lean stock maintenance and minimise risk of wrong build on assembly line. Key components of a heater are

- 1) Heating element with insulated sheath
- 2) A body to encapsulate water around the element and provide a flow path
- 3) Electrical connectors

There are many off the shelf heaters, which are used in electric showers or as immersion heaters in a storage tank, but these are not suitable for the application. The heater body should be packaged between the heater panels and integrate with the bespoke control system.

Hence based on the concept three possible designs have been proposed in

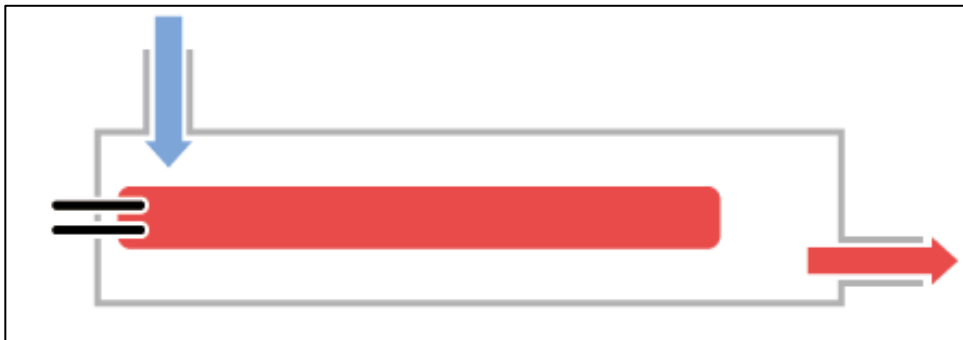


Figure 4-13 Heater with straight element

The first design is the simplest with a straight heating element of 15mm OD (outer diameter) packaged inside a standard 28mm tube. The heating element is electrically isolated from the outer tube. One end of the 28mm tube is sealed with electrical connectors and the system has an inlet and outlet for fluid circuit. The main advantages of this design are

- 1) The heating element used in the design is readily available in a range of power outputs and
- 2) The simplicity of the design offers significant cost saving over the other designs.

But the design has some disadvantages as well

- 1) Mass flow rate of the fluid around the element is restricted, which may lead to local hot spots in higher wattage heaters
- 2) The length of the element is approximately 250 mm and this gives package restrictions.

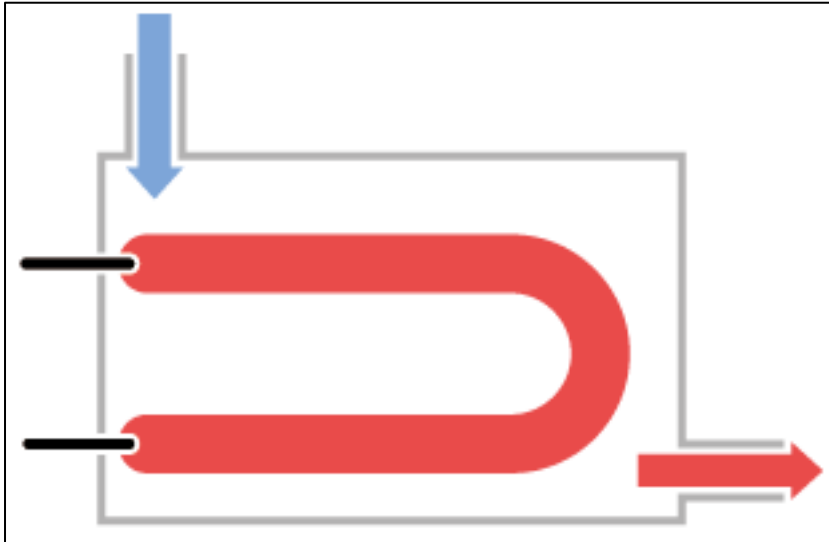


Figure 4-14 Heater with U shaped element

The second design in Figure 4-14 Heater with U shaped element is similar to the design one where the heating element is smaller in diameter (6.8 mm), bent in U shape offers the same advantages and overcomes the package issue but still has the mass flow rate issue.

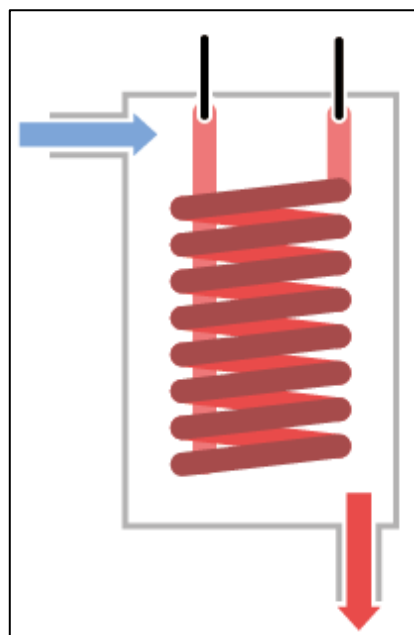


Figure 4-15 Heater with coil element and increase flow volume

The third design in Figure 4-15 is significantly different as the heating element is bent into a coil and packaged in a vertical tubular body. The coil increases the diameter of the tubular body to 60mm but reduces the length. This revised design can be packaged between the radiator panels. Increased diameter also allows for a better mass flow of the fluid mitigating the risks in the 1st design. Although this design offers a better solution the major disadvantage is the construction of the heater body. As discussed in previous section the radiator system can reach up to 8 bar of pressure and the proposed design with cylindrical heater body is packaged between the radiator panels with very low tolerance. Due to high ductility of copper, unlike the previous design proposal the heater body cannot be made using standard copper tubing due to strength and availability. Steel body has been proposed to overcome the issue. Using steel body design makes the design robust gives higher accuracy but increases the cost due to increase in material and labour costs. Table 4-15 summarises the cost and quality of the three design proposals.

	Heater 1	Heater 2	Heater 3
Package	250mm long – block air flow	Compact	Very compact
Flow	Restricted	Restricted	Un-restricted
Complexity	Simple	Simple	Complex

Table 4-15 Comparison of heater for stand-alone radiators

Based on the comparative analysis it can be seen that the design proposal three offers significant quality benefit over the other designs. In order to reduce the risk in the new product and develop a robust design proposal three has been selected.

Element power and rating calculation

The process of producing heat from a by passing electricity through a conductor is called Joule heating or resistive heating. Using Ohm’s law [65]

$$V = I \times R$$

Equation 4-4 Potential difference as a function of current and resistance

$$P = V \times I$$

Equation 4-5 Power as a function of potential difference and current

Substituting current from Equation 4-4 in Equation 4-5 we get Equation 4-6

$$P = \frac{V^2}{R}$$

Equation 4-6 Power as a function of Current and resistance

Hence for power output of 500W and 2000W a wire with resistance of 105.8 Ω and 26.45 Ω [66] respectively is required. These heater would consume 2.17 A and 8.69 A based on a 230V domestic supply voltage. Once the power rating and current draw is known the diameter and length of the element is determined.

Detailed design

Heater is comprised of a steel shell encapsulating helical coiled heating element with terminals on the top of the boiler unit. The element's core has been tightly packed with magnesium oxide [67] powder within a 6.5 mm metal tube with M6 threaded ends on either ends. This process has been specially developed to ensure no local hot spots are generated under operation. The helical element is brazed on a 57.2 mm diameter circular plate. The plate in turn is vacuum brazed to a 60 mm diameter steel tube. Inlet and outlet tubes are nickel brazed in the same operation. Careful selection of the grade of steel and brazing material was paramount as the unit had to conform to tight tolerance of the assembly at all temperatures and withstand load and shocks during the manufacturing process. Selection of nickel brazing is key to ensure a copper block can be mounted on the top plate. The copper block has been a critical feature, as it provided a heat sink for the high power electronics that control the heater and the pump. The heaters were built with elements of different wattage in order to cater to various sizes.

4.3.3.3 Pumps

DFMEA carried out in concept development phase has highlighted that oil filled radiators purely rely on convection to circulate the hot fluid in the radiator. This results in temperature variation in the radiator. Another major disadvantage of the oil filled radiator is thermal lag. The time required for the oil filled radiator to get to full operation temperature (+50°C) is significantly high due to specific heat capacity of oil. Water based system cover the shortcoming of the oil-based radiators due to higher thermal conductivity but pose a significant challenge. Due to higher specific heat compared to oil, water when in contact with the heating element would have the tendency to boil locally and produce steam. The steam would raise the pressure of the system exponentially. In order to avoid localised kettling (boiling), it is important to circulate the water at the correct rate. If the flow rate is

too slow, water around the heating element will boil, if it is too fast there will be system losses.

$$m = \frac{Q_{heating\ element}}{C_{pw} \times \Delta T}$$

Equation 4-7 mass flow rate of water in a stand-alone system

Where

m – mass flow rate of water in a stand-alone system (kg/s)

C_{pw} - Specific heat capacity of water (kJ/(kg-K))

ΔT - Temperature differential between the heating element and water (K)

$Q_{heating\ element}$ - Power of the heating element (kW)

Using Equation 4-7 to maintain a temperature differential of 50°C per kW a water based system needs a flow rate of 0.0047kg/s which is equivalent to 0.00477 litres per second. Hence a 2kW heating element will heat 0.0095 litres of water from 20°C to 70°C in 1 sec. The heating element at 100°C in the current design is in direct contact with maximum of 0.2 litres of water (water in the heater unit). If the system does not have a pump the water adjacent to the element will reach boiling temperature in 33.469 secs and 70°C in 21.05 secs. Hence to avoid boiling the pump has to operate at 0.0161 lps. Based on this it can be seen that the largest radiator proposed would reach max operating temperature in 11.07 minutes. A standard central heating pump operates between 0.2 lps and 0.8 lps where the head varies between 60kPa and 20kPA. In a stand-alone system the expected head losses are lower than the central heating system due simple single radiator and plumbing layout. Although the calculation suggest that a central heating pump will be over the required specification, to reduce development time and risk an off the shelf unit has been purchased which can operate within the temperature, pressure and package constraints.

Two commonly used pumps (Laing and Grundfos) [68,69] have been benchmarked to establish the best fit. A comparative study has been carried out in Table 4-16

	Grundfos	Laing
Power	30W	25W
Flow rate	30lpm	10lpm
Ambient temperature	0-40°C	0-80°C
Bearing	Mechanical ball bearing	Ceramic
Orientation	Horizontal	Vertical
IP rating	IP 42	IP 42

Table 4-16 Comparison of common central heating pumps

It can be seen that the Laing pump offers the following benefits

- 1) Better package as it pump orientation occupies less space (vertical as opposed to horizontal)
- 2) Ceramic bearing offers lower noise and wear –which is turn improves product life
- 3) Higher operating temperature (in the stand-alone system the pump is packaged between the panels which can reach 70°C)
- 4) Laing pump has a lower power consumption

For all the above reasons a Laing pump has been selected. An exploded view of the pump is shown in Figure 4-16



Figure 4-16 Exploded view of Laing pump [68]

4.3.3.4 Control system

A PCB (printed circuit board) has been developed by a third party to integrate with the heater and the pump unit and control to deliver the heating demand. Design details for the PCB are not in scope for this work but the technical specification developed to deliver the product attributes have been detailed below

Input voltage	220V to 240V
Current	Upto 13 amp
Heater control	Triac to control heater upto 2 kW
Pump control	S/W to include a pre and post run for the pump to avoid overheating of water
Manual control	Manual over-ride to control temperature
RF control	Primary temperature control using a radio frequency controller at 433 Mhz compliant domestic appliance regulation

Figure 4-17 Technical specification for a PCB used in a stand-alone system

Design

PCB must control heater up to 2kW and a 25W pump. The pump must operate continuously at the stated speed to ensure there are no local hotspots or kitting effects in the heater. The triac on the PCB must be able to switch up to 3kW (factor of safety) heater without overheating. PCB must monitor room air temperature, water temperature and local air temperature to ensure safe operation.

The PCB takes input from three different sources.

- 1) A thermostat has been integrated in the PCB (printed circuit board) with the control accessible to the user. The user can adjust the heating demand manually with this feature.
- 2) The PCB has a RF (radio frequency) receiver to receive signals from a remote room thermostat that measures the air temperature in the room.
- 3) In addition a local thermostat is mounted on the PCB and located at the bottom of the radiator away from hot surfaces to monitor local temperatures and ensure the radiator is not overheating.

Fail-safe

A high temperature (90°C) thermal cut-off has been incorporated on top of the heater. The mains supply to the control PCB has been routed through the thermal cut-off unit to add an extra layer of safety. If due to system fault the pump stops working or the control PCB is short, the thermal cut-off unit will isolate the mains power supply to the entire system once the heater unit exceeds 90°C.

Safety

A special plastic box has been designed to fit on top of the boiler assembly and enclose the circuit board. The box has been designed to comply with IP 45 ingress protection rating to prevent water ingress around the electrical circuit and isolate the high voltage circuitry from user interface. A clip on fascia unit has been designed to improve the aesthetics of the product and protect accidental damage to the control knob.

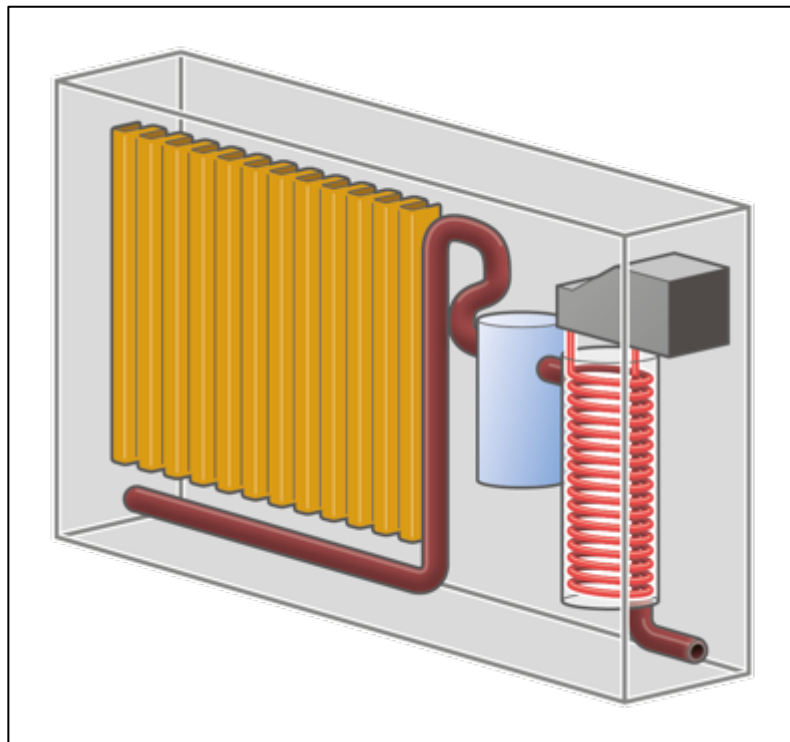


Figure 4-18 Isometric illustrative view of stand-alone water filled radiator

4.3.3.5 Operating fluid

Operating fluid in the stand-alone system is very important. Although thermodynamically the two systems would produce the same amount of heat for a given radiator size and power consumption, a water filled system aims to overcome the lag (time to temperature) in an oil filled system. As discussed in the boiler design, using water introduces its own challenges, as the water has to maintain a specific flow rate to avoid boiling. In addition water causes severe oxidation of the metal radiator panels. The

oxidisation causes debris in the system, which hampers the performance. Similar to central heating system, water used in a stand-alone system has to be treated with glycol rust inhibitor. The fluid mix has to be carefully balanced to ensure good corrosion protection without compromising the thermal properties.

Chemicals:- Fernox Alphi -11 [70] anti-rust and anti-freeze chemicals are mixed with water to protect the radiator. These chemicals react with water and produce effervescence. If the fluid mix is introduced in a sealed stand-alone system, it can lead to pressure build up in the system over a period of time. Once the system undergoes a few heating and cooling cycles, the pressure reaches critical levels causing leaks through the fittings used in the radiator. To overcome this problem the chemicals are pre-mixed in a tank and allowed to de-aerate before the system is filled.

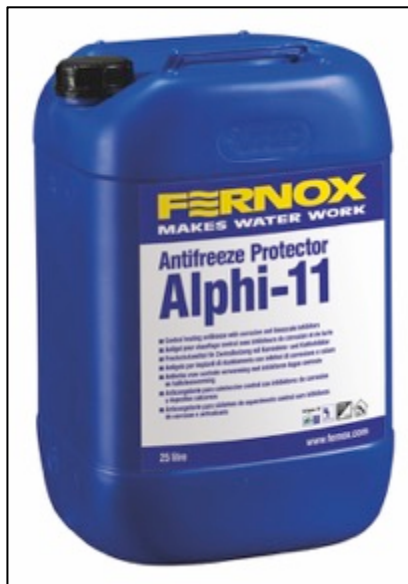


Figure 4-19 Fernox Anti freeze and anti rust [70]

Bacteria: - The chemicals used are glycol based and can react with any microbes in the system. This also results in some undesirable effects (effervescence) and pressure build up. To mitigate development of bacteria biocide is also premixed to the fluid.



Figure 4-20 Fernox biocide [71]

The exact percentages of the rust inhibitors and the biocide cannot be disclosed as they are protected by the confidentiality agreement with the company.

4.3.4 Design for Manufacture and Assembly (DFMA)

Once the components have been designed and selected to deliver the performance, a lean and simple manufacturing process is required to ensure a good product quality. The manufacturing process has to be structured, well laid out and intuitive. Considering manufacturing feasibility during the design process enables early assessment of any potential problems and planning mitigation actions thereof. Design for manufacture and assembly (DFMA) is a design method of products for ease of manufacturing and assembly. This is also an effective tool to reduce overall part cost by minimising complexity and using common geometric features to align components and systems.

As per the bespoke product development process for stand-alone radiators shown in figure 4-4, robust modular product architecture is developed. The architecture along with manufacturing feasibility delivered a well-defined layout. The flexible and modular approach in the bespoke process along with due consideration for product specification has resulted in a single design for boiler with 3 power outputs, one pump, PCB and control box design to cover the entire range of power and radiator sizes. Further optimisation has been carried out to reduce the number of radiator sizes in the product portfolio by eliminating uncommon sizes with outputs same as another radiator with more common applications. The bespoke process requires parallel assessments of sub-systems and components to reduce development time. As discussed in 4.1.2 primary constraints for the development process has been limited labour and financial resource to develop the stand-alone radiator. In order to optimise the design and testing phase, utilising “off the shelf” components/systems with proven performance has reduced development time and improved reliability as the component testing is outsourced to the supply chain.

In order to perform detailed functional analysis a full BoM (bill of materials) and process flow has been created. Functional analysis helps ascertain essential and non-essential parts, error proofing requirements and critical quality check requirements.

Full BoM is given in Table 4-17 where each bought out assembly/component is a level 2 part and the complete assembly is at level 1. Details on bought out assembly details are not given to protect product IP.

Level	Part Name	Quantity	Number of interfaces
1	Stand-Alone radiator system	1	
2	Radiator	1	9
2	Heater	1	6
2	Pump	1	3
2	PCB	1	2
2	Control box lower	1	4
2	Control box lower	1	4
2	Control Knob	1	1
2	O-ring	1	2
2	Air temperature sensor	1	1
2	Heater Temperature sensor	1	2
2	Ground Wire	1	2
2	Power lead	1	2
2	Grommets	2	2
2	Elbow connector	1	2
2	Elbow connector push fit	1	2
2	Male- Female Straight connector	2	2
2	Female -Female straight connector	1	2
2	Bleed Valve	1	1
2	Filler connector	1	1
2	25 mm copper pipe	1	2
2	Copper pipe	1	2
2	Tie wraps	2	2
2	Spacer block	1	4
2	Facia cover	1	3
2	Facia panel	1	5
2	Back panel	1	3
2	Top panel	1	3
2	Bottom panel	1	4
2	Safety label	1	1
2	Radiator label	1	1
2	M6 nuts	5	2
2	M4 hex screw	1	2
2	M6 button head screws	4	2
2	M4 self tapping screws	2	2
2	Power lead clip	1	2

Table 4-17 Manufacturing BoM for stand-alone radiator

The process flow has been used to estimate time for every stage of manufacturing process. Summing up each process, it can be seen that the total manufacturing time is 22 mins and additional 12 mins and 60 mins for filling and final testing respectively. To improve process and increase productivity the production layout has been designed to run 4

activities in parallel. This increased the production to 5 radiators in an hour from start to finish. In order for the parallel process to work seamlessly product quality is paramount. If there are any issues/failure in one of the station, it will have an impact on the work stream causing line stoppage. For instance, if one stand-alone system fails at the final testing net output will be affected and it will be difficult to identify the root cause of the failure. In order to improve the robustness of the process and build the product “right first time”, interim quality check and test process have been introduced. By following the DFMA process a robust reliable manufacturing and quality process has been developed. Details of the manufacturing shown in the process chart and the test process have been explained in section 4.3.1.

4.3.5 DFMEA (Design Failure Mode Effect and Analysis)

System and component development has been undertaken to mitigate the risk highlighted in the DFMEA study undertaken in concept phase. Upon completion of the design phase it is important to review the DFMEA and compare the RPN score.

Function	Potential failure mode	Potential failure effect	Severity	Potential Cause of failure	Probability	Current Design detection	Detection Score	RPN Score	Recommendations
Stand-alone system to effectively and efficiently heat the surrounding air	System does not expel adequate heat	Poor performance	8	Design offers 2 heated panels and further maximises convection as well	2	Enclosed system tested during manufacturing	2	32	N/A
		Customer dissatisfaction							
	Air circulation around the radiator is restricted	Poor performance		Control box encapsulated within the radiator with minimum obstruction	2	Inherent to architecture	2	32	N/A
		Customer dissatisfaction							
	System has hot and cold spots	Poor performance		System checked and tested during assembly	2	Difficult to detect unless full diagnosis is done	1	16	N/A
		Customer dissatisfaction							
Stand-alone system should operate safely	System is over pressurised	Occupants in vicinity exposed to hot water and burnt	10	System pre-filled, tested and bled during manufacturing process	1	100% Product testing	1	10	N/A
	System has hot spots/ areas which could cause burns	Occupants in vicinity exposed to hot surface and burnt	10	System is IP45 rated with no access to hot surface and surface temperature limited to 70°C	2	System design to enclose hot surface	1	20	N/A
Installation time and cost are high	Does provide any benefit over current systems	Customer dissatisfaction and loss of sales	9	Stand-alone system mounted on brackets	2	Stand-alone system with just a electrical lead	1	18	N/A
System requires maintenance	Does provide any benefit over current systems	Customer dissatisfaction and loss of sales	9	Stand-alone self-contained system.	2	Current architecture requires maintenance	1	18	N/A

Table 4-18 DFMEA on completed stand-alone radiator

RPN score in Table 4-6 were 180 for effective heating. The score is reduced to 32 by incorporating the heater and pump unit between the 2 panels of a K2 radiator and the design now offers 2 complete surfaces for radiant energy and further convective energy by maximising the fins in the panels and exposing the hot pipes and heater to the airflow between the panels. Similarly the RPN score for safe operation has reduced to 10 for pressurisation and 20 for hotspots compared to concept phase where the scores were 800 and 180 respectively. This has been achieved by

- 1) Pre-filling and bleeding the stand-alone radiators during the manufacturing process and
- 2) Designing the stand-alone system to meet an ingress protection (IP) 45 standard.

Product design will be completed only if the RPN score is low and acceptable for a given failure mode. DVP (design verification process) has been used to test individual components and the system to ensure the robustness and reliability. DFMA process has been used to develop a lean manufacturing process and introduce testing process in the manufacturing phase to eliminate any lost time due to leaks, airlocks or component failures in the finished product.

4.4 Stand-alone water filled radiator manufacturing

Most critical phase after product development is product manufacturing. It is expected that the desired product is easily manufactured, meets quality targets and production volumes within target cost and timing. Hence the tools and process like, DVP, DFMA and DFMEA are used to develop robust manufacturing process. As stated in section 4.2.4 a detailed manufacturing process has been developed and the learning from the DVP has helped incorporate interim testing to deliver a high quality product. The process has been divided in 2 main processes

- 1) Sub assembly process and quality assessment
- 2) Final assembly and testing

Details are given in the following sections

4.4.1 Sub-Assembly process and Quality assessment

To ensure quality whilst increasing the production volumes the pump, heater unit and electronic circuit board are pre assembled into a sub unit. A customised jig (Figure 4-21)

has been manufactured to maintain the angular and linear tolerance for the sub assembly. The fixture has a base to hold the pump and pin and slider system to adjust the gap between the pump and the heater unit. The control box is fastened on the boiler with an O-ring to seal the inner compartment. The PCB is fixed using additional locator pins in the box. Each crimp joint on the power cable, pump power cable and the sensors are checked using a pull test (2 N) to ensure the connection is secure. Once assembled the sub-unit is sent to the testing station.

The sub-units are tested on a test bench figure 4-22 designed to accommodate the pump and boiler unit. The purpose of the rig is to test sub units for water leaks, electrical connections and accuracy of the thermostat to ensure quality and reduce failures on the manufacturing line. In order to meet production timing and improve efficiency the rig can test up to six units simultaneously. The base of the pump in the sub-unit is fixed in a circular recess on the test bed. The elbow connectors on the boiler assembly are connected to the mains water supply using a flexible hose. The pump inlet has been connected to a pipe network. The pipe network is connected to a drain and back again to the boiler forming a closed loop. Isolator valves and non-return valves are in place to ensure the mains water filled the loop and the flow is unidirectional (in the direction of the pump flow). The circuit also has an air bleed valve to vent air in the system. Opening the mains water supply and closing the drain fills the hydraulic circuit and ensuring air is vented out of the loop. Once filled, each sub unit is connected to an isolated mains power supply.

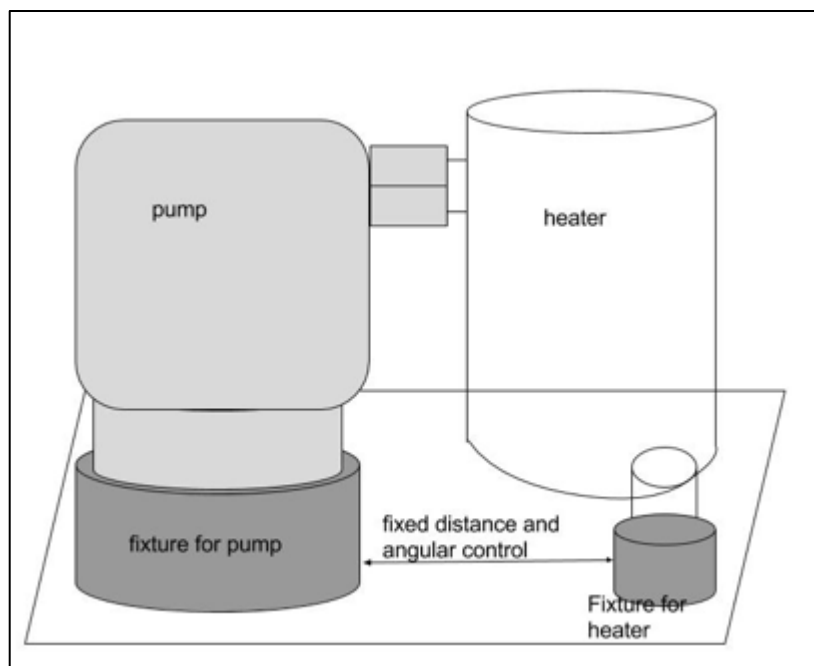


Figure 4-21 Pump and heater jig

Careful consideration has been made for health and safety of the operators. A clear acrylic protective cover has been designed to isolate the units from the operator during the test. Each mains connector has been enclosed in an IP 56 rating enclosure. A RCD (residual current device) has been incorporated in the mains connection to the power supply to further protect the user in case of any current leakage or failures.

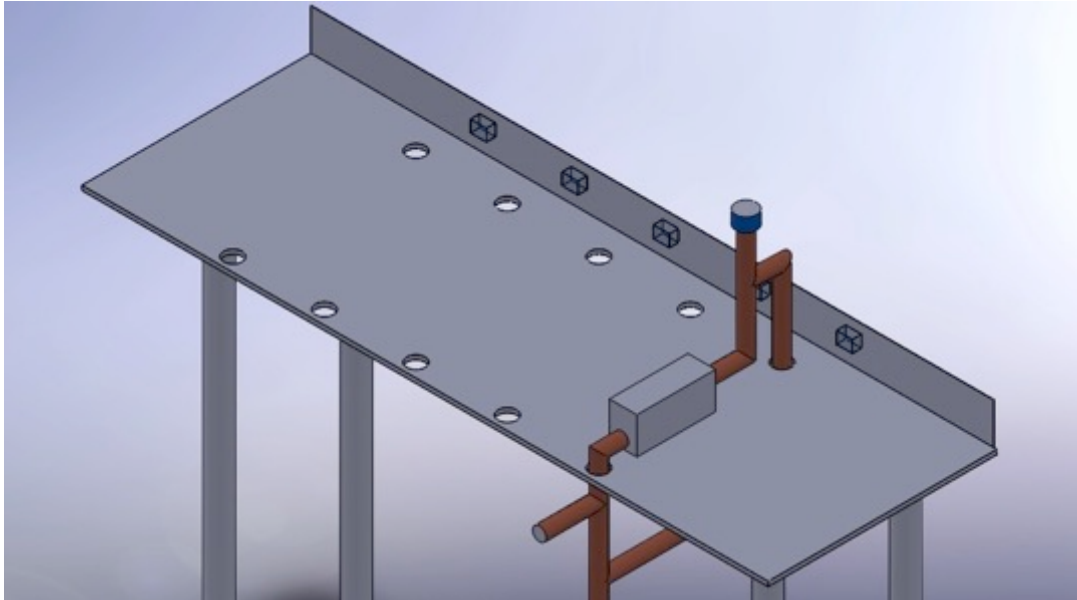


Figure 4-22 Test Bench for Sub Units

On completion of the test each unit is sealed with the control box cover and a safety label with sub-unit number and power rating is attached. A computer system logs the power, flow, temperature, and serial number of each unit. In addition the system is also designed to log date, time and ID of operator. The data is kept on records to trace any faults. Tested and certified sub units are then ready to be assembled in the radiator

4.4.2 Final assembly and testing

While the sub-units are built, a parallel process is undertaken to prepare the radiator units for the final assembly. The radiator unit is placed on a workbench facing up and clamped. Due care is taken to ensure no cosmetic damage is done to the radiator. A bleed valve and a filler connector are fastened to the top left and right T joint respectively. A male-female straight connector is fastened to the two bottom T-joints. The radiator is flushed with water remove any debris from manufacturing and transport process. Metallic debris in the system can damage the pump impeller, especially if it is magnetic it can get stuck and stop the impeller from rotating.

Based on the DV (design variation) analysis carried out during product design bottom right T- joint of the specially designed radiator is the primary datum. The tested sub-units

are referenced and fixed to the bottom right T-joint. A 25 mm (based on DVA) copper tube is used to trend set the assembly and achieve a flush finish of the fascia to the edge of the radiator. A copper pipe is connected between the bottom left connector and the elbow push fit attached to the end of the pigtail pipe of the pump. All joints and connections are checked with a spanner to ensure the joint is secure.

The radiator assembly is then transferred to a purpose built jig Figure 4-23. The jig comprises a sliding bracket clamp mounted on a ply wood base with a 20mm shaft. This unit is mounted on a 1.5 m post using bearings and break system. The clamp is made using six, 1.2m long x 0.2m wide 3 mm thick sheet metal panels. The panels are cut and folded to form radiator support brackets. Three plates are stacked on top of one another in order to provide mounting for a 300mm, 400mm and 600mm high radiator. Another set of 3 plates are welded on linear bearing, which is mounted on the plywood base. A toggle clamp is used to control the movement of the three plates. The top and bottom plates together form the brackets to hold the radiator securely when the jig is rotated. The design of the jig has been critical to ensure that the diagonal of a radiator is perpendicular to the ground plane with the bleed valve facing up. This ensures that all the air in the radiator and the pipes is drawn out.

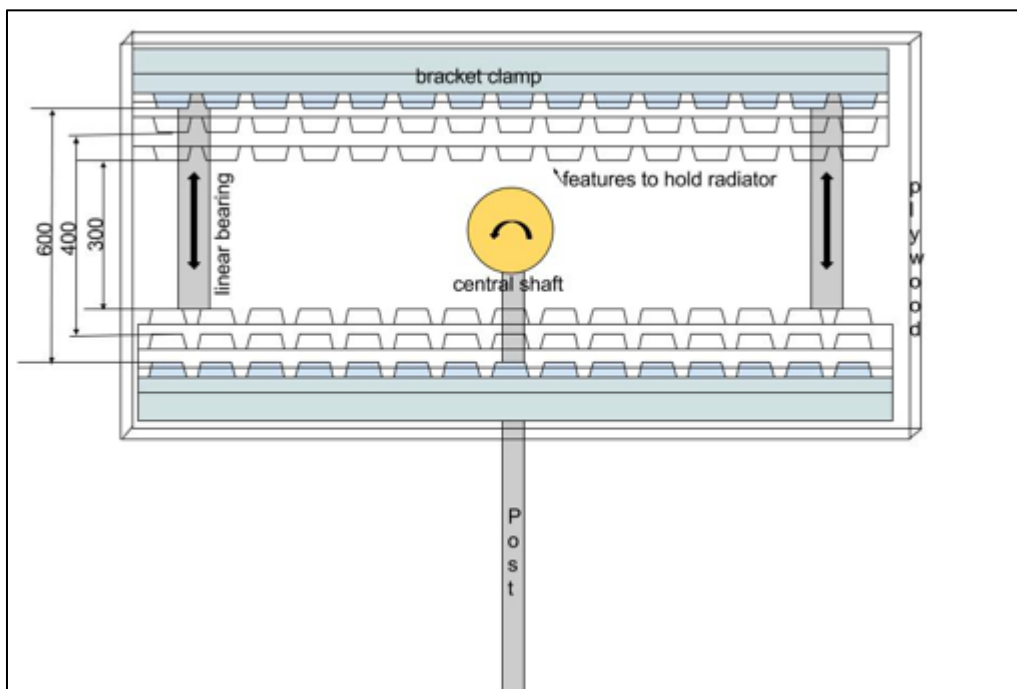


Figure 4-23 Filling jig for radiators

Once the connections are made the radiator is filled with pre-mixed water and glycol mixture. Using the data in Table 4-8 a metered amount of pre-mixed liquid is fed into the radiator, during this procedure the rig is turned to purge all the air out of the system. The

pump is allowed to run to ensure no air is trapped in the pipe work. Once this is achieved 0.5% of fluid is drawn out of the system and then the system is closed. This has been done to allow expansion of fluid when the system reaches peak operating temperature. Nevertheless drawing water from a closed system lowers the pressure, which affects pump operation and increases risk of kettling. Hence compressed air is injected into the radiator such that the system pressure rises to 1.2 bar at room temperature. Pneumatic lines with pressure control valves are installed on the production line to ensure the process is consistent and also eliminate operator errors. Once filled the radiator were sealed and checked for leaks.

The radiator is then set on heat soak cycle for 60 minutes and the temperature is recorded. Upon successful completion of the test, finisher panel are attached which enclose the control box between the radiator panels and provide an aesthetic appeal. Finished product can be seen in Figure 4-24.



Figure 4-24: Stand-Alone water filled radiators [72]

4.4.3 Product performance evaluation

Performance evaluation for domestic heating systems has to be carried out in accordance with British standards. BS EN 442-1 and BS EN 442-2 give a detailed guideline of the test setup, means and accuracy of measurement. Thermal Performance evaluation (in compliance with BS) has to be carried out in a temperature-controlled room. The specification of the room and the test are

- 1) Dimension of the room 4m x 4m x 3m with the walls, ceiling and floor with a minimum thermal resistance of $2.5 \text{ m}^2\text{K/W}$.
- 2) Emissivity greater than 0.9
- 3) The heater unit should be installed as per manufactures installation guideline (in this case 50 mm from the wall and 110mm from the floor.
- 4) There should not be another source of heat
- 5) In case of electric heaters power consumption should be logged over 1 hour period
- 6) Room reference air temperature should be set to 20°C .
- 7) Room air temperature should be measured using K-type thermocouples placed at 0.75 m from the radiator in central vertical plane of the room as per Figure 4-25. Additional measurements are made at 0.05m and 1.5 m above the floor and 0.05 m from ceiling in the same plane.
- 8) In addition a thermal camera has been used to measure the absolute surface temperature and temperature distribution.

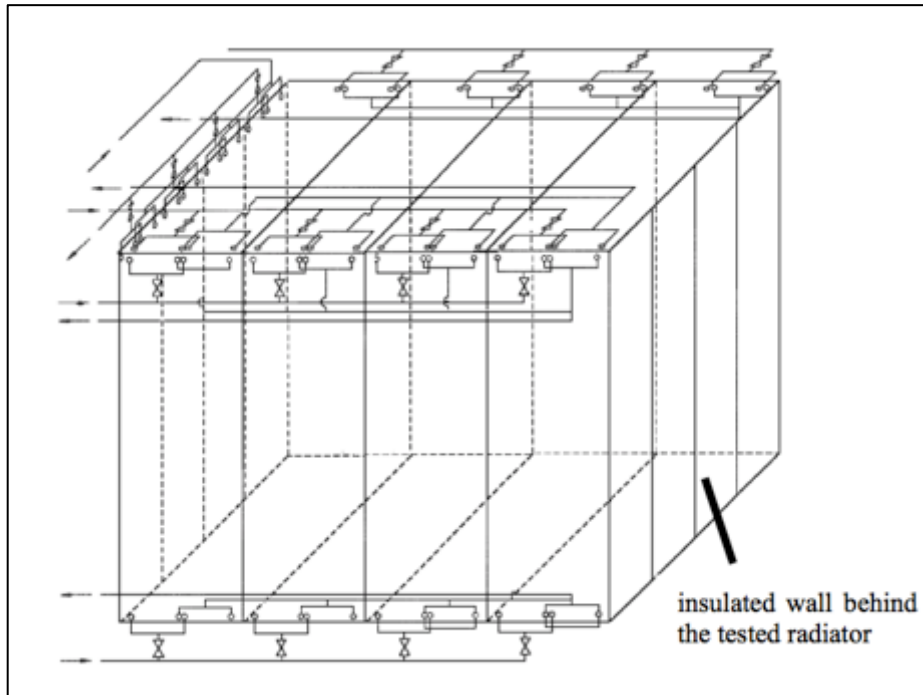


Figure 4-25 Test room BS EN 442 [50]

Heat output is calculated from the temperature data collected from above mentioned points in a steady state test. Steady state is achieved once the temperature of reference point does not vary more than 2°C. Using the equations in the BS EN 442 [13] a standard characteristic equation is generated for the radiator.

$$\log \Phi = \log K_m + n \cdot \log \Delta T$$

Equation 4-8 Characteristic equation of radiator BS EN 442

Where

Φ - Thermal output

ΔT - excess temperature (temperature difference between radiator surface and air)

K_m and n are calculated based on Equation 4-9 and Equation 4-10

$$\log K_m = \frac{\sum(\log \Phi) \cdot \sum[(\log \Delta T)^2] - \sum(\log \Delta T \cdot \log \Phi) \cdot \sum(\log \Delta T)}{N \sum[(\log \Delta T)^2] - (\sum \log \Delta T)^2}$$

Equation 4-9 K_m - characteristics equation of radiator BS EN 442

$$n = \frac{N \sum[(\log \Delta T \cdot \log \Phi)] - \sum(\log \Delta T) \cdot \sum(\log \Phi)}{N \sum[(\log \Delta T)^2] - (\sum \log \Delta T)}$$

Equation 4-10 n characteristic equation of radiator BS EN 442

Where

$$K_m = 10^{\frac{A \cdot B - C \cdot D}{N \cdot B - D^2}}$$

Equation 4-11 Factor based on EN 442

$$n = \frac{N \cdot C - D \cdot A}{N \cdot B - D}$$

Equation 4-12 Factor based on EN 442

Where N is the number of test points and A, B, C and D are

$$A = \sum (\log \Phi)$$

$$B = \sum [(\log \Delta T)^2]$$

$$C = \sum (\log \Delta T \cdot \log \Phi)$$

$$D = \sum (\log \Delta T)$$

Using the standard equations for the radiators under test and using the manufacturers data the following two equations have been developed to calculate heat output from a single panel and double panel radiator.

$$Q_{\text{radiator-single}} = L \times \left[564 + \left(\frac{(h - 0.3)}{0.1} \times 152 \right) \right]$$

Equation 4-13 Heat output from a single panel radiator

$$Q_{\text{radiator-double}} = L \times \left[1115 + \left(\frac{(h - 0.3)}{0.1} \times 275 \right) \right]$$

Equation 4-14 Heat output from a double panel radiator

Results of the test conducted according to EN 442-1 and EN 442-2 to quantify the thermal output of the radiators are given in Table 4-19.

	3100	6100
Heater size in radiator	900 w	2000 w
Thermal Output	770.36 W	1537.029 W
Efficiency	98.76%	97.4%

Table 4-19 Thermal output of stand-alone radiators as per BS EN 442 test

The results indicate that the stand-alone radiators are over 97% efficient for the largest radiator and 98.76% for a small radiator. Although the radiators are very efficient, thermal imaging carried out during the test show that the temperature on the radiator surface is not uniform. This suggests that the entire surface of the radiator is not effective in both convective and radiated heat transfer as they are a function of area. Thermal images have shown that significant area of the radiator at lower temperature than design intent. This is primarily due to reduced or no flow in areas of the radiator. The flow may be restricted due to pressure variation within the radiator. An investigation into local pressure variation would give an insight into flow distribution. Improving flow and consequently the temperature distribution on the radiator surface will increase the affective area and improve the performance.

4.5 Summary

A bespoke product development process has been developed that delivers a methodical approach to design a new stand-alone radiator whilst accounting for performance attributes, customer requirements, manufacturability and quality assurance system for robust product delivery. Based on this approach new stand-alone water filled radiator has been developed which offers the benefit of a central heating radiator system without the complexity of plumbing, installation and maintenance. Following unique points have been noted in the process and stand-alone system development process

- Compared to the existing stand-alone range, the new process has improved modularity, functionality and significantly improved quality assurance process, that reduces warranty issues.
- Detailed market research and benchmarking has revealed that there is no competition with a similar product in the market.
- The product offers significant cost benefit over traditional central heating system for new builds and extensions.

- The product is safe and certified by Nemko [73]
- New stand-alone radiators are over 97% efficient
- Unique components and systems have been analytically developed with due consideration to performance, manufacturing feasibility and cost.
- Product has been successfully launched in the market within 2 years with the projected sales increase of 70%.

In the new product development process, both mechanical and hydraulic considerations have been accounted for to ensure a safe, robust and commercially viable product is developed.

Although the product has been tested according to standard and found to be very efficient, there is scope to improve the effectiveness of the stand-alone system. As discussed, market and customer requirements keep evolving and there is a constant push to improve efficiency and reduce cost for the consumer products. As per the literature review in chapter 2 it can be seen that there has been limited investigation on internal flow parameters of domestic radiators. The key to improve the efficiency and effectiveness is to investigate opportunities to improve the heat distribution, reduce pressure drop in the system to reduce pumping power consumption and reduce overall cost. MK 2 of the stand-alone radiator system will be developed based on the outcomes of the flow investigations in chapter 5 and 6 where experimental and numerical analysis has been carried out to quantify the flow parameters of radiator. Chapter 7 investigates the costs of owning and operating a hydraulically improved stand-alone system.

5 CRITICAL PERFORMANCE ANALYSIS OF STAND-ALONE WATER FILLED RADIATORS

During the early stages of this work, for commercial reasons time was dedicated to product development, with little focus on detailed flow analysis, performance optimisation and possibility of design optimisation. As shown in figure 4-5, TVM (total value management) is important to carry out critical analysis of the designed product to investigate opportunities to optimise the product. Critical performance analysis to understand critical flow characteristics of the new stand-alone radiator is required to understand losses in the flow circuit, improve the flow and in turn heat distribution.

Detailed literature review has been undertaken to understand current research in domestic heating. The literature review suggested that the research in the area varied from detailed experimental work on central heating radiator system to performance of radiators in a room. Previous work has also suggested that there were large range of parameters influencing radiator performance. The literature thus far quantifies the impact of some of the parameters but does not cover the flow within the radiator. Present work aims to study micro flow parameters in a radiator. Quantify the effect of flow rate and flow configurations on pressure and heat distribution over a panel. Optimise the flow parameters to minimise the cost of operation and manufacture of a radiator. Transfer this to a complete domestic heating system and a stand-alone system

The performance of radiators can be quantified by comparing the characteristics of radiators under a range of operating parameters. Key performance characteristics of the radiator to be evaluated are

1. Pressure drop across a radiator – to quantify hydraulic losses and affect on pumping power
2. Pressure variation – to understand flow distribution and its affects the temperature distribution
3. Velocity profiles – to understand flow distribution

As discussed earlier these are evaluated under the following variables

1. Point of entry → BBOE and BTOE

2. Flow rates → Range of 5 flow rates
3. Size effect → 2 radiator sizes

5.1 Temperature distribution analysis of double and single panel radiators with two flow configurations

In the following, the effect of point of entry of fluid in a stand-alone radiator system has been analysed both qualitatively and quantitatively. Both double and single panel radiators have been analysed to quantify the difference between the two radiators.

5.1.1 Double Panel BBOE Configuration

Figure 5-1 shows the temperature distribution in a standalone double panel radiator with BBOE configuration. It can be seen that the temperature distribution is not uniform. It can be seen that the maximum temperature in the system is 67.2 °C which is recorded at the inlet of the radiator. The minimum temperature that can be seen is 59.3 °C at the center of the radiator.

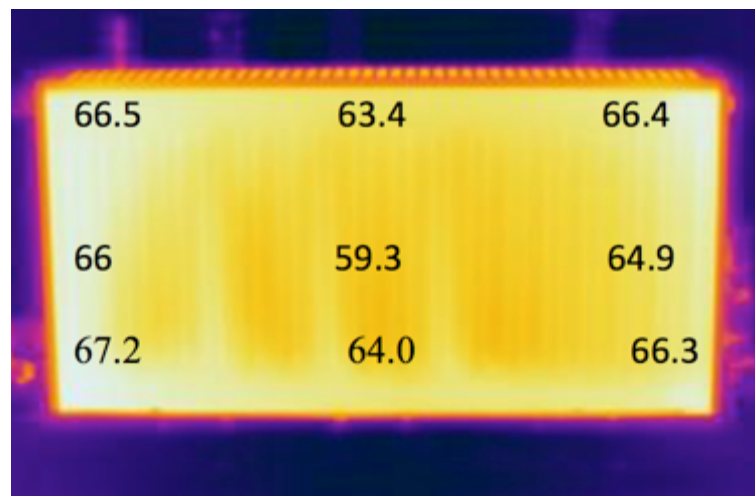


Figure 5-1 Temperature profile double panel radiator - °C (BBOE) [59]

Along the bottom edge of the radiator the temperature first drops to 64 °C at the center and shows a recovery to a temperature of 66.3 °C at the exit point of fluid from the radiator. It has also been observed that the temperature is fairly uniform along the left edge of the radiator near the entry point. This suggests that the water rises once it enters the system and flows towards the top. The temperature profile also suggests that the part of the hot water flow along the top of the radiator and a small portion flows down and to the center of

radiator. To further quantify the non-uniformity in temperature field the thermal images have been digitized and temperature values obtained at different points in the flow field.

5.1.2 Single Panel BBOE Configuration

Figure 5-2 shows the temperature distribution in a standalone single panel radiator with BBOE configuration. It can be seen that the temperature distribution is not uniform. It can be seen that the maximum temperature in the system is 68.3 °C which is recorded at the inlet of the radiator. The minimum temperature that can be seen is 63.4 °C at the center of the radiator.

Similarly along the lower edge the temperature first drops to 65.6 °C at the center and shows a recovery to a temperature of 67.5 °C at the exit point of fluid from the radiator. Similar to the double panel radiator the temperature is fairly uniform along the left edge of the radiator near the entry point suggesting that the water rises once it enters the system and flows towards the top. The temperature profile also suggests that hot water primarily circulates along the outer periphery of the radiator.

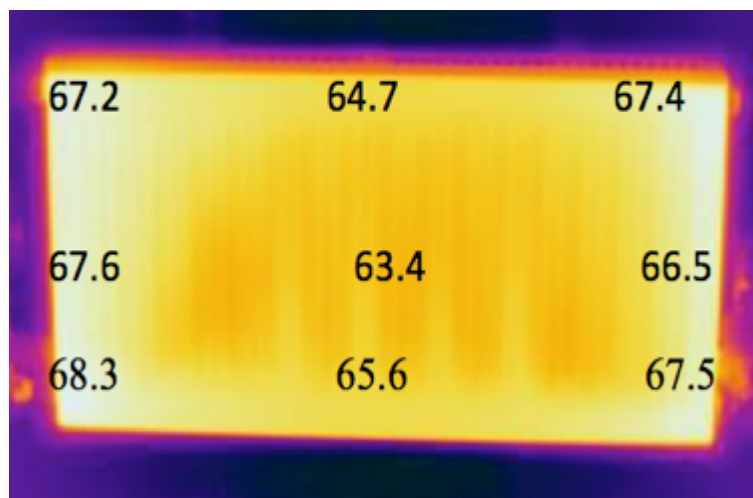


Figure 5-2 Temperature profile in a single panel radiator - °C (BBOE) [59]

To eliminate small variations in the inlet temperature between the two experiments and do comparative analysis, dividing temperature values at different points by the inlet temperature has normalized the temperature field. This is shown in Figure 5-3 for a double panel BBOE system and Figure 5-4 for a single panel BBOE system. The arrow shows the point of entry of fluid in the radiator.

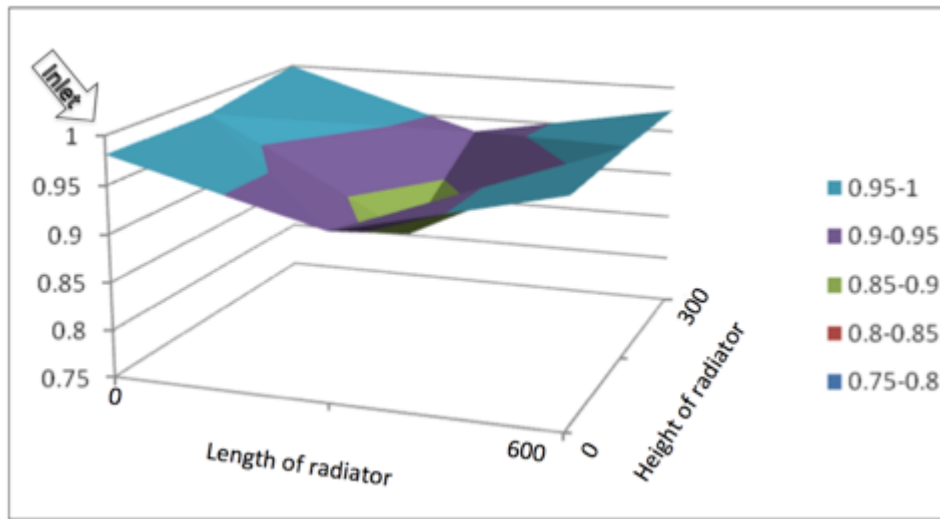


Figure 5-3: Normalised temperature Variance with respect to inlet - double panel (BBOE) [59]

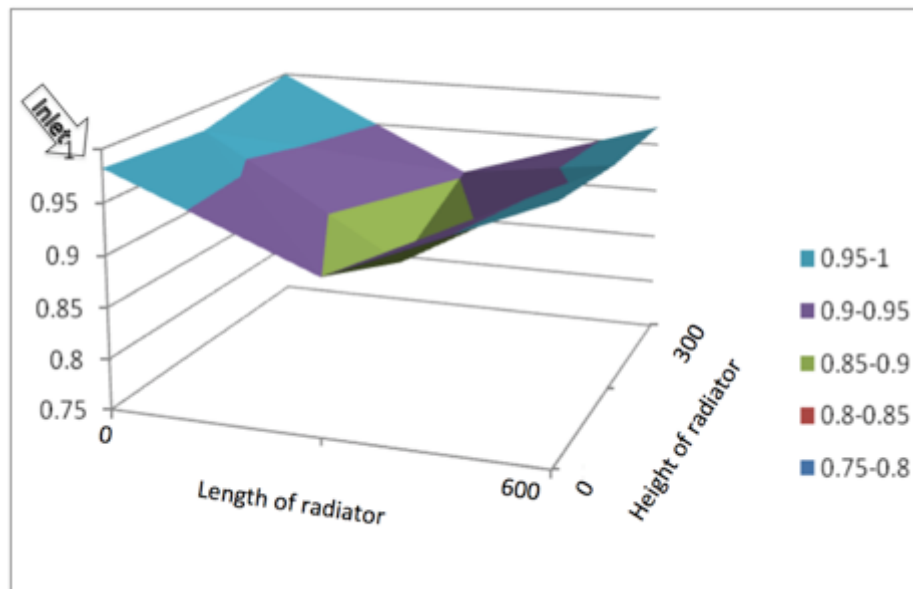


Figure 5-4: Normalised temperature Variance with respect to inlet single panel (BBOE) [59]

The two graphs show that the temperature drops to 95% and 90% along the horizontal for the two radiators respectively. Also the temperature along the vertical axis at the center of the radiator drops to a minimum of 85% in a single panel BBOE system. The effect is limited to dead centre for the double panel radiator. The overall temperature drop between the inlet and outlet temperature of the fluid is marginal. Single panel configuration shows marginally more variation in temperature compared to double panel. The information on temperature distribution is very important in understanding flow distribution in the radiator, as there are no directly means to measure the local flows in the radiator. It would be useful to compare the velocity profiles from the CFD based internal flow analysis in chapter 6 and co-relate the temperature distribution.

5.1.3 Double Panel BTOE Configuration

Similarly Figure 5-5 shows the temperature distribution in a standalone radiator double panel with BTOE configuration. Having the fluid exit diagonally opposite modifies the path. The resultant temperature drop between the entry and exit is greater. It can be seen that the maximum temperature in the system is 77.2 °C that is recorded at the inlet of the radiator. The minimum temperature that can be seen is 64.2 °C at the center of the radiator.

Along the bottom edge of the radiator the temperature first drops to 69.4 °C at the centre and shows a recovery to a temperature of 71.0 °C at the exit point of fluid from the radiator. The temperature profile also suggests that hot water primarily circulates along the outer periphery of the radiator. The difference between the inlet and the outlet fluid temperature is highest (4.9 °C) in this particular configuration.

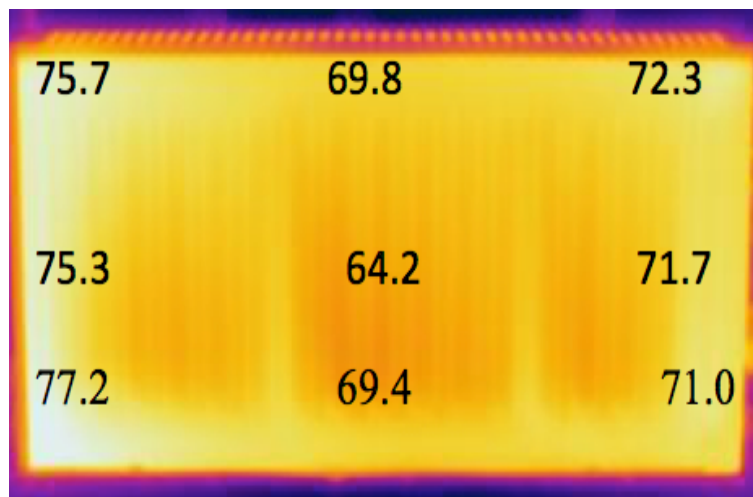


Figure 5-5 Temperature profile on a double panel - °C (BTOE)

5.1.4 Single Panel BTOE Configuration

Similarly investigations are shown in Figure 5-6. Having the fluid exit diagonally opposite modifies the path. It can be seen that the maximum temperature in the system is 68.3 °C which is recorded at the inlet of the radiator. The minimum temperature that can be seen is 64.8 °C at the centre of the radiator. The temperature distribution is very uniform in this particular configuration. The temperature drop is better than the two BBOE systems but less than the double panel BTOE configuration.

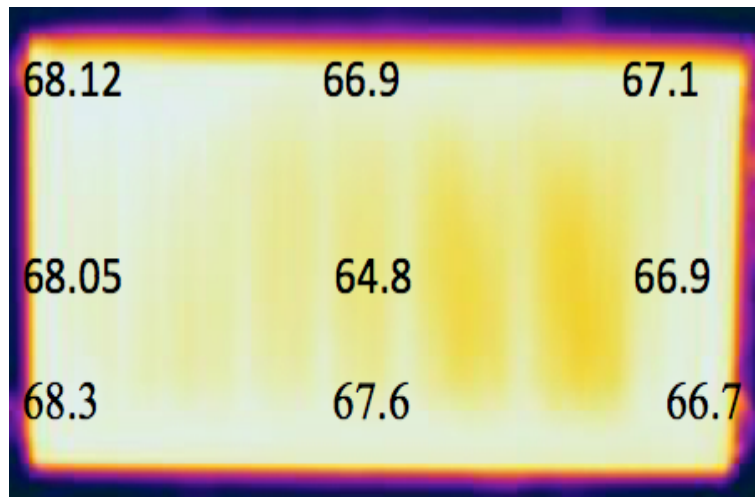


Figure 5-6 Temperature profile in a Single panel - °C (BTOE)

The temperature variances for the double and single panel radiator configuration are shown in Figure 5-7 and Figure 5-8. The arrow shows the point of entry of fluid in the radiator. The plot for the double panel very clearly shows the non-uniformity with the maximum temperature drop to 82% at the centre of the radiator. In a double panel BTOE unlike the BBOE system there is a temperature drop along the x-axis at both top and bottom of the radiator.

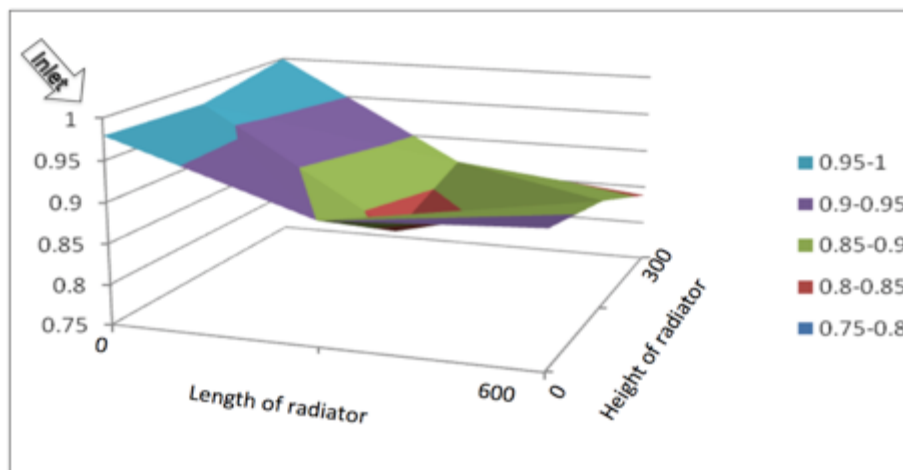


Figure 5-7: Normalised temperature Variance with respect to inlet (double BTOE)

The temperature variance for the single panel BTOE system illustrated in Figure 5-8 shows uniformity along both x and y-axis. The temperature drops to 98.2% at the exit with the coldest region being the centre at 94.9%.

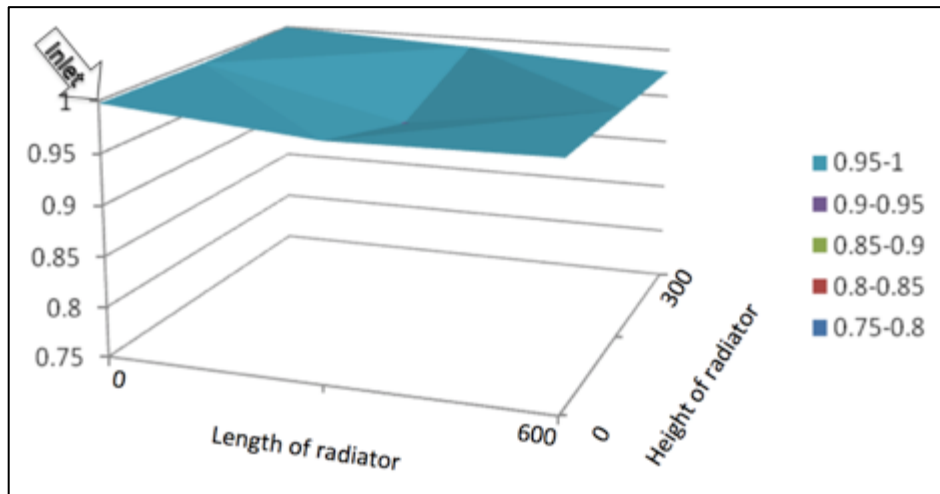


Figure 5-8: Normalised temperature variance with respect to inlet (single BTOE)

To further quantify the effect of point of entry on temperature distribution a non-dimensional parameter “n” has been used. This parameter is defined as a ratio of the temperature at the centre of the radiator and the average temperature at the four corners of the radiators. The parameter is coined to normalize the temperature whilst accounting for both cold and hot zones on the surface. Higher “n” value signifies more uniform temperature distribution. Figure 5-9 shows the value of this non-dimensional parameter for different combinations of radiator panel and entry condition. The results show that both double and single panel radiators in a BBOE system have similar values. A single panel BTOE system shows maximum uniformity in the temperature field.

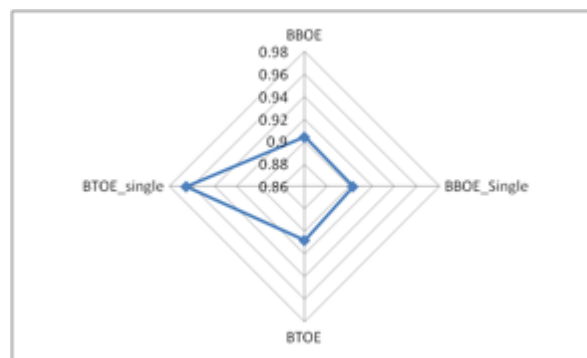


Figure 5-9: Variation of the non-dimensional parameter with respect to different radiator combination.

5.1.5 Summary of temperature distribution in double and single panel radiator

Experimental investigation has revealed that under full flow condition the thermal field is non-uniform and the non-uniformity depends on the radiator configuration and the point of fluid entry into the radiator. BTOE system gives the best results in terms of uniform

temperature field and temperature drop in the radiator. Higher temperature drops results in greater heat transfer from the fluid into the radiator.

Above investigation has also shown that there is minimal variation between a double and single pane radiator. The results do have a good co-relation to the observations from Akin [52] where the temperature drop is maximum in the centre of the radiator. Of the two flow configurations BTOE has shown better temperature distribution and higher temperature drop, but due to package constraints BBOE layout is preferable.

The investigation is also carried out at a single flow rate and temperature. Ward [29] has suggested that operating temperature has significant impact of radiator output. Following section investigates the effect of water temperature at the inlet of radiator and the effect of flow rate.

5.2 Temperature distribution analysis to quantify the effect of temperature and flow rate

To evaluate the thermal performance K-type thermocouples have been used to measure the inlet and outlet temperatures of water. For the purpose of the study the temperature distribution has been measured at three different boiler temperatures and two flow rates. The temperatures are 75°, 65° and 55 °C and the inlet water velocities are 0.32 m/s and 0.25 m/s, corresponding to two valve positions (100% and 50%).

c	Description
T	Temperature
ν	Mass flow rate
K_T	Constant

Table 5-1 description of parameters

To start the experiment the rig is set for the required temperature and flow rate as described in chapter 3. The experiments have been carried out in a temperature-controlled environment to ensure maximum thermal load on the system. Once the room temperature is stabilised the thermocouples, flow meter and pressure sensors are connected to the computer via the data logger. The operating temperature of the radiator is set using a radio frequency controller. The experiments are conducted using a needle valve and the flow rate of the

system is set to 50% [0.25m/s] and 100% [0.32m/s] valve opening position. The data logger software and a thermal camera are set to capture the readings and images at 10 sec interval. The thermal camera captures the flow of hot fluid within the radiator. The images are used to quantify the radiator surface temperature and help visualize the fluid path. The radiator turned on and left running for 60 minutes. The data for the present study are recorded once the system reached a steady state during heating phase.

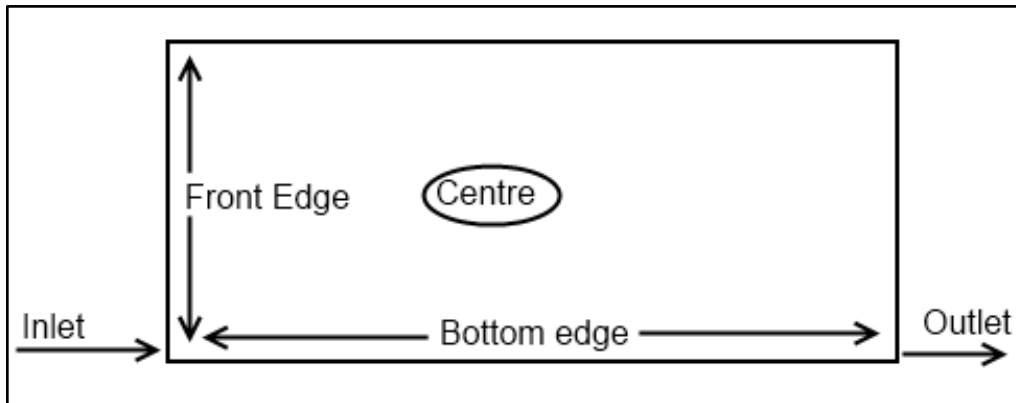


Figure 5-10: Schematic of panel layout

Temperature distribution on a single panel radiator has been analysed both qualitatively and quantitatively under two different flow rates and three temperature settings. The thermal images have been digitized to obtain the absolute temperature. The thermal images show temperature recorded at 9 set points on the panel. Due to the operating tolerance of the thermostat on the boiler, it has been observed that the inlet water temperature varied by a maximum of 4 °C. To quantify the non-uniformity of the inlet temperature a non-dimensional number K_T has been established by dividing each of the recorded temperatures by the inlet temperature. This non-dimensional number K_T is used to establish a relationship between flow rate and temperature distribution. The variation of the K_T value on the panel has been quantified in the graphs where, 0 on 'Length of radiator' axis represents the inlet and the 0 on the 'Height of radiator' axis represents the bottom edge of the radiator.

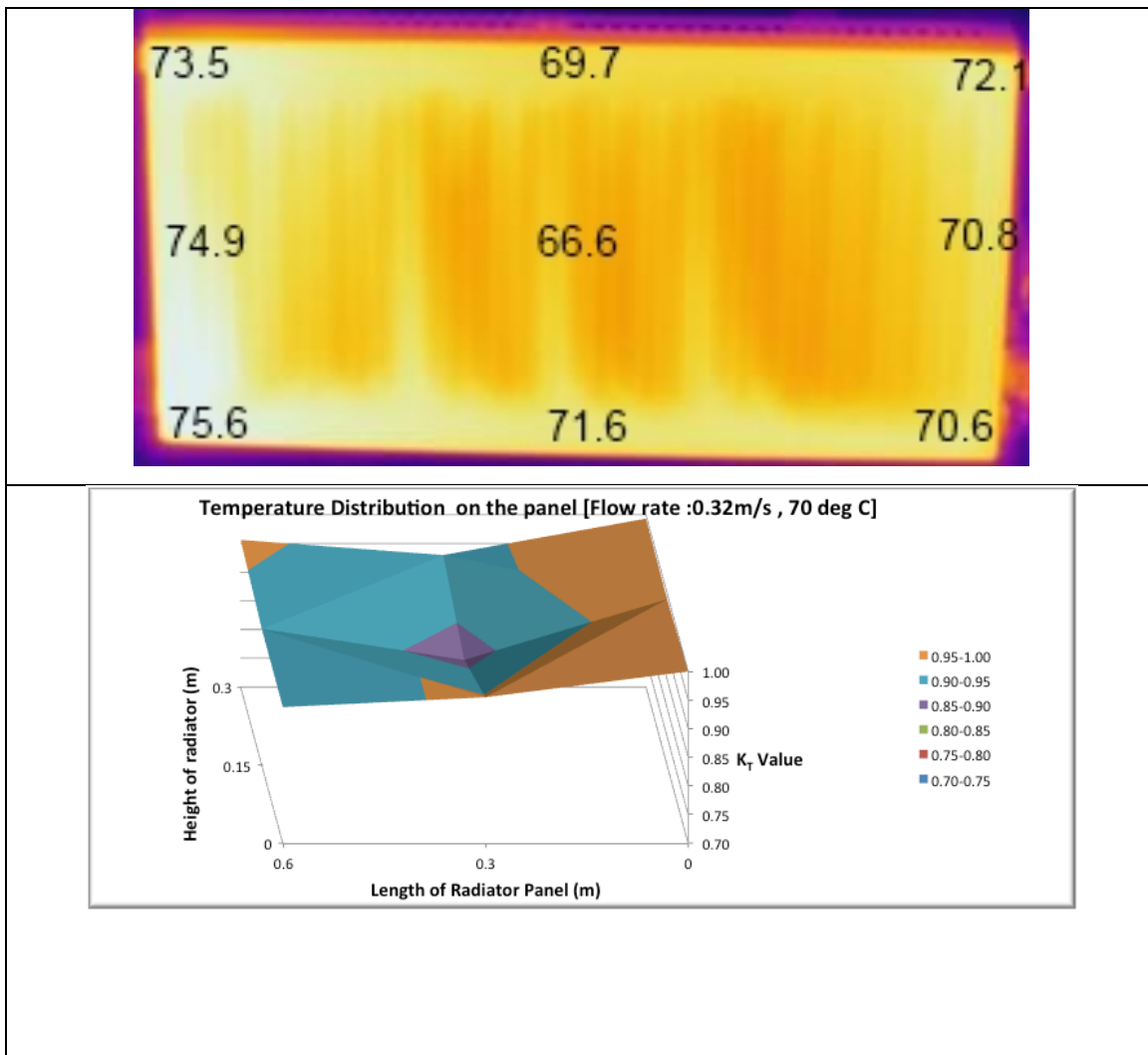


Figure 5-11: Temperature Distribution on Panel [Flow rate 0.32 m/s, 70 °C]

Figure 5-11 shows the temperature distribution at 70 °C and a flow rate of 0.32m/s. Maximum temperature of 75.6 °C is recorded at the inlet of the radiator. Consistent with previous findings it is observed that high percentage of the water rises up along the front edge as it enters the radiator and the temperature drops to 73.5 °C at the top. The temperature profile also suggests that the part of the hot water flow along the top of the radiator and a small portion flows down and to the centre of radiator. Along the bottom edge the temperature drops to 71.6 °C mid way and further to 70.6 °C at the outlet. The lowest temperature of 66.6 °C is recorded at the centre of the radiator suggesting limited flow in the centre. The graph show that the K_T value is above 0.9 along the outer edges of the radiator and the gradually drops towards the centre with K_T value of 0.88. The average K_T value for the given flow rate and temperature is 0.95. Higher average K_T values indicate more uniform temperature distribution.

Figure 5-12 represent temperature distribution at 70 °C and a flow rate of 0.25m/s. Due to the tolerance in the thermostat it can be seen that although the temperature was set to 70 °C using the controller the inlet temperature is 71 °C. For this flow rate it can also be seen that the temperature drop along the front edge is greater than 0.32m/s [100%] flow rate. Along the bottom edge, contrary to 100% flow rate the temperature drop between the midway and outlet point is negligible. Lowest temperature of 54.6 °C is recorded at the centre of the radiator, corresponding to a K_T value of 0.77 as opposed to 0.88 at 0.32m/s.

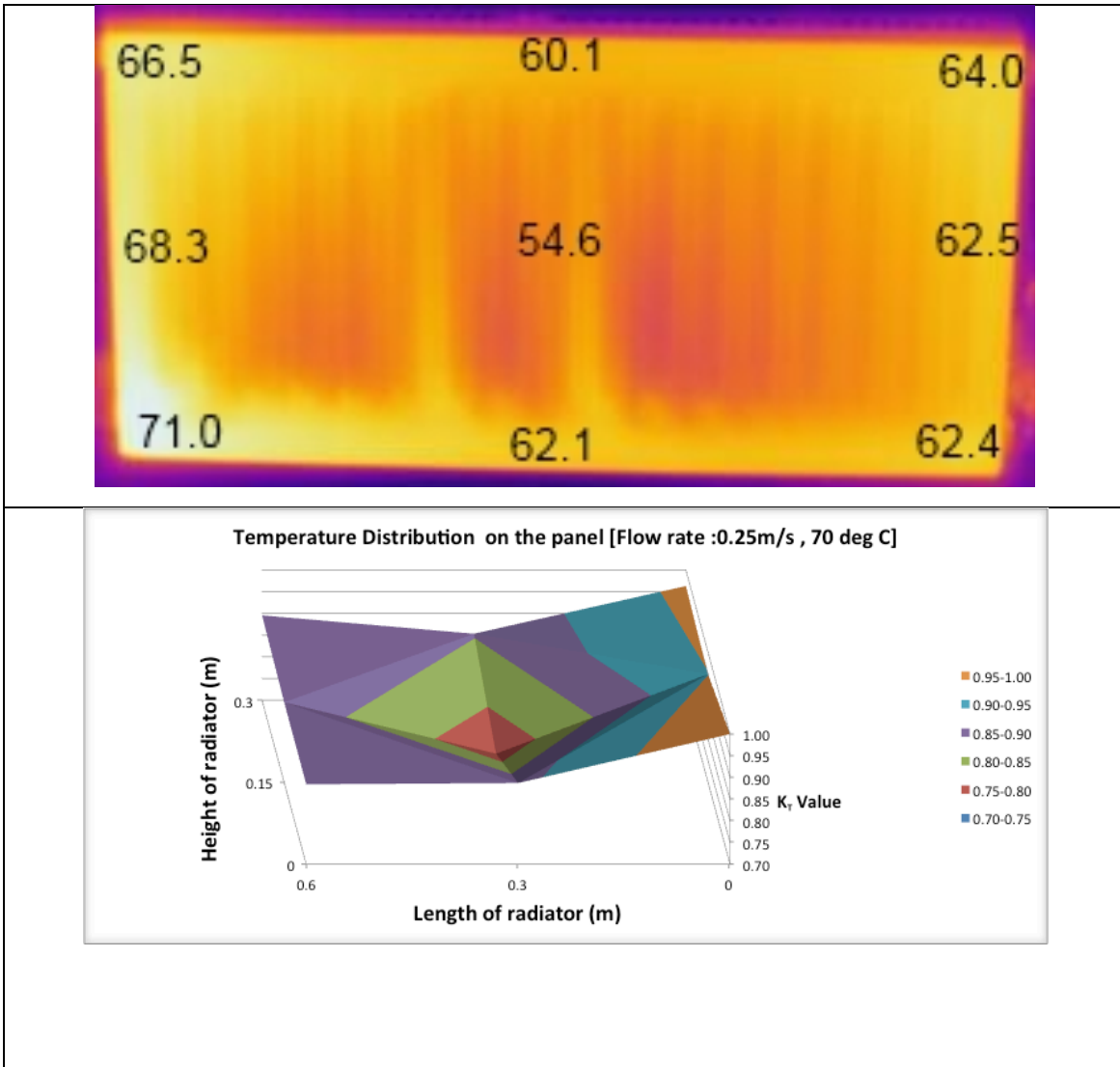


Figure 5-12: Temperature Distribution on the panel [Flow rate: 0.25 m/s, 70 °C]

The graph clearly indicates that the variation in K_T value is very high compared to 100% flow rate. The temperatures at far edge are fairly uniform with K_T values of 0.88 suggesting continuous flow along the edge. For 0.25 m/s flow rate the average K_T value is 0.90, which is 5.8% less than the average K_T value at 0.32 m/s flow rate.

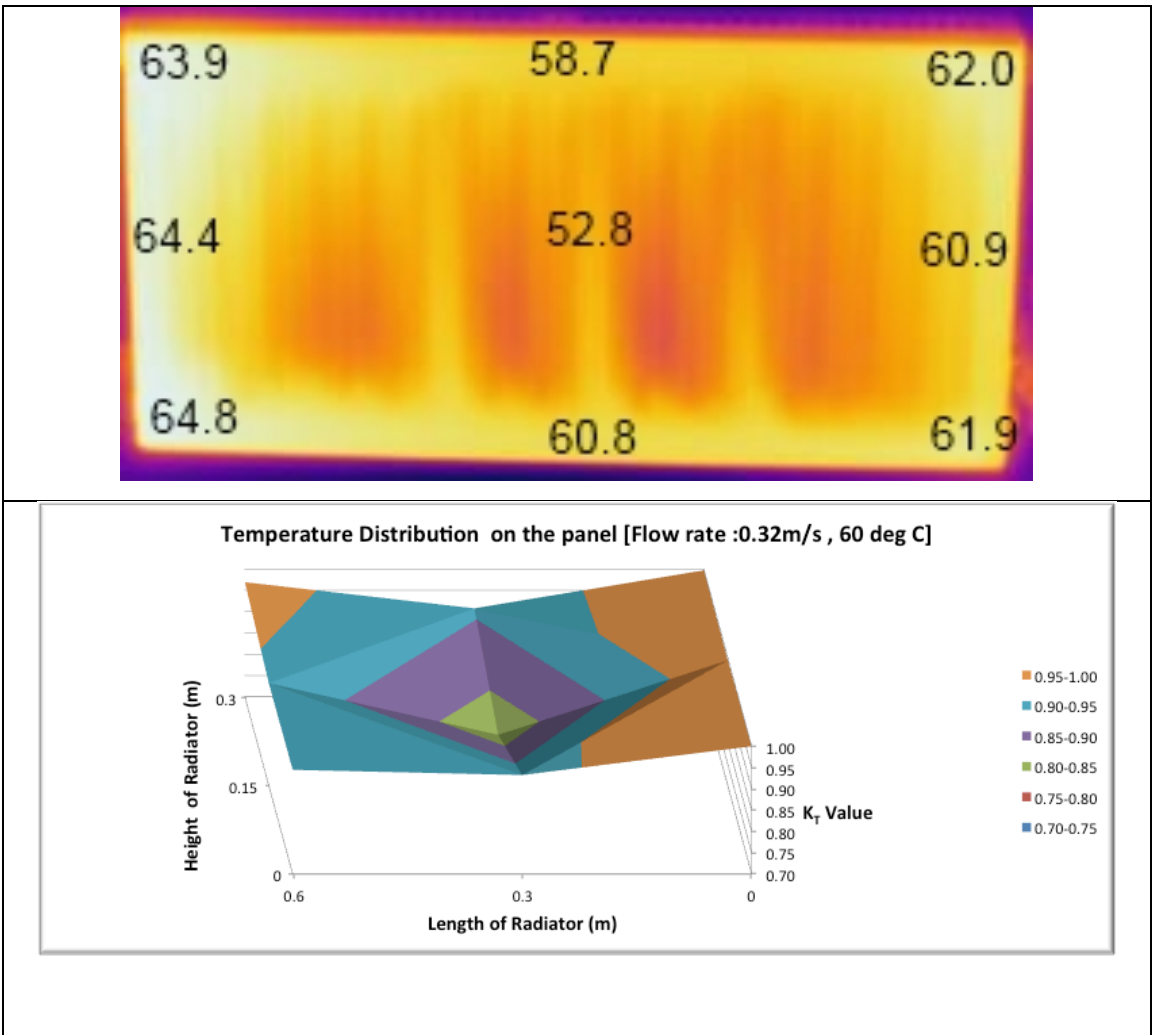


Figure 5-13: Temperature distribution on the panel [Flow rate: 0.32m/s, 60 °C]

Temperature distribution at 60 °C and a flow rate of 0.32m/s is shown in Figure 5-13. A maximum temperature of 64.8 °C is recorded at the inlet of the radiator. In general the trend is very similar to the radiator at 70 °C and 0.32 m/s flow rate. The temperature along the front edge is fairly uniform with K_T values of 1, 0.99 and 0.99 for the three points on the edge. The top edge shows a drop in the K_T value at the centre to 0.9 and a rise to 0.97 corresponding to 62.0 °C. Lowest temperature of 52.8 °C is recorded at the centre of the radiator, corresponding to a K_T value of 0.82. For this setup the average K_T value is 0.95, which is the same as the radiator at 70 °C and 0.32 m/s flow rate.

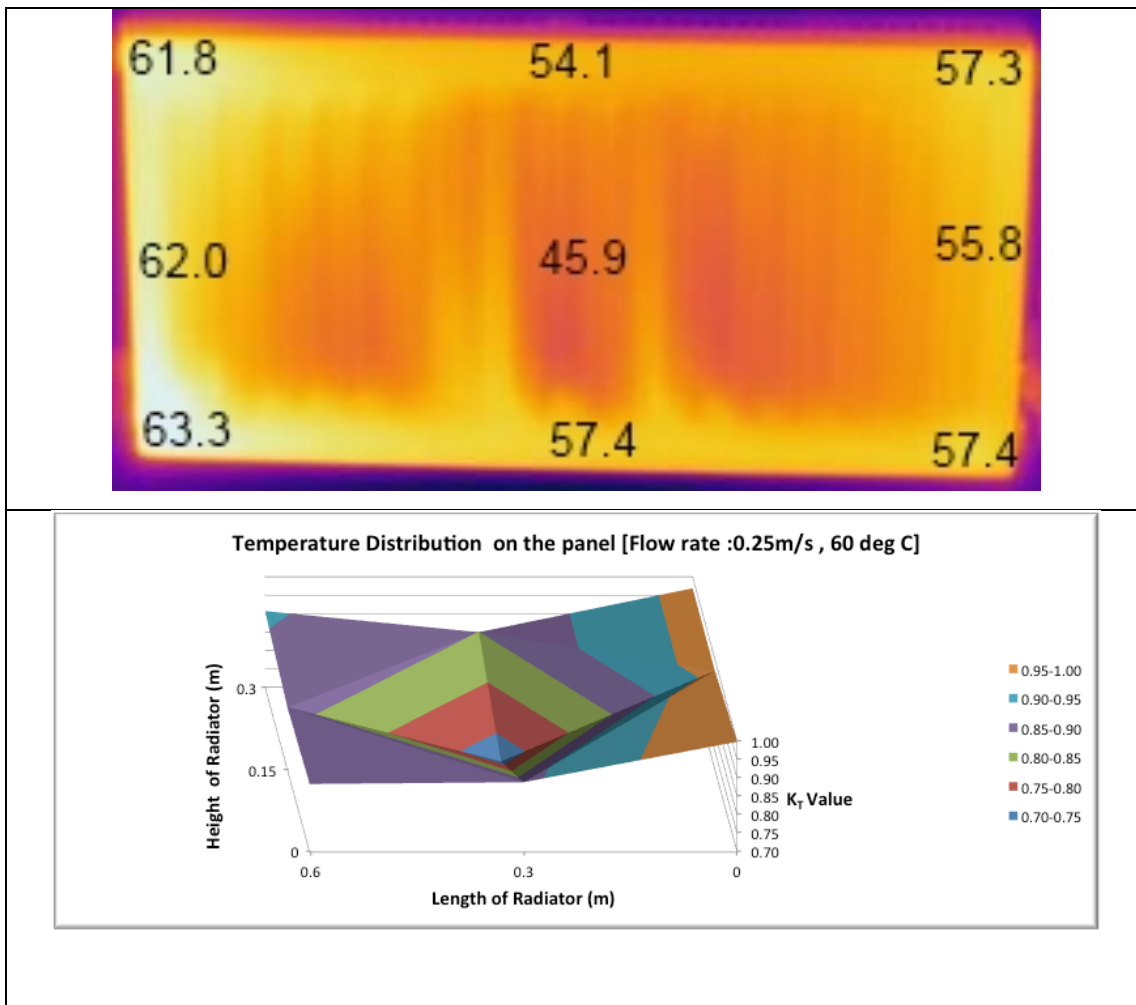


Figure 5-14: Temperature Distribution on the panel [Flow rate: 0.25m/s, 60 °C]

Figure 5-14 represent temperature distribution at 60 °C and a flow rate of 0.25m/s. The inlet temperature is 63.3 °C. The relative temperature along the front edge is lower than the radiator at 60 °C and 100% flow rate but with a similar trend of K_T values; 1, 0.97 and 0.97 respectively. At the bottom edge the temperature drop between the inlet and the midway point is 5.9 °C as opposed to 4 °C at 100% flow rate. It is also observed that in this configuration, along the bottom edge the temperature drop between the midway and outlet point is negligible. Lowest temperature of 45.9 °C is recorded at the centre of the radiator, corresponding to a k value of 0.72 as opposed to 0.82 at 0.32m/s at 60 °C. For 0.25 m/s flow rate at 60 °C the average K_T value is 0.90 which is the same the 50 % flow rate at 70 °C.

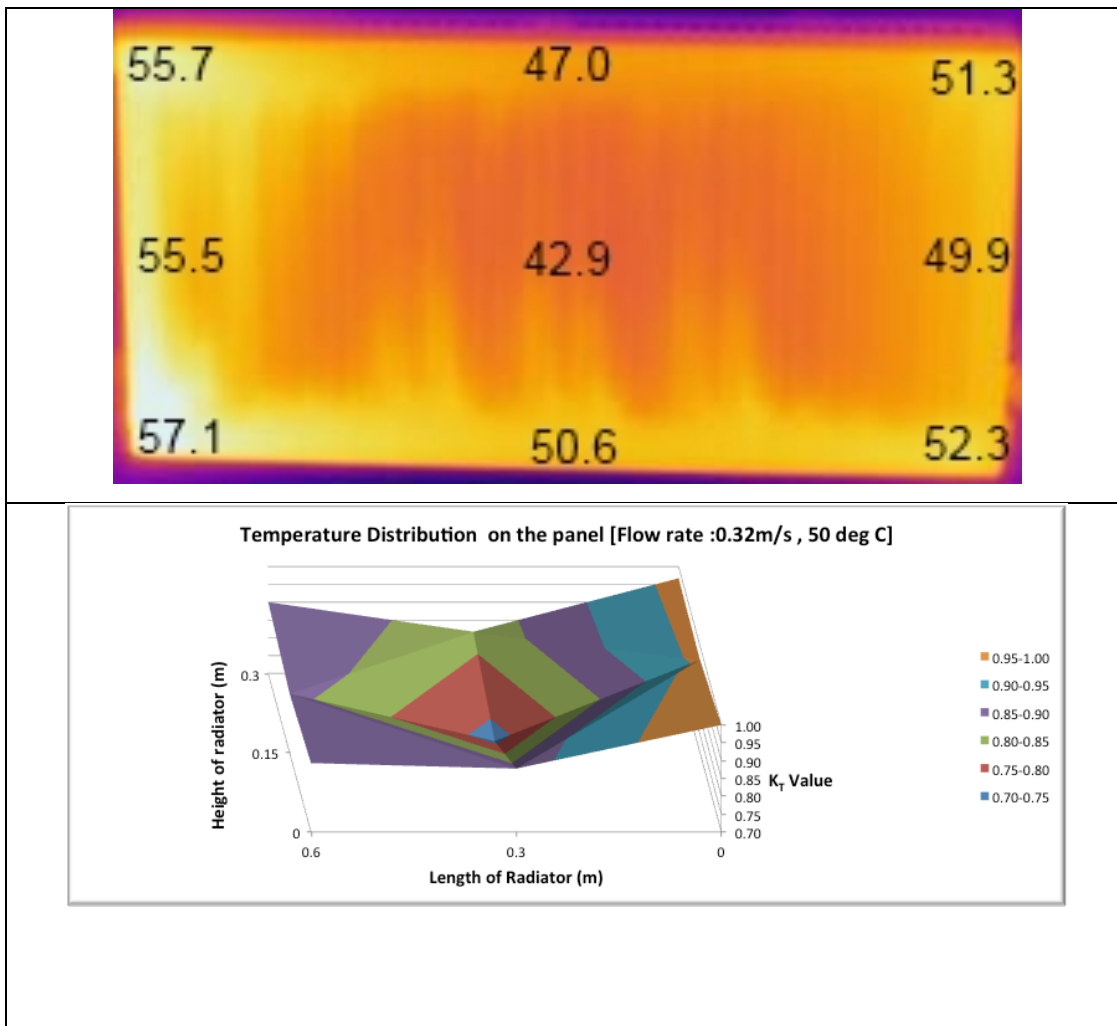


Figure 5-15: Temperature distribution on the panel [Flow rate: 0.32m/s, 50 °C]

The temperature profile on the panel at 50 °C at 0.32 m/s (100%) flow rate is very similar to profiles observed at 70 °C and 60 °C at the same flow rate. It can be seen in Figure 5-15 that the highest temperature is at the inlet at 57.1 °C and the temperature along the front edge is also fairly uniform suggesting that maximum flow is along this edge as the water enters the radiator. Minimum temperature of 42.9 °C is recorded at the centre of the radiator with a K_T value of 0.73. The average K_T value is 0.89 which lower than the average K_T values at 70 °C and 60 °C at the same flow rate.

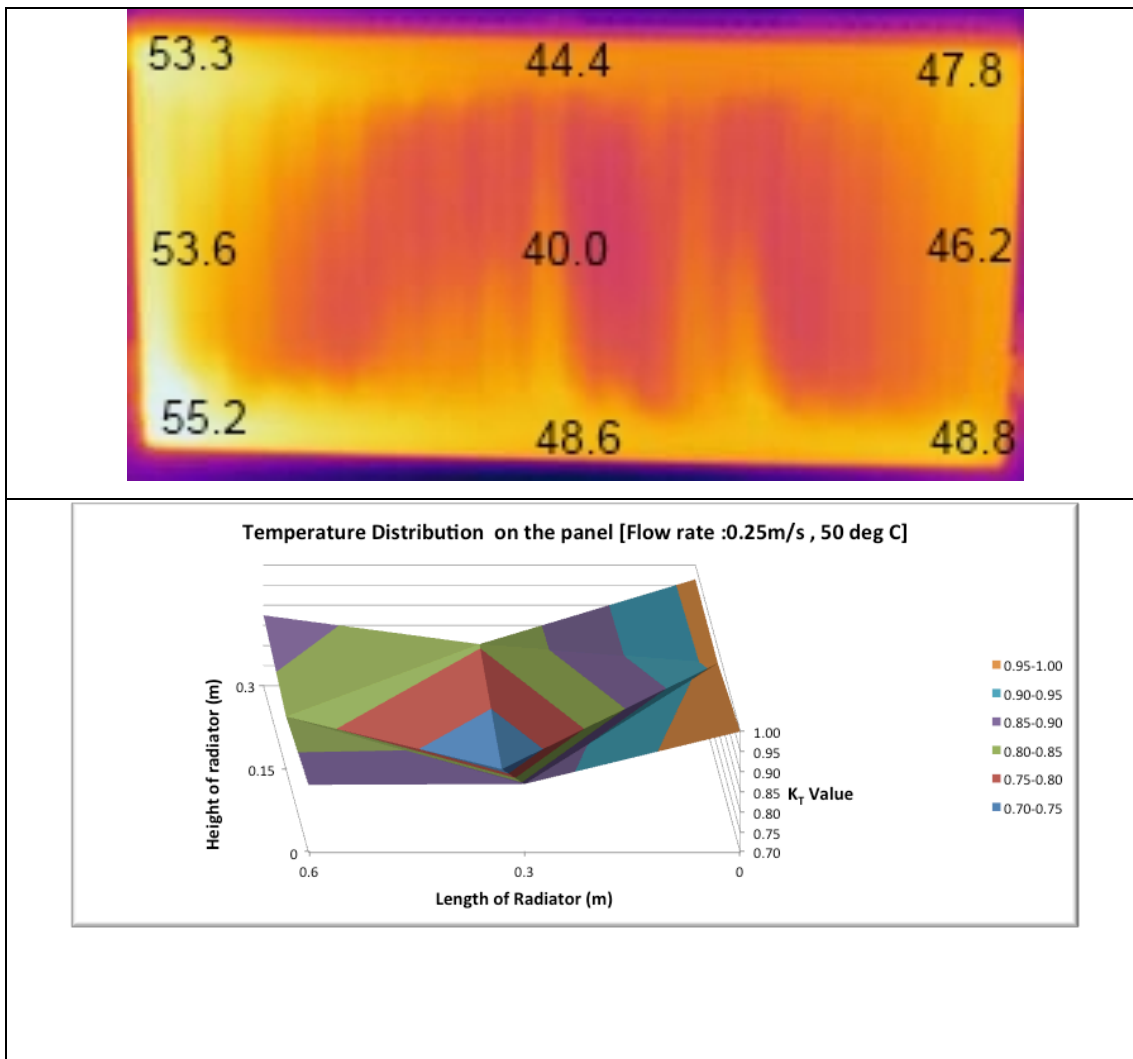


Figure 5-16: Temperature distribution on the panel [Flow rate : 0.25m/s, 50 °C]

Figure 5-16 shows the temperature distribution on the panel at 50 °C and 0.25 m/s flow rate. Along the front edge it drops from 55.2 °C at the inlet to 53.6 °C to the centre of the front edge and then stays fairly uniform to the top. The K_T values are 1, 0.96 and 0.96 respectively. The temperature drops by 6.6 °C between the inlet and the midway of the bottom edge with a marginal rise to the outlet of radiator. Minimum temperature of 40.0 °C is recorded at the centre of the radiator with a K_T value of 0.70. The average K_T value is 0.88 which is very similar to the average values at 50% flow rate at 70 °C and 60 °C.

The study has given a clear indication of the flow path of hot water in each of the cases. It has been observed that the flow path is unique for each of the cases. This indicates that the flow rate and flow configuration along with the buoyancy effect of the hot water plays a significant role in the temperature distribution on the panel. The operating temperature would in turn affect the buoyancy. Table 5-2 summarises the average K_T values, K_T values at the centre and temperature drop between inlet and outlet.

Table 5-2: Summary of key factors

Setup	Average K_T Value	K_T value at the centre	Temperature drop between inlet and outlet (°C)
70 °C @0.32 m/s	0.95	0.88	4.7
70 °C @0.25 m/s	0.90	0.77	8.2
60 °C @0.32 m/s	0.95	0.82	3.6
60 °C @0.25 m/s	0.90	0.72	7.4
50 °C @0.32 m/s	0.89	0.73	6.2
50 °C @0.25 m/s	0.88	0.70	7.4

The results clearly indicate that the most uniform temperature distribution is achieved at 0.32 m/s (100%) flow rate at 70 °C and 60 °C, but maximum heat output is achieved with maximum temperature drop between inlet and outlet. The above results show that maximum temperature drop between inlet and outlet is achieved at 70 °C at 0.25 m/s (50%) flow rate. Although the average K_T value is 0.9, it is an acceptable compromise specially when the temperature drop is almost double and also reduced flow rate would result in lower pumping power, which in turn will reduce operational cost.

5.2.1 Summary of temperature distribution at different flow rates

Thermal investigation has shown that the flow rate and flow configurations have a significant impact on the temperature distribution and temperature drop across the radiator. Operating temperature of the water also contributes towards the performance of radiators. The investigation has been carried out on a 300 mm x 600 mm radiator only. It is important to understand the flow parameters in the radiator and quantify pressure drop and flow distribution as a function flow rate, configuration and radiator size. Hence further investigation is undertaken in 5.3, 5.4 and chapter 6 to quantify the flow parameters independent of temperature.

5.3 Pressure drop across the radiator

Head loss in standalone alone system can be mainly attributed to loss at entry, loss in the radiator panel and loss at the exit. Where, loss in the radiator is a combination of frictional loss and the losses associated with complexity of fluid path for the given condition. As seen in Figure 3-3, to capture the effect of inlet and outlet connectors and the radiator, care was taken that the pressure gauge 3 was located at the upstream of inlet connection and gauge 6 at the downstream outlet connector and flow control valve. For a set valve position, it has been observed that there is approximately 10% variation in the flow velocity. Head loss in a system is computed by Equation 5-1. It is very difficult to determine the surface friction coefficient for the radiator due to the complexity of the geometry and access to the flow path. Hydraulic diameter is typically calculated by using Equation 5-5. Due to wide range of path length within the radiator for different pipe layouts and panel configuration, hydraulic diameter of the inlet pipe has been used as for the study. 'K' is a constant for the system under consideration dependant on friction co-efficient of system and hydraulic diameter.

$$H_f = f_c Leq \frac{V^2}{2gDh} = K \frac{V^2}{2g} = \frac{\Delta P}{\rho g}$$

Equation 5-1 Head loss in a pipe

Where

$$K = F(f_c, Leq, D_H)$$

Equation 5-2 Loss co-efficient as a function of friction and hydraulic diameter

Therefore

$$K = \frac{H_f \times 2g}{V^2} = \frac{2 \times \Delta P}{\rho V^2}$$

Equation 5-3 Loss co-efficient as function of head loss

$$R_e = \frac{\rho V D}{\mu}$$

Equation 5-4 Reynolds number

$$D_H = \frac{4A}{P}$$

Equation 5-5 Hydraulic diameter of pipe

Above equations have been used to analyse the pressure drop that has been measured across two radiator sizes for two flow configuration and five flow rates.

The rational for selecting the criteria for investigations are as mentioned below

Rationalisation of Flow Configuration

Literature review has suggested that the TBOE (Top Bottom Opposite End) and BBOE (Bottom Bottom Opposite End) are common flow configurations with TBOE layout offering maximum temperature drop across the radiator. Package constraints discussed in chapter 4, have suggested that the only two configurations possible in a stand-alone system are BBOE and BTOE. Hence it is suggested that for the current investigation flow configurations are limited to BBOE and BTOE.

Rationalisation of Flow range

Selection of the pump is discussed in detail in chapter 4 as part of the design and development of a stand-alone radiator. The pump selected for the system has a max flow rate of 11 lpm and does not have an electronic control for the for flow rate. As stated above, flow is controlled using a needle valve. It has been observed that a quarter turn (90°) of the needle valve corresponds to approximately 1 lpm. In addition during the thermal evaluation of the radiator, the flow rate could not be reduced below 5 lpm, as the fluid around the boiler would start boiling. This resulted in reducing the initial range discussed in Table 3-1 to 6 lpm to 11 lpm with 5 increments.

Rationalisation of Radiator size

Stand-alone radiators are made in a range of sizes as tabulated in Table 6-1. Experimental investigation is limited to the smallest and the largest radiator. This allows investigation to capture the effect of length and height over the entire range.

By Rationalising the flow configuration, flow rate, and radiator configuration and size, the experimental work has reduced to a manageable size, without compromising the quality and scope of information. The ranges of parameters are tabulated in the following section.

Hence in summary the radiator sizes used are

300 mm x 600 mm (height x length) → Single panel K1 radiator

600 mm x 1000 mm (height x length) → Single panel K1 radiator

The above radiators were used in following configurations

BBOE → Bottom - Bottom Opposite End

BTOE → Bottom – Top Opposite End

5.3.1 Pressure drop analysis in a 3060 radiator

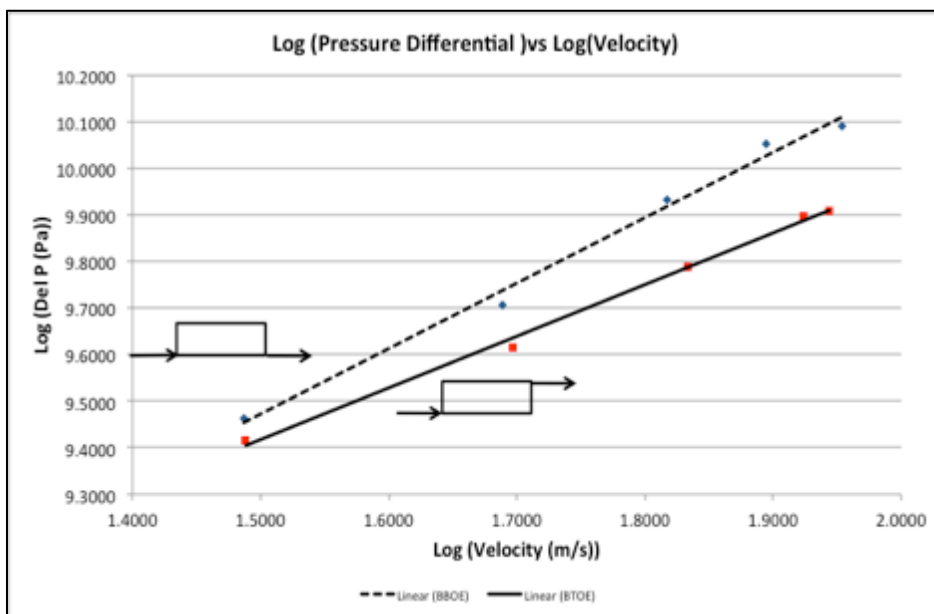


Figure 5-17 Variation of pressure differential with velocity (300 x 600 mm radiator)

Pressure drop against velocity has been illustrated in Figure 5-17 to study the trend for frictional head loss in a 300 mm x 600mm. Two flow configurations BBOE and BTOE have been illustrated in the graph. Log of pressure differential has a linear co-relation to the log

of the velocity for both the configurations. The pressure drop slope for the BBOE trend line suggests that the pressure drop is greater than the BTOE flow configuration. The pressure differential at initial flow rate is comparable between the two configurations with a variation of only 300 Pa. BTOE flow configuration has a more gradual slope compared to BBOE. The pressure drop is 24112 Pa in a BBOE whereas the pressure drop is 20112 Pa for the BTOE layout at peak flow velocity of 7 m/s. The pressure drop in a BBOE system is higher than BTOE by 4000 Pa.

5.3.2 Loss Co-efficient analysis in a 3060 radiator

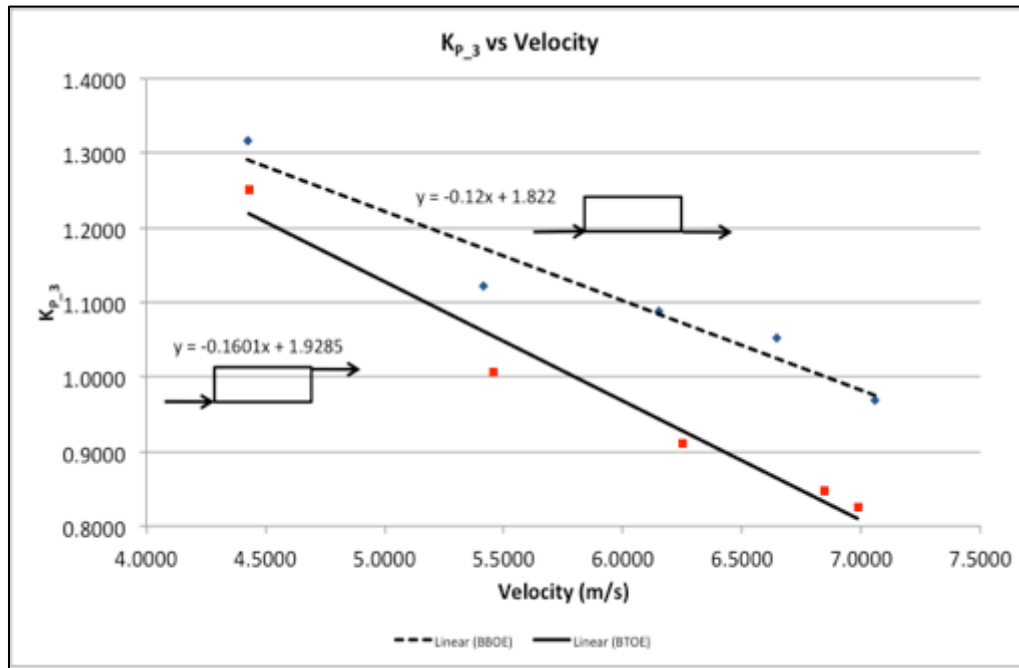


Figure 5-18 Variation of Loss co-efficient with change in velocity (300 x 600 mm radiator)

The pressure measured at the inlet and outlet of the radiator was used to compute the pressure drop, which in turn was used to compute the loss co-efficient based on Equation 5-3. Figure 5-18 compares the non-dimensional loss co-efficient for flow configurations. Loss co-efficient against velocity has been illustrated in Figure 5-18 to study the trend for the two pipe layouts in a single panel radiator. BBOE and BTOE configurations have similar trends, where the value for the loss co-efficient K drops with the increase in velocity. BTOE configuration has a lower loss co-efficient than BBOE configuration at all velocities. K at 4.2m/s for a single panel radiator in a BBOE layout was 1.31 and 1.25 for a BTOE layout. The loss co-efficient was found to be 0.968 and 0.824 at peak velocity of 7 m/s for BBOE and BTOE configurations respectively. The slopes vary by 25% for the two layouts with BTOE having a higher slope. The two systems show differences as the flow develops, and the path becomes more complicated.

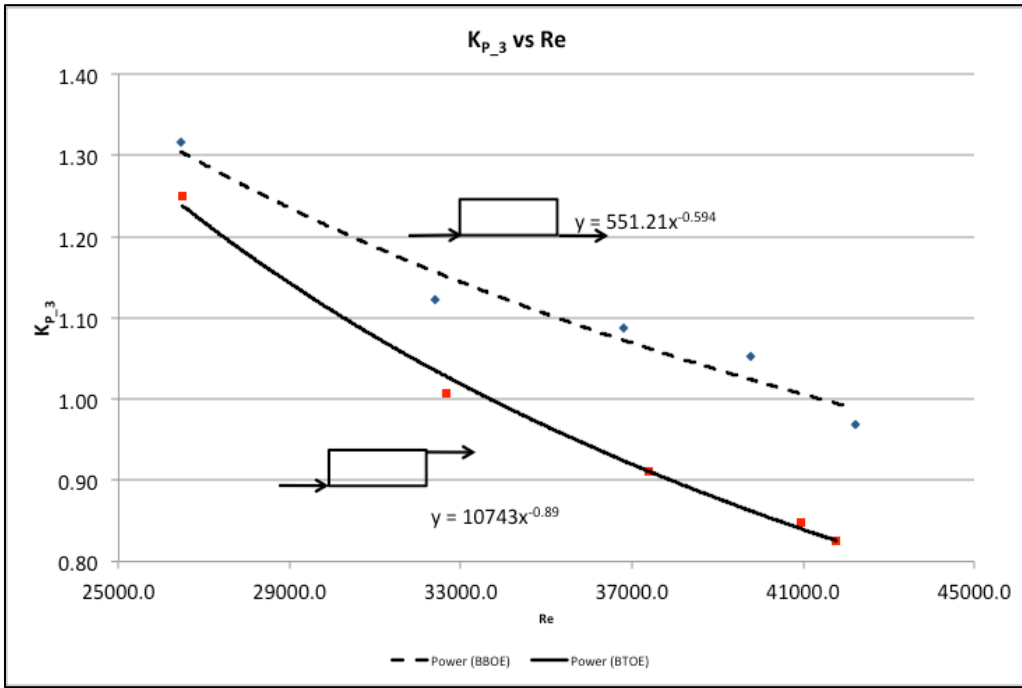


Figure 5-19 Variation of Loss co-efficient with the change in Reynolds Number (300 x 600 mm radiator)

For a straight pipe the frictional co-efficient is expressed by Equation 5-6 [8], where A is constant for a system depending on fouling. Loss co-efficient, being a function of frictional co-efficient and hydraulic diameter, can effectively be expressed as a function of the Reynolds number.

$$f_c = \frac{A}{Re^{0.145}}$$

Equation 5-6 Friction loss as function of Reynolds number

As indicated by the curves in Figure 5-19, the loss coefficient in the radiator decreases with an increase in Reynolds number for both pipe layouts investigated. In the BBOE configuration the loss co-efficient is 1.32 at 26460 Reynolds number and 0.97 at 42209.3 Reynolds number. The loss co-efficient for a BBOE configuration can be expressed as a function of Reynolds number by Equation 5-7.

$$K_{P_3B_Exp} = \frac{551.21}{(Re)^{0.594}}$$

Equation 5-7 Loss co-efficient for 3060 radiator – BBOE Exp

The loss co-efficient in the BTOE configuration is smaller than in the BBOE layout with the K value of 1.25 at 26503.4 Reynolds number and 0.82 at 41775.8 Reynolds number. Similarly BTOE configuration can be expressed by Equation 5-8

$$K_{P_3T_Exp} = \frac{10743}{(Re)^{0.89}}$$

Equation 5-8 Loss co-efficient for 3060 radiator – BTOE Exp

On comparing Equation 5-7 and Equation 5-8 it can be observed that the constant A for the BBOE configuration is 551.21 while in a BTOE layout it is 10743.

The exponent values for the Reynolds number are 0.594 (eq.6) and 0.89 (eq.7) for the BBOE and BTOE layouts in a 300 x 600 radiator. The exponents vary by 33.25%.

RADIATOR SIZE	LOSS COEFFICIENT	A	x
3060_BBOE	$K_{P_3B_Exp}$ $= \frac{551.21}{(Re)^{0.594}}$	551.21	0.594
3060_BTOE	$K_{P_3T_Exp}$ $= \frac{10743}{(Re)^{0.89}}$	10743	0.89

Table 5-3 Loss co-efficient 300 x600 radiator

5.3.3 Pressure drop analysis in a 6100 radiator

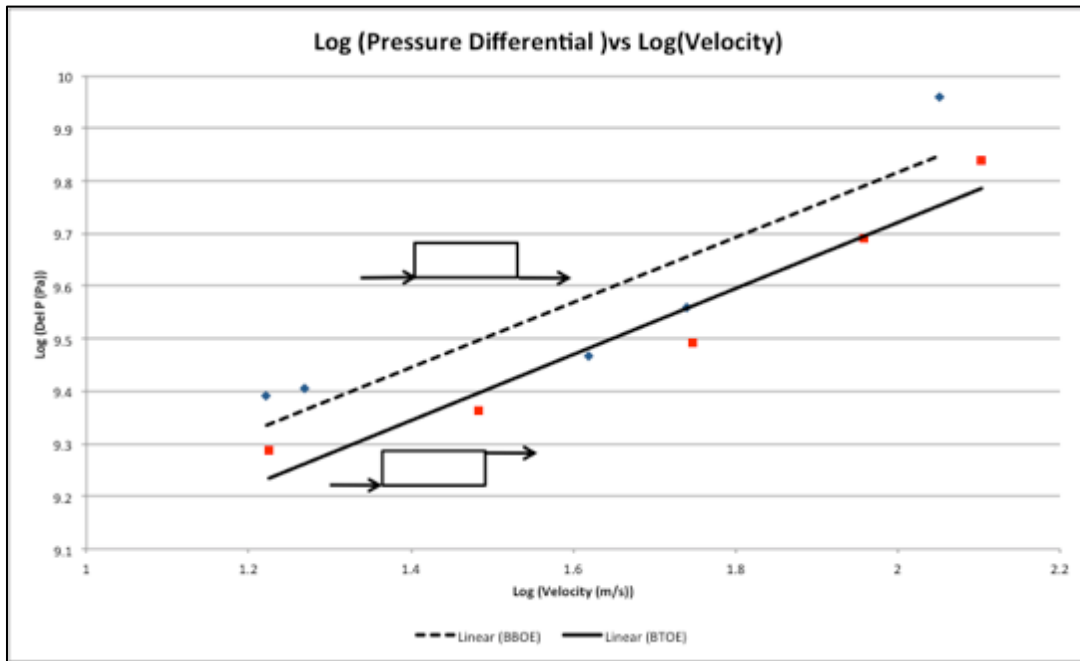


Figure 5-20 Variation of pressure differential with velocity (600 x 1000 mm radiator)

Pressure drop against velocity has been illustrated in Figure 5-20 to study the trend for frictional head loss in a 600 mm x 1000mm. Two flow configurations BBOE and BTOE have been illustrated in the graph. Log of pressure differential has a linear co-relation to the log of the velocity for both the configurations. The pressure drop slopes for the BBOE and BTOE flow configuration are very similar. BTOE flow configuration is consistently lower than BBOE over the range of flow rates. The pressure drop is 21173.75 Pa in a BBOE whereas the pressure drop is 18774.75 Pa for the BTOE layout at peak flow velocity. The pressure drop in a BBOE system is higher than BTOE by 2399 Pa at similar velocities 300 x 600 mm radiator had a variation of 4000 Pa between BBOE and BTOE.

5.3.4 Loss Co-efficient analysis in a 6100 radiator

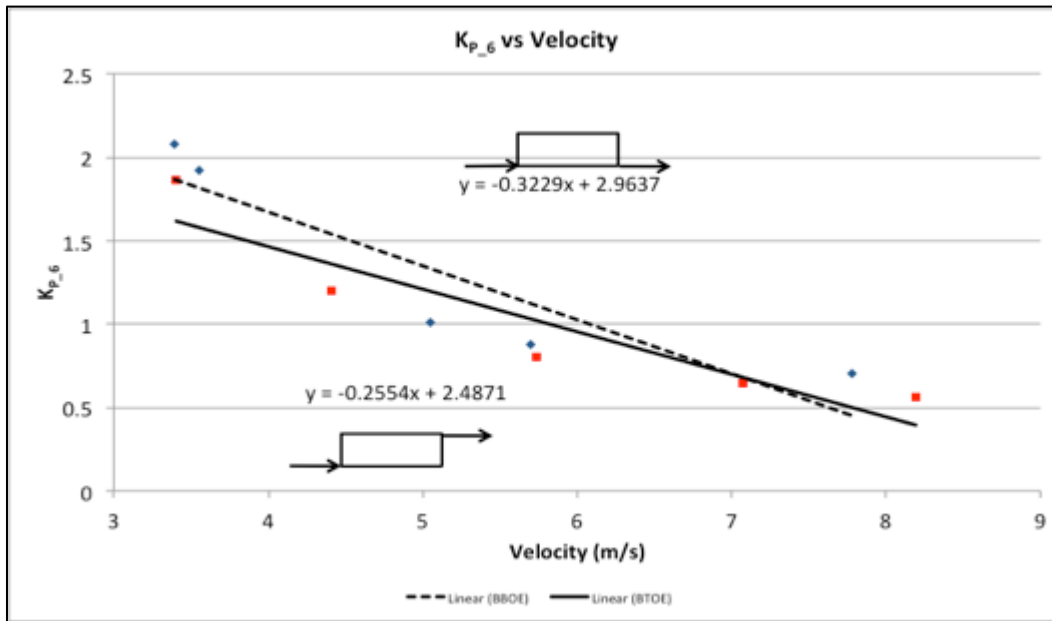


Figure 5-21 Variation of Loss co-efficient with change in velocity (600 x 1000 mm radiator)

Figure 5-21 compares the non-dimensional loss co-efficient for flow configurations. Loss co-efficient against velocity has been illustrated in Figure 5-21 to study the trend for the two pipe layouts in a single panel 600mm x 1000 mm radiator. BBOE and BTOE configurations have different slopes, where the value for the loss co-efficient K drops with the increase in velocity. BTOE configuration has a lower loss co-efficient than BBOE configuration at lower velocities. K at 3.4m/s for a single panel radiator in a BBOE layout was 2.01 and 1.86 for a BTOE layout. The loss co-efficient was found to be 0.699 and 0.559 at peak velocity of ~8 m/s for BBOE and BTOE configurations respectively. In BTOE configuration larger radiator 600mm x 100mm has a loss coefficient of 0.64 at 7 m/s compared to 0.82 in a 300 mm x 600 mm radiator.

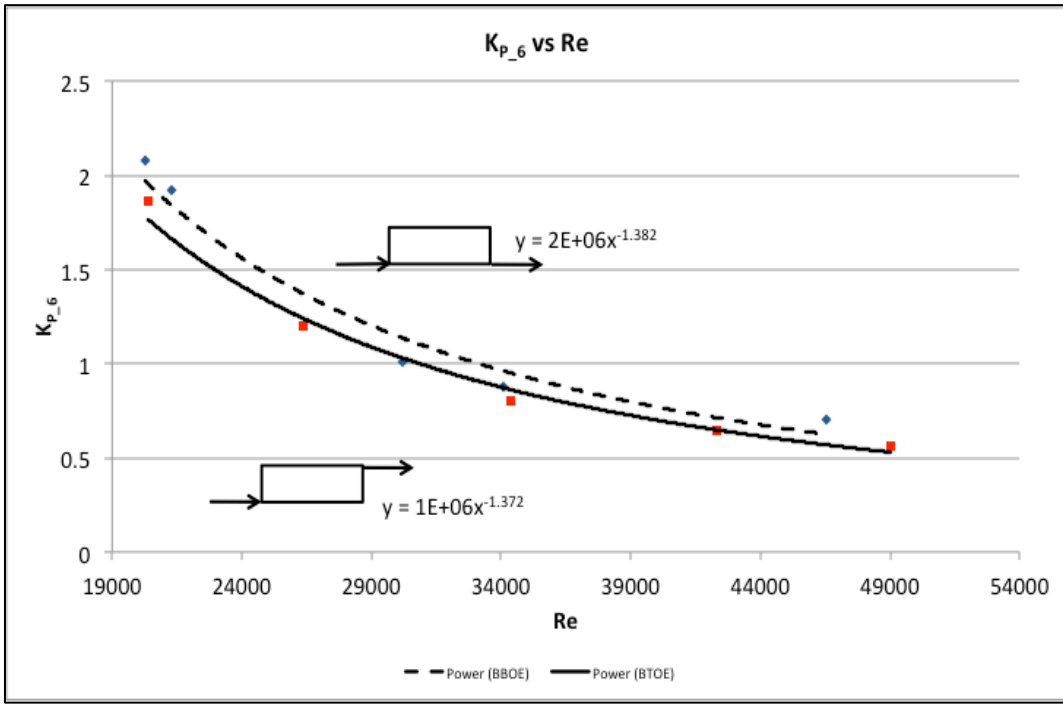


Figure 5-22 Variation of Loss co-efficient with change in Reynolds number (600 x 1000 mm radiator)

Similar to 300 x 600 mm radiator the curves in Figure 5-22 indicate that the loss coefficient in the radiator decreases with an increase in Reynolds number for both pipe layouts investigated. In the BBOE configuration the loss co-efficient is 2.08 at 20304.45 Reynolds number and 0.699 at 46529.35 Reynolds number. The loss co-efficient for a BBOE configuration can be expressed as a function of Reynolds number by Equation 5-9

$$K_{P_6B_Exp} = \frac{2 \times 10^6}{(Re)^{1.382}}$$

Equation 5-9 Loss co-efficient for 6100 radiator – BBOE Exp

The loss co-efficient in the BTOE configuration is greater than in the BBOE layout with the K value of 1.86 at 20364.25 Reynolds number and 0.559 at 49011.72 Reynolds number. Similarly BTOE configuration can be expressed by Equation 5-10.

$$K_{P_6T_Exp} = \frac{1 \times 10^6}{(Re)^{1.372}}$$

Equation 5-10 Loss co-efficient for 6100 radiator – BTOE Exp

On comparing Equation 5-9 and Equation 5-10 it can be observed that the constant A for the BBOE configuration is 2e6, while in a double panel BTOE layout it is 1e6.

The exponent values for the Reynolds number are 1.382 and 1.372 for the BBOE and BTOE layouts in a 600 X 1000 mm radiator. The exponents vary by 0.7% compared to 33% in 3060 radiators.

RADIATOR SIZE	LOSS COEFFICIENT	A	x
6100_BBOE	$K_{P_6B_Exp}$ $= \frac{2 \times 10^6}{(Re)^{1.382}}$	2×10^6	1.382
6100_BTOE	$K_{P_6T_Exp}$ $= \frac{1 \times 10^6}{(Re)^{1.372}}$	1×10^6	1.372

Table 5-4 Loss co-efficient for 600 x1000 mm radiator

5.3.5 Summary of pressure drop across radiator

Detailed experimental evaluation of radiators under different flow configurations and flow rates for a 3060 (300 mm x 600 mm) radiator and 6100 (600 mm x 1000 mm) radiator have been conducted. The port diameter for the two radiators is same at 6mm effective diameter. Pressure drop across the radiator between the inlet and the outlet port have been measured over a range of flow velocities. It can be seen that for a given radiator as the flow velocity increases the pressure drop increase. A non-dimensional loss co-efficient K has been developed to observe the behaviour with the change in Reynolds number.

5.4 Pressure variation analysis in a radiator

For a domestic radiator key function is to heat surrounding area as quickly and as effectively as possible. Effectiveness of radiator depends on operating temperature and temperature distribution. As mentioned in literature review it is very important to have a high temperature exponent to maximise the heat transfer rate. Temperature distribution is directly affected by the flow distribution, where a uniform flow distribution is expected to result in an almost uniform temperature distribution. It is very difficult to quantify the flow distribution in an opaque metal radiator with multiple channels. Flow distribution is dictated by the pressure distribution. As flow always occurs from high-flow energy zone to low-energy zone, knowing the pressure distribution in a radiator helps us predict the flow profile in a radiator.

In figure 5-28 we have compared a 300 mm x 600mm single panel K1 radiator in two different flow configurations. In the first column we have the BBOE (Bottom-Bottom Opposite End) configuration and in the second column we have the BTOE (Bottom-Top Opposite End) configuration. Each of the flow configurations have been compared over five flow rates ranging between 3.2 m/s to 8.5 m/s. Pressure was measured at the inlet, outlet and six points around the periphery of the radiator as shown in Figure 5-23. The measured data was digitally processed. Local pressures (1-6) were divided by the inlet pressure for the given flow rate and configuration in order to normalise the values.



Figure 5-23 Radiator setup for pressure distribution

5.4.1 Pressure variation analysis in a 3060 radiator

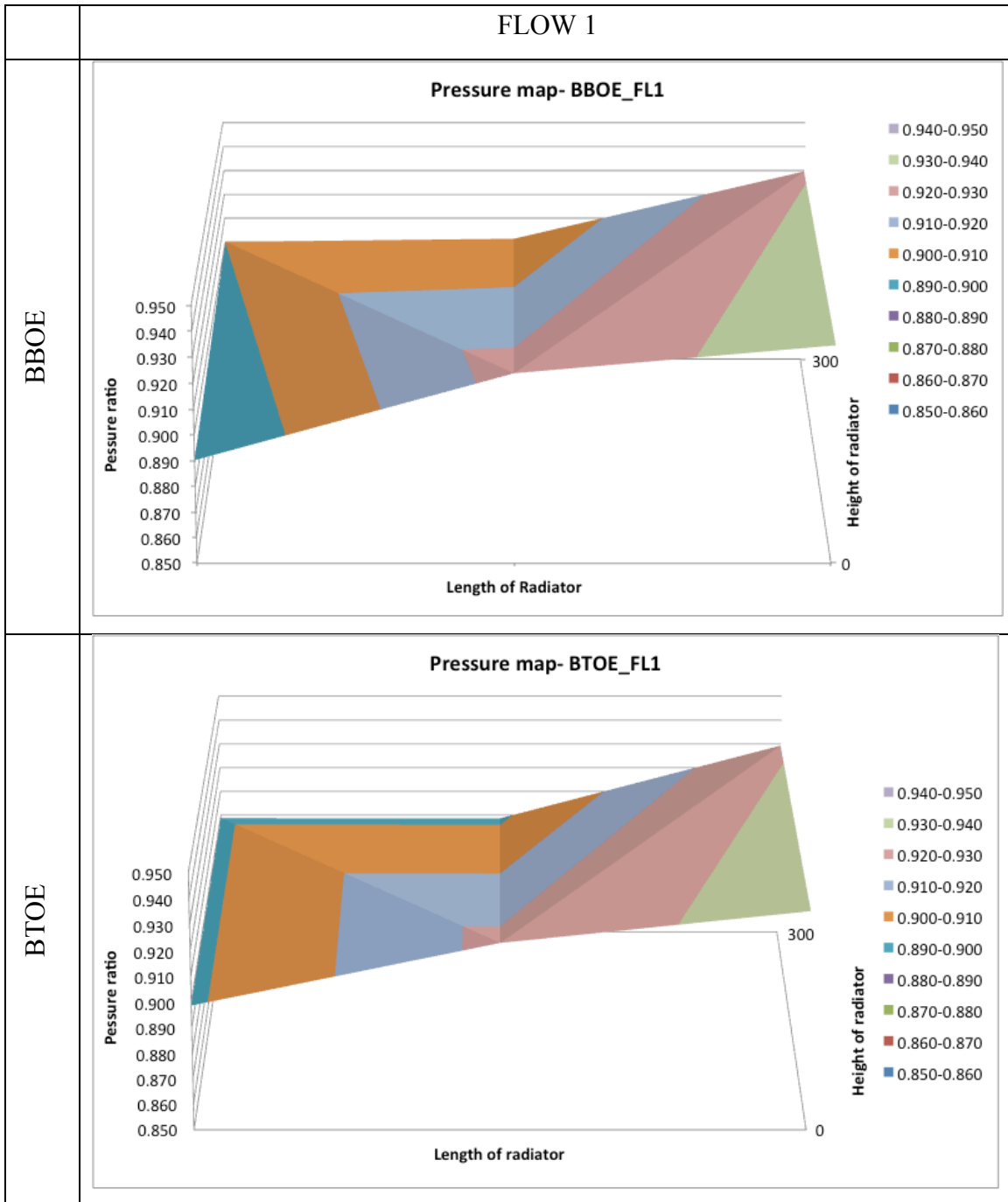


Figure 5-24 Normalised pressure variation in 3060 radiator - Flow 1

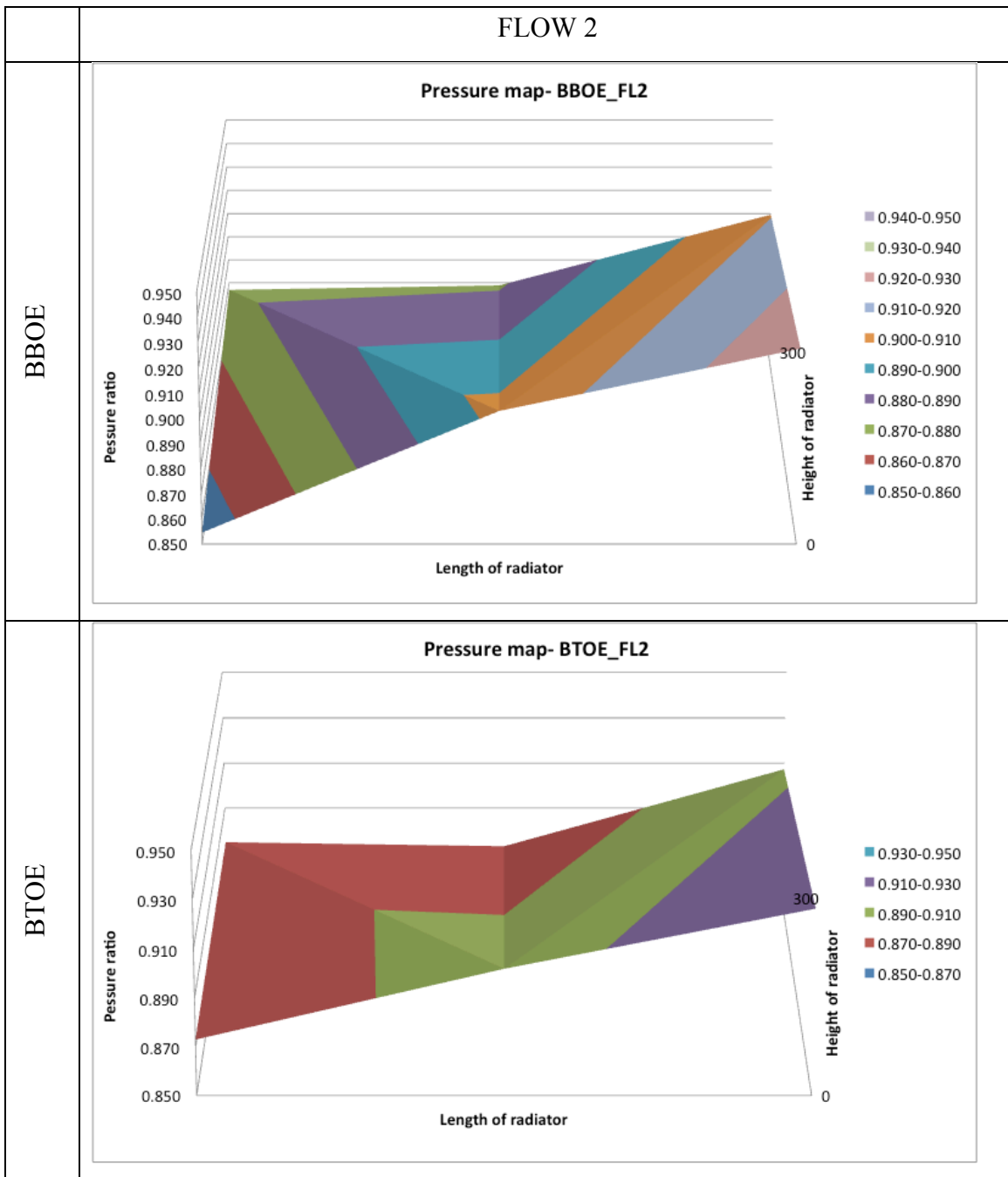


Figure 5-25 Normalised pressure variation in 3060 radiator - Flow 2

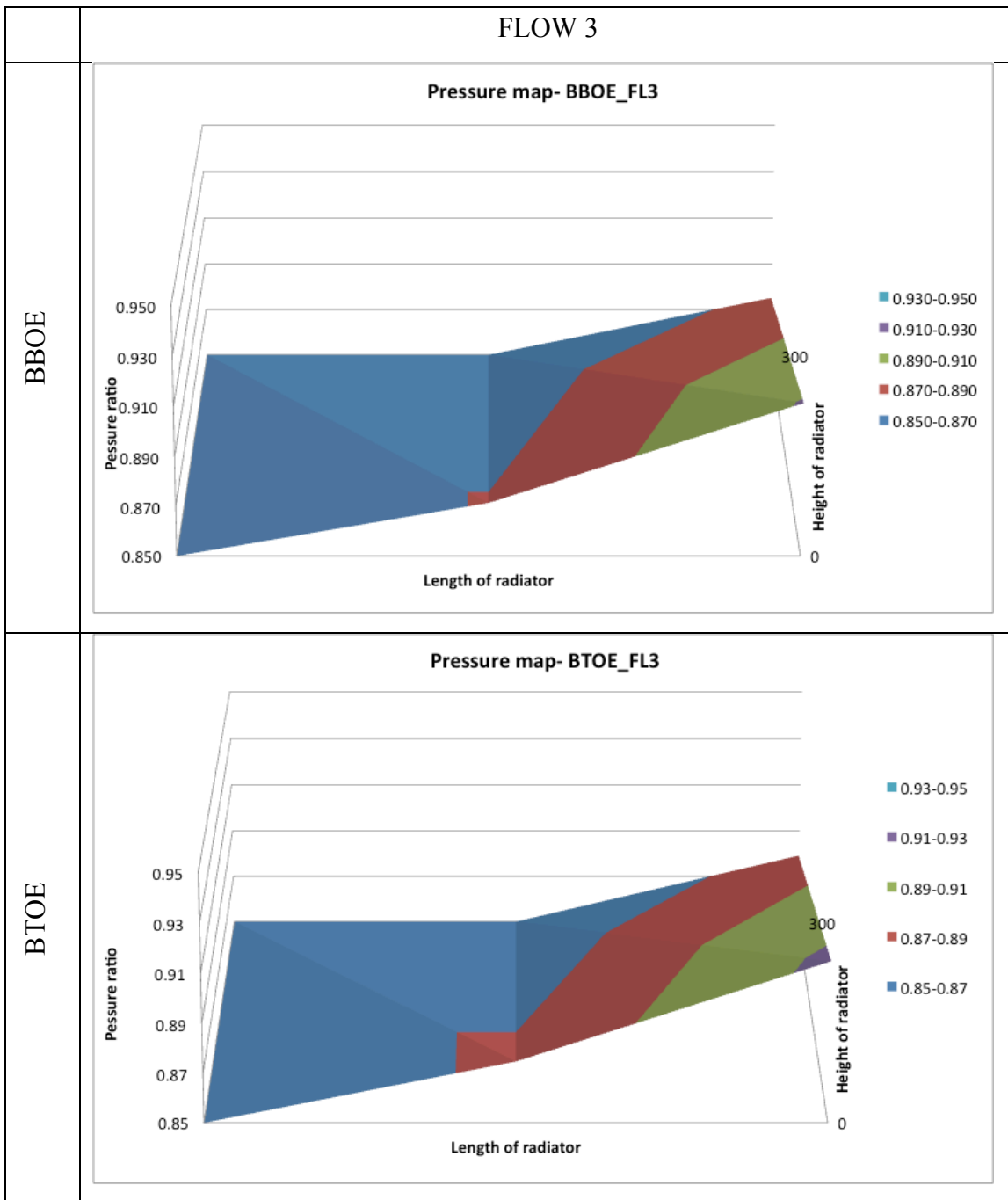


Figure 5-26 Normalised pressure variation in 3060 radiator - Flow 3

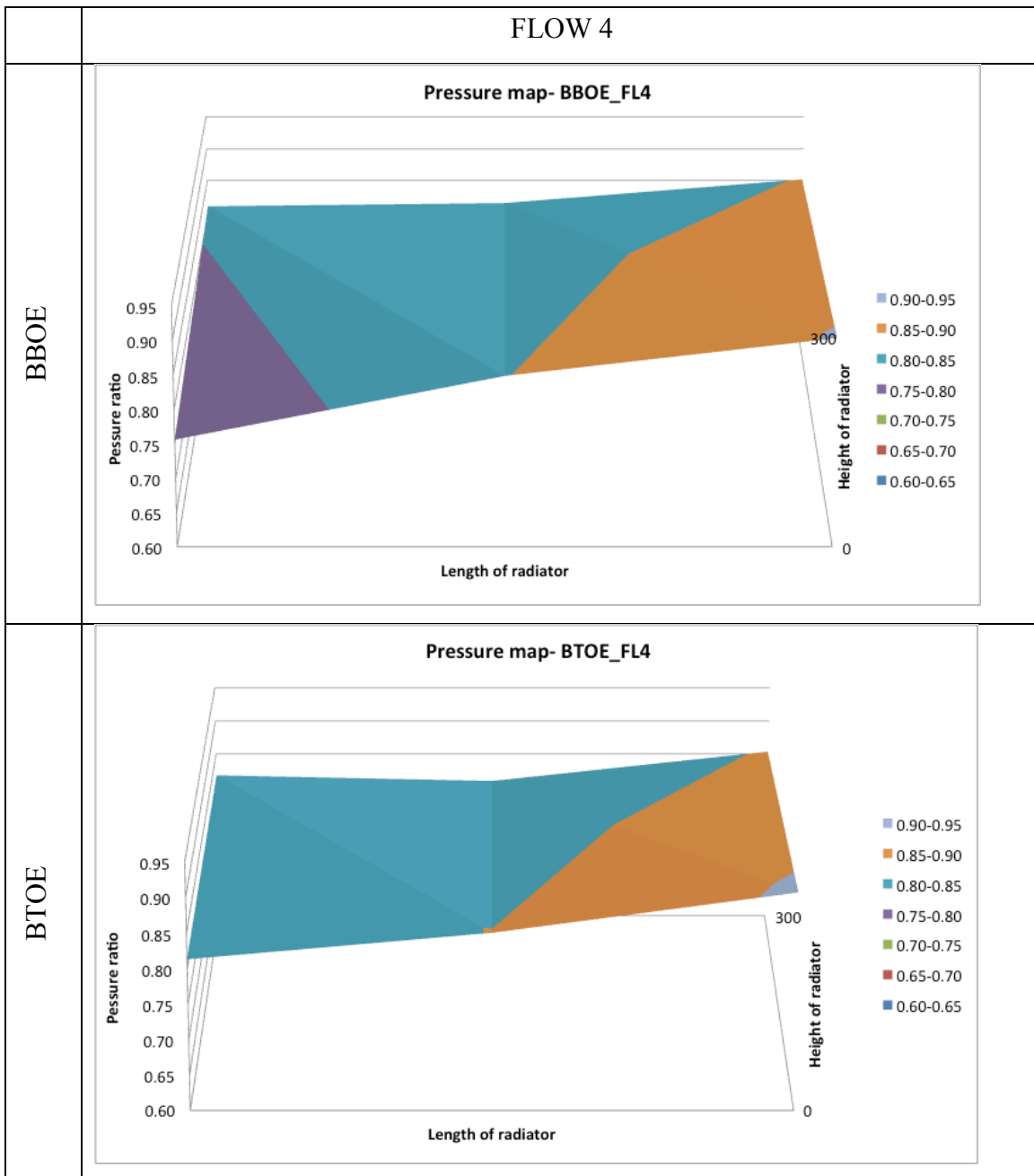


Figure 5-27 Normalised pressure variation in 3060 radiator - Flow 4

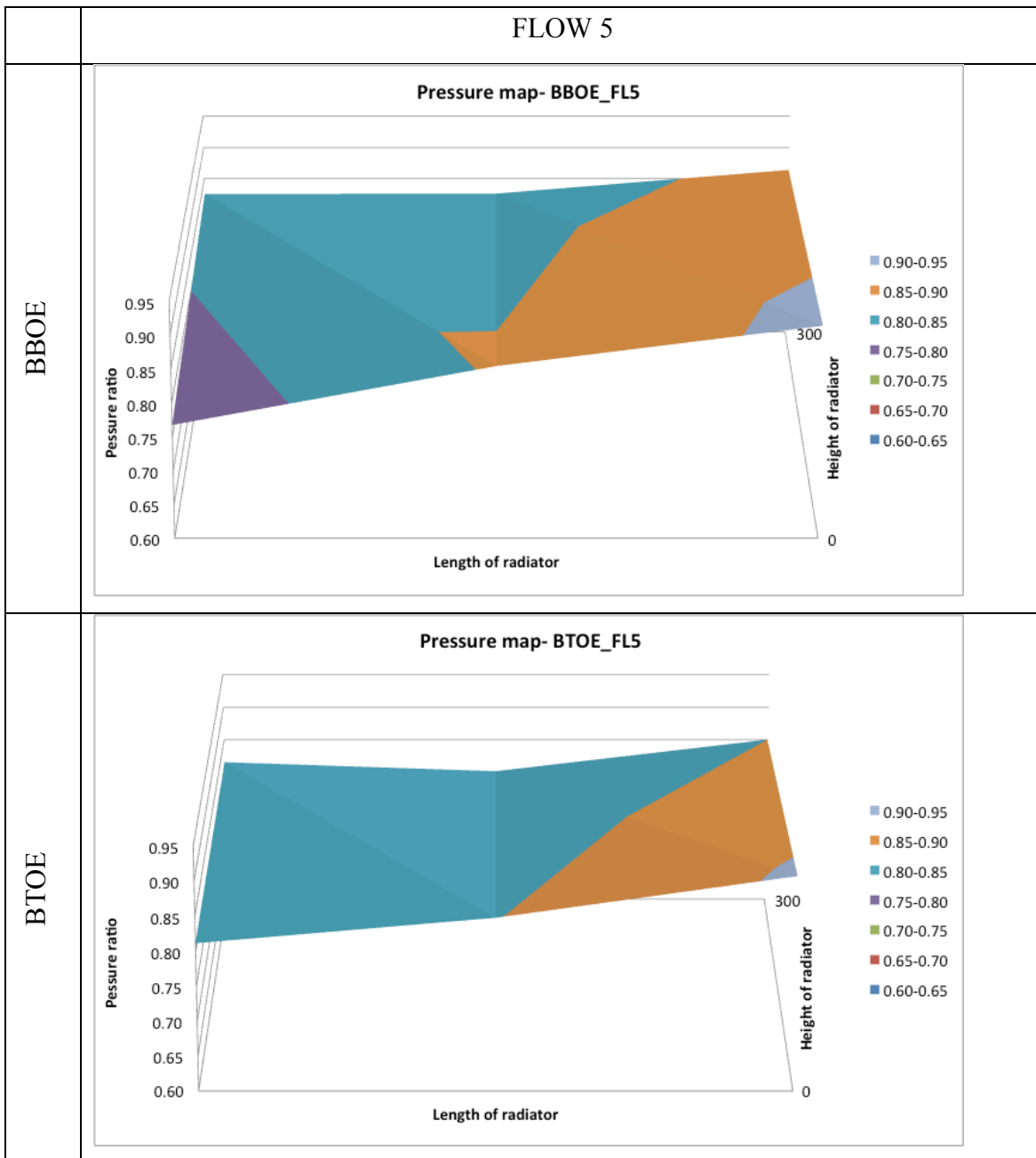


Figure 5-28- Normalised pressure variation in 3060 radiator - Flow 5

In Figure 5-24, Figure 5-25, Figure 5-26, Figure 5-27 and Figure 5-28 a comparison of pressure variation in a 3060 radiator over a range of five flow velocities and 2 flow configuration has been conducted. In we can see that the pressure variation is minimal at lower flow rate of 4.4 m/s for both BBOE and BTOE configuration. The pressure distribution ratio values vary from 0.935 to 0.89, the lowest pressure at the outlet is 0.89. The five flow velocities are shown in Table 5-6. The pressure distribution ratio at pressure point 1 for flow 2 is lower than flow 1. As the flow increases the losses at the inlet increase resulting in lower pressure distribution ratio at point 1 for both BBOE and BTOE. The pressure fluctuation is not significant flow 2 for both configurations. The ratio varies from

0.928 to 0.855 in BBOE whereas the ratios in BTOE are comparable with maximum ratio of 0.926 at point 1 and minimum of 0.873 at point 5.

BBOE at flow 3 has a pressure distribution ratio variation between 0.911 and 0.796 with max and min values at point 1 (downstream of inlet) and point 5 (upstream of outlet) respectively. The trend matches the previous flows but variation is pronounced with a net variation 12.6%. BTOE at flow 3 has a variation of 8.19% with max and min values of 0.915 and 0.840 at point 1(downstream of inlet) and point 5 similar to BBOE

As the flow rate increases the pressure variation increases across the radiator. With a flow velocity of 6.6 m/s in BBOE the pressure distribution ratio fluctuates from 0.903 to 0.757. This gives a net pressure variation of 16.17%. Pressure distribution ratio of 0.814 at point 3 (top centre) is 9.6% lower than point 1 (closer to inlet). These differences ensure that the flow would develop towards the top of the radiator and not just straight from inlet to outlet in a BBOE layout. BTOE layout at similar flow rate has pressure distribution ratio fluctuation 0.907 to 0.814. Net pressure variation is only 10.25% as opposed to 16.17% in a BBOE layout.

Flow 5 has a pressure distribution ratio of 0.907 at point 1 and 0.815 at point 4 (close to outlet) in a BTOE layout, whereas point 1 is 0.914 and point 5 is 0.769 (close to outlet) in a BBOE layout. Average pressure distribution ratio in BTOE is 0.839 compared to 0.842 in a BBOE layout. The pressure variation is more in BBOE layout across all flow velocities compared to BTOE.

A pressure distribution ratio co-efficient \bar{K} has been developed by taking an average of pressure distribution ratios across the radiator for a given flow rate and configuration. This co- efficient gives us valuable information to compare the variation in pressure across the radiator as a function of velocity.

BBOE					BTOE				
0.876	0.900	0.901	0.930	1	0.882	0.899	0.899	0.929	1
	0.890	0.924	0.935			0.899	0.923	0.935	
0.833	0.877	0.879	0.910	1	0.848	0.875	0.873	0.907	1
	0.855	0.903	0.928			0.873	0.902	0.926	
0.770	0.836	0.839	0.875	1	0.805	0.842	0.837	0.879	1
	0.796	0.871	0.911			0.840	0.875	0.915	
0.724	0.809	0.814	0.852	1	0.772	0.817	0.808	0.853	1
	0.757	0.849	0.903			0.814	0.851	0.907	
0.728	0.825	0.826	0.864	1	0.767	0.815	0.801	0.850	1
	0.769	0.855	0.914			0.812	0.849	0.907	

Table 5-5 Normalised pressure distribution in a 300 x 600 mm radiator

Key observations –

Pressure drop at point 1 (down stream of inlet) increases with increase in flow velocity for both BBOE and BTOE layout. Pressure at point 5 is the lowest in the radiator for a given flow velocity for both BBOE and BTOE. The trend for both BBOE and BTOE is same but BBOE is lower than BTOE layout as seen in Figure 5-29. Pressure distribution ratio co-efficient ζ has maximum variation of 3.5% in BBOE and 3.2% in BTOE ref Table 5-6. Pressure distribution ratio co-efficient ζ is a key design parameter in order to achieve uniform flow distribution and in turn uniform temperature on the radiator surface.

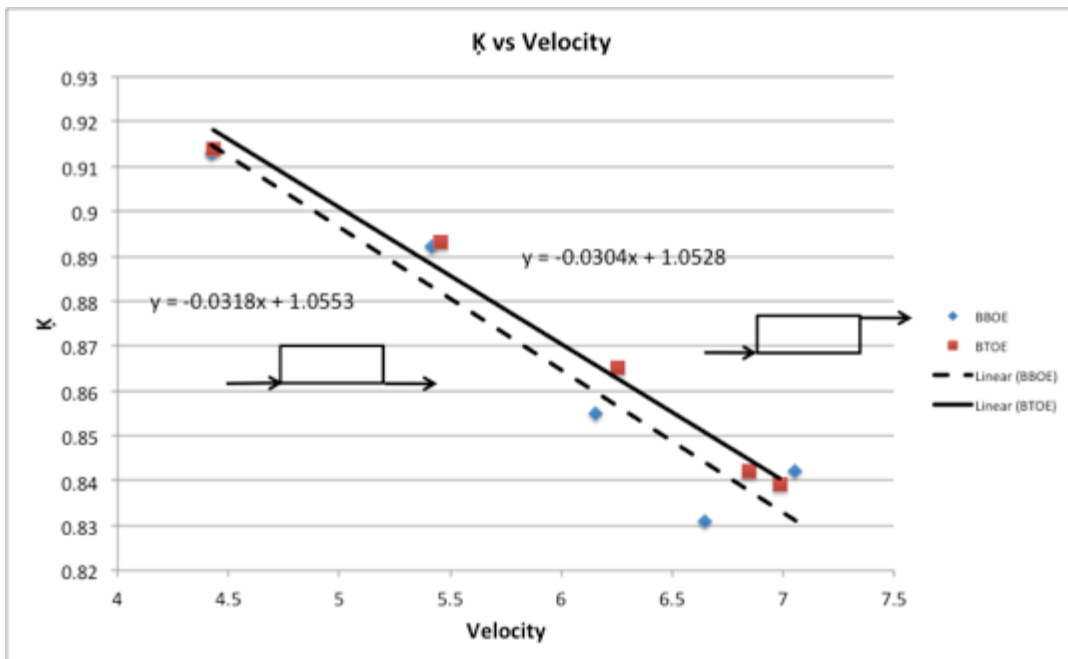


Figure 5-29 Pressure distribution ratio co-efficient vs velocity (300 mm x 600 mm radiator)

Velocity	ζ _BBOE	ζ _BTOE	Velocity
4.423	0.913	0.914	4.430
5.413	0.892	0.893	5.459
6.153	0.855	0.865	6.252
6.647	0.831	0.842	6.848
7.056	0.842	0.839	6.984

Table 5-6 Pressure distribution ratio co-efficient for BBOE and BTOE (300mm x 600mm radiator)

Figure 5-29, shows that in a 3060 radiator, BTOE has higher, pressure distribution ratio co-efficient than BBOE through the range of flow velocities. The difference is similar through the range of flow velocities. For both configurations it can be seen that the pressure distribution ratio co-efficient is higher at lower velocities. In BBOE and BTOE ~60% increase in flow velocity drops the pressure distribution ratio co-efficient by 8%. BBOE and BTOE have very comparable trends in a 3060 radiator.

5.4.2 Pressure variation analysis in a 6100 radiator

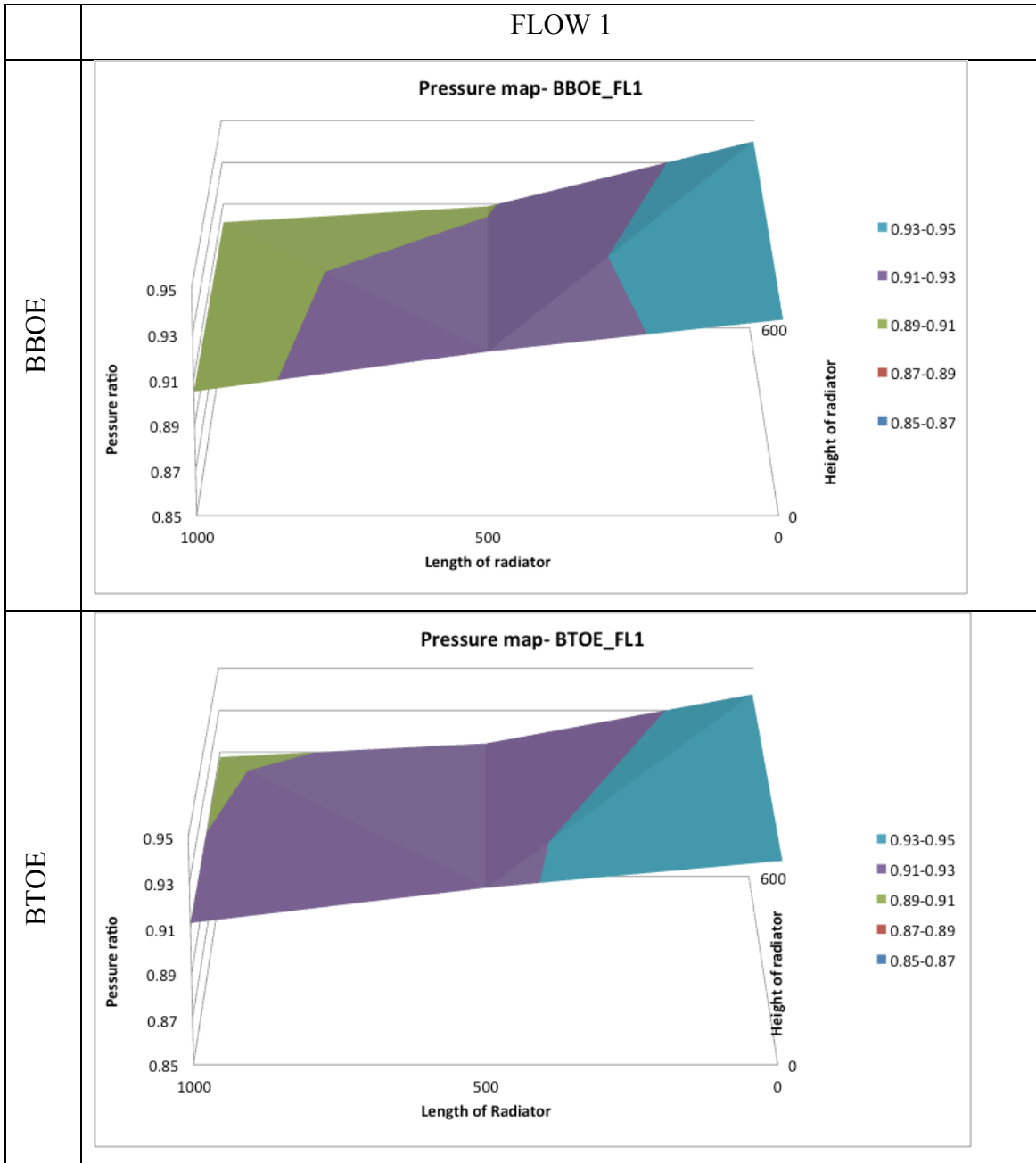


Figure 5-30 Normalised pressure variation in 6100 radiator - Flow 1

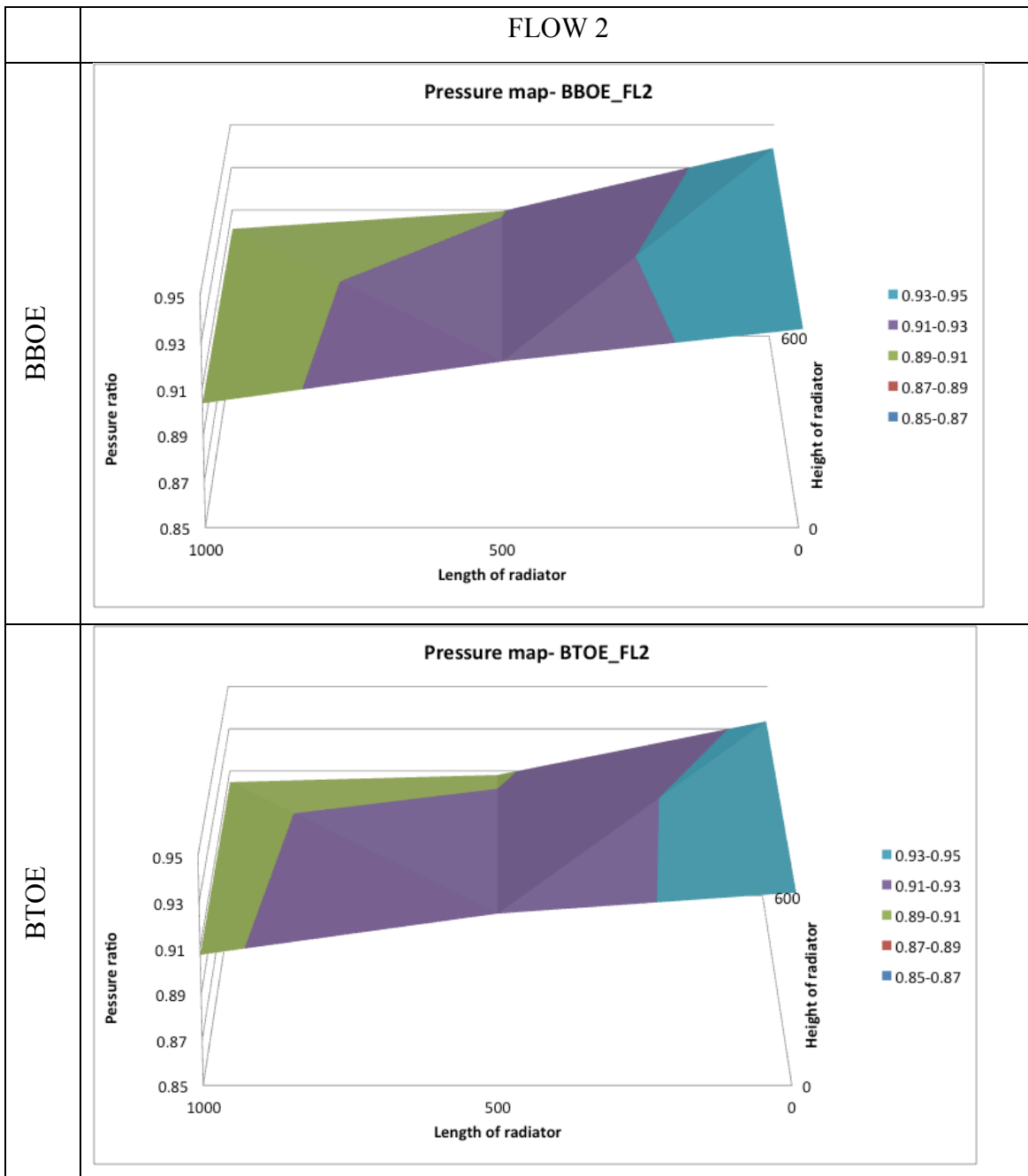


Figure 5-31 Normalised pressure variation in 6100 radiator - Flow 2

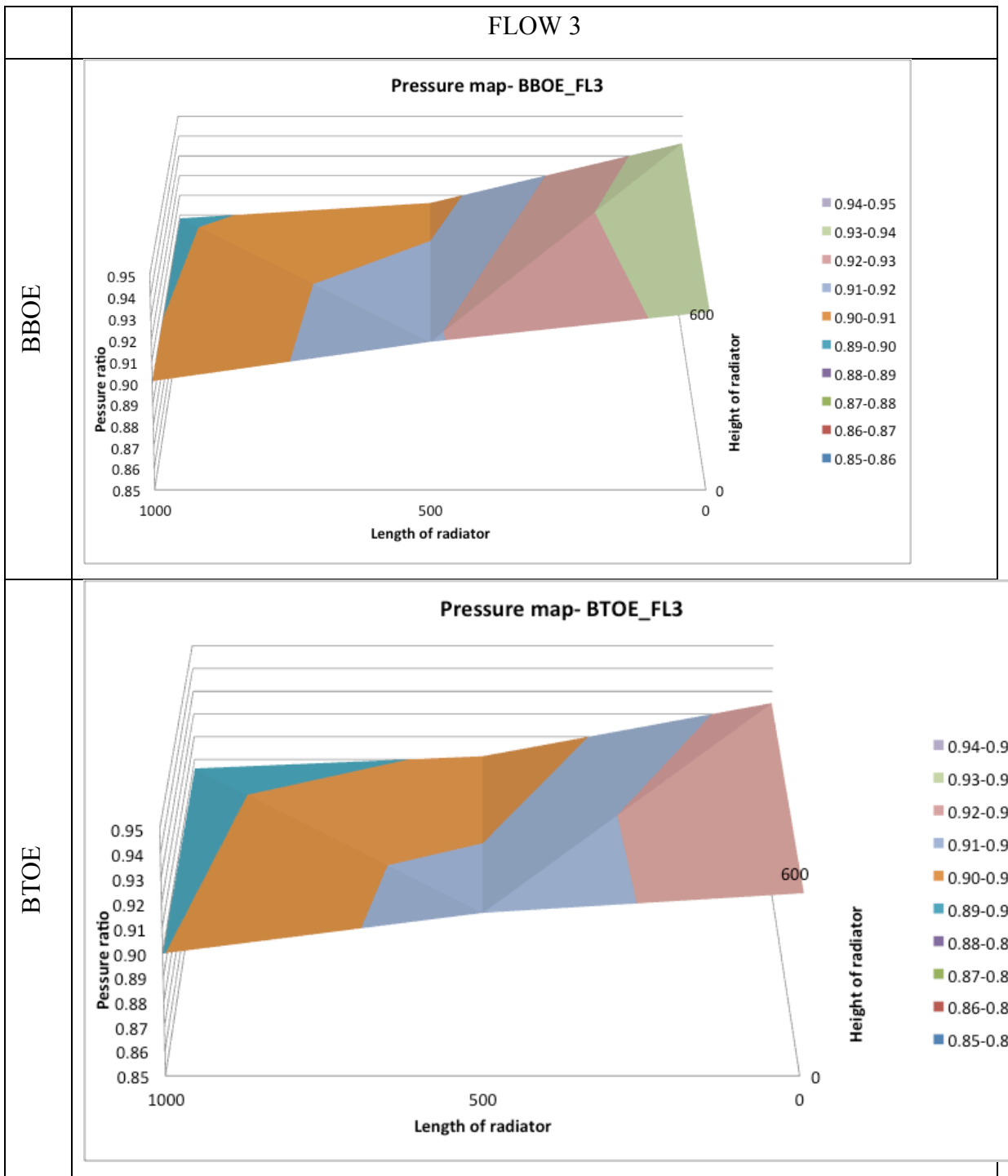


Figure 5-32 Normalised pressure variation in 6100 radiator - Flow 3

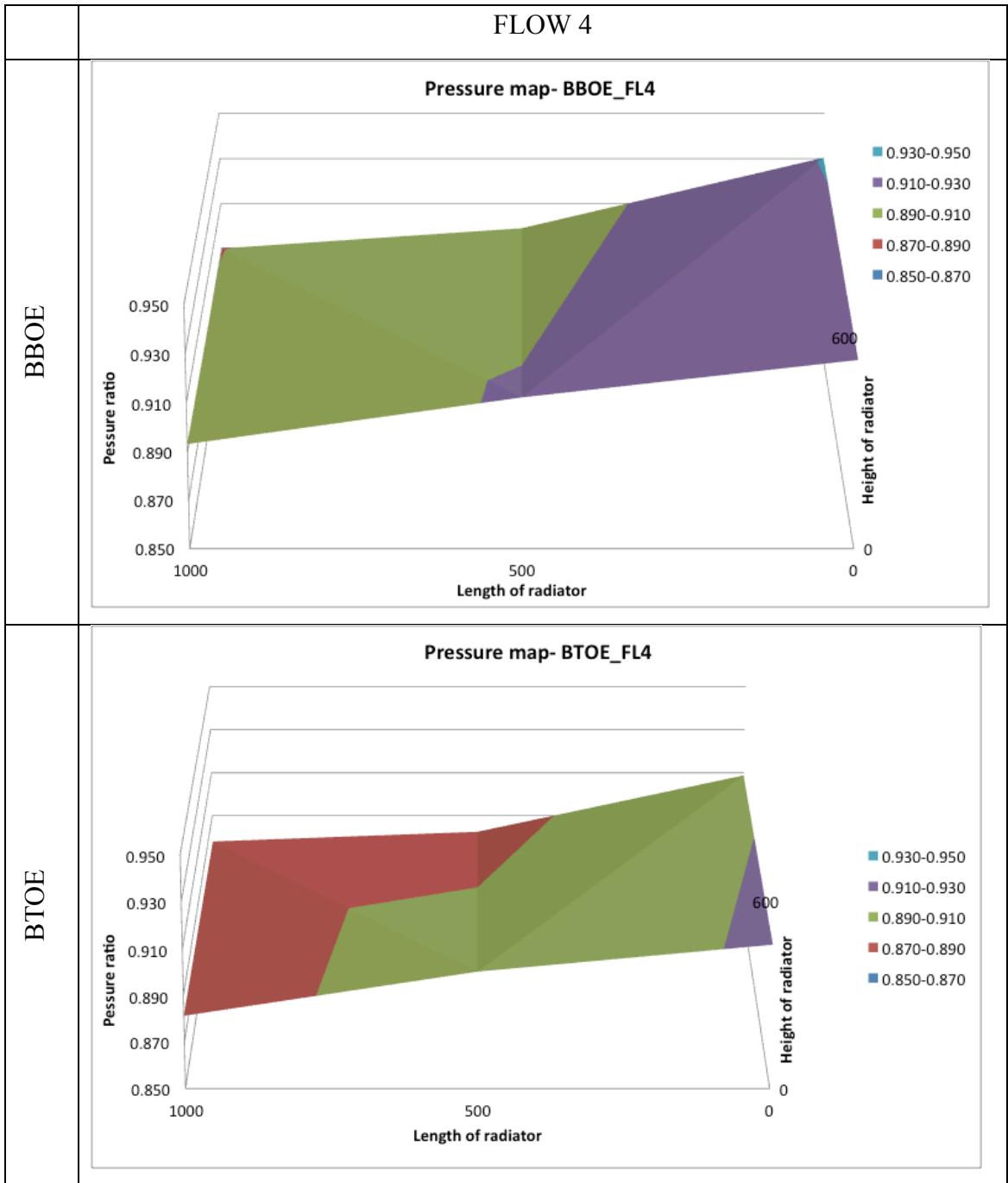


Figure 5-33 Normalised pressure variation in 6100 radiator - Flow 4

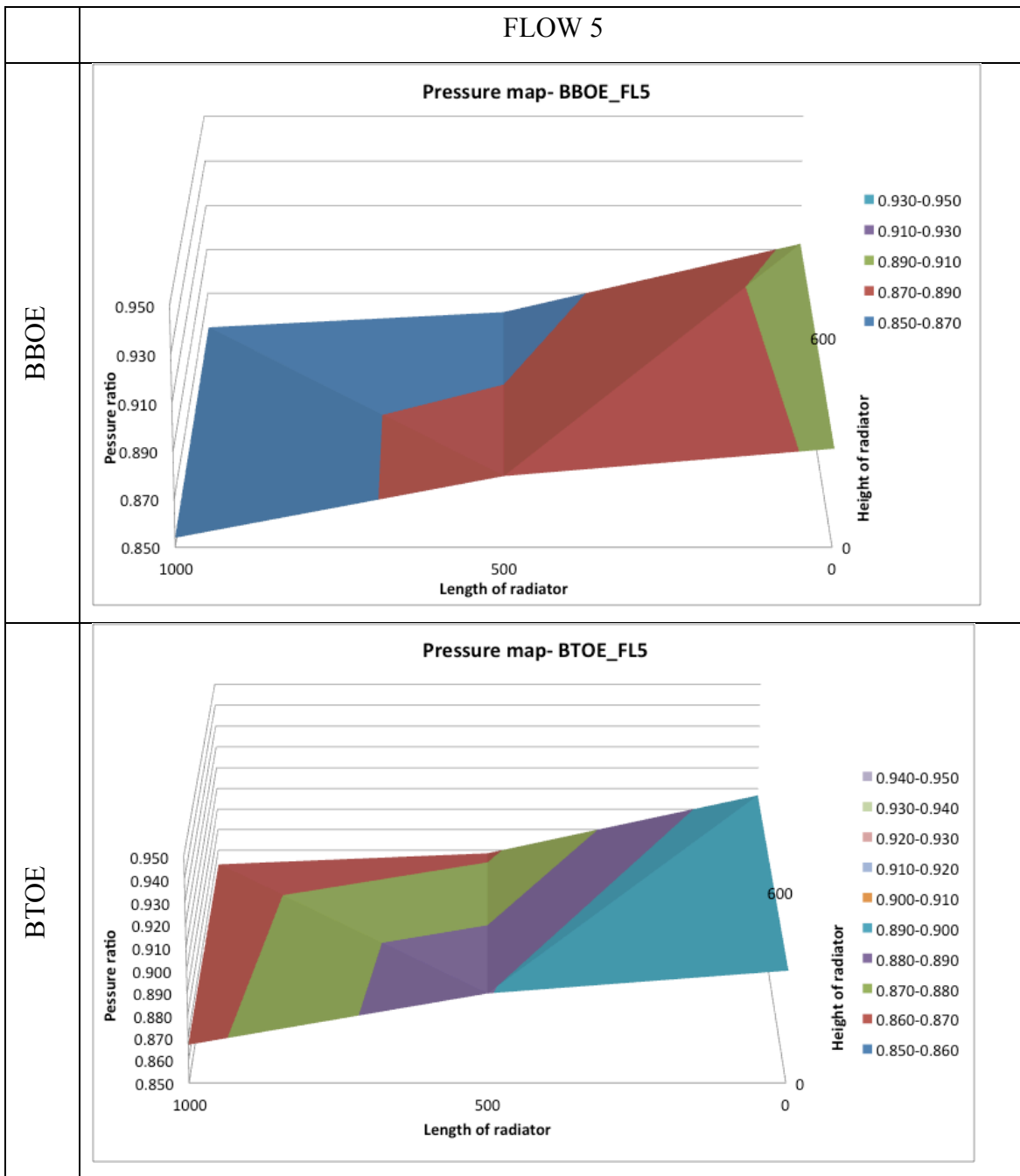


Figure 5-34 Normalised pressure variation in 6100 radiator – Flow 5

In Figure 5-30, Figure 5-31, Figure 5-32, Figure 5-33 and Figure 5-34 graphical comparison of the pressure distribution ratio over a 600mm x 1000mm radiator for BBOE and BTOE flow configurations is shown. The comparison has been carried out over a range of five flow velocities between 3.39 m/s to 8.19 m/s (detailed in Table 5-8). The maximum and minimum pressure distribution ratio values are 0.936 and 0.901 respectively for a BBOE layout flow 1. In BBOE configuration unlike the smaller 300mm x 600mm radiator the lowest pressure distribution ratio is observed at point 4 and not at point 5. This trend is consistent for all the flow velocities. At a similar flow velocity of 3.4 m/s BTOE has a maximum pressure distribution ratio of 0.940 and minimum value of 0.908 at point 4

(upstream of outlet). For flow two, pressure variation is 3.74% and 3.1% in BBOE and BTOE layout respectively with the average pressure of 0.919 for both. The ratios vary from 0.936 to 0.901 in BBOE and 0.934 to 0.904 in BTOE. Pressure distribution ratio co-efficient reduces with the increase in flow velocity. At flow 3, the pressure at point 1 is 0.933 and 0.924 in BBOE and BTOE respectively. Point 4 has a value of 0.896 and 0.898 for BTOE and BBOE respectively. Point 5 in BBOE (closest to the outlet) has a pressure distribution ratio of 0.901. Pressure variation in BBOE configuration for flow velocity of 5.59 m/s is 4.01% and 3.7% in a BTOE configuration at flow velocity of 7.07 m/s.

In BBOE configuration, compared to 300mm x 600mm radiator the pressure variation is significantly lower in a larger radiator of 600mm x 1000mm. In the smaller radiator we observed pressure varying up to 16% compared to 4.15% in the larger radiator. The pressure drop observed in a smaller radiator was 27.2% in BBOE configuration and 23.3% in BTOE configuration. The larger radiator has lower pressure drop of only 21.7% in BBOE and 19.5% in BTOE.

BBOE					BTOE				
0.887	0.901	0.909	0.940	1.000	0.899	0.908	0.914	0.938	1.000
	0.905	0.922	0.936			0.913	0.928	0.940	
0.884	0.901	0.909	0.939	1.000	0.890	0.905	0.908	0.934	1.000
	0.904	0.922	0.936			0.907	0.925	0.934	
0.874	0.898	0.906	0.936	1.000	0.872	0.896	0.901	0.925	1.000
	0.901	0.919	0.933			0.900	0.916	0.924	
0.860	0.890	0.899	0.930	1.000	0.838	0.878	0.882	0.909	1.000
	0.893	0.912	0.928			0.881	0.900	0.912	
0.783	0.854	0.861	0.893	1.000	0.805	0.863	0.868	0.897	1.000
	0.854	0.880	0.891			0.867	0.890	0.900	

Table 5-7 Normalised pressure distribution in 600mm x 1000mm radiator

Pressure distribution ratio co-efficient for 600mm x 1000mm radiator varies from 0.919 to 0.872 for BBOE and 0.923 to 0.881 for BTOE. In Figure 5-35 we have compared the trend of pressure distribution ratio co-efficient for the two flow layouts. The trend is similar but not the same. Pressure distribution ratio co-efficient has a co-relation to the velocity and layout.

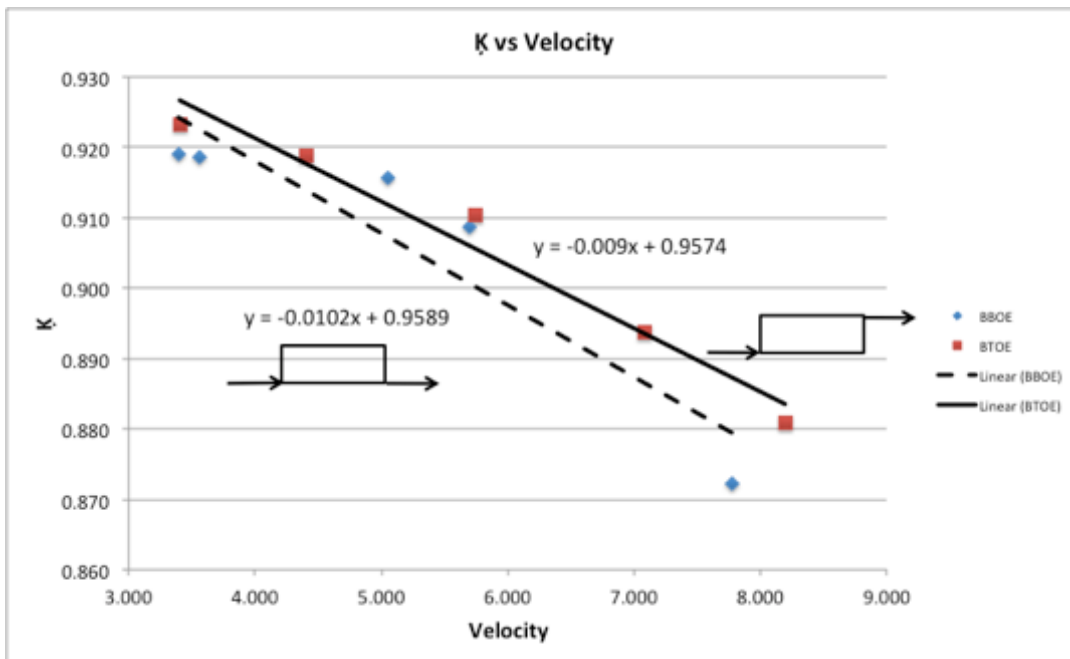


Figure 5-35 Pressure distribution ratio co-efficient vs velocity (600mm x 1000mm radiator)

Velocity	BBOE	BTOE	Velocity
3.394	0.919	0.923	3.404
3.556	0.919	0.919	4.408
5.051	0.916	0.910	5.742
5.697	0.909	0.894	7.078
7.778	0.872	0.881	8.193

Table 5-8 Pressure distribution ratio co-efficient for BBOE and BTOE (600mm x 1000mm radiator)

Figure 5-35, shows that BTOE has higher pressure distribution ratio co-efficient than BBOE through the range of flow velocities. The difference is lower at low velocities but increases with the increase in flow velocity. For both configurations it can be seen that the pressure distribution ratio co-efficient is higher at lower velocities. In BBOE a 110% increase in flow velocity drops the pressure distribution ratio co-efficient by 5% where as in BTOE for similar increase in velocity pressure distribution ratio co-efficient drops only by 3%.

5.4.3 Summary of pressure variation in a radiator

Similar to 3060 radiators, pressure drop at point 1, (downstream of inlet) increases with increase in flow velocity for both BBOE and BTOE layout. Pressure at point 5 is the lowest in the radiator for a given flow velocity for both BBOE and BTOE. In the smaller radiator we observed pressure varying up to 16% compared to 4.15% in the larger radiator. The trend for both BBOE and BTOE is same as seen Figure 5-35 slope for BBOE is -0.0102 and BTOE is -0.009. Pressure distribution ratio co-efficient ζ has max variation of 1.98% in BBOE and 1.77% in BTOE ref Table 5-8. This information in conjunction with the data for loss co-efficient would help determine a radiator configuration with minimal pressure drop, maximum pressure distribution and optimum flow velocity.

5.5 Summary

Detailed experimental evaluation of radiators under different flow configurations and flow rates for two radiator sizes have been carried out. The results obtained from the investigation have been quantified and graphically represented. Two key parameters to quantify pressure loss and pressure variations in a radiator have been developed. The resulting equations have been critiqued and compared back to experimental results to validate the accuracy of the equations.

Relationship of pressure drop to flow velocity has been developed and it is of the form

$$\log(\Delta P) = \log(v) + C$$

- 1) Non dimensional parameter, loss co-efficient K has been developed as a function of effective Reynolds number and the resulting relationship is in the form $K = \frac{A}{Re^x}$
- 2) Individual equations for each size and configuration has been developed
- 3) We have investigated the effect of flow velocity on the pressure variation in a radiator – which gives us valuable information regarding the flow distribution.

Due to complex nature of the geometry with varying number of vertical channels and horizontal channels the effective diameter considered in the investigation was the diameter of the inlet port. The investigation thus far has been limited to one type of radiator, which has an effective inlet diameter of 6mm. This has an impact on the resulting Reynolds number and loss co-efficient. Combined study of Loss co-efficient and pressure distribution ratio co-efficient has shown us that the effective diameter has a significant impact on the results. The study thus far suggests that for a given flow rate increasing the port diameter would reduce the pressure drop across the radiator for each size and flow configuration.

It is not practically possible to modify the radiators for different inlet diameters and re-run the experiments. Furthermore due limitations on accessibility of sensor in the radiator, detailed internal flow analysis could not be carried out. In order to overcome these concerns, computational models (as explained in chapter 3) have been developed, which were 1:1 in size and limited only to the fluid path.

A detailed investigation on 3 different radiator sizes with constant inlet diameter has been undertaken to quantify the effect of size on flow patterns. Further a 3060 radiator with three different inlet diameters has been investigated to understand the effect of inlet diameter.

6 QUANTITATIVE ANALYSIS OF GEOMETRIC PARAMETERS IN RADIATORS

6.1 Introduction

Experimental investigation discussed in chapter 5 helped establish a relation between loss co-efficient and Reynolds number. This information is key to quantify pressure loss in radiators. The experimental work is limited to only two radiator sizes. This limitation is mainly driven by cost and time constraints. In order to establish a stable equation for pressure drop minimum three data sets are required. Due to manufacturing constraints, it was not possible to modify port diameters for the radiators hence experimental investigation could not quantify the effect of inlet and outlet port diameter. CFD analysis would also allow us to evaluate the effect of inlet diameter on the loss co-efficient and pressure distribution.

In order to validate the CFD model and process, initially a CFD model is developed, which represents the 300 mm X 600 mm radiator, used in experiments. Output from the CFD models has been compared with the experimental work to quantify any variations and validate the accuracy of the numerical approach.

CFD techniques have been applied to numerically simulate the flow of water through the radiator. Detailed flow field analysis has been carried out to evaluate the effects of radiator size on pressure drop and pressure distribution. Based on the finding a size independent pressure drop model has been developed. Flow characteristics in a radiator under different flow configurations have also been analysed. Pressure variation in a radiator has been analysed to quantify pressure distribution, which affects flow, and temperature distribution. Finally internal flow analysis has been carried out to visualise flow in the radiator, which was not possible in an experimental setup.

6.2 Validation and comparison of Computational and experimental analysis

6.2.1 Comparative study of pressure drop in BBOE configuration

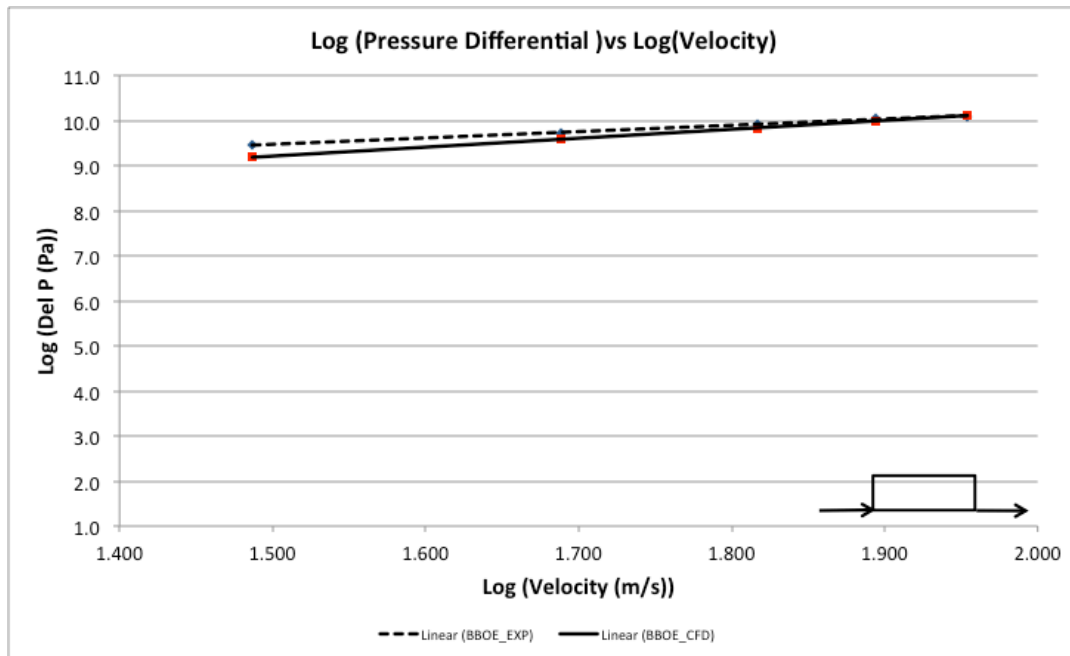


Figure 6-1 Experimental to CFD comparison- Pressure loss against velocity - Base model BBOE

Pressure drop against velocity has been illustrated in Figure 6-1 to study the trend for frictional head loss in a 300 mm x 600mm. Experimental and CFD results have been illustrated in the graph. Log of pressure differential has a linear co-relation to the log of the velocity for both the configurations. The pressure drop for the BBOE CFD at 1.487 m/s inlet velocity is lower than the experimental work by 2.9 %. The variation at flow velocities 2, 3 and 4 are 1.29%, 0.99% and 0.68% respectively. The pressure differential at initial flow velocity is marginally deviated but as flow velocity increases the two trend lines converge. The deviation from theoretical values can be attributed to the accuracy of experimental system which has a tolerance of ~ 3%.

6.2.2 Comparative study of pressure drop in BTOE configuration

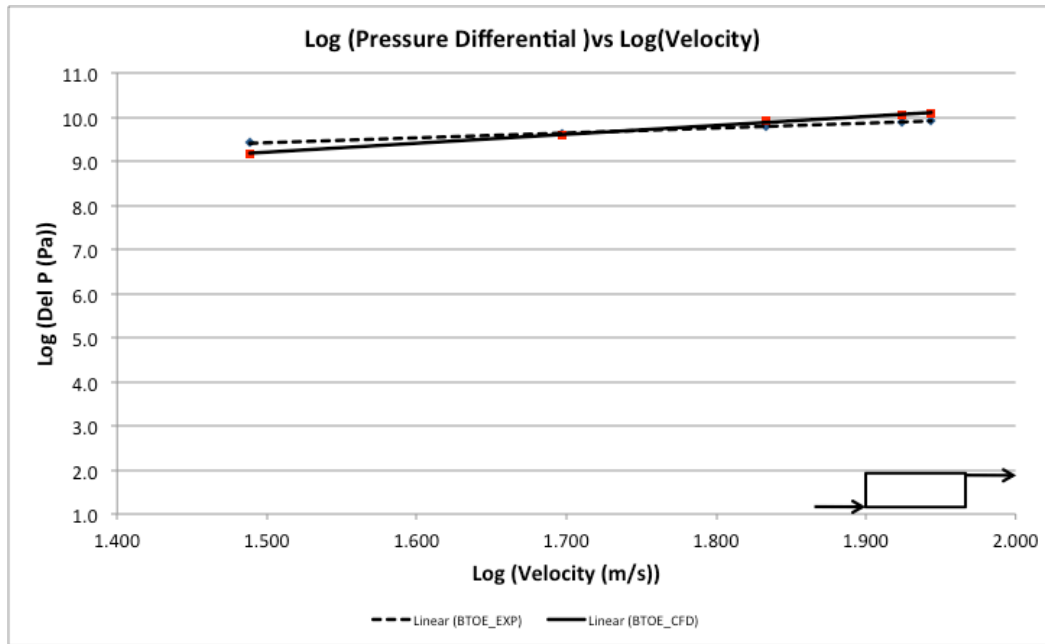


Figure 6-2 Experiment to CFD comparison- Pressure loss against velocity - Base model –BTOE

Similar to previous comparative study, pressure drop against velocity has been illustrated in Figure 6-2 to study the trend for frictional head loss in a 300 mm x 600mm in BTOE configuration. Experimental and CFD results have been illustrated in the graph. The pressure drop for the BTOE CFD at 1.489 m/s inlet velocity is lower than the experimental work by 2.55 %. The variation at flow velocities 2, 3 and 4 are 0.17%, 1.28% and 1.85% respectively. Average variation is 0.4% with the two trend lines crossing at 1.73 m/s. Similar to the BBOE configuration, deviation from theoretical values can be attributed to the accuracy of experimental system which has a tolerance of ~ 3%.

6.2.3 Comparative study of Pressure distribution ratio Co-efficient in BBOE configuration

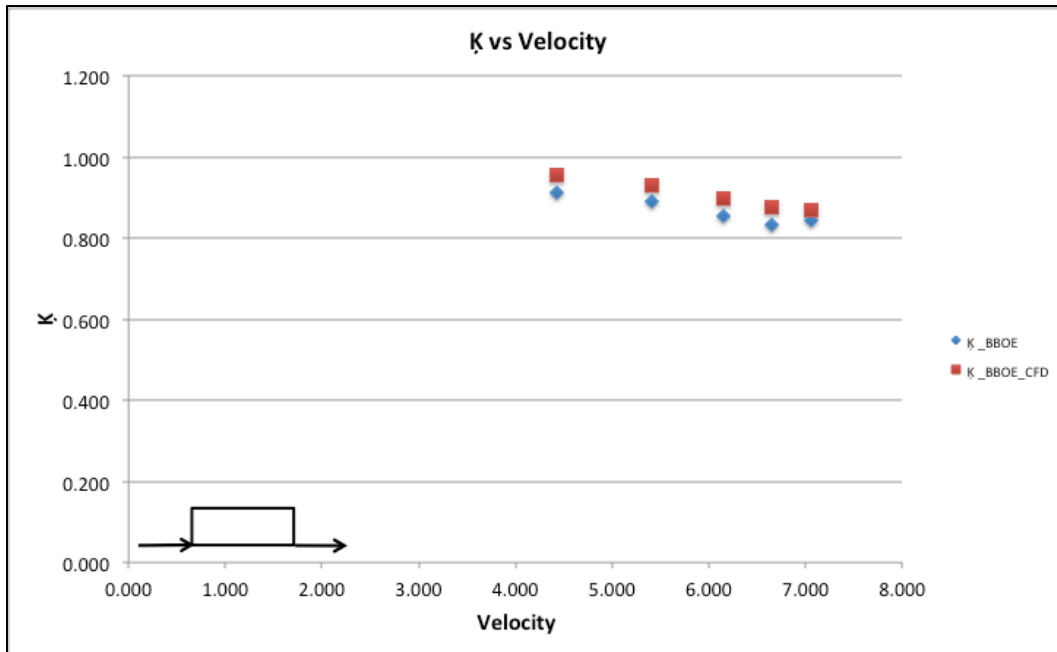


Figure 6-3 Experiment to CFD comparison- Pressure distribution ratio- Base- BBOE

Comparing the pressure distribution ratio co-efficient in a 300 x 600 radiator in a BBOE pipe configuration we see that trend lines have similar slopes between experimental results and numerical results. The variation is only 7.5%. Through the range of flow velocities CFD analysis predicts a higher value for the pressure distribution ratio co-efficient than the experimental results. Maximum variation is at flow velocity 4 (6.65 m/s) with the average being 4.27%. This suggests a good co-relation and gives confidence to further develop numerical models to have a better understanding and visualisation of the flow parameters inside the radiator.

6.2.4 Comparative study of Pressure distribution ratio Co-efficient in BBOE configuration

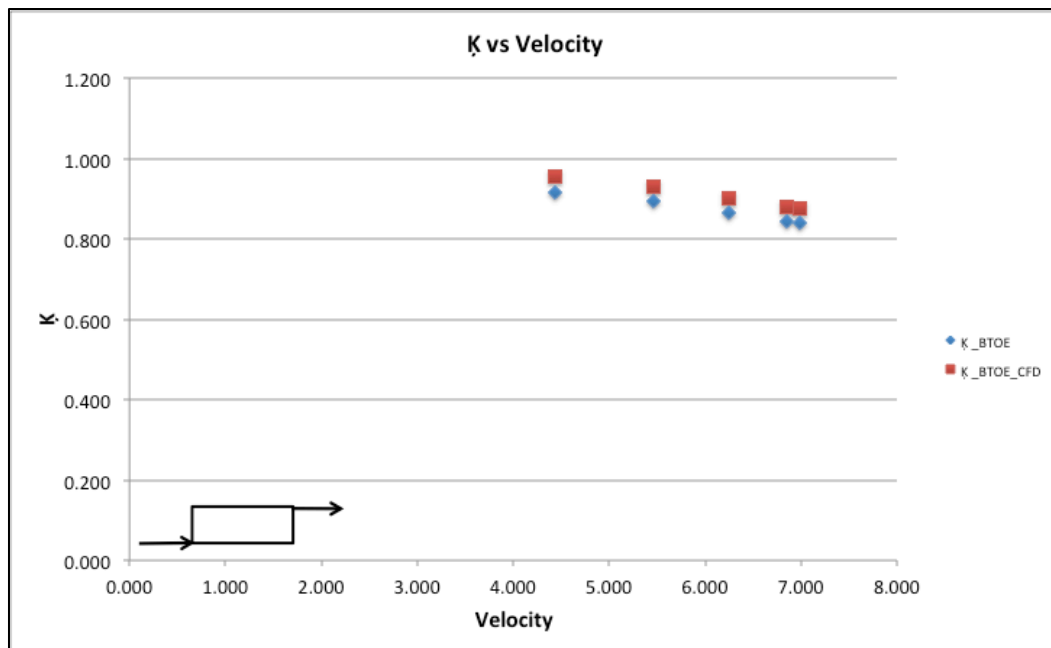


Figure 6-4 Experiment to CFD comparison- Pressure distribution ratio- Base- BTOE

Similar to section 6.2.3 numerical results and experimental results for the BTOE pipe layout in a 300 mm X 600 mm radiator have been compared. Figure 6-4 shows trend lines for the two data sets to have similar slopes with a variation of 5.2%. CFD analysis predicts marginally higher values than the experimental results with maximum variation of 4.26 % at flow velocity 4.43 m/s (velocity 1) and a minimum variation of 3.95% at flow velocity of 5.46 %. Average variation across the flow velocities is 4.11 %, which can be accounted to variation in experimental setup. BTOE configuration also shows good co-relation to the experimental setup.

6.2.5 Key observation

Results from the computational model developed has shown high level of co-relation to physical setup and validated the CFD model.

6.3 Quantitative analysis of radiator size on internal flow parameters

6.3.1 Introduction

As discussed in Chapter 4, stand-alone radiators have been developed in a range of sizes. Radiators are available in three heights 300mm, 400mm and 600mm. Lengths ranged from 600 mm to 1000 mm with increments of 100mm. In order to rationalise the product range and reduce manufacturing complexity certain sizes have been eliminated, as their thermal outputs are very similar. Summary of all the sizes is given below. For the purpose of this investigation three radiators have been selected to cover range of radiator heights and lengths (highlighted in the table). The inlet and outlet port diameters for the models is taken as 8mm

Height	Length										
	600	700	800	900	1000	1100	1200	1300	1400	1500	1600
300	Y	-	-	-	Y	-	-	-	Y		Y
400	-	Y	-	-	Y	-	-	-	Y		Y
600	Y		Y	-	Y	-	-	-	-	-	-

Table 6-1 Stand-alone radiator sizes

Review of previous work carried out in chapter 2 has suggested that the pressure loss in the system increases with the size of the radiator but there has been no analytical work done to quantify the effect of size. There is also limited research on the point of entry for a given radiator size. In this section work has been undertaken to investigate the trends of pressure loss between inlet and outlet ports of radiators for three different sizes. Geometric parameters like, channel size, inlet and outlet diameter and pipe configuration have been kept the same to quantify the effect of radiator size.

6.3.2 Pressure drop in BBOE configuration

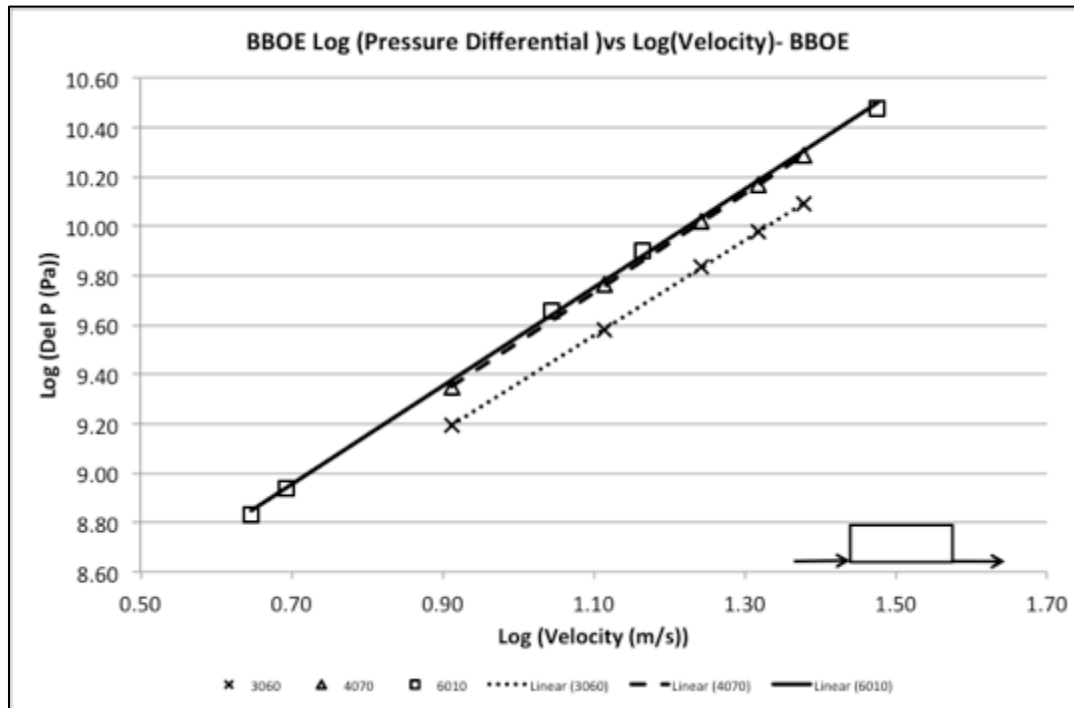


Figure 6-5 Comparison of pressure drop in 3 radiators of varying sizes - BBOE

Pressure drop between inlet and outlet of the radiator has been evaluated for five inlet flow velocities in Figure 6-5. The graph represents the characteristics for BBOE (Bottom-Bottom-Op-posite-End) flow configuration in three radiators 3060 (300mm X 600 mm), 4070 (400 mm X 700 mm) and 6100 (600 mm X 1000 mm). The trend lines for the three radiators have very similar slopes. Pressure drop in 4070 radiator is 3.9% higher than the pressure drop in a 3060 radiator whereas the same for 6100 radiator is 3.16% higher than 3060 radiator. It is intended that the flow velocities for numerical evaluations be kept the same across the three radiators but the larger radiator (6100) required a wider range of flow velocities to produce a stable trend. Absolute pressure drop values for a given flow velocity are identical for 4070 radiator and 6100 radiator with an average offset of 1.8% to the pressure drop values in a 3060 radiator at the same flow velocity. Although a 6100 radiator has significantly higher surface area, it could be possible that there is no flow through some of the channels and alternatively in a 4070 radiator it could be possible that the flow is prevalent in all the channels. As a result the effective flow length in both 4070 radiator and a 6100 radiator is higher compared to effective flow length in a 3060 radiator.

6.3.3 Pressure drop in BTOE configuration

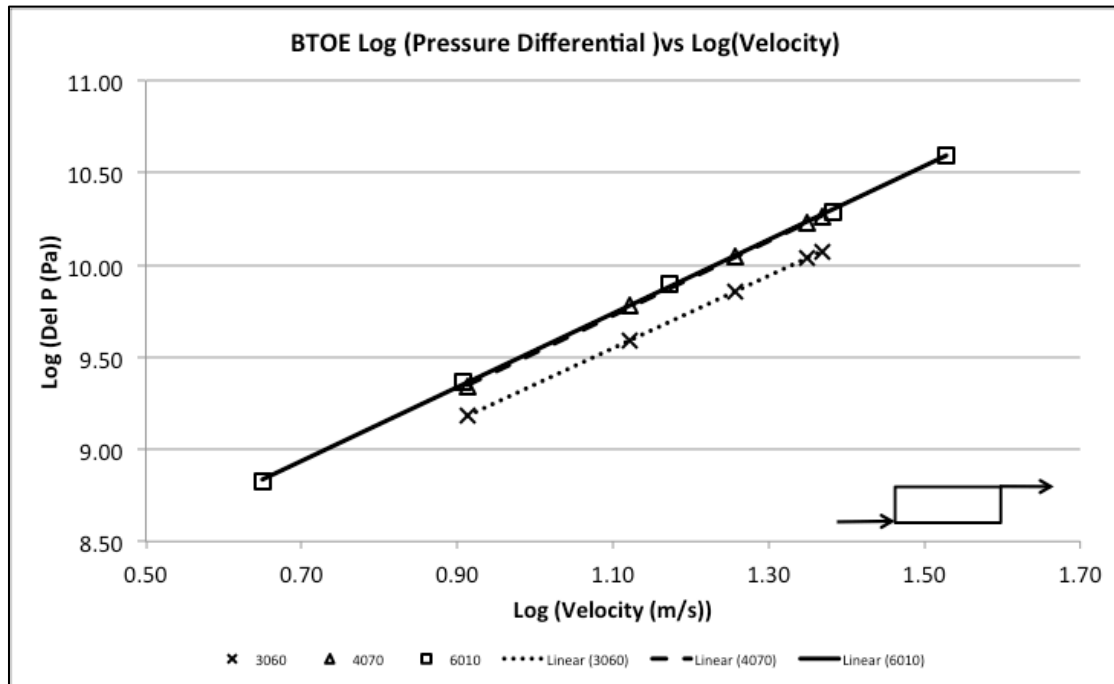


Figure 6-6 Comparison of pressure drop in 3 radiators of varying sizes - BTOE

Figure 6-6 illustrates pressure drop against velocity to study the trend for pressure drop between inlet and out points of the three radiators in a BTOE (Bottom- TOP- Opposite End) configuration. The pressure drop slope for the BTOE flow configuration in the three radiators is similar with a minimal variation. Similar to the BBOE configuration 4070 and 6100 have the same pressure drop (within 0.1%) for given flow rate, while the 3060 radiator has an average offset of 1.8 %. Pressure drop in the two configurations, BBOE and BTOE are similar as shown in Figure 6-5 and Figure 6-6 respectively. BBOE and BTOE curves for 3060 radiator varies by an average of 0.14% in the numerical model opposed to 1.27% in the experimental setup as shown by Figure 5-17. BBOE and BTOE curves for 4070 radiator and 6100 radiator vary by 0.16% and 2.35% respectively. The study suggests that the flow configuration has insignificant effect on smaller radiators and very small effect on the largest radiator.

6.3.4 Loss coefficient in BBOE configuration

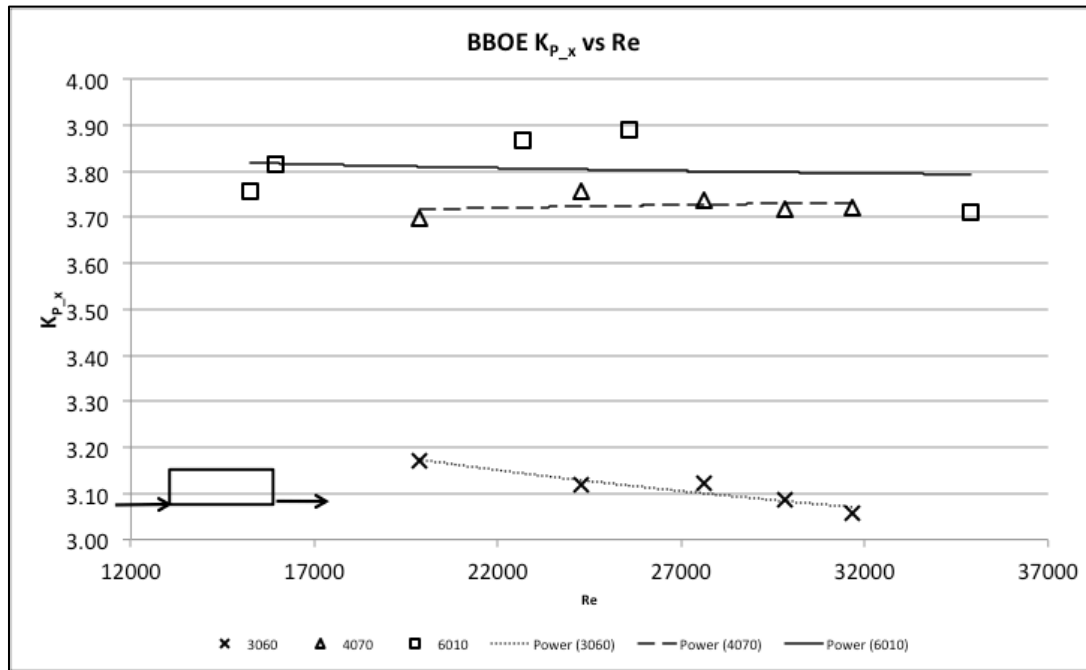


Figure 6-7 Comparison of Loss Co-efficient in 3 radiators of varying sizes – BBOE

In Chapter 5 pressure loss co-efficient has been developed which is a non-dimensional parameter to quantify pressure drop across the inlet and outlet of the radiator. Table 5-3 and Table 5-4 summarise the equations for loss co-efficient for 3060 and 6100 radiator respectively. Figure 6-7 illustrates loss co-efficient against Reynolds number to study the trend of the three radiators in a BBOE (Bottom- Bottom- Opposite End) configuration. Trend for the loss co-efficient in the three radiators are similar with respect to Reynolds number where the fouling factor constant A for 3060, 4070 and 6100 radiators are 6.4068, 3.4197 and 4.1283 respectively. Loss co-efficient in 3060 varies by 3.77% but the variation in Reynolds number, which is a function of flow velocity, is 37.3 %. Likewise in 4070 and 6100 radiator the loss co-efficient varies only by 0.6% and 1.18% respectively through the measured range of Reynolds number. This trend suggests that the non-dimensional loss co-efficient parameter is almost independent of the flow velocity but varies with radiator size in BBOE configuration.

6.3.5 Loss co-efficient in BTOE configuration

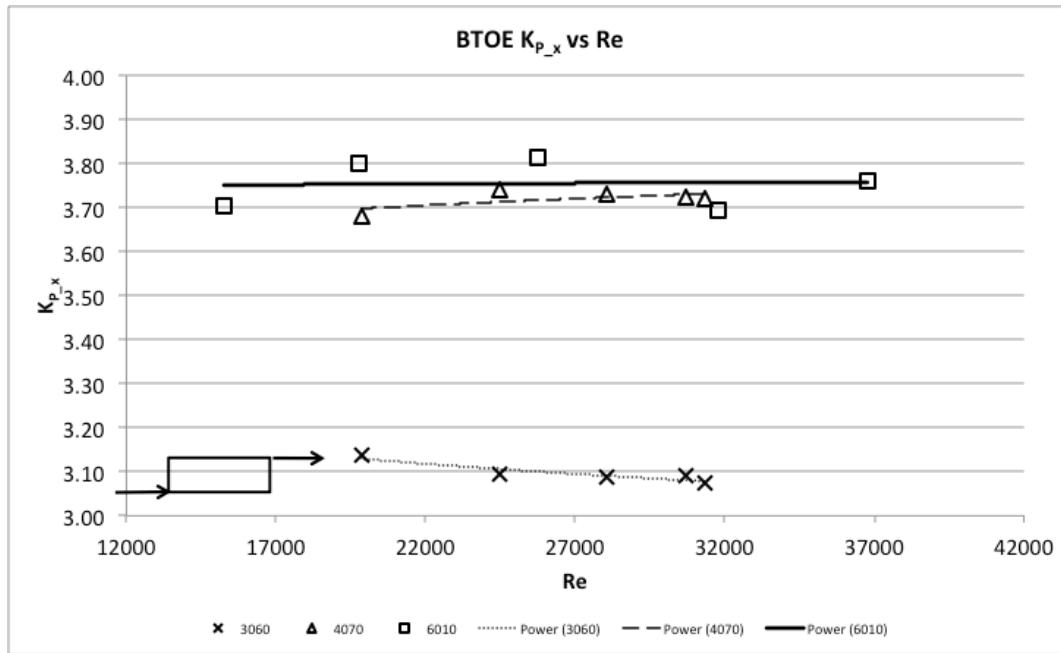


Figure 6-8 Comparison of Loss Co-efficient in 3 radiators of varying sizes – BTOE

Figure 6-8 illustrates loss co-efficient against Reynolds number to study the trend of the three radiators in a BTOE (Bottom- Top- Opposite End) configuration. To highlight the differences, Y-axis scale has been modified to a lower range. Trend for the loss co-efficient in the three radiators are similar with respect to Reynolds number where the fouling factor constant A for 3060, 4070 and 6100 radiators are 4.481, 3.052 and 3.6736 respectively. Loss co-efficient in 3060 varies by 2.0% but the variation in Reynolds number, which is a function of flow velocity, is 37.3 %. Likewise in 4070 and 6100 radiator the loss co-efficient varies only by 1.03% and 1.52% respectively through the measured range of Reynolds number. This trend suggests that similar to BBOE configuration, the non-dimensional loss co-efficient parameter is independent of the flow velocity but varies with radiator size in BTOE configuration. As discussed earlier, the loss co-efficient is higher for a 6100 radiator mainly due to increased length of the flow path compared to a 3060 radiator. Qualitative analysis discussed in 6.3.8 reveals the local flow velocity in the three radiator sizes.

6.3.6 Loss co-efficient as a function of radiator size

It can be seen from both BBOE and BTOE that the loss co-efficient varies with radiator size. In the BBOE configuration loss co-efficient has an average value of 3.114, 3.7262 and 3.8080 for 3060, 4070 and 6100 radiator respectively. In BBOE configuration, the loss factor varies by 18.3% between a 3060 and 6100 radiator and by 16.5% between a 3060 and 4070 radiator where the volume change is 64.8% and 30.74%. Likewise in BTOE configuration, loss co-efficient has an average value of 3.0971, 3.7194 and 3.7554 for 3060, 4070 and 6100 radiator respectively. In BTOE configuration, the loss factor varies by 17.5% between a 3060 and 6100 radiator and by 16.7% between a 3060 and 4070 radiator where the volume change is 64.8% and 30.74%. There is a marginal change in loss co-efficient between 4070 and 6100 radiator for both configurations. In this section geometric parameters of the radiator are reviewed to establish a correlation between loss-coefficient and a non-dimensional geometric parameter.

Based on the figure key geometric parameters that change with the change in size are

- 1) Length of the radiator – L (m)
- 2) Height of radiator – h (m)
- 3) Frontal area of radiator – $A_r = L \times h$
- 4) Number of channels in the radiator – $n=f(L)$
- 5) Diagonal length – $L_d = f(L, h)$

$$n = \text{Int}\left(\frac{L \times 1000}{16.66}\right)$$

Equation 6-1 Number of channels in the radiator

$$L_d = \sqrt{L^2 + h^2}$$

Equation 6-2 Diagonal length of the radiator

- 6) Volume of fluid in a radiator is given in Table 4-8, can also be expressed as a function of L and h.

$$V_w = f(L, h)$$

$$V_w = (L \times [1.81 + \frac{(h - 0.3) \times 0.43}{0.1}]) \times 0.001$$

Equation 6-3 Volume of fluid in the radiator

A non-dimensional geometric factor is proposed to account for radiator size. $G_f = f(V_w, A, L_d, n)$

$$G_f = \frac{n \times V_w}{A \times L_d}$$

Equation 6-4 Geometric factor

The geometric factor is non-dimensional and based on net volume of fluid circulated in the system, which is determined, by the height and length of the radiator. Volume of fluid is very important, as it is the primary means of transferring heat from the heater unit to the radiator panel. Numbers of channels determine the flow path and heat distribution on the radiator panel. The area of the radiator panel is directly proportional to the heat output capacity of the radiator in both convective and radiative modes. Last factor that is important is the diagonal length as it helps differentiate radiators with similar area.

Substituting Equation 6-1, Equation 6-2 and Equation 6-3 in Equation 6-4, geometric factor a non-dimensional number is expressed as a function of length and height of the radiator.

$$G_f = \frac{\text{Int}\left(\frac{L \times 1000}{16.66}\right) \times \left(L \times \left[1.81 + \frac{(h - 0.3) \times 0.43}{0.1}\right]\right) \times 0.001}{(L \times h) \times \sqrt{L^2 + h^2}}$$

Equation 6-5 Geometric factor as a function radiator dimensions

Based on this geometric factor for the three radiators investigated in the study are

	Height	Length	Volume	Diagonal length	Area	n	Geometric Factor G_f
	(m)	(m)	(m ³)	(m)	(m)		
3060	0.3	0.6	0.0011	0.671	0.18	18	0.162
4070	0.4	0.7	0.0016	0.806	0.28	21	0.146
6100	0.6	1	0.0031	1.166	0.60	30	0.133

Table 6-2 Geometric factor based on radiator size

In Table 6-2 geometric parameters influencing the size of the radiator are summarised. Using Equation 6-5, G_f has been computed. From Equation 6-3 it can be seen that the volume of water in the radiator increases with the increase in size. Volume change between 3060 and 4070 radiators is 30.74% whereas the volume change from a 3060 to 6100 radiator

is 64.97%. Increase in area for the same are 35.71% and 70% respectively. Geometric factor changes with the radiator size with the variation between 3060 and 6100 is 21.8%, 3060 and 4070 is 10.9% and 4070 and 6100 is 9.75%.

As discussed in previous section, loss co-efficient is almost independent of flow rate but changes with size in both flow configurations. In order to quantify the effect of radiator size on loss co-efficient further investigation has been undertaken as shown in Figure 6-9 and Figure 6-10 for BBOE and BTOE configurations.

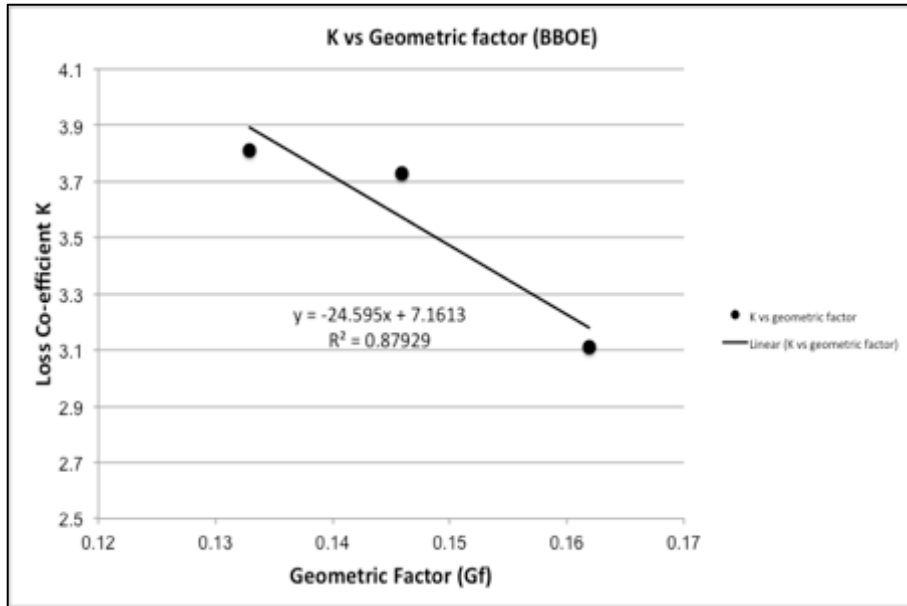


Figure 6-9 Loss co-efficient as a function of geometric factor – BBOE

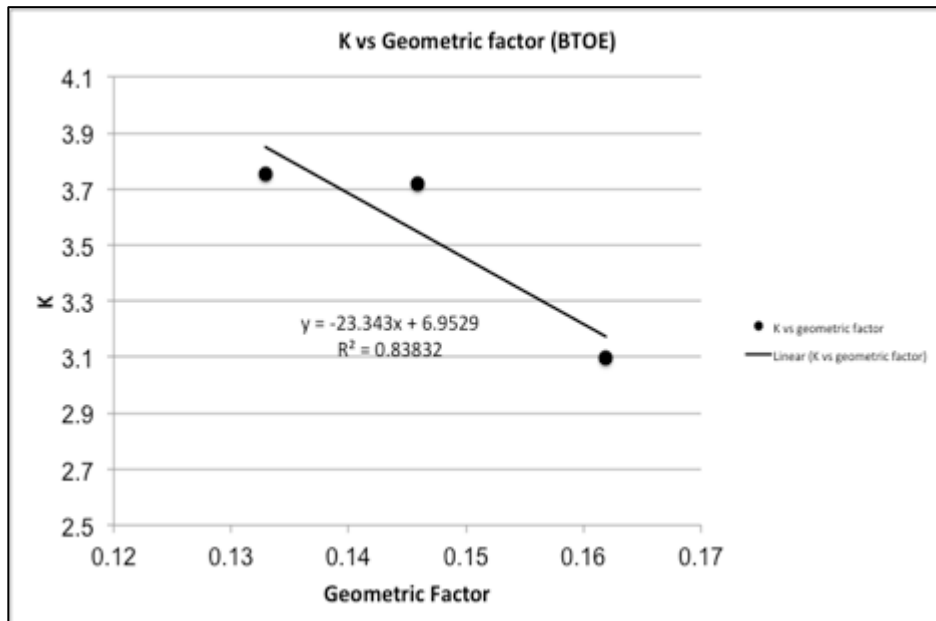


Figure 6-10 Loss co-efficient as a function of geometric factor – BTOE

As expected, loss co-efficient increases with the increase in size of the radiator with 3.808 for 6100 and 3.1114 for 3060 radiators. The length of the complex flow path in the radiator effectively increases with the increase in size. The geometric factor reduces as the radiator size increases, with a value of 0.16, 0.15 and 0.13 for 3060, 4070 and 6100 respectively. The trend is linear with the slope of the line being -24.595. From Figure 6-10, it can be seen that BTOE configuration has a similar trend where loss co-efficient increases with the increase in size of the radiator with 3.7554 for 6100 and 3.0971 for 3060 radiators. The geometric parameters are the same. Comparing BBOE and BTOE, the loss co-efficient varies marginally. Using the Equation 6-6 generated by the curve in Figure 6-9, a common loss co-efficient curve is established to cover the range of radiators given in Table 6-1.

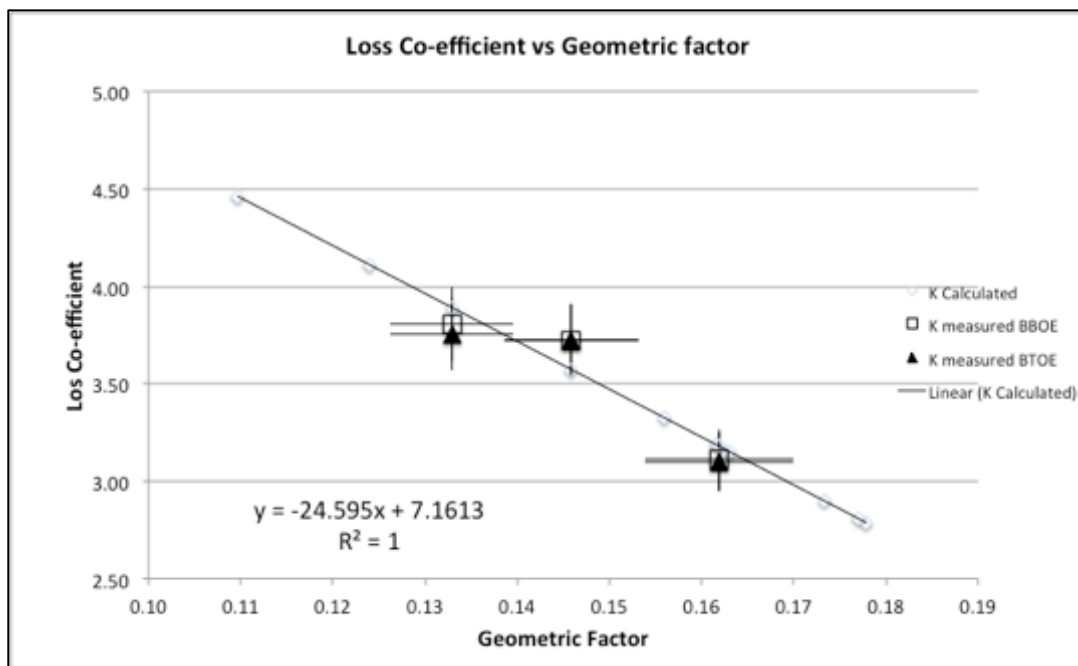


Figure 6-11 Loss co-efficient vs Geometric factor for both configurations

Hence loss co-efficient is given by

$$K = -24.595 \times \left[\frac{\ln \left(\frac{L \times 1000}{16.66} \right) \times \left(L \times \left[1.81 + \frac{(h - 0.3) \times 0.43}{0.1} \right] \right) \times 0.001}{(L \times h) \times \sqrt[3]{L^2 + h^2}} \right] + 7.1613$$

Equation 6-6 Equation to determine Loss co-efficient

Figure 6-11, compares measured (using CFD) loss co-efficient for both BBOE and BTOE against the common equation. The curve shows good co-relation with the BBOE loss co-efficient varying only by 2.19%, 4.10% and 2.21% for 3060, 4070 and 6100 respectively. BTOE loss co-efficient varies by 2.59%, 4.08% and 3.51% for the three radiators. Based on

low variation it can be seen that the co-relation established between loss co-efficient and the geometric factor is valid and independent of flow rate and flow configuration. Using Equation 6-6 loss co-efficient for the range of stand-alone radiators have been identified in Table 6-3

Height	Length	Area	n	Volume	Diagonal	K calculated	Geometric factor
(m)	(m)	(m ²)		(m ³)	(m)		
0.3	0.6	0.18	18	0.0011	0.67	3.18	0.16
0.3	1	0.3	30	0.0018	1.04	2.90	0.17
0.3	1.4	0.42	42	0.0025	1.43	2.81	0.18
0.3	1.6	0.48	48	0.0029	1.63	2.79	0.18
0.4	0.7	0.28	21	0.0016	0.81	3.57	0.15
0.4	1	0.4	30	0.0022	1.08	3.32	0.16
0.4	1.4	0.56	42	0.0031	1.46	3.19	0.16
0.4	1.6	0.64	48	0.0036	1.65	3.15	0.16
0.6	0.6	0.36	18	0.0019	0.85	4.47	0.11
0.6	0.8	0.48	24	0.0025	1.00	4.11	0.12
0.6	1	0.6	36	0.0031	1.17	3.89	0.13

Table 6-3 Geometric factors and loss-co-efficient for stand-alone radiators

6.3.7 Analysis of radiator size on pressure distribution

As discussed in chapter 3, Akin [34] has shown that the velocity magnitudes of fluid flow in a radiator are low in the centre of the radiator. Flow magnitude is influenced by the pressure distribution in the radiator. In order to study the pressure distribution and quantify its effect a pressure distribution ratio constant is required. To develop the constant, absolute pressure is recorded at inlet, outlet and 6 points across the radiator as shown in Figure 5-23. A ratio of absolute pressure and inlet pressure is taken to develop a non-dimensional pressure distribution ratio representing each point. Pressure distribution ratio co-efficient K_p has been developed by taking an average of pressure distribution ratios across the radiator for a given flow rate and configuration. A higher value for pressure distribution ratio co-efficient signifies more even distribution, which leads to even flow and temperature distribution. The co-efficient gives us valuable information to compare the variation in pressure across the radiator as a function of velocity. In this section, pressure distribution ratio co-efficient for three radiator sizes has been investigated at 5 flow velocities and 2 flow configurations to identify optimum velocity with minimal pressure variation, which in turn would give maximum flow distribution. Three radiator sizes are also compared at a given velocity to assess pressure distribution across the radiator. A sample of pressure distribution ratio in the two flow configurations is shown in Table 6-4 and graphically represented in Figure 6-12, Figure 6-13 Figure 6-14. In general it can be observed that the pressure distribution ratio is high in the centre of the radiator for both flow configurations.

BBOE						BTOE					
3060		0.883	0.883	0.885		3060	0.736	0.878	0.887	0.889	
	0.728	0.874	0.883	0.873	1			0.889	0.888	0.874	1
4070		0.849	0.849	0.850		4070	0.697	0.848	0.853	0.854	
	0.687	0.844	0.850	0.847	1			0.853	0.854	0.852	1
6100		0.840	0.841	0.843		6100	0.660	0.821	0.833	0.836	
	0.682	0.832	0.841	0.830	1			0.832	0.833	0.821	1

Table 6-4 Pressure distribution ratio in three radiators

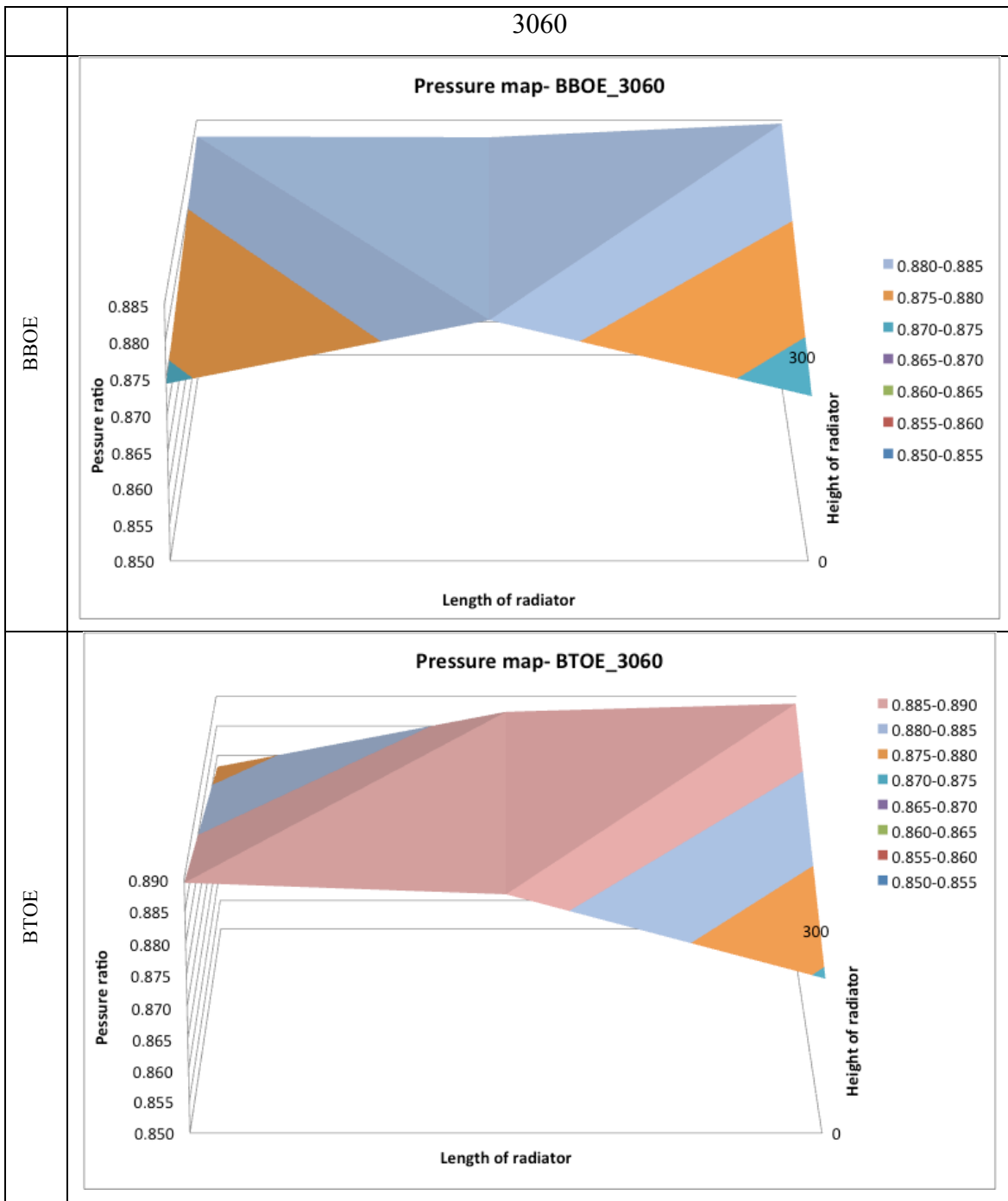


Figure 6-12 Normalised pressure variation in 3060 radiator

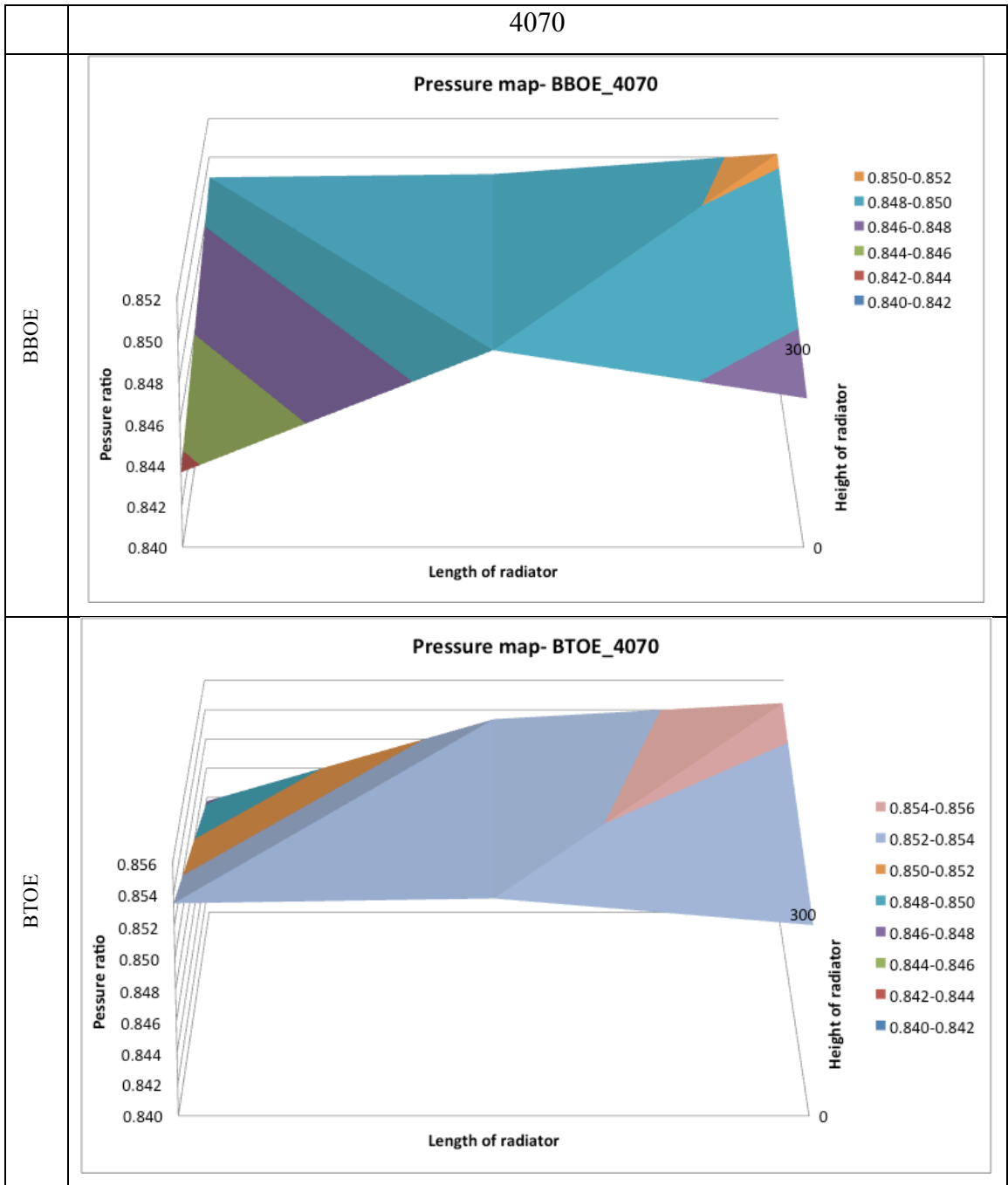


Figure 6-13 Normalised pressure variation in 4070 radiator

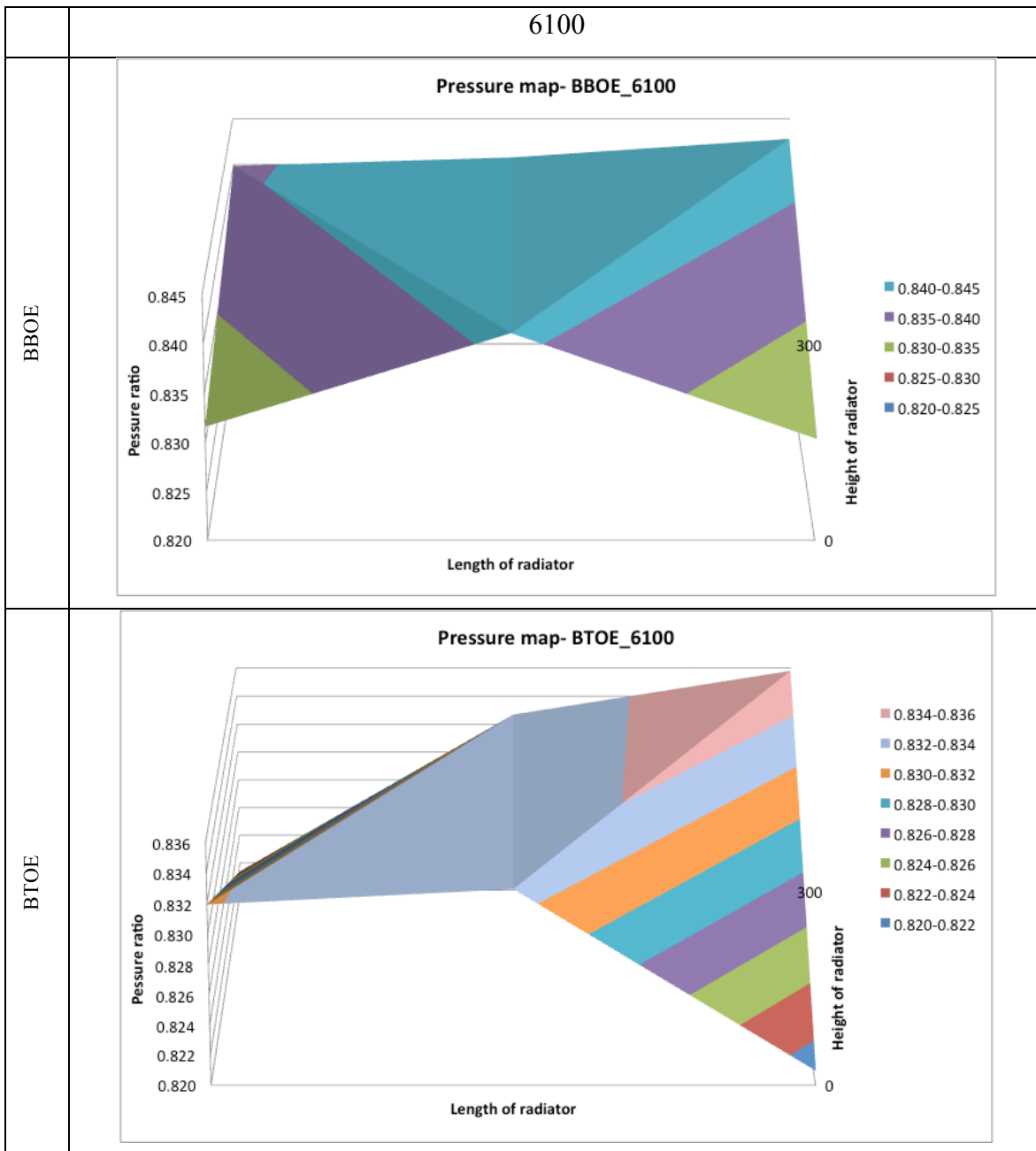


Figure 6-14 Normalised pressure variation analysis in 6100 radiator

Lowest pressure is at the outlet, but pressure in the radiator just upstream of the outlet is comparable to the pressure observed just downstream of the inlet. In both flow configurations, top right hand corner has the highest pressure, suggesting that flow is restricted to this zone.

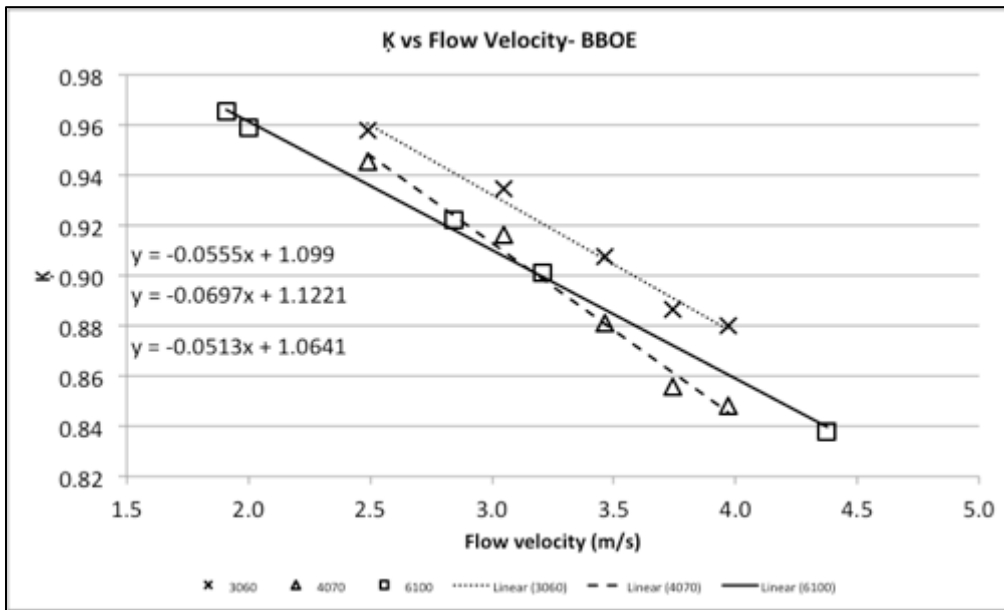


Figure 6-15 Pressure distribution co-efficient vs flow velocity for 3 radiators- BBOE

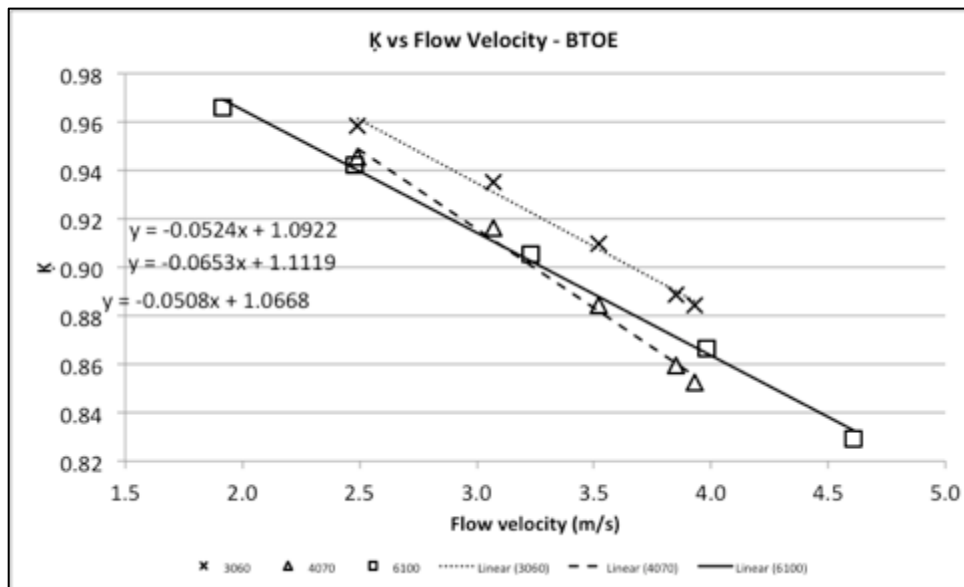


Figure 6-16 Pressure distribution co-efficient vs flow velocity for 3 radiators - BTOE

In Figure 6-15 pressure co-efficient for 3060, 4070 and 6100 radiators are compared over the range of flow velocities in BBOE configuration. To highlight the differences, Y-axis scale has been modified to a lower range. 3060 radiator has higher values for pressure distribution co-efficient compared to 4070 and 6100 for given flow rate. At higher velocities 4070 radiator has the lowest pressure distribution ratio of the three radiators. All three radiators have a similar trend with comparable slopes of -0.0555, -0.0697 and -0.0513 for 3060, 4070 and 6100 respectively. The three radiators also show higher pressure distribution ratio co-efficient at lower flow velocities, suggesting an even flow distribution. On an average 3060 radiator has 2.22% higher pressure distribution ratio co-efficient than the

pressure distribution ratio co-efficient for a 6100 radiator and 2.86% than the pressure distribution ratio co-efficient for a 4070 radiator. On average pressure distribution ratio co-efficient in a 4070 radiator is 0.67% lower than the pressure distribution ratio co-efficient in a 6100.

In Figure 6-16 pressure co-efficient for 3060, 4070 and 6100 radiators are compared over the range of flow velocities in BTOE configuration. Similar to BBOE configuration, 3060 radiator has higher pressure distribution ratio co-efficient than 4070 and 6100 across all flow velocities. The slopes of the trend lines in BBOE and BTOE are comparable. Comparing pressure distribution ratio coefficient for each flow velocity in BBOE and BTOE configuration, it can be seen that the variation is only 0.47%, 0.44% and 0.51% for 3060, 4070 and 6100 radiator respectively. Based on this it can be concluded that the flow configuration does not influence the pressure distribution ratio coefficient.

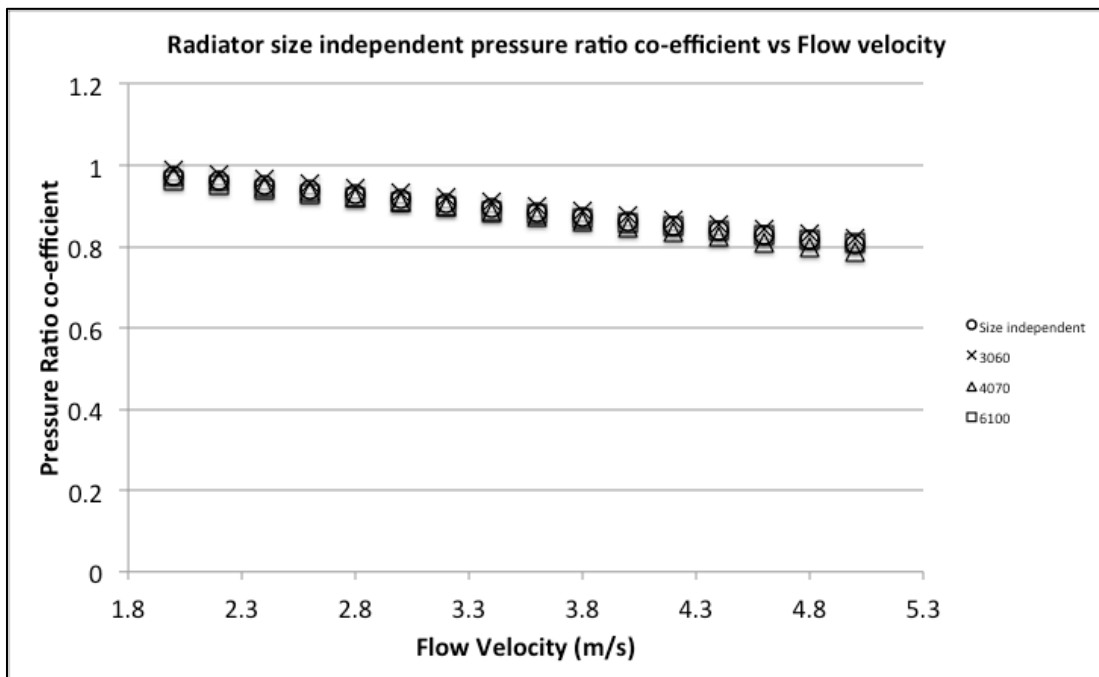


Figure 6-17 Pressure distribution ratio co-efficient as function of flow velocity independent of radiator size and flow configuration

During heating system design for a built environment and radiator selection and for a given room, this is equation would help quantify the pressure variation and consequently the flow and temperature distribution in a radiator. It is desirable to have even flow distribution in order to achieve good temperature distribution. In Figure 6-17, pressure distribution ratio co-efficient independent of radiator size and flow configuration has been developed and compared to individual radiator pressure distribution ratios over range of flow velocities. This has been done to quantify any deviations of the new empirical relationship between

pressure distribution ratio co-efficient and radiator size to the values computed by the numerical analysis. Taking an average of the ratios across three radiators at a flow velocity has developed the size independent pressure distribution ratio. The trend line generated shows a good correlation to all three radiators. Pressure distribution ratios have a maximum deviation of 2.08%, 2.43% and 1.31% for 3060, 4070 and 6100 respectively. Over the range of flow velocities, comparing the pressure distribution ratios co-efficient calculated from the equation generated in Figure 6-15 and size independent pressure distribution ratio co-efficient equation in Figure 6-17 an average deviation of 1.72%, 1.19% and 0.53% in 3060, 4070 and 6100 respectively. This suggests a good co-relation. Further comparing the pressure distribution ratio co-efficient from CFD results for the three radiators with the calculated pressure distribution ratio co-efficient a good co-relation is observed with an average deviation of only 1.66%. Flow velocity and the radiator size influence the pressure distribution in the radiator. To achieve an even distribution and low losses a smaller radiator at lower flow velocity is recommended for a BBOE configuration.

6.3.8 Qualitative analysis of velocity variation

Investigations carried out in Section 6.3.6 and 6.3.7 have shown that flow in the radiator geometry is complex. In this section results from the CFD simulation have been reviewed to analyse variation in velocity profiles, distribution, vectors and magnitude across three radiator sizes. As discussed in chapter 3, CFD model is setup with a velocity inlet and a pressure outlet. In Figure 3-8 primary reference planes have been created to capture X, Y and Z velocity profile. XY plane also helps visualise the velocity vector and magnitude as cross the radiator. A further reference plane has been developed to in XZ plane across the mid height of the radiator to review the velocity in individual vertical channels of the radiator. Inlet for all the radiators is on the bottom right. The outlet for BBOE is on bottom left whereas the outlet for BTOE is on top right of the radiator

Plane a_b is a XZ plane central to the bottom horizontal channel

Plane a_b1 is a XZ plane at the bottom of the vertical channels

Plane a_c is a XZ plane at mid height of the vertical channels

Plane a_t1 is a XZ plane at the top of the vertical channels

Plane a_t is a XZ plane central to the top horizontal channel

There are 18, 21 and 36 channels in a 3060, 4700 and 6100 radiator respectively.

X is in horizontal direction – flow to right is positive vector, left is negative vector

Y is in vertical direction – Upward flow is positive vector, down ward is negative vector

Z is perpendicular to the XY plane

6.3.8.1 X- Velocity profiles across the radiator- 8mm

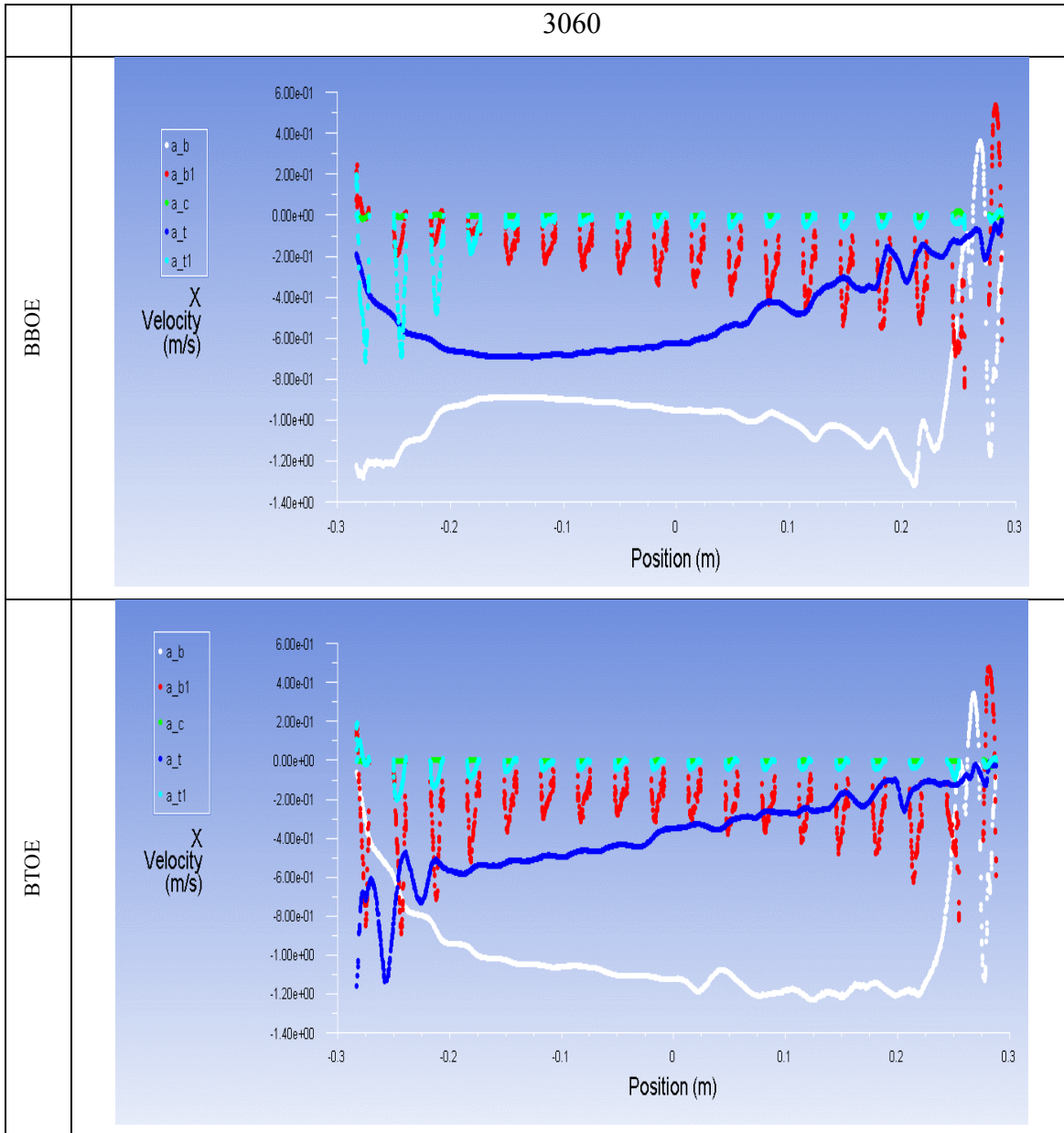


Figure 6-18 X - Velocity profiles in a 3060 radiator

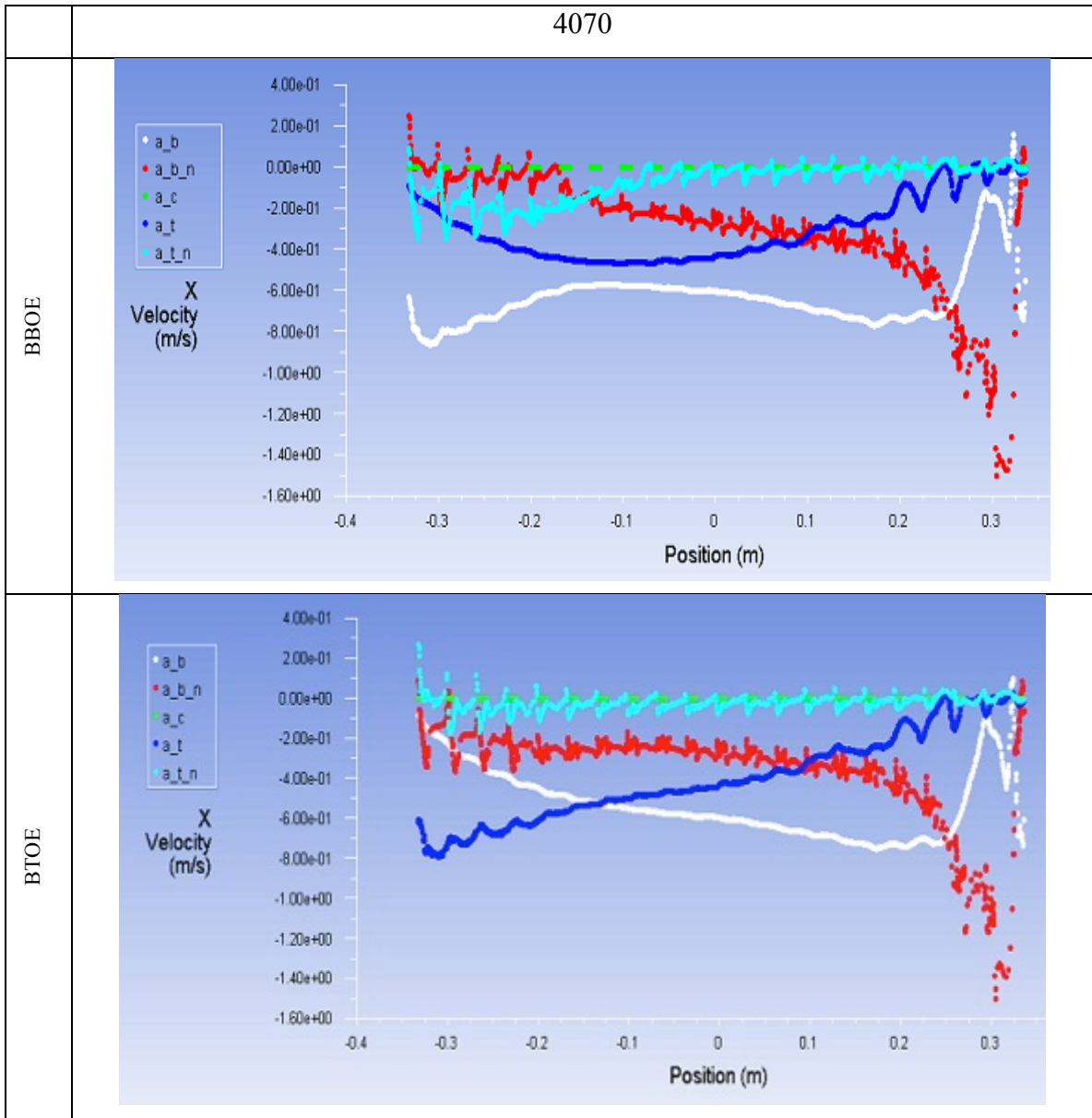


Figure 6-19 X- Velocity profiles in 4070 radiator

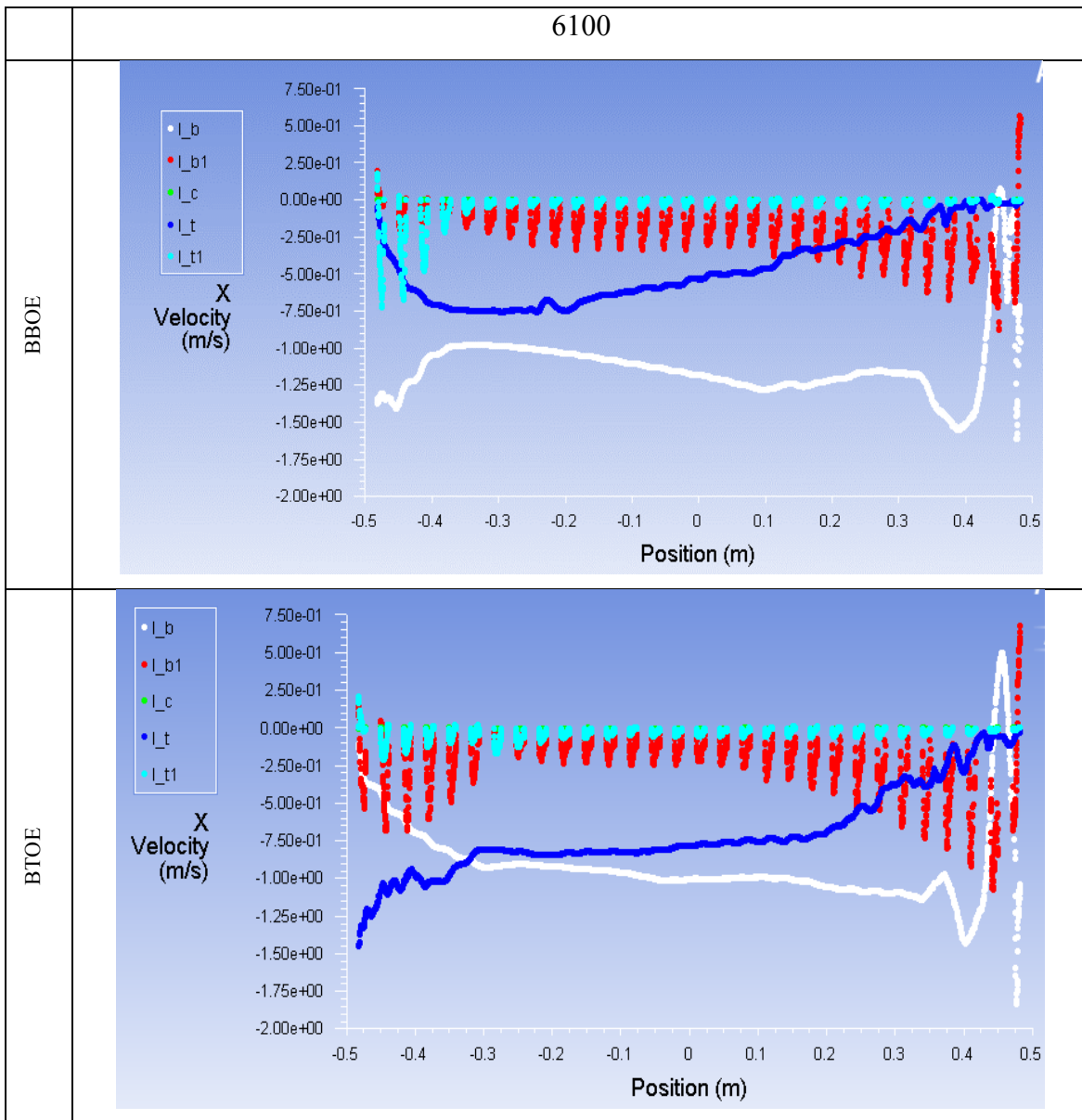


Figure 6-20 X velocity profiles in a radiator

In Figure 6-18, Figure 6-19 and Figure 6-20 velocity profiles in the three radiators are studied. The graph shows the velocity in x direction along the 5 reference planes shown in Figure 3-8. X velocity is along the length of the radiator. It can be seen that for a given flow configuration the three radiators have a similar trend, there is no flow in X direction in the vertical channels (in green). Maximum flow velocity can be observed in the bottom channel in the BBOE configuration with a peak of 1.5 m/s in 6100 1m/s in 4070 and 1.2 m/s in 3060. In the BTOE configuration flow velocity increases in the top horizontal channel towards the exit. In the planes tangential to the vertical channels there is minimal flow in X direction.

6.3.8.2 Y- Velocity profiles across the radiator- 8mm

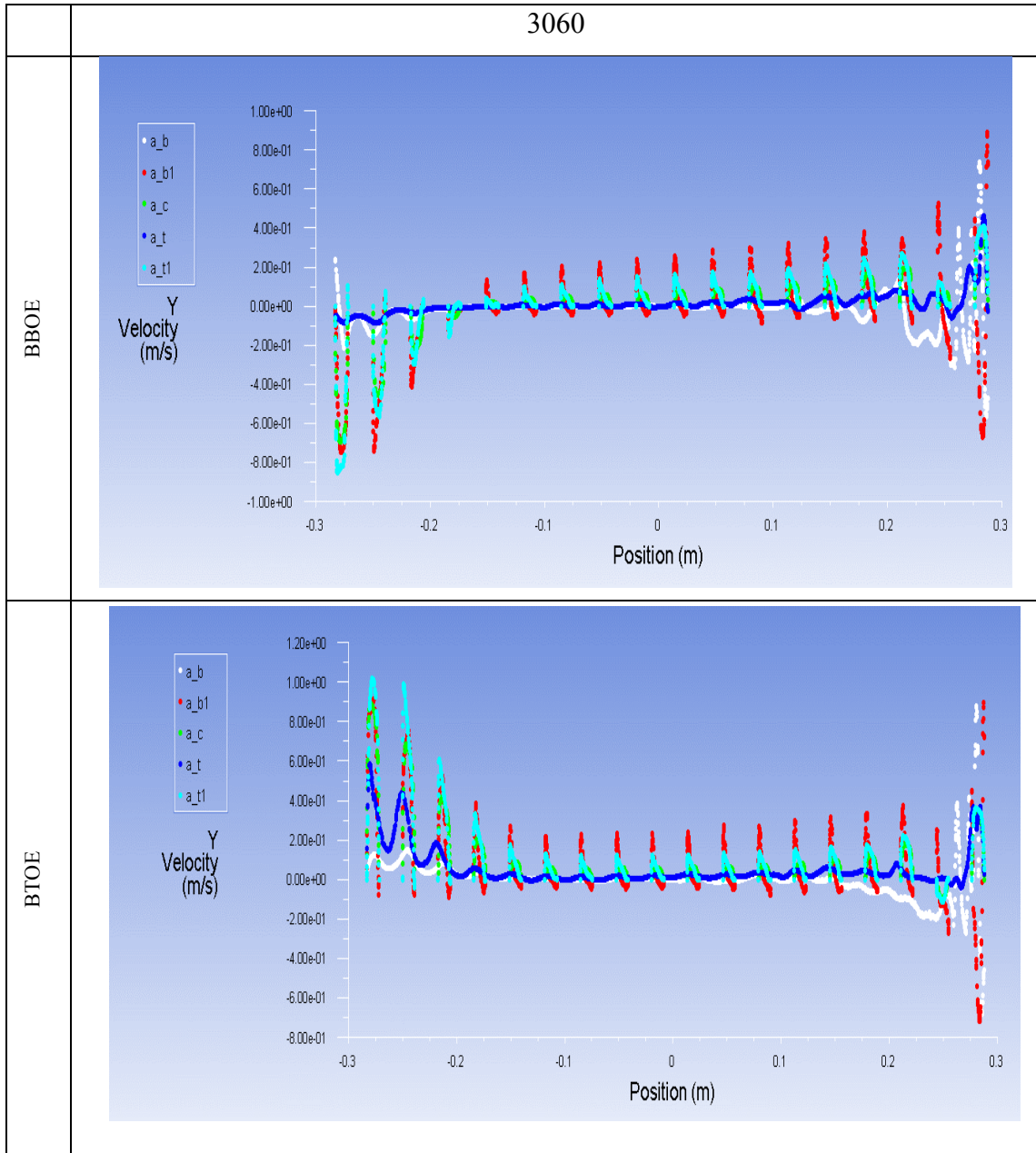
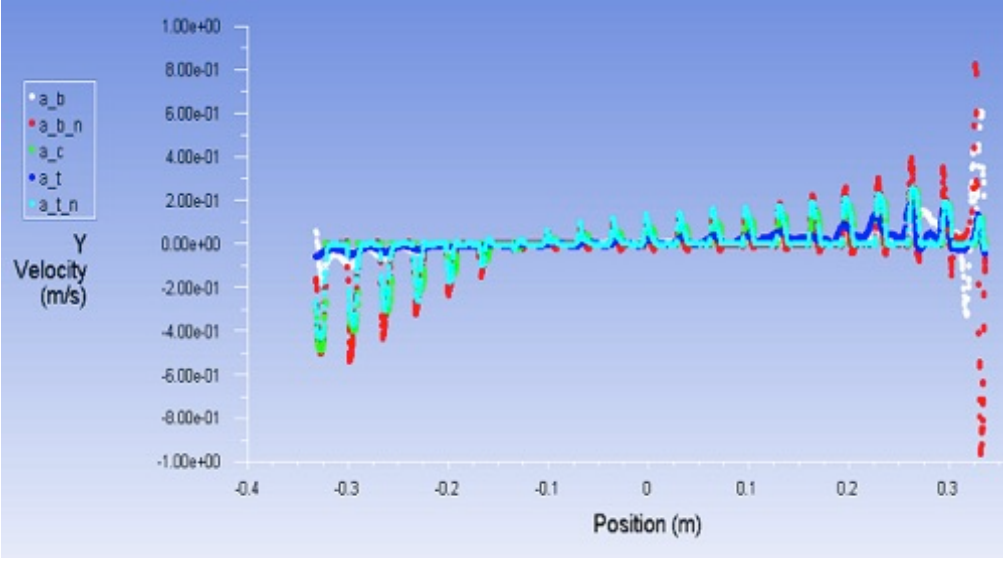


Figure 6-21 Y- Velocity profiles in 3060 radiator

4070

BBOE



BTOE

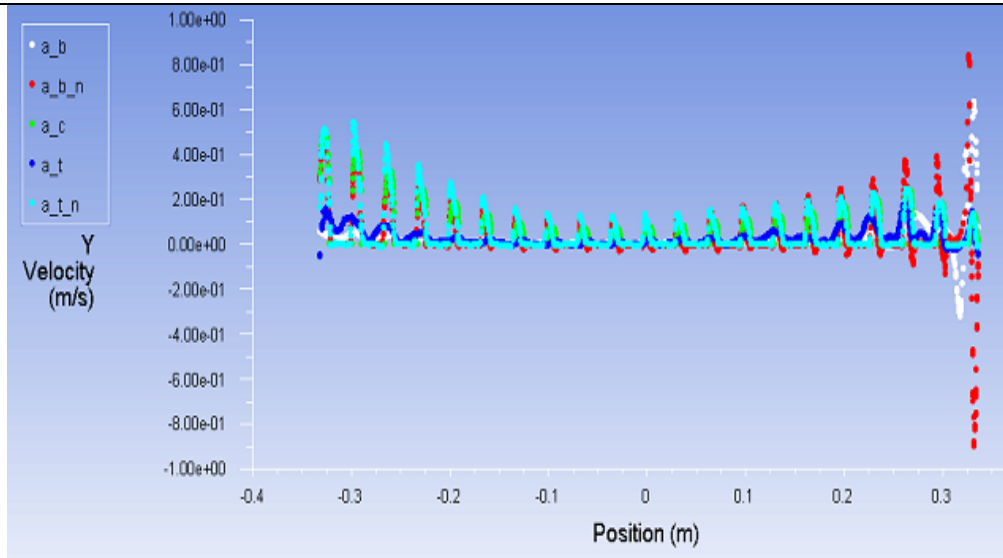


Figure 6-22 Y - Velocity profiles in 4070 radiator

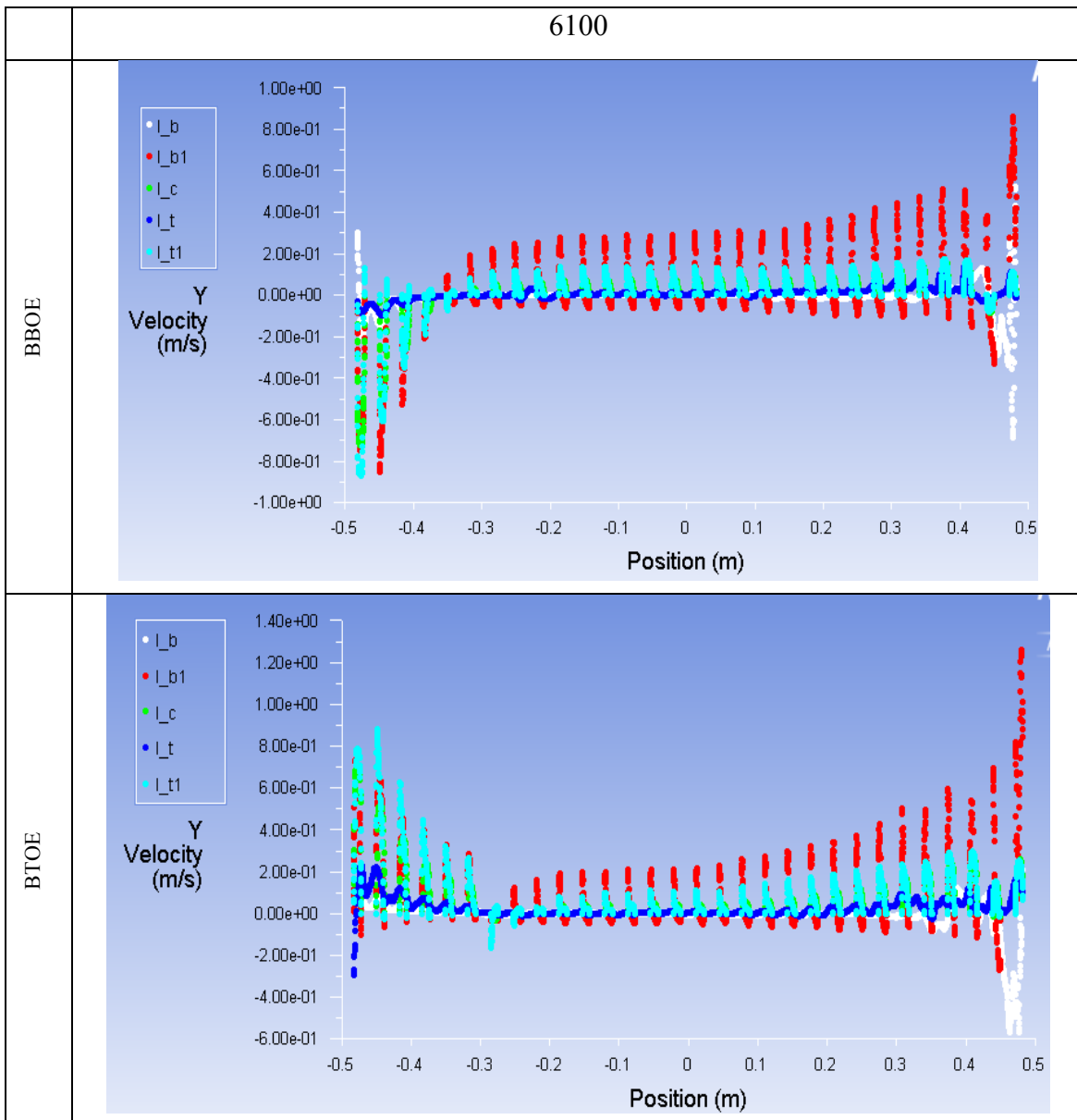


Figure 6-23 Y velocity profiles in 6100 radiator

In Figure 6-21, Figure 6-22 and Figure 6-23 Y velocity profiles in the three radiators are studied. The graph shows the velocity in Y direction along the 5 reference planes. Y velocity is along the height of the radiator. In BBOE and BTOE there is no flow in vertical direction in the plane a_b and a_t, which are central to the bottom and top horizontal channels. In BBOE maximum velocity is seen in the first and last vertical channel in all three radiators, where the velocity is approximately 0.8 m/s. In BTOE maximum velocity is in the first channel where it reaches 1.2 m/s in 6100, 0.9 m/s in 4070 and 0.85 m/s in 3600 radiator. BBOE and BTOE layout are significantly different across all three, radiator size. There is no flow in down ward direction in the BTOE configuration. Approximately central 200 mm of the 4070 radiator has negligible flow in both BBOE and BTOE. This suggests that the resulting temperature distribution will not be uniform and will lead to cold spots.

3060 and 6100 radiators also have a maximum velocity of 0.4 m/s in the mid vertical channels in BBOE.

6.3.8.3 Z- Velocity profiles across the radiator - 8mm

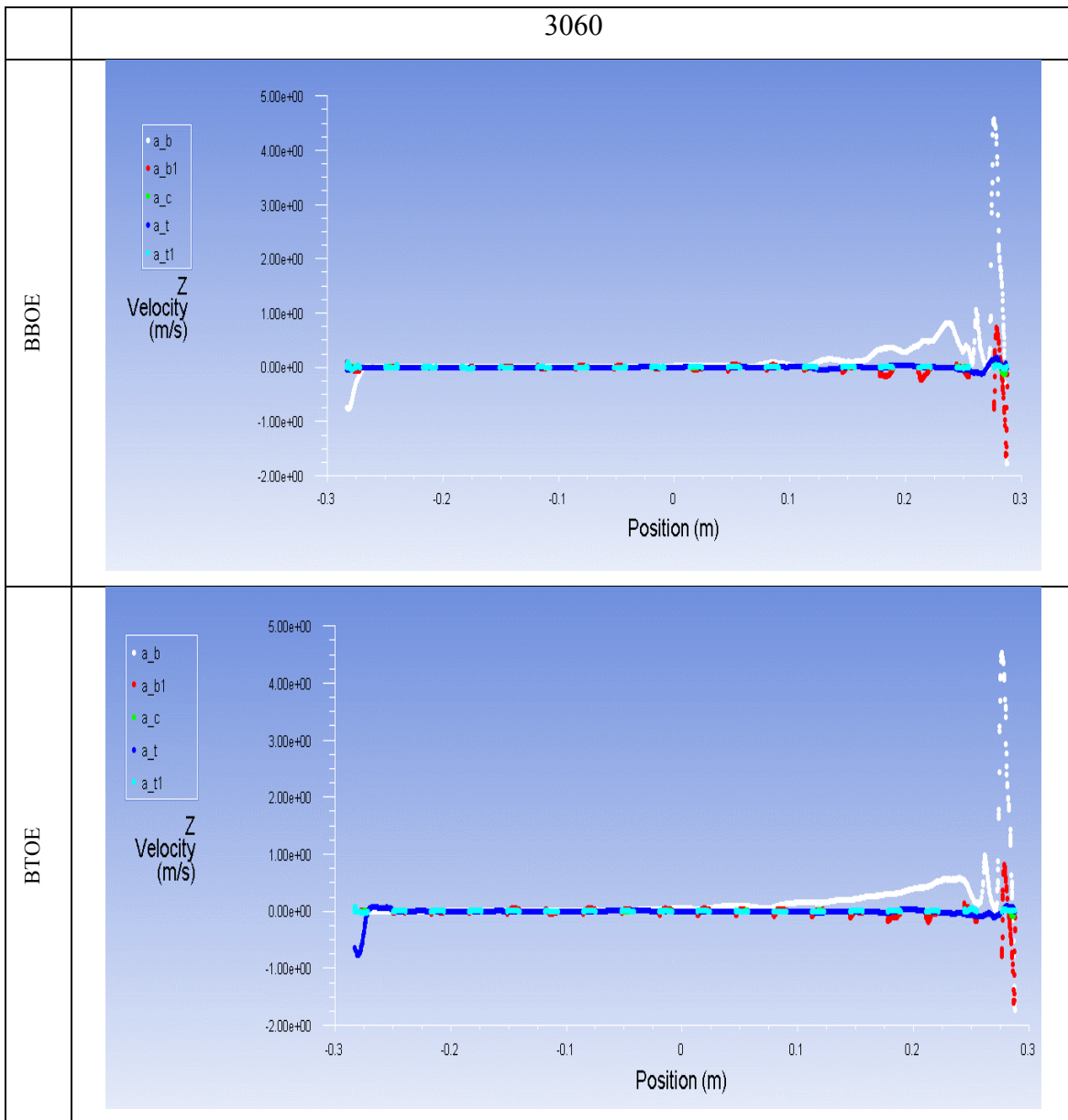
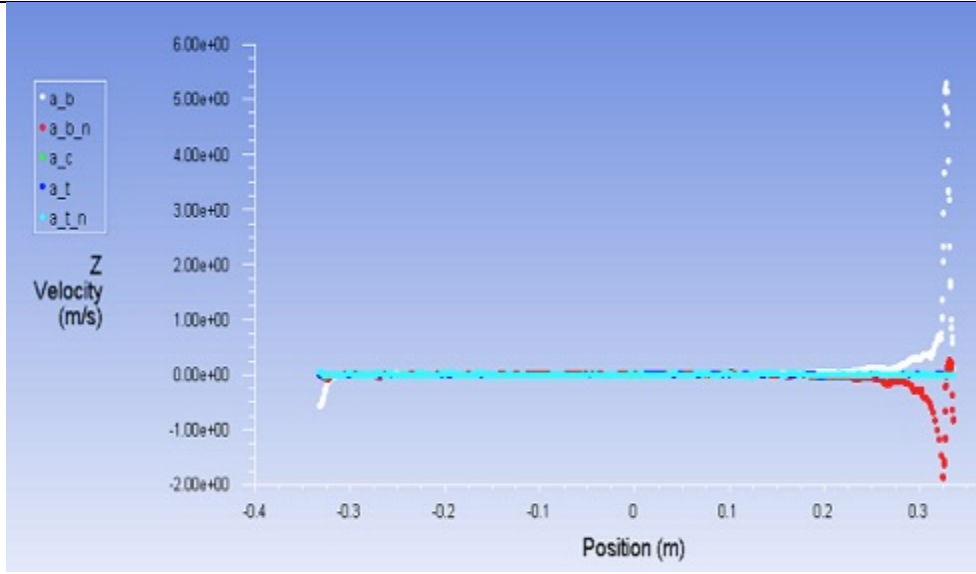


Figure 6-24 Z - Velocity profiles in 3060 radiator

4070

BBOE



BTOE

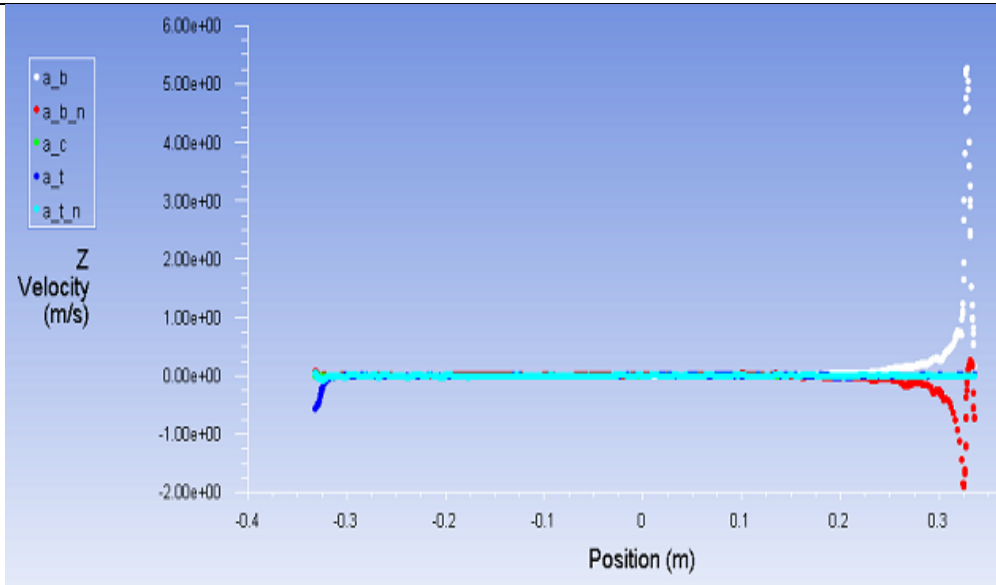


Figure 6-25 Z -Velocity profiles in 4070 radiator

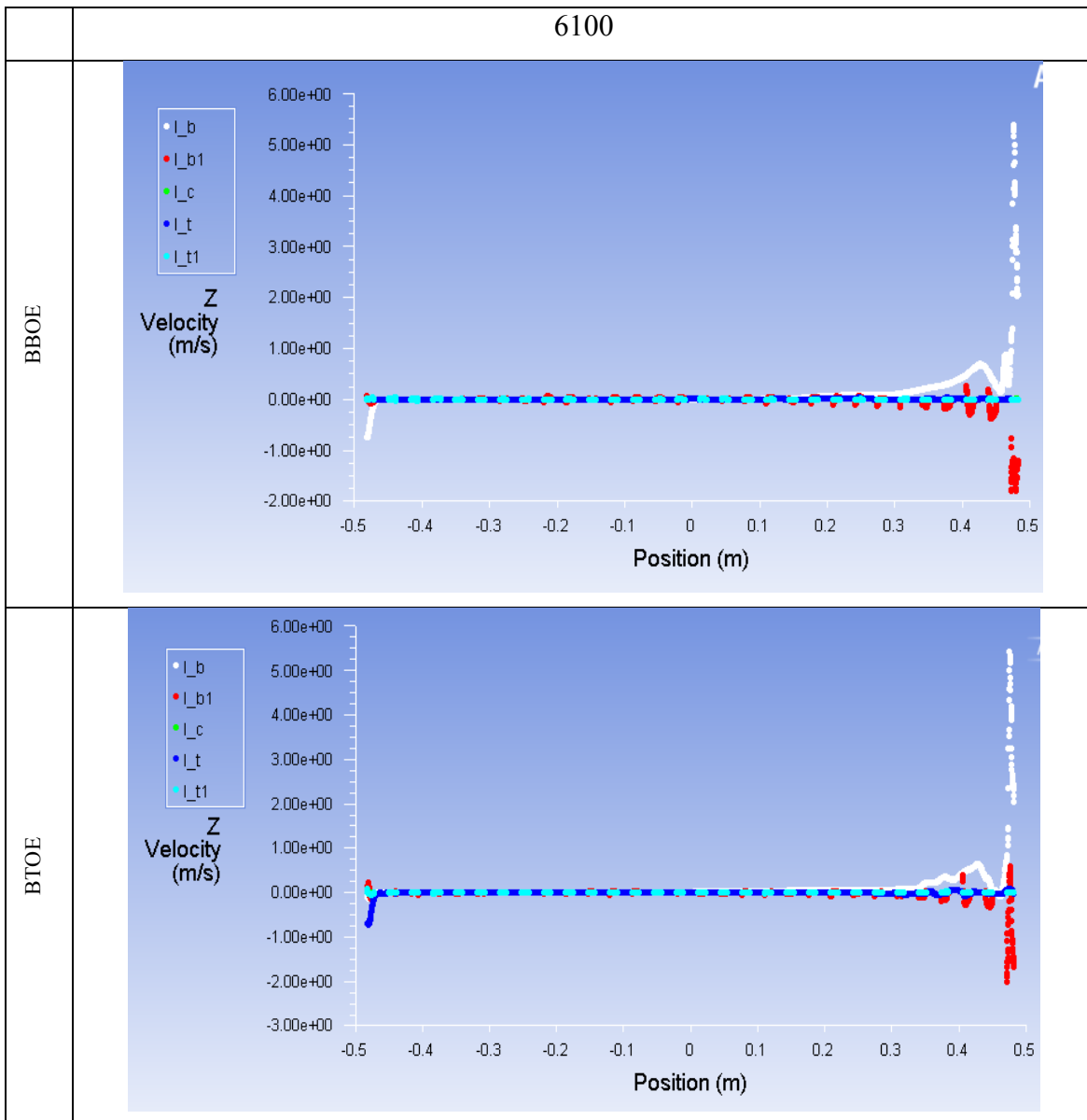


Figure 6-26 Z velocity profiles in 6100 radiator

In Figure 6-26 Z velocity profiles in the three radiators are studied. The graph shows the velocity in Z direction along the 5 reference planes. Z velocity is perpendicular to the XY plane of the radiator. In both BBOE and BTOE there is no flow in in Z direction in most of the channels. Hence based on Figure 6-20, Figure 6-23 and Figure 6-26 it can be concluded that the flow in the vertical channels is only in Y direction. The plane a_b shows up to 5 m/s flow velocity in the + Z direction. This is primarily due to the flow into the radiator from the inlet port located at the bottom right of the radiator in both flow configurations. In BBOE configuration a small rise in velocity can be observed in the bottom central plane close to the exit port. Similarly in BTOE configuration a small raise of 0.5 m/s can be observed in the top central plane close to the exit port. In both cases the vales are negative indicating the flow is away from central XY plane.

6.3.8.4 Y- Velocity distribution in the central plane – 8mm

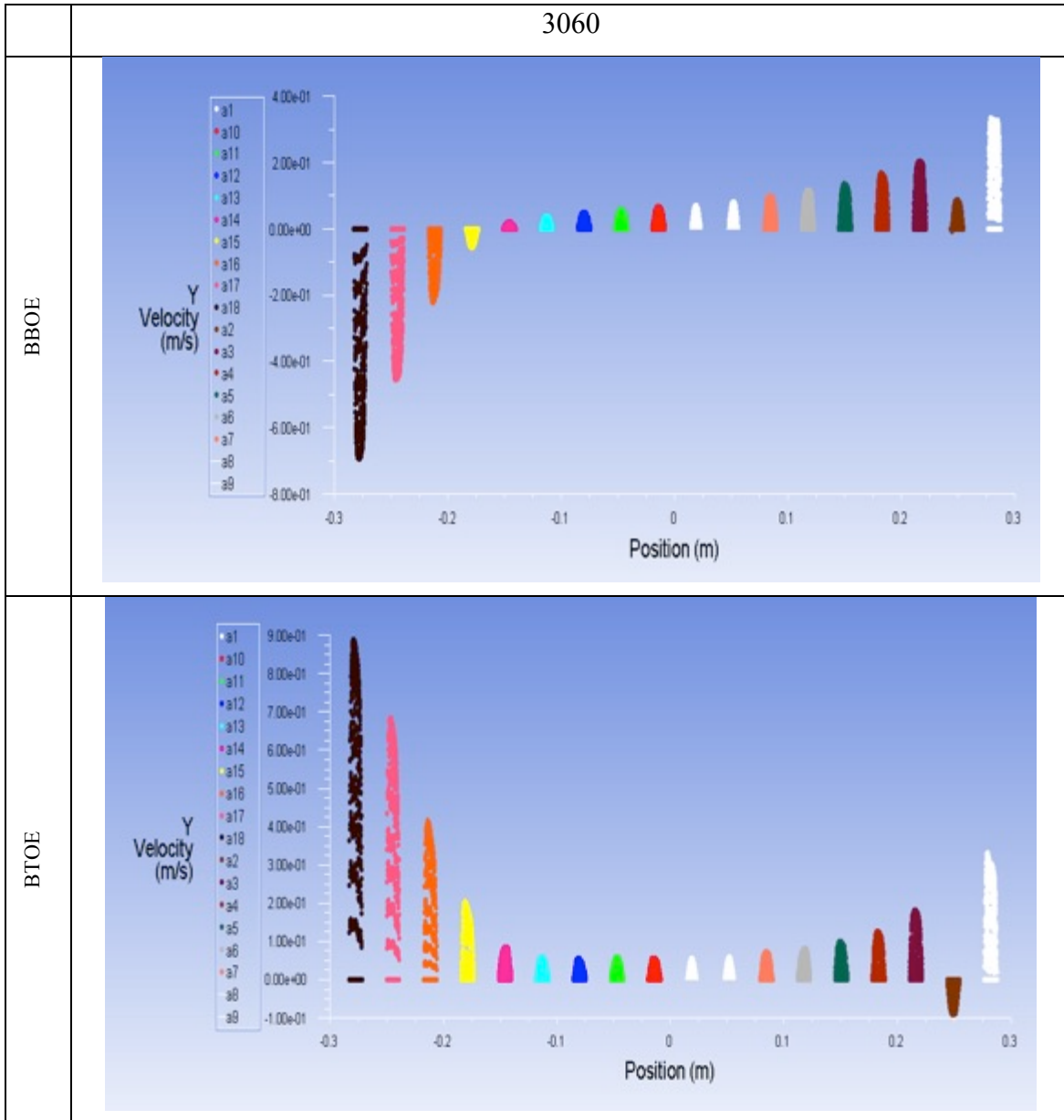


Figure 6-27 Y Velocity distribution along the central plane in 3060 radiator

Comparing the Y velocity distribution for a 3060 radiator in BBOE configuration to the temperature distribution in Figure 5-6 it can be seen that there is a good co-relation. The vertical channels (on either end of the radiator), which show high temperature, correspond to the channels with higher velocity distribution and the cold spots match with the channels with low velocity in the channels.

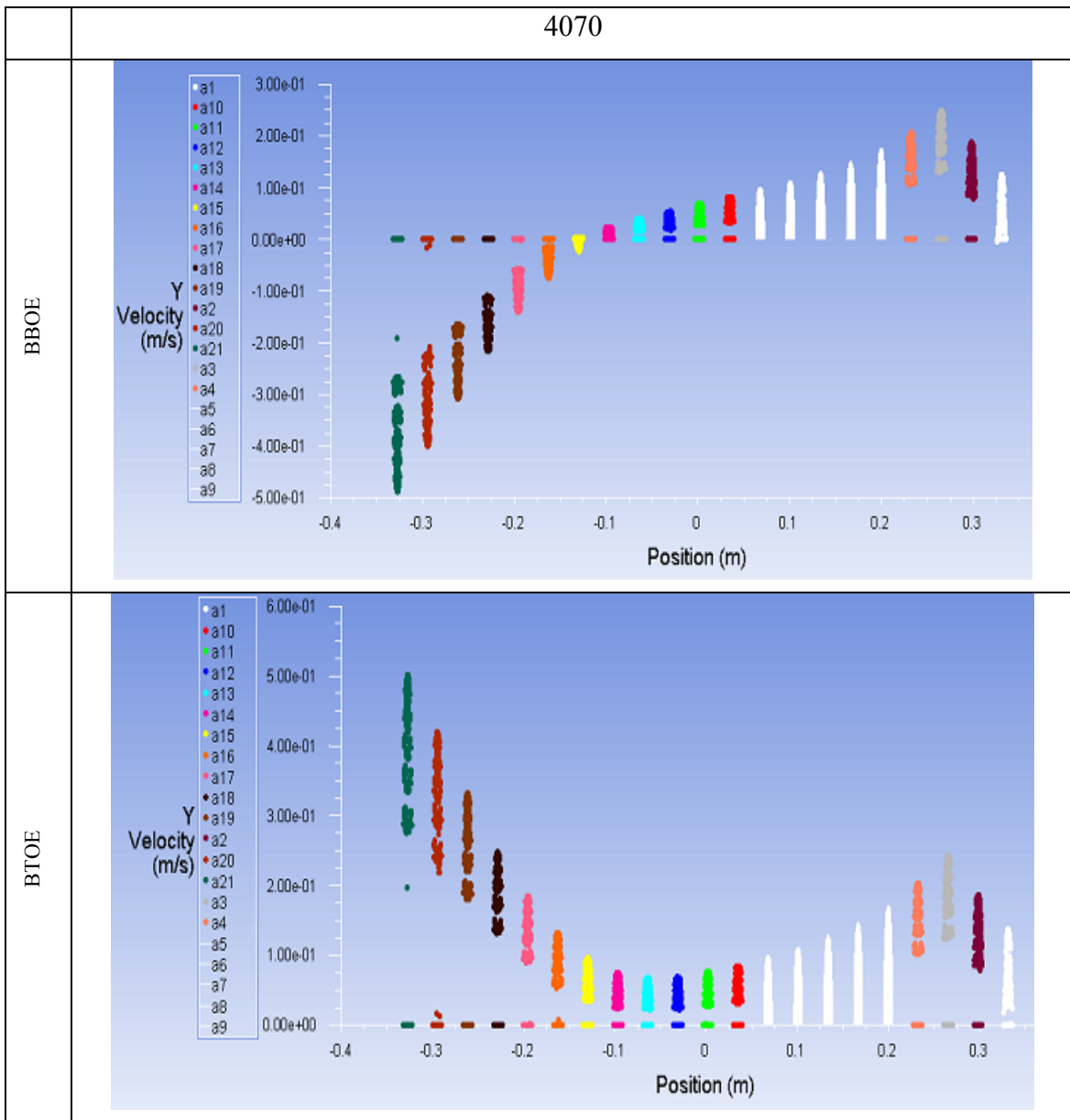


Figure 6-28 Y velocity distribution along central plane in 4070 radiator

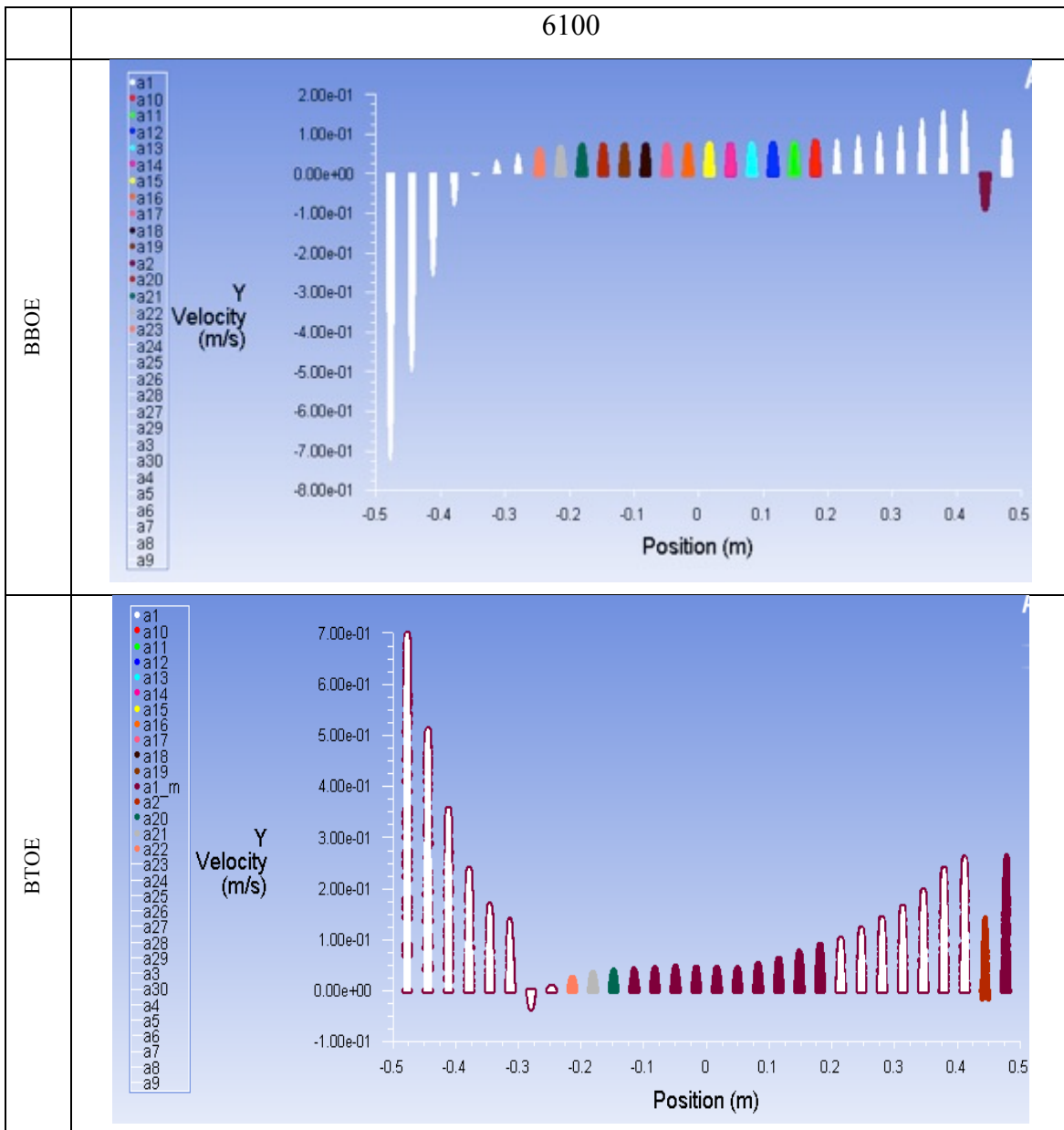


Figure 6-29 Y velocity distribution along central plane in 6100 radiator

In Figure 6-27, Figure 6-28 and Figure 6-29 velocity distribution in the Y direction from the central reference plane are studied in the three radiators. Y velocity is along the height of the radiator. It is very evident from the graphs that in BTOE configuration above the central reference plane, the flow is in the upward direction in majority of the vertical channels. In BBOE configuration, 83% of the channels have the flow going up with only 17% with downward flow, which are closer to the outlet. Similarly in 6100 over 80 % have flow going up with the last 4 channels having flow going down. Peak velocity in the radiator is on the last channel, closer to the exit port. In BBOE the configuration, 0.7 m/s, 0.5 m/s and 0.7 m/s are recorded in the last vertical channel for 3060, 4070 and 6100 respectively. Similarly in BTOE configuration, 0.9 m/s, 0.5 m/s and 0.7 m/s are the peak velocities recoded for 3060, 4070 and 6100 respectively. The cross sectional area of each of the vertical channels for all

three radiators is the same. Hence the hydraulic diameter is the same. Using Equation 5-5, hydraulic diameter for the hexagonal vertical channel with 7mm sides is 0.0122 m. Reynolds number for each radiator in BBOE and BTOE configuration is given in Table 6-5. Based on the calculated Reynolds it can be seen that the flow is turbulent.

	Reynolds number (BBOE)	Reynolds number (BTOE)
3060	8641.4	10878.9
4070	6043.9	6043.9
6100	8641.4	8641.4

Table 6-5 Peak Reynolds number in vertical channels

6.3.8.5 Velocity magnitude contours – 8mm

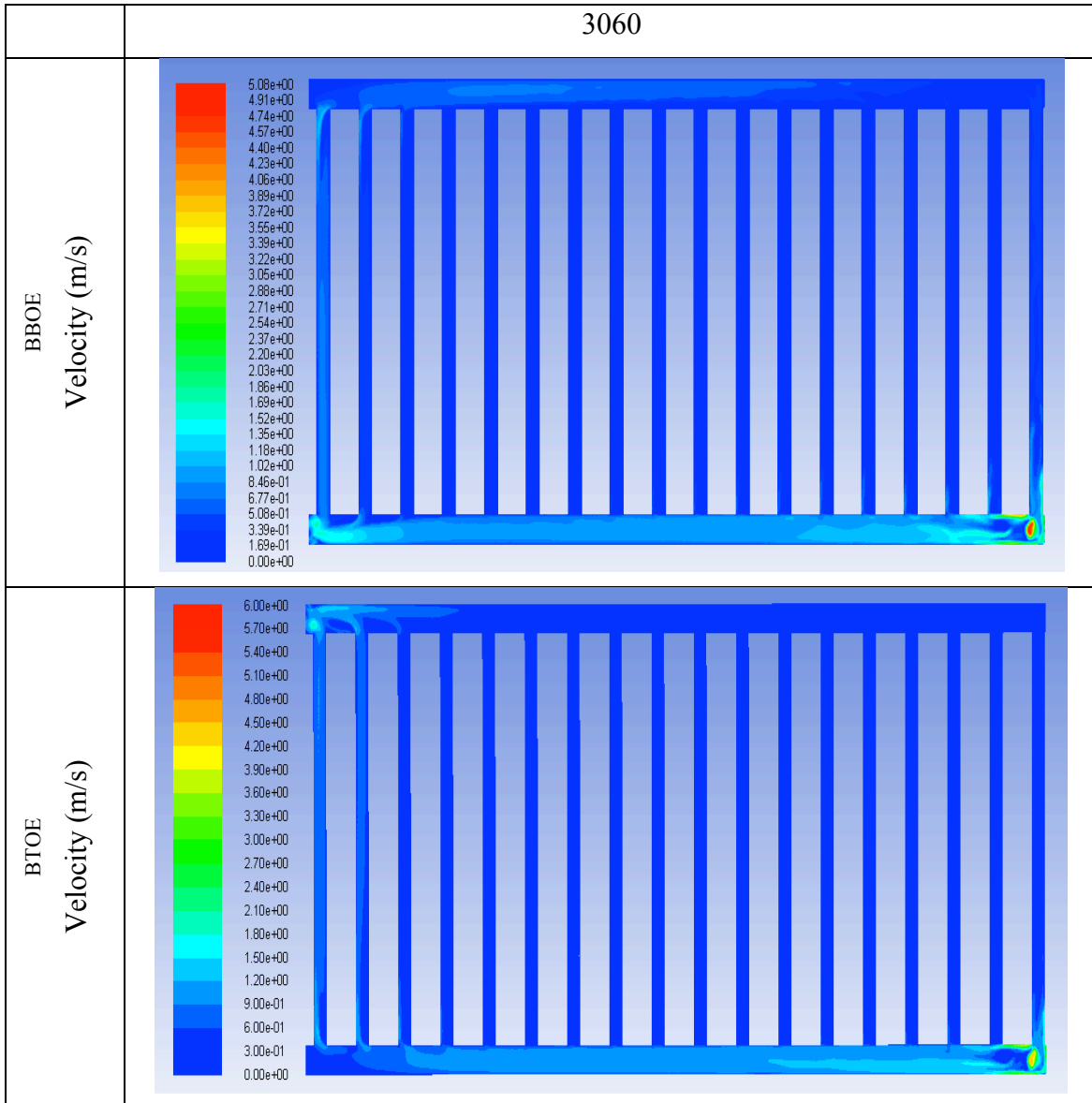


Figure 6-30 Velocity magnitude contours in 3060 radiator

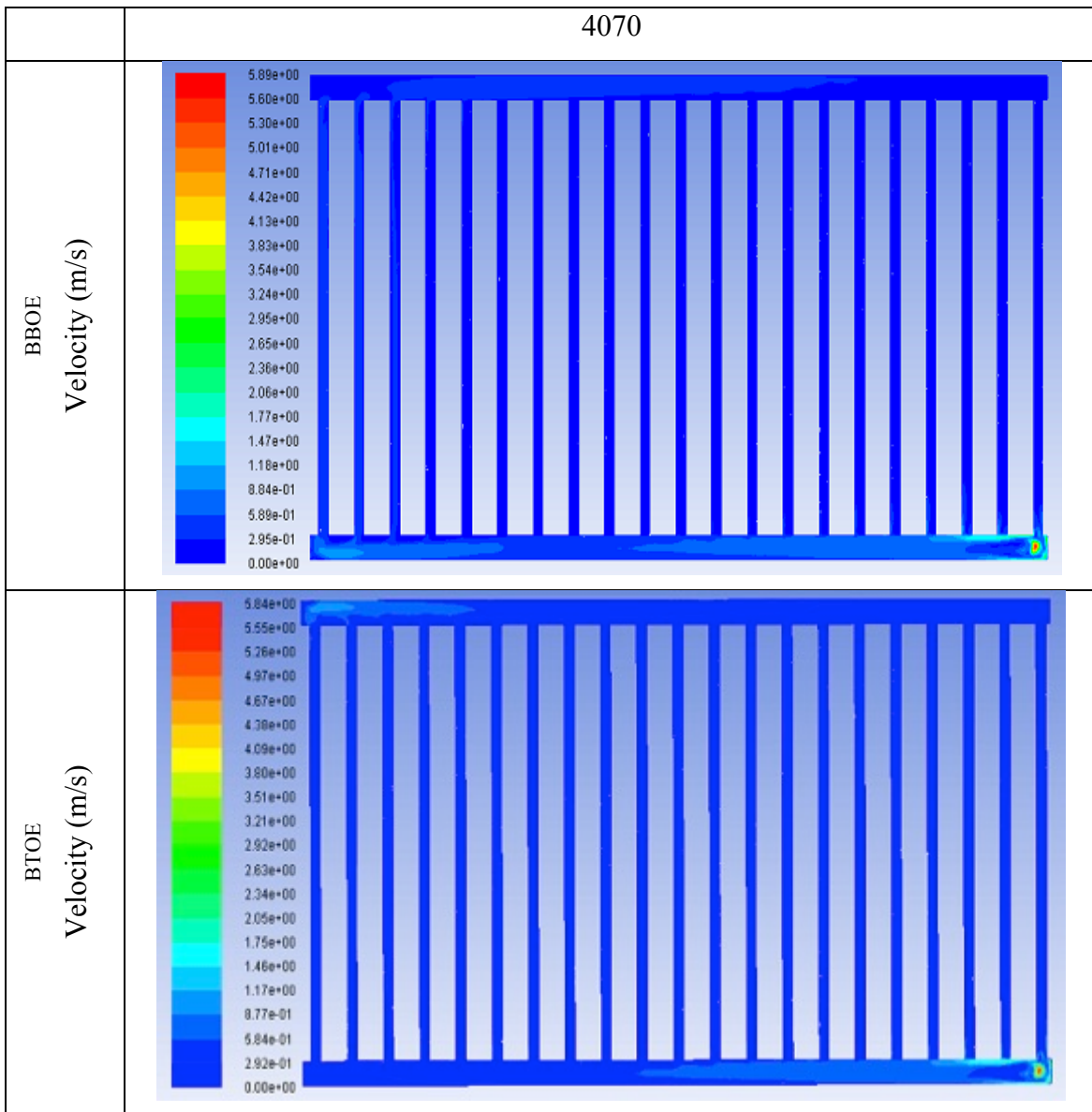


Figure 6-31 Velocity Magnitude contours in 4070 radiator

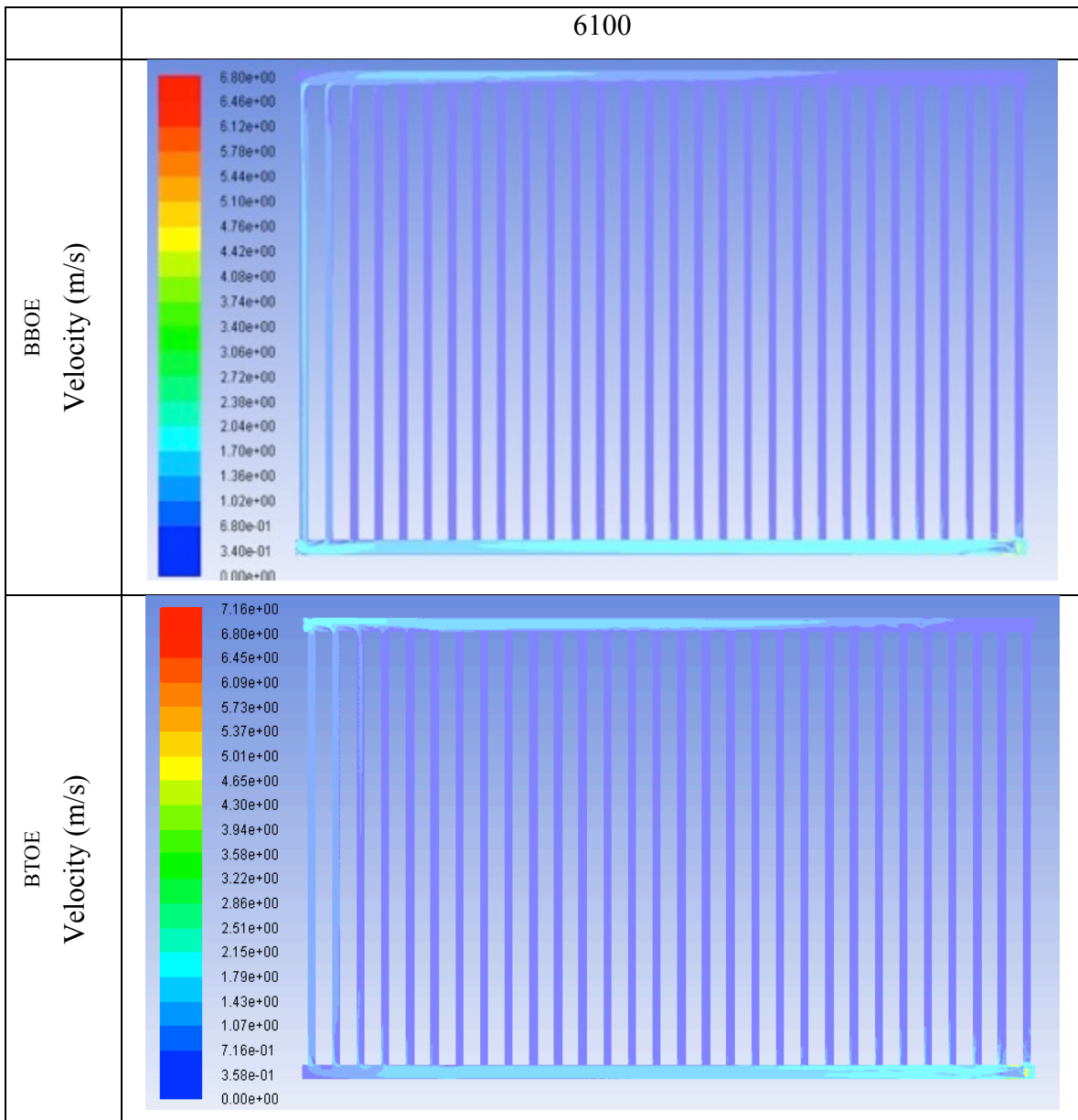


Figure 6-32 Velocity magnitude contours in a 6100 radiator

In Figure 6-30, Figure 6-31 and Figure 6-32 velocity magnitude in the three radiators are studied. The graph shows the velocity magnitude in the XY reference plane, which is central placed to capture the flow distribution. Maximum velocity is observed at the inlet as the fluid enters the radiator from a 8mm inlet port. In a 6100 radiator, average velocity across the inlet face is 4.5 m/s and as the distance from the inlet increases velocity in the vertical channels drops. Lowest velocity of 0.0039 is recorded in the channel 23 of the 6100 radiators. Majority of the channels have a low velocity with an average of 0.07 m/s, 0.12 m/s and 0.01 in 6100, 4070 and 3060 respectively. As discussed earlier, velocity distribution, directly impact the temperature distribution.

6.4 Quantifying the effect of inlet and outlet port diameter

As discussed in chapter 2 Ward's [29] work has identified that lower flow rate results in mixing of circulated water and the supply hot water. Also lower flow rate results in lower return temperature, which enhances the problem. Giesecke [30] has found that in a central heating radiator frictional head loss increases with the increase in flow rate. In section 6.3 effect of radiator size on pressure loss and pressure distribution have been quantified, where loss co-efficient increases with increase in radiator size and pressure variation increases with increase in flow rate. Hence it is important to investigate other geometric parameters that may influence the flow. As per Equation 5-1, in a straight pipe head loss is indirectly proportional to hydraulic diameter of the pipe.

Review of standard radiators in central heating systems has shown that the geometry of the inlet and outlet ports is complex and affects the flow distribution in the radiator. In this section the effect of diameter of the inlet and outlet ports has been investigated. In order to quantify the influence, a 300mm x 600mm radiator is used with 5 flow rates, 2 flow configurations and three inlet port diameters. Both inlet and outlet diameters have been kept the same for the three diameters investigated. In a stand-alone radiator, a standard panel radiator with modified T joints is used, which is manufactured in Turkey. The inlet and outlet connections to a radiator are made to a T joint which is a ½" BSP standard fitting. The T joint is welded to the panels where a circular flow distribution port is fixed between the two plates of a panel. In the investigation the geometry (diameter) of the ports are modified to reduce pressure drop and improve pressure distribution

6.4.1 Geometry of the ports

6mm port design – The port in a baseline design (used in current stand-alone radiators) is a 25mm diameter circular disc with an 8 mm diameter cutout in the centre. The height of the disc is 11 mm. Five 3 mm holes are drilled around the perimeter. Water enters the port from the T joint through the 8 mm hole and disperses radially towards the 3 mm holes to enter the channels of the radiator. The radial holes help distribute the flow in X and Y direction but provide a hydraulic diameter of 6mm.

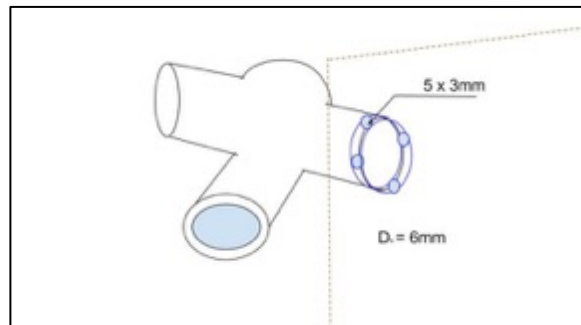


Figure 6-33 6mm port diameter

8mm port design – The height of the disc is previous design is 11 mm (restricted by radiator dimension) and a 3mm hole allows only 3.5 mm to the edge of the disc. In order to increase the effective hydraulic diameter compared to the above design, hole sizes on the disc have to be increased and this cannot be achieved due to manufacturing constraints. Hence in this design the circular disc is eliminated allowing the water to enter the radiator panels from the T-joint directly through an 8 mm hole. This design reduces the restriction in the flow path compared to the base design giving a hydraulic diameter of 8mm.

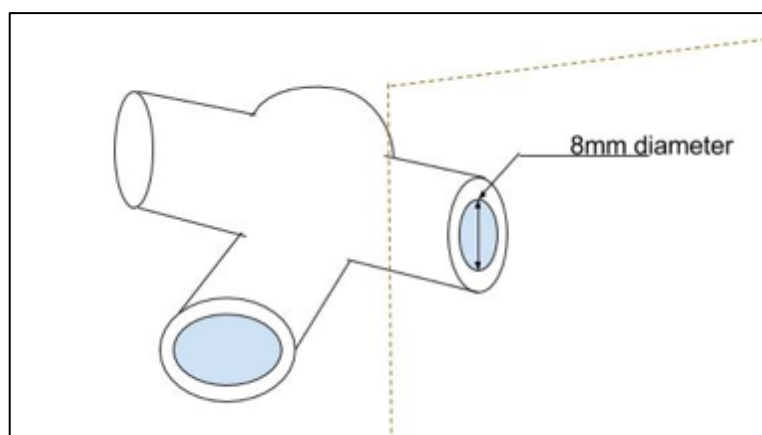


Figure 6-34 8 mm port diameter -CFD

12mm port design – This design is similar to the 8 mm port design where the circular disc is eliminated but the inlet and outlet diameter is increased to 12 mm. The stand-alone system uses 15 mm copper pipes, which have an inner diameter of 12 mm. As copper pipe is fixed to the T-joint with a 12 mm ID brass connector the design aims to eliminate sudden change in hydraulic diameter and potentially reduce pressure loss for a given flow rate and improve pressure variation.

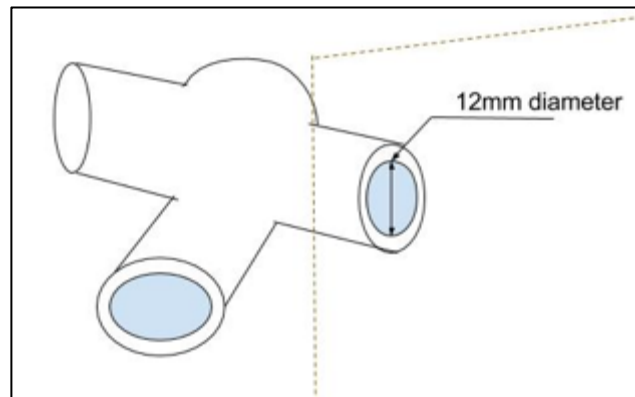


Figure 6-35 12mm port diameter -CFD

6.4.2 Analysis of port diameter on pressure drop in a system

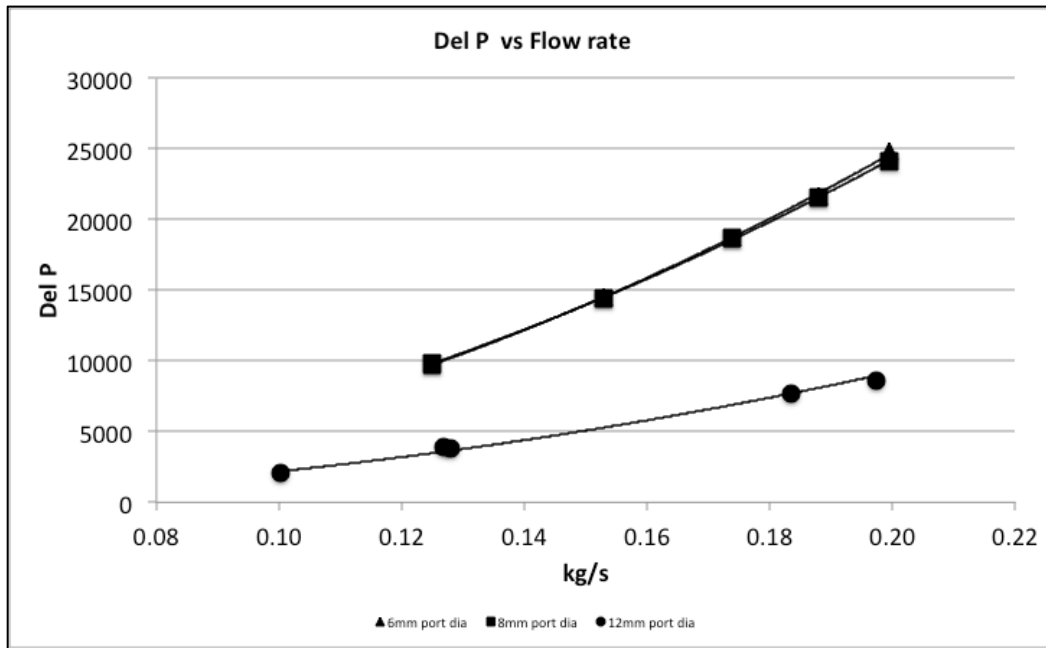


Figure 6-36 Pressure drop across radiator vs flow rate with change in port diameter

Figure 6-36 shows the variation of pressure drop across a radiator with change in flow rate for three different port diameters for a 3060 (300 mm x 600 mm) radiator. The data for base line (6 mm port diameter) have been calculated by taking a small difference in the CFD and experiments in to account and a combined trend has been shown. The difference between the 6mm and 8mm is minimal but the variation in values for the radiator with 12 mm port diameter is significant. For the same flow rate velocity decreases as the diameter and or area increase. An average of 173% lower pressure drop is observed in the radiator with 12 mm port diameter. Lower pressure drop across the radiator is beneficial to reduce the pumping power in the system.

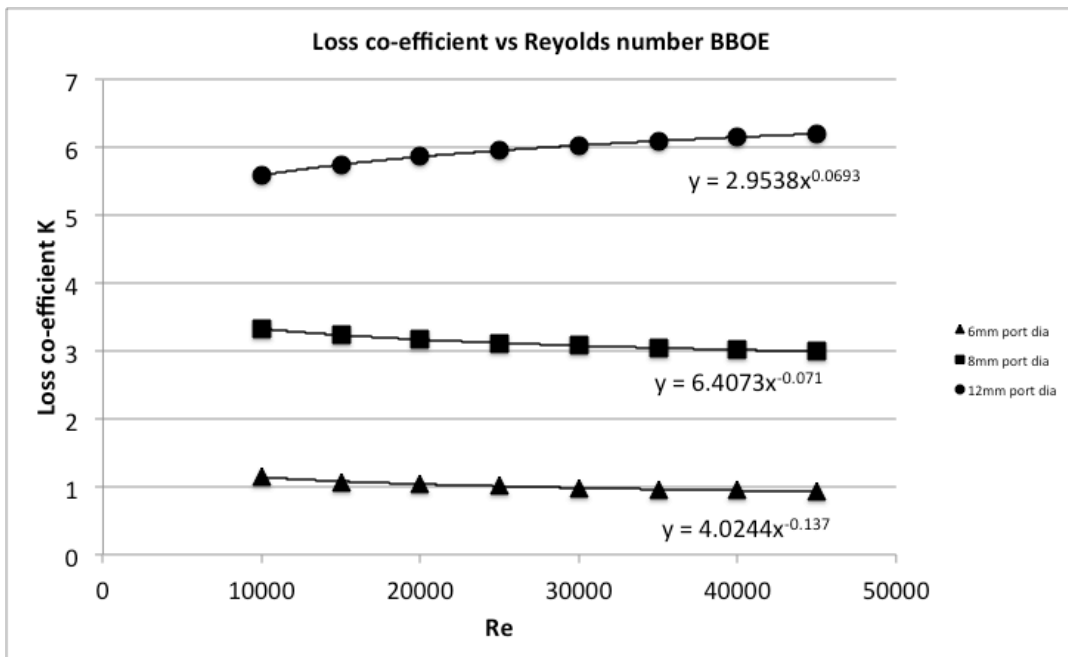


Figure 6-37 Effect of port diameter on loss co-efficient in a radiator

In Figure 6-37 loss co-efficient of the radiator is compared for three different port diameters over a range of Reynolds number in BBOE configuration. As discussed in section 6.3.6, loss co-efficient is constant for a given port diameter over the range of Reynolds number. However the value of loss co-efficient K does change with change in port diameter. Loss co-efficient increases with increase in port diameter. As discussed in previous section, increase in port diameter decreases the velocity. K is inversely proportional to the square of velocity. Hence with the increase in port diameter, velocity reduces and K increases.

Radiator with 8 mm port diameter has higher K values compared to a radiator with 6 mm port diameters by an average of 214%. Port diameter of 12 mm has significantly higher K values compared to a 6 mm port diameter radiator by 481%. K values vary by 85% between a radiator with 8 mm and 12 mm port diameter. This is mainly due to the effect of port diameter on flow velocity. As the port diameter increases flow velocity reduces for the same mass flow rate.

To quantify the effect of port diameter on loss co-efficient, the values are normalised against loss co-efficient corresponding to 6mm port diameter. Figure 6-38, shows the trend of the normalised values for 8mm and 12 mm port diameter with the reference line of 1 representing port diameter of 6mm.

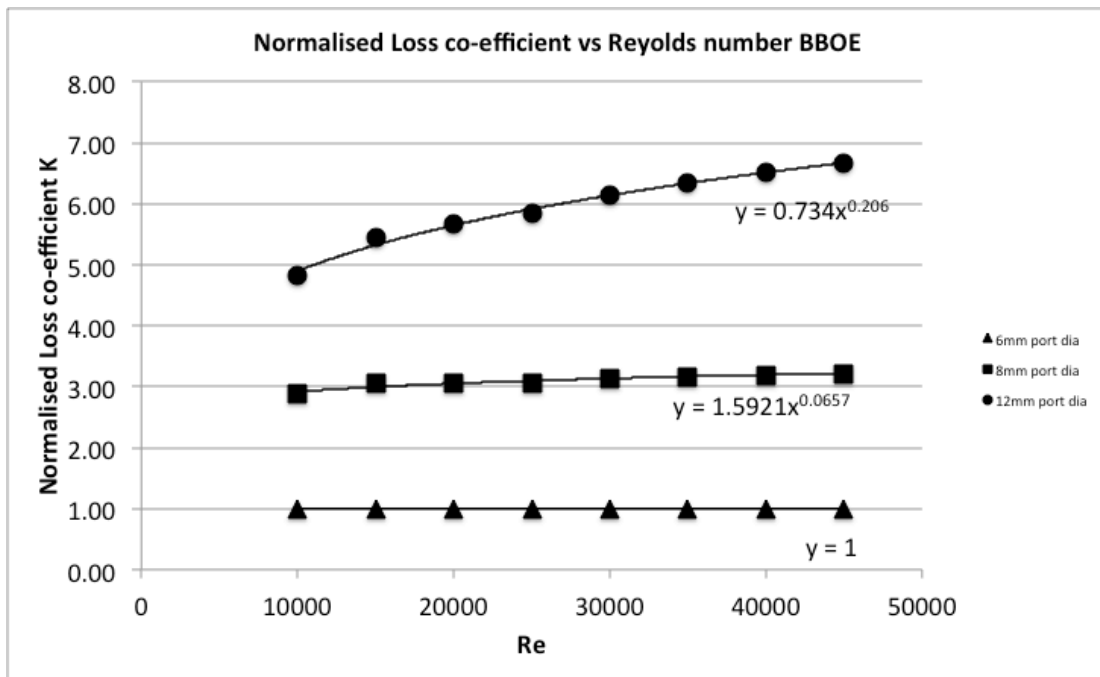


Figure 6-38 Normalised loss co-efficient vs Reynolds number.

The trend is similar to the trends seen in Figure 6-37, with almost constant offset to the 6mm port diameter. In Figure 6-39, loss co-efficient K for 8 mm and 12 mm port diameter is shown as a function of loss co-efficient with port diameter of 6 mm. It can be seen that the trend for 8 mm port diameter is increasing with increase in loss co-efficient for 6mm. Similar trends can be seen, primarily due to relatively small change in diameter.

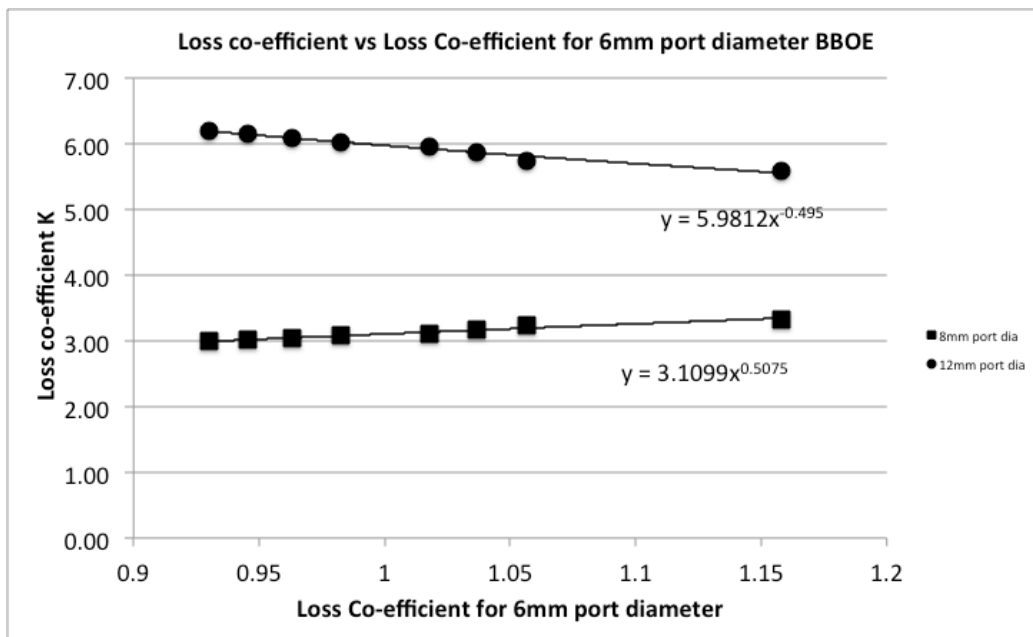


Figure 6-39 Loss Co-efficient vs Loss co-efficient for 6mm port diameter

On contrary, the trend for the 12 mm port diameter is decreasing with the increase in loss co-efficient values for port diameter of 6mm. With a 100% increase in port diameter the change in velocity is significant which affects the loss –coefficient. From the trend lines the following equations can be created.

$$K_{8mm} = 3.11 \cdot (K_{6mm})^{0.5075}$$

Equation 6-7 Loss co-efficient of 8mm port dia as function of loss co-efficient of 6mm port dia

$$K_{12mm} = 5.98 \cdot (K_{6mm})^{-0.495}$$

Equation 6-8 Loss co-efficient of 12mm port dia as function of loss co-efficient of 6mm port dia

Substituting K_{6mm} we get

$$K_{8mm} = 3.11 \cdot \left(\frac{1.1967}{Re^{0.018}}\right)^{0.5075} \quad \text{equals} \quad K_{8mm} = \frac{3.41}{Re^{0.0091}}$$

and

$$K_{12mm} = 5.98 \cdot \left(\frac{1.1967}{Re^{0.018}}\right)^{-0.495} \quad \text{equals} \quad K_{12mm} = \frac{5.47}{Re^{-0.0089}}$$

These can be used to compute the loss co-efficient.

6.4.3 Analysis of port diameter on pressure distribution

Non-dimensional pressure distribution ratio co-efficient developed in chapter 5 is used to quantify pressure distribution in a radiator. In section 6.3.7 pressure distribution ratio co-efficient was analysed for three different radiator sizes and the investigation has shown that pressure distribution is independent of radiator size but dependent on flow velocity. In this section a 300mm x 600 mm radiator with three different port diameters has been analysed to quantify their affect on pressure distribution.

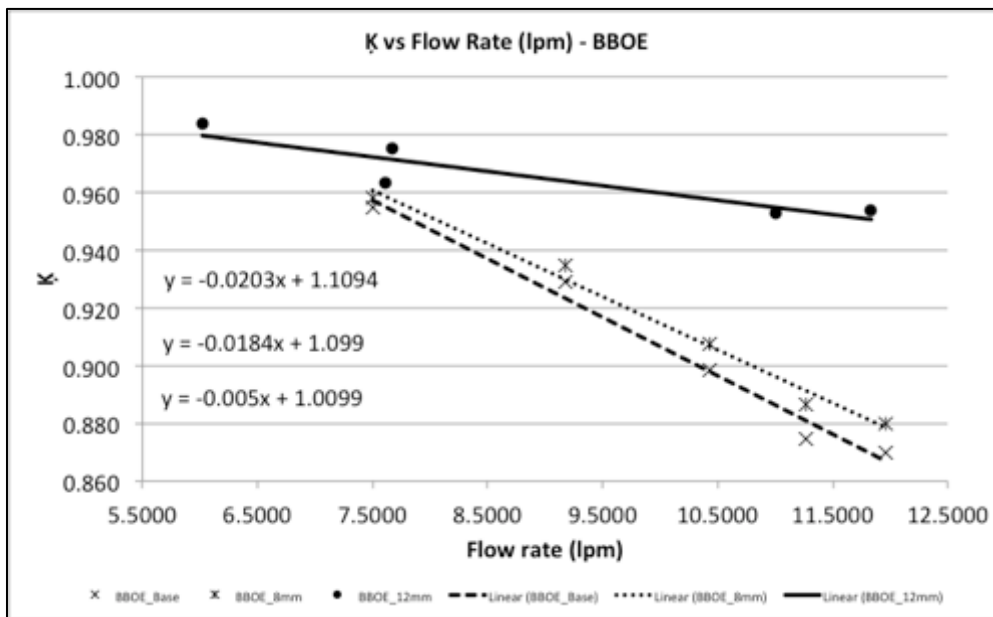


Figure 6-40 Pressure distribution ratio as function of flow rate for different inlet and outlet port diameter – BBOE

In Figure 6-40, a 6 mm port diameter and 8mm port diameter radiator have a similar slope, with pressure distribution ratio co-efficient reducing with increase in flow rate in BBOE configuration. This would result in pressure variation and uneven flow distribution. This can be mainly attributed to flow velocity in radiator. For a given flow rate, change in port diameter reduces the effective velocity at the port but the channels in the radiator are the same. This has an affect on the flow distribution in the radiator as flow rate increases. Similarly for BTOE configuration, Figure 6-41 shows that a 6 mm and 8 mm port diameter radiator have same slope but the 8mm port diameter has average 4.7% lower pressure distribution ratio co-efficient than the 6mm port radiator for a given flow rate.

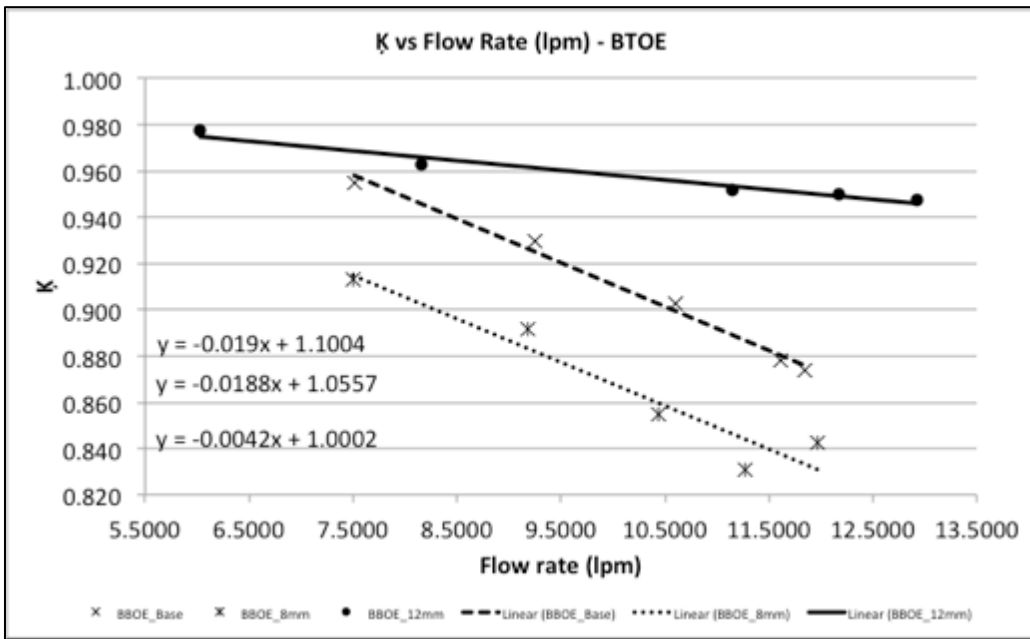


Figure 6-41 Pressure distribution ratio as a function flow rate for different inlet and outlet port diameter - BTOE

In BBOE and BTOE configuration, pressure distribution ratio co-efficient in a radiator with 12 mm port diameter is high, suggesting that the pressure variation is low allowing uniform flow distribution. Increased port diameter reduces flow velocity for the same radiator panel, which will reduce the turbulence and formation of eddies in the narrow channels. This results in lower variation. The pressure distribution ratio co-efficient varies only by 3.03% with a 96.5% change in flow rate in BBOE configuration and 3.06% with 114% change in flow rate. The trend for pressure distribution ratio co-efficient in BBOE and BTOE is similar with average 0.3% variation for flow rates between 5 lpm and 12 lpm. Hence it can be concluded that the pressure variation in a radiator with 12 mm port diameter is independent of flow rate and flow configuration. 12 mm port diameter also has significantly better flow distribution, which will provide uniform temperature distribution.

6.5 Summary

Detailed analysis to quantify the effect of radiator size and the port diameter under different flow configurations and flow rates has been discussed. This investigation has led to further understanding of radiator size and port diameter on pressure drop and pressure variation in the radiator. Generic equations for loss coefficient (K) and pressure distribution ratio coefficient (ζ) have been developed. The results obtained from the investigation have been quantified and graphically represented. Detailed flow analysis in different radiator sizes and radiator with different port diameter has revealed the following.

- Loss coefficient K is independent of flow velocity
- Loss coefficient K is a function of radiator size
- An equation for loss coefficient as a function of radiator length and height has been developed
- Pressure distribution ratio coefficient ζ is independent of size
- Pressure distribution ratio coefficient ζ is dependent on flow velocity
- Flow velocity in the central channels of the radiator is limited.
- Port diameter has a significant impact on loss coefficient of the radiator
- 12 mm port diameter also has high pressure distribution ratio coefficient, which results in a uniform pressure distribution. Uniform pressure distribution would result in uniform flow distribution and consequently uniform temperature distribution.

As discussed in chapter 4 stand-alone radiator is designed, developed and launched in the market. This design has been experimentally evaluated in chapter 5 and detailed investigation undertaken in this chapter has provided critical information on understanding the affect of radiator geometry on pressure drop and pressure distribution in the radiator. The information of loss coefficient and geometric factor can be used to develop pumping cost and radiator cost. The following chapter focuses on development of these cost models and method for minimising the overall cost.

7 DEVELOPMENT OF COST MODEL AND OPTIMISED STAND-ALONE WATER FILLED RADIATOR FOR BUILT ENVIORNMENT

Following the development of stand –alone radiator system discussed in chapter 4 TVM analysis is carried out where the design has been experimentally evaluated in chapter 5 and based on the results obtained from chapter 6 a radiator cost model with optimum size and configuration has been developed in this chapter. The co-relations developed for geometric function and pressure distribution in previous chapters for radiator has been used to develop the cost model and optimise the design. Asim [59] has developed an optimisation model for HCPs (Hydraulic Capsule Pipelines) based on hydraulic design. The model makes use of least cost principle, which states the total cost of the system is minimum, where the total cost refers to sum of operating cost and manufacturing cost. Using similar principle a cost model has been developed to quantify system cost and then further analysis is carried out to reduce the cost of the stand-alone radiator.

7.1 Optimisation of radiators

Stand-alone radiator has been designed and developed for mid-scale manufacturing with an estimate of 6000 units per year. The bill of materials (BoM) cost, assembly cost, factory overheads and logistics costs fall under manufacturing cost of the radiator. A profit margin is calculated based on the business plan and added to the manufacturing cost to determine the sales price. In addition to the sales price the end consumer also has to account for the operating cost. The total of the manufacturing cost, sales margin and the operating cost are taken into account to compare the viability of the heating system against other stand-alone or central heating systems. Hence optimisation of the stand-alone water filled radiator is essential for its commercial viability.

As stated above, the least cost principle refers to minimum total cost for the heating system. The total cost for the stand-alone water filled radiator includes

$$C_{Total} = C_{Manufacturing} + C_{Operation}$$

Equation 7-1 Total cost for stand-alone radiator

In this case for simplicity profit is considered as a fixed percentage of the manufacturing cost, hence included in the manufacturing cost.

In this case manufacturing cost can be further divided into cost of radiator which varies with size, cost of heater which varies with power requirements and fixed cost for components required in all radiators, consumables and labour.

$$C_{Total} = C_{radiator} + C_{heater} + C_{fixed} + C_{power-pump} + C_{power-heater}$$

Equation 7-2 Total cost of radiator (detailed)

7.2 Cost of radiator

Weight of the radiator panel is a function of height and width. Increase in the dimension of the radiators requires additional material, which in turn increases weight. The weight of radiator per unit length and height of radiator is given by Table 7-1

Height	300	400	500	600	700
Weight/meter length of radiator	8.53	11.44	14.35	17.26	20.17

Table 7-1 Weight per unit length of radiator [60]

$$W_R = (L \times [8.53 + \frac{(h - 0.3) \times 2.91}{0.1}])$$

Equation 7-3 Weight of radiator as a function of length and height

The cost of radiator is a function of the weight of the panel, which in turn is a function of the length and height of the radiator. The cost can be expressed as

$$C_{radiator} = C_1 \cdot W_R$$

Equation 7-4 Cost of radiator as a function of radiator weight

Where C_1 is a constant representing cost per unit weight of radiator panel that includes the material, manufacturing and shipping cost (£/kg).

Similar to the radiator, the panel areas are also function of the height and the width. Hence constant C_1 is selected such that it also accounts for the cladding/ finishing metal panels used in the radiator assembly. As per the bill of materials (BoM) in chapter 4, there are a total of four panels.

Hence

$$C_{radiator} = C_1 \cdot (L \times [8.53 + \frac{(h - 0.3) \times 2.91}{0.1}])$$

Equation 7-5 Cost of radiator as a function of radiator length and height

7.3 Cost of heater

As discussed in chapter 4, a range of heaters are required to ensure optimum heat output from the stand-alone radiator. In order to achieve this, the heat generated by the heater should be more than the heat output capacity of the radiator. The heat output capacity of the radiator panels are given by the manufacturer based on the test conducted in accordance with BS EN 442. The heat output for K1 radiators are given by Table 7-2

Height	Length	Power
m	m	W
0.3	0.6	338.4
0.4	0.7	501.2
0.3	1	564
0.6	0.6	612
0.4	1	716
0.3	1.4	789.6
0.3	1.6	902.4
0.6	0.8	816
0.4	1.4	1002.4
0.6	1	1020
0.4	1.6	1145.6

Table 7-2 Max heat output from K1 radiator [60]

Hence the heater capacity should range from range from 500W to 2000W. In order to minimise the inventory and optimise the assembly process 3 heaters have been selected to cater for the entire range. The selection was made to ensure for any given setup (heater + radiator) maximum heat output achieved. Hence this resulted in a 900W, 1500 W and 2000 W heater. The cost of the heater is a function of the wattage.

Hence

$$C_{heater} = C_2 \cdot Q_{heater}$$

Equation 7-6 Cost of heater as a function of wattage

$$C_{heater} = C_2 \times Q_{heater}$$

Where

Q_{heater} - Power rating of the heater (kW)

C_2 - is a constant cost per unit power (£/kW)

For a steel construction with nickel brazing as described in chapter 4, C_2 is ~£30/kW

7.4 Fixed Cost

As discussed in chapter 4, a number of components in the BoM (bill of materials) are common across the range of radiators and independent of size. The cost of these components adds to the overall costs of the radiator. It can be seen from the initial BoM that these components account for approximately 40 to 60% of the net cost, hence it is important to quantify these in the cost model for the radiator as it would impact the sales price of the stand-alone radiator system and the sales price of the radiator has an impact on cost of ownership. The components, which are common across all radiators, are

Level	Part Name	Quantity
2	Pump	1
2	PCB	1
2	Control box lower	1
2	Control box lower	1
2	Control Knob	1
2	O-ring	1
2	Air temperature sensor	1
2	Heater Temperature sensor	1
2	Ground Wire	1
2	Power lead	1
2	Grommets	2
2	Elbow connector	1
2	Elbow connector push fit	1
2	Male- Female Straight connector	2
2	Female -Female straight connector	1
2	Bleed Valve	1
2	Filler connector	1
2	25 mm copper pipe	1
2	Tie wraps	2
2	Spacer block	1
2	Safety label	1
2	Radiator label	1
2	M6 nuts	5
2	M4 hex screw	1
2	M6 button head screws	4

2	M4 self tapping screws	2
2	Power lead clip	1

Table 7-3 Common components contributing towards fixed cost

The cost of the components may change due to change in production volumes, commercial negotiations and market trends. For the purposes of this investigation constant C_3 , represents the fixed cost of the components.

Similarly the labour cost for the assembly of the components also contributes towards the overall manufacturing cost. The volume of the fluid required for the stand-alone radiator varies with the radiator size which has an impact on the time required to complete the assembly. For this study the time for assembly is assumed constant as the difference between the smallest and the largest radiator is marginal.

C_4 represents the cost of labour to assemble the parts. From early trials and production rates, it is expected that a single radiator will take 0.9hr. Based on semi-skilled requirements, for this study an hourly rate of £15 is assumed.

Hence

$$C_{fixed} = C_3 + C_4$$

Equation 7-7 Fixed cost of radiator

7.5 Total manufacturing cost

Based on Equation 7-1 and Equation 7-2, total manufacturing cost be expressed as

$$C_{Manufacturing} = C_{radiator} + C_{heater} + C_{fixed}$$

$$C_{Manufacturing} = C_1 \cdot (L \times [8.53 + \frac{(h - 0.3) \times 2.91}{0.1}]) + (C_2 \cdot Q_{heater}) + C_3 + C_4$$

Equation 7-8 Total manufacturing cost

7.6 Operating cost

7.6.1 Pumping cost

The cost of power consumption for pumping per unit watt is given by

$$C_{Power-pump} = C_5 P_{pump}$$

Equation 7-9 Cost for pumping the fluid in radiator

Where P_{pump} is the power requirement of the stand-alone radiator pump. The power can be expressed as:

$$P_{pump} = \left[\frac{\dot{m} \times \Delta P_{Total}}{\eta_{pump}} \right] \cdot \tau_{pump}$$

Equation 7-10 Power consumption of pump

Where \dot{m} is the flow rate of the fluid, ΔP_{Total} is the total pressure drop across the radiator inlet and outlet, η_{pump} is the efficiency of the pumping unit and τ_{pump} is the utility factor for the pump. Based on the manufactures catalogue it can be assumed that the efficiency of pumping unit ranges between 75 to 80%. The total pressure drop can be calculated from the relations developed in the previous chapters over a range of flow rate for various radiator sizes and port diameters.

$$C_{Power-pump} = C_5 \cdot \left[\frac{\dot{m} \times \Delta P_{Total}}{\eta_{pump}} \right] \cdot \tau_{pump}$$

Equation 7-11 Cost of pumping the fluid in radiator as function of pressure drop and flow rate

7.6.2 Heating cost

The cost of power consumption for heating per unit watt is given by

$$C_{Power-heating} = C_6 P_{heating}$$

Equation 7-12 Power consumption cost for heating

Where P_{pump} is the power requirement of the stand-alone radiator pump. The power can be expressed as:

$$P_{heating} = \left[\frac{I^2 \times R}{\eta_{heater}} \right] \cdot \tau_{heater}$$

Equation 7-13 Power consumption for heating

Where

I is the current consumption in Amperes,

R is the wire resistance based on the design,

η_{heater} is the efficiency of the heating unit and

τ_{heater} is the utility factor for the heater.

Based on the component testing and evaluation carried out in chapter 4 efficiency of heating unit ranges between 98.5 to 99.2%. Current draw and time can be measured for a test case based on heating element design specification and duration of operation.

$$C_{Power-heating} = C_6 \cdot \left[\frac{I^2 \times R}{\eta_{heater}} \right] \cdot \tau_{heater}$$

Equation 7-14 Power consumption cost for heating

Hence total cost of operation can be given as

$$C_{Operation} = C_5 \cdot \left[\frac{\dot{m} \times \Delta P_{Total}}{\eta_{pump}} \right] \cdot \tau_{pump} + C_6 \cdot \left[\frac{I^2 \times R}{\eta_{heater}} \right] \cdot \tau_{heater}$$

Equation 7-15 Total operating cost

7.7 Effect of diameter on pumping cost

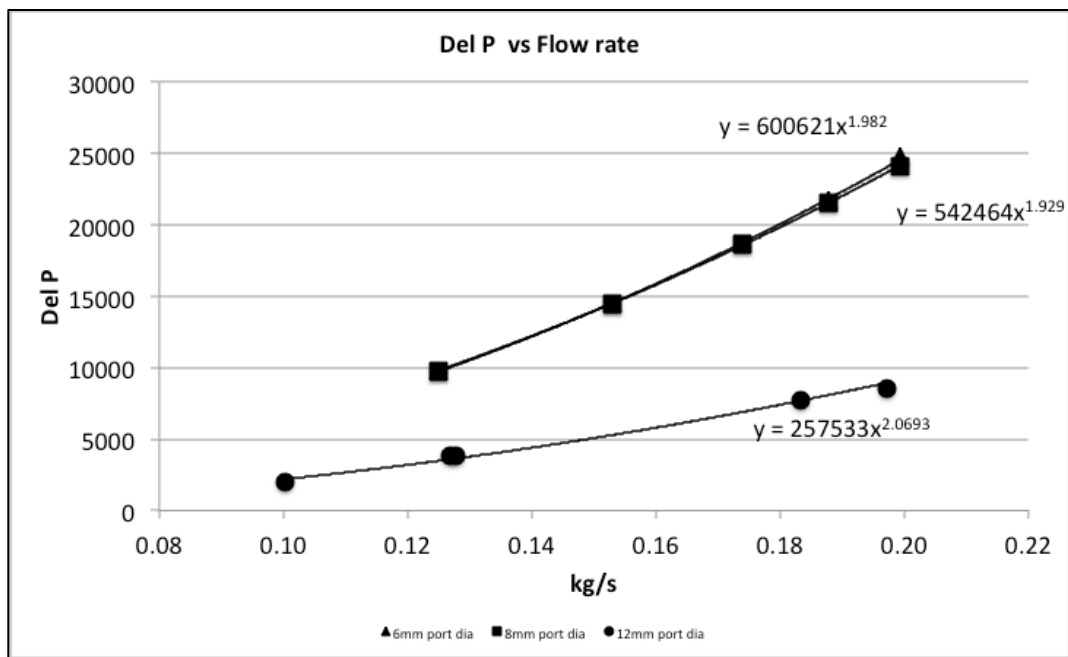


Figure 7-1 Pressure drop vs flow rate for three port diameters

As discussed in chapter 4, loss co-efficient can be calculated based on the port diameter and flow rate. Using the same numerical models, pressure drop is compared for three port diameters across a range of flow rates in a 300 mm x 600 mm radiator. Figure 7-1 shows the pressure drop trend for 6 mm, 8 mm and 12 mm port diameters. It can be seen that 6 mm and 8 mm have a very similar trend but 12 mm port diameter shows a significant reduction in pressure drop across the inlet and outlet.

The study has been extended further where the relation between pressure drop and flow rate for respective port diameters have been used to calculate pressure drop over a wider range. The corresponding pressure drop and flow rate have been used in Equation 7-11 to compute the operating cost of the pump. Efficiency is taken as 0.8 and as discussed in chapter 4 the pump is required to run 100% of the time, to ensure there is no localised boiling adjacent to the heating element. Hence

$$\eta_{pump} = 0.8$$

$$\tau_{pump} = 1$$

Based on the statistics shown in heating trends in the UK, it is assumed that the radiator is operated for 5 hours a day. Hence multiplying $C_{power-pump}$ by 5 produces the operating cost

per day. Resulting cost in pence have been tabulated in Table 7-4 and graphically represented in Figure 7-2

	$C_{\text{power-pump}}$		
Flow rate	6mm port dia	8mm port dia	12mm port dia
Kg/s	Pence/day	Pence/day	Pence/day
0.1	0.78	0.80	0.27
0.12	1.35	1.36	0.48
0.14	2.13	2.14	0.77
0.16	3.18	3.16	1.16
0.18	4.52	4.47	1.67
0.2	6.18	6.08	2.30
0.22	8.22	8.04	3.09
0.24	10.65	10.37	4.03

Table 7-4 Pump operating cost with three port diameters and range of flow rates

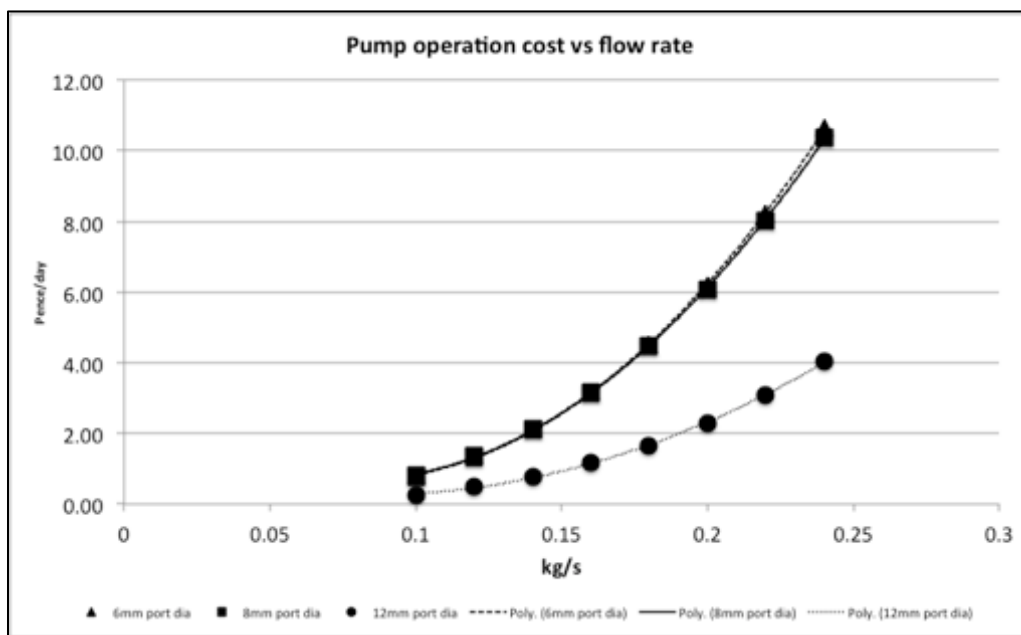


Figure 7-2 Pump operating cost for three port diameters over range of flow rates

Compared to a port diameter of 6 mm, a 12 mm port diameter has an average of 63% lower running cost for the same flow rate and radiator size. Trend for 6 mm and 8 mm is almost identical and has an average variation of 0.6%. As seen in chapter 6 a 12 mm port diameter at lower flow rates of 0.12kg/s to 0.14 kg/s gives a pressure distribution with the ζ values being as high as 0.97 and significantly lower pressure drop across the radiator. The pumping cost at these conditions is 0.5 to 0.7 pence/day. Compared to the heating cost this

is a significantly low number. Although the geometric benefits of port diameter for pressure drop and temperature distribution are significant the pump operating cost can be ignored for the optimisation process. Based on the above benefits it is recommended that a port diameter of 12 mm is assumed used for cost models.

7.8 Cost of ownership

The above approach has outlined the process for calculating the manufacturing cost and the operating cost. Heating costs for a household are generally reported annually or per day. For the purposes of this study the cost will be calculated based on cost per day.

Using Equation 7-8 we get the total manufacturing cost. As discussed in chapter 4 stand-alone radiator has been designed to work maintenance free for 10 years. In order to account the price of the stand-alone radiator in cost of ownership, the sales price of the unit is amortised over 5 years. Hence the cost of cost of ownership per day for the unit is

$$C_{ownership/day} = \frac{[C_1 \cdot (L \times [8.53 + \frac{(h - 0.3) \times 2.91}{0.1}])] + (C_2 \cdot Q_{heater}) + C_3 + C_4}{5 \times 365} * C_7$$

Equation 7-16 Total cost of ownership per day

C_7 is the sales margin. (assumed 15% - 25% for this study)

Using Equation 7-15 the operating cost of the stand-alone system can be calculated. From section 7.7 it can be concluded that the pumping cost is insignificant compared to the overall operating cost and hence can be neglected. To calculate cost of operation per day it is assumed that on an average there is 5 hours of usage per day. Hence the total cost of operation per day is given by

$$C_{operation/day} = 5 \times C_6 \cdot \left[\frac{I^2 \times R}{\eta_{heater}} \right] \cdot \tau_{heater}$$

Equation 7-17 Total cost of operation per day

Hence total cost of heating per day can be calculated by combing the ownership cost and the operation cost.

$$C_{heating/day} = \frac{[C_1 \cdot (L \times [8.53 + \frac{(h - 0.3) \times 2.91}{0.1}])] + (C_2 \cdot Q_{heater}) + C_3 + C_4}{5 \times 365} * C_7$$

$$+ 5 \times C_6 \cdot \left[\frac{I^2 \times R}{\eta_{heater}} \right] \cdot \tau_{heater}$$

Equation 7-18 Total heating cost per day

If a radiator size is known, geometric factor, heat output, manufacturing cost, operation cost and total heat cost per day can be computed from the equations given in section 7.6 and 7.8. As a design guide to assist with radiator selection Figure 7-5 and Figure 7-7 graphically represent the variation of key parameters with the change in geometric factor from Equation 6-5.

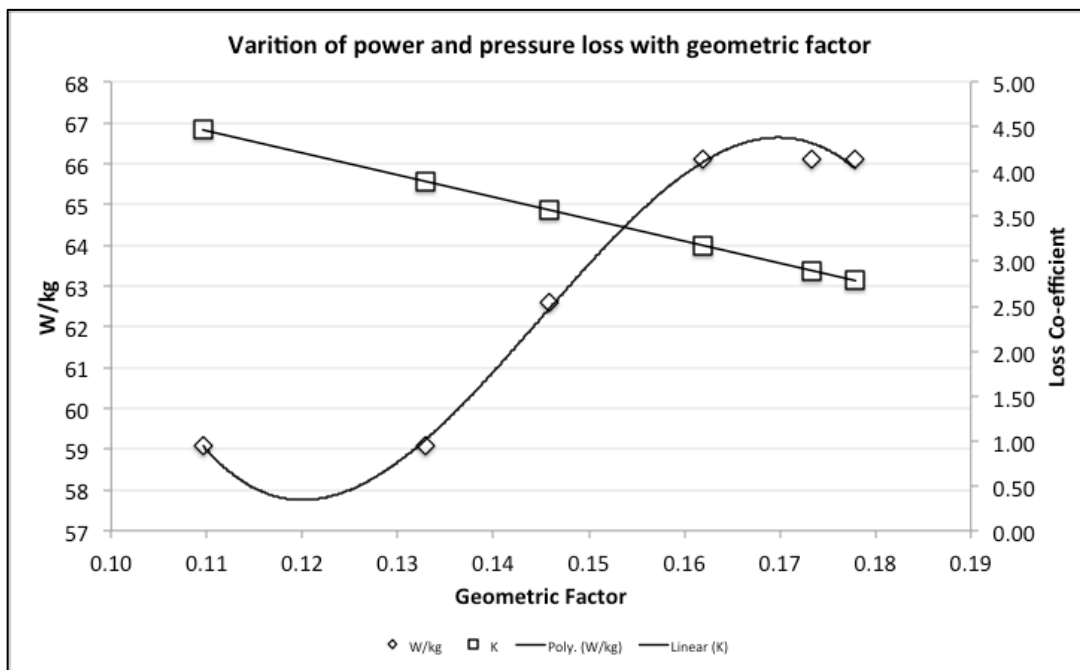


Figure 7-3 Variation of power and pressure loss with geometric factor

Figure 7-5 shows variation of power per unit mass of the radiator and loss co-efficient with the change in geometric factor. It can be seen that the loss co-efficient drops with the increase in geometric factor but power per unit mass is nearly constant between 0.105 and 0.135 and then increase linearly till 0.165 after which it is once again nearly becomes constant. This would suggest that geometric factor influences the rate of increase of thermal output per unit mass only in a range. Also radiators with higher geometric factors have lower pressure loss.

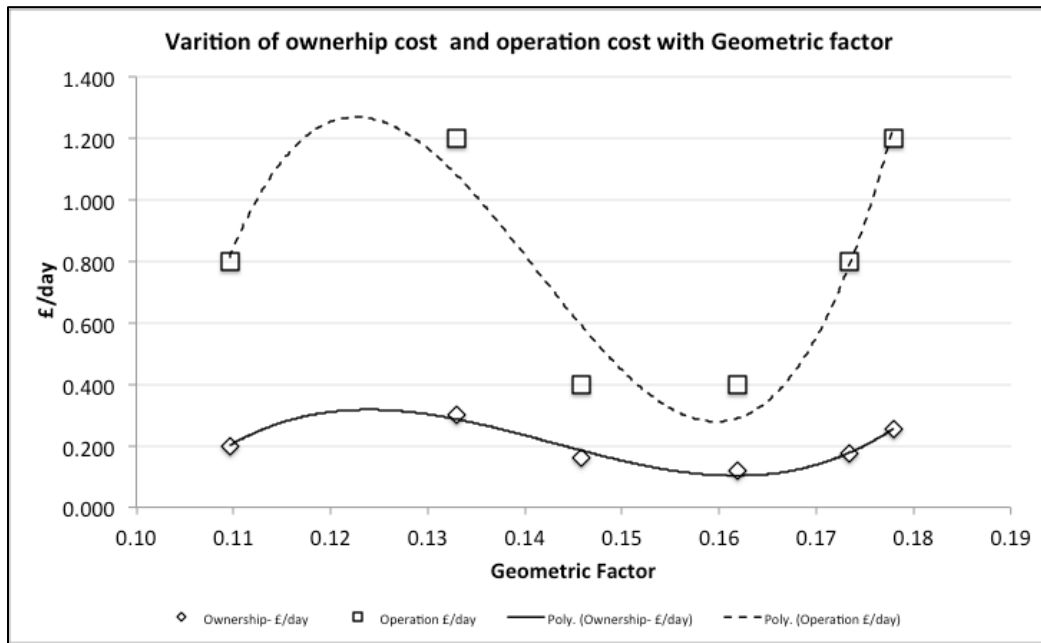


Figure 7-4 Variation of ownership cost and operation cost with geometric factor

Figure 7-7 shows variation ownership cost per day of the radiator and operation cost per day with the change in geometric factor. It can be seen that the operation cost per day has minimal variation as it is primarily driven by heater size and as discussed in chapter 4 to optimise the production process only three heaters are used across the range of radiator sizes. Ownership cost per day varies significantly with the geometric factor with the least cost at 0.162. The operating cost is also low at this point. The total cost is only £0.534 per day based on 5 hours of usage per day. The highest cost can be seen for geometric factor of 1.33 with the operating cost per day of £1.2 and ownership cost of ~£0.3.

These graphs can be used as guide for radiator selection for basic estimates. In order to accurately compute heating cost for a built environment during the design phase a detailed methodology has been developed and discussed in the following sections.

7.9 Computing heating cost for a room

The following steps should be followed to run the heating cost model. The input to the model is room dimension.

1. Assume a value of port diameter (12 mm)
2. As discussed in literature review for a given room size with standard ceiling height of 2.4 m the thermal requirement for the radiator (s) is known [61].
3. Assume a height (h) of the radiator (from standard heights of 0.3 m, 0.4 m and 0.6 m)
4. Calculate the radiator length using Equation 4-13
5. Calculate the geometric factor
6. Calculate the loss co-efficient
7. Calculate the weight of the radiator
8. Calculate the manufacturing cost of the stand-alone system
9. Calculate the operating cost of the radiator based on 5hr/day
10. Amortise the cost over 5 years
11. Compute cost of ownership per day
12. Repeat steps 3 to 11 for various values of h until that value is reached at which the total cost of the radiator is minimum.

7.10 Design Example for heating a room

Heating source is required to warm a room with the length, width and height of 3 m x 3 m x 2.4 m is used in the study.

Find the heating cost per day of the stand-alone radiator required for this purpose.

Solution: According to the product design and development process undertaken in chapter 4 and current energy tariffs and, the values of different constants involved in the optimisation process are:

$$C1 = 25 \text{ £/kg} \quad C2 = 30 \text{ £/kW} \quad C3 + C4 = \text{£}75 \quad C5 = 0.2\text{£/kWh [61]} \quad C6 = 0.2\text{£/kWh[61]}$$

The floor space for the room is 9 m^2 . It is assumed the room has average insulation. As disused in chapter 2 the heat demand for the room with average insulation is 107.64 W/m^2 .

Total demand on the heating system is $107.64 \times 9 = 968.76 \text{ W}$

Assuming a radiator height of 0.6 m and following the steps described in computing the heating cost, the following results are obtained for the initial radiator height assumption.

Length	m	1.00	0.80	0.60
Height	m	0.60	0.60	0.60
K calculated		3.89	4.11	4.47
Geometric factor		0.13	0.12	0.11
Weight	Kg	17.26	13.81	10.36
Heater (input)	kW	1.50	1.50	1.00
Radiator output	kW	1.02	0.82	0.61
total man cost	£	551.50	465.20	363.90
Sale Cost	£	689.38	534.98	418.49
Ownership	£/day	0.38	0.29	0.23
Operation	£/day	1.20	1.20	0.80
Total cost per day	£/day	1.58	1.49	1.03
W/kg		59.10	59.10	59.10

Table 7-5 Geometry and cost for radiator with height 0.6 m

The results presented in Table 7-5 depicts that a radiator with a height of 0.6 m and heat output requirement of 990 W would require a radiator with a length of 1 m. The heat output

from the radiator would be 1.02 kW and power consumption would be 1.2 kW. Total manufacturing cost is £551.5, which gives a sales price of £634. Based on amortising the cost of ownership over five years and averaging 5 hours per day through the year, total cost of heating per day is £1.578 for a single room. The above calculation is based on pump utility factor of 1 and heater utility factor of 0.8.

The heat output for a 600 mm x 1000 mm radiator is 3% higher than the design requirements. This would lower the utility factor of the radiator and effectively reduce the power consumption. Nevertheless the cost of ownership is constant for the given radiator. In order to optimise the cost for a given demand, selecting smaller stand-alone radiators, which will deliver net heat demand, can reduce total cost of heating per day.

7.11 Optimisation of total heat cost per day by varying radiator size

We have developed a cost model, which accounts for total manufacturing cost and operating cost of the radiator per day. In this section, an optimisation process is developed to minimise the total heat cost per day for a given heat demand for a room. The process investigates if a combination of smaller radiators ilo of larger radiator offers any cost benefit. Figure 7-5 shows the variation of power input and power output with the change in weight of the radiator and Figure 7-6 shows variation of power input and output with the change in geometric factor of the radiator. Weight of the radiator is a direct function of the radiator dimensions. As discussed in chapter 4, as the area of the radiator increases the heat out capacity of the radiator increases.

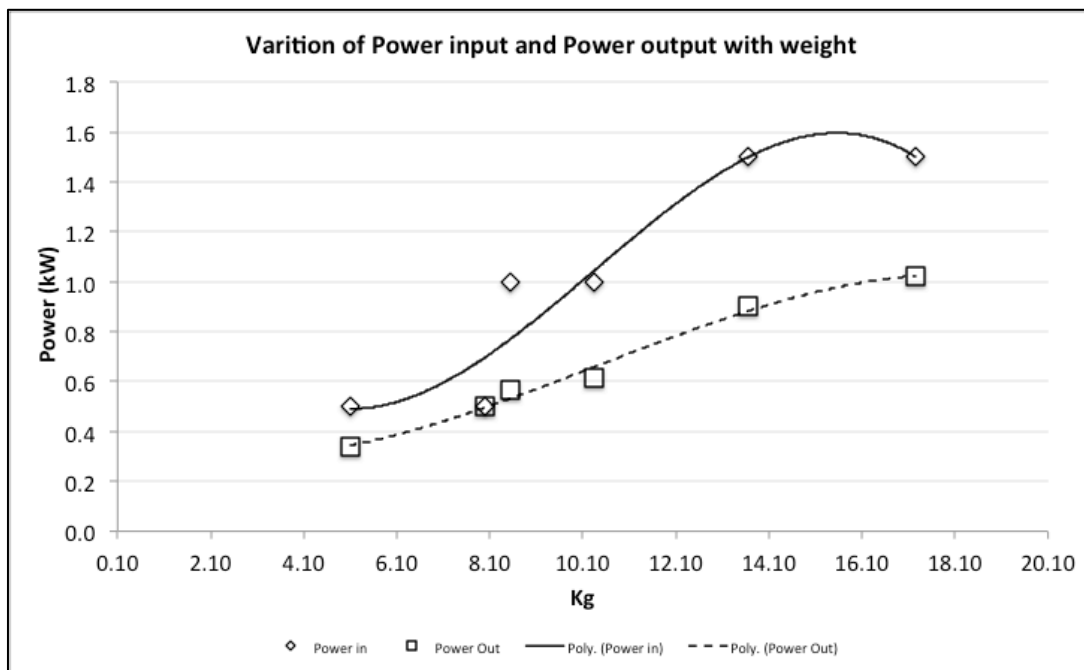


Figure 7-5 Variation of power input and output with weight of radiator

It can be seen that the power output increases linearly with the increase in weight of the radiator. Power input increases in steps due to three heater units commonised across the radiator sizes. An important point to note is, this does not result in reduced efficiency but reduced utility factor and effectiveness.

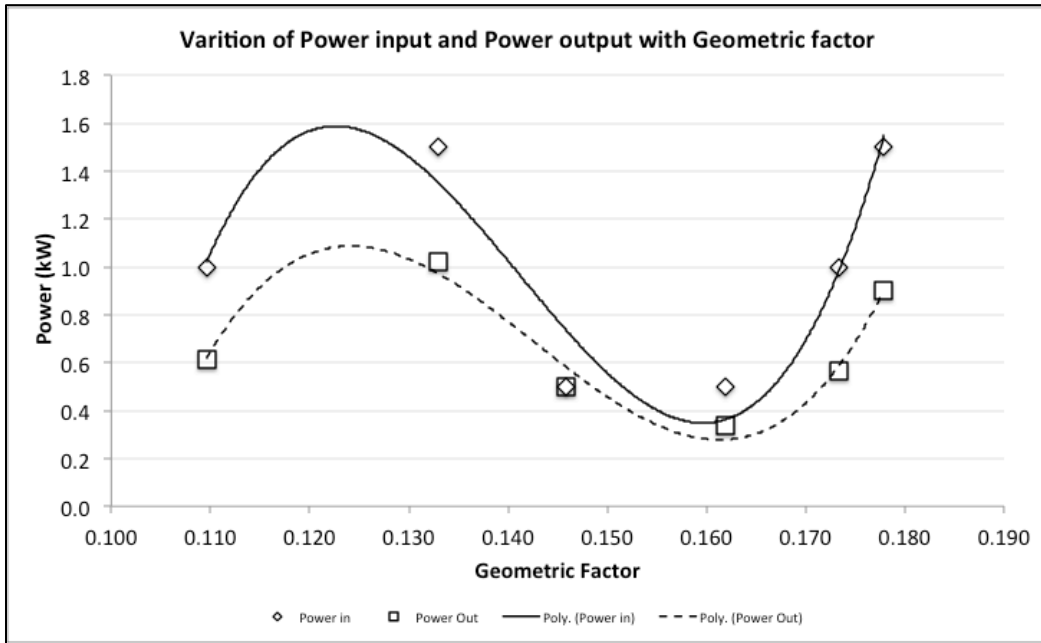


Figure 7-6 Power input and output variation with geometric factor

In this case it can be seen that both power input and power output are a polynomial function of the geometric factor. The trend is very similar to the one seen in Figure 7-5, where the difference between the power input to power output is least for smaller radiators and increases with the increase in size. The information is very useful in selecting the right radiator for a given heat demand in the room. It can be seen that for 0.9kW one can select a radiator with geometric factor of 0.115, 0.135 and 0.178. This presents the opportunity to optimise radiator selection to either minimise cost or room layout.

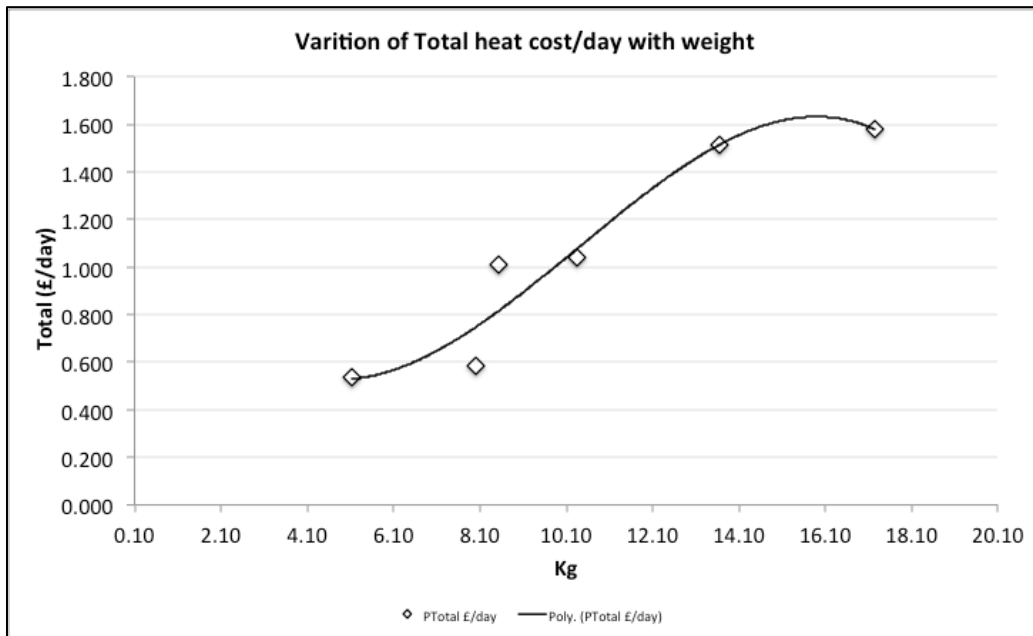


Figure 7-7 Variation of Total heat cost per day with weight

Figure 7-7 shows variation of total heating cost with change in weight of radiator panel. It can be seen that the total cost/day increases with the increase in radiator size. The trend is nearly constant between 14.1 kg and 16.10 kg due marginal increase in weight and no change in operational cost due to same heater wattage and assuming the same utility factor.

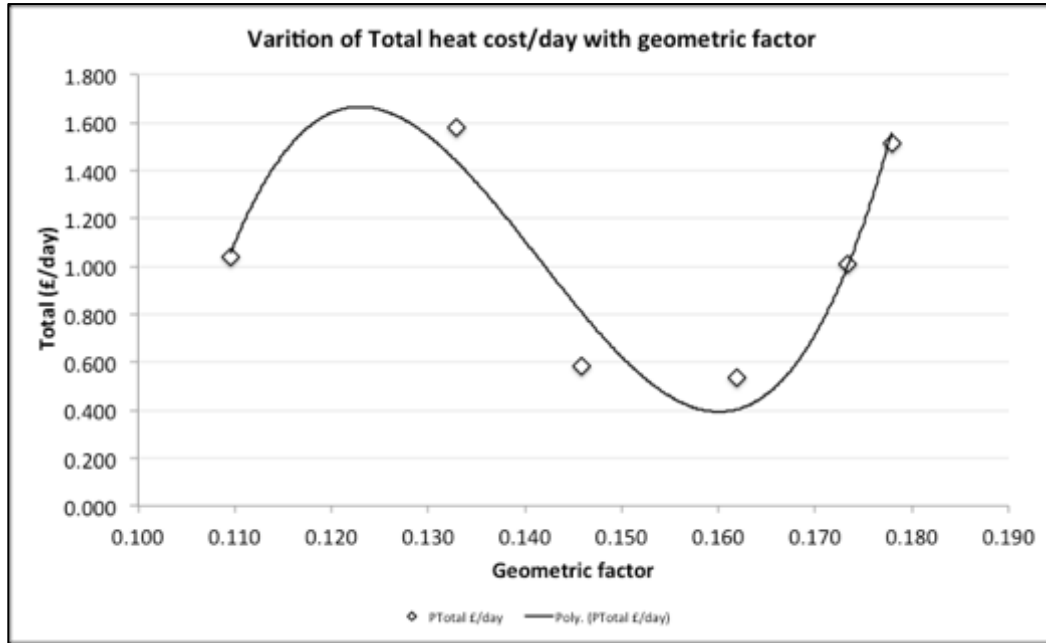


Figure 7-8 Variation of total heat cost per day with geometric factor

Figure 7-8 shows variation in total heating cost per day with change in geometric factor. It can be seen that the total cost/day varies with the increase in geometric factor for radiator. This is an important graph for radiator selection for a given application. If used in conjunction with Figure 7-6 where geometric factor for a desired heat output is selected, corresponding total heat cost can be ascertained from this graph.

Figure 7-9, breaks the total heat cost per day into ownership cost and operation cost. It can be seen that the operation cost increases linearly with increase in the radiator size. The ownership cost is nearly constant for larger radiators; this is mainly due to the usage of same heater and pump module. The trend for ownership cost is almost linear up until 13 kg radiators due variation in heater sizes.

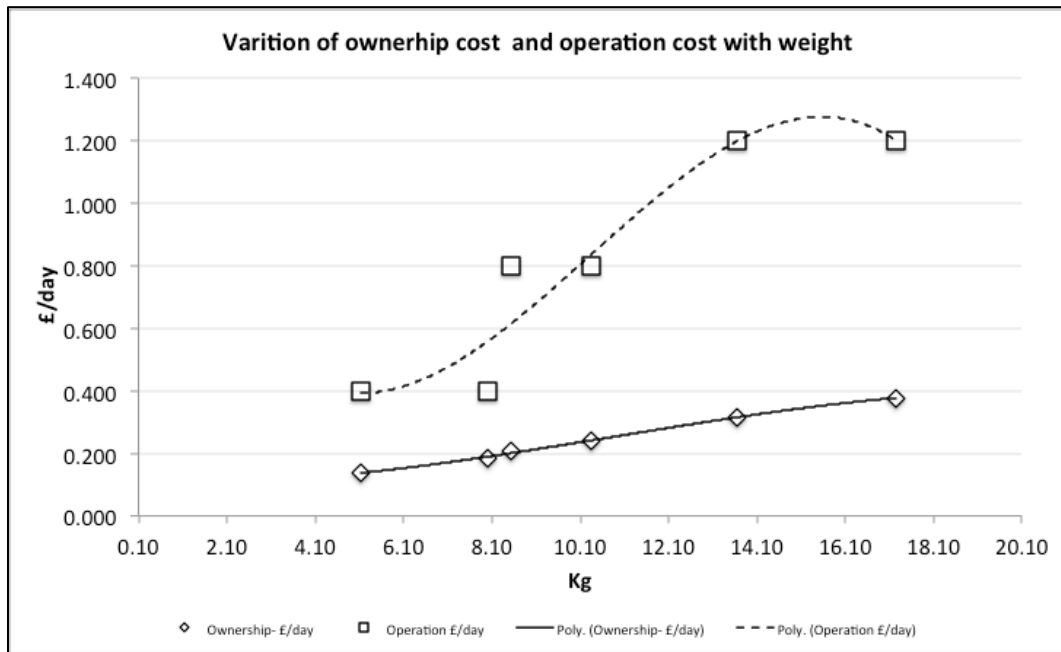


Figure 7-9 Variation of ownership cost and operation cost with weight

Design problem

To optimise for least cost, using the same example room (3 m x 3 m x 2.4 m) but selecting two radiators from Figure 7-6, which collectively provide a comparable output would require a radiator with geometric factor 0.162 and 0.110. This will be two radiators with height of 0.3 m x 0.6 m and 0.6 m x 0.6 m with net output equating to the heat demand of ~ 990W. Using the graph in Figure 7-8, total heat cost/day can be computed. Ownership cost/day and operation cost/day and can be computed using the graph in Figure 7-9. Using the graph in Figure 7-7 the weight of the system can be computed. The same can also be calculated using the equations discussed in section 7.6.

Hence recommended radiators are 300 mm x 600 mm and 600 mm x 600 mm which give a heat output of 340 W and 612 W respectively. Cumulative total heating cost/day is £1.577. This cost is lower than one 600 mm x 1000 mm radiator for the same room.

7.12 Comparative study of stand-alone radiator to a central heating system

With the development of cost model and an optimisation approach it is important to compare the total heat cost per day for a stand-alone radiator with a central heating system for a same built environment. This approach would objectively quantify the cost advantages and dis-advantages of the stand-alone system.

As discussed in literature review Arup [60] have presented the finding of their survey that quantified the total cost of heating for a given built environment, ranging from a single room studio apartment to a 4-bedroom house. The cost included energy cost, standing charge, system maintenance cost and repair cost. The finding suggested, a cost of £0.52 /kWh for a single room, £0.27/kWh for a studio apartment and £0.12/kWh for a four bed house. The floor area of each of the built environments are given in Table 7-6

	Area (m ²)
Single room	9
Studio apartment	12
4 bedroom house	120

Table 7-6 Floor area of test built environments

Hence total heating cost /day based on gas central heating (GCH) would be would be as per

	Area	Heat demand	GCH	GCH	GCH
	m2	kW	£/kWh	£/kW-day	£/day
Single room	9	0.97	0.52	2.6	2.52
Studio apartment	12	1.29	0.27	1.35	1.74
4 bedroom house	120	12.92	0.12	0.6	7.75

Table 7-7 Heat demand and total heat cost per day for gas central heating

For a comparable study with the stand-alone system discussed in the previous section a usage of 5 hr/day and an assumption that all rooms have average insulation has been used. As discussed in chapter 2, a typical central heating system comprising of a boiler, plumbing and radiators would cost ~ £3000. To compute the cost of ownership/day if the initial

investment cost and the cost of installation is amortised over 5 years, the cost of ownership/day is £1.64. The revised total heat cost per day for gas central heating would be

	GCH	GCH- Amortise	GCH
	£/day	£/day	£/day
Single room	2.52	1.64	4.16
Studio apartment	1.74	1.64	3.38
4 bedroom house	7.75	1.64	9.39

Table 7-8 Total heat cost per day for gas central heating including investment and installation

Using floor areas for the respective built environments, stand-alone radiator (s) system (s) have been identified by following the steps detailed in section 7.9. The resulting total heats cost per day based on stand-alone system are presented in Table 7-9.

	Area	Heat demand	Stand-alone	
	m ²	kW	£/day	Comments
Single room	9	0.97	1.58	Based on a 3060 and 6060 radiator
Studio apartment	12	1.29	2.12	Based on 3060 and 6100 radiator
4 bedroom house	120	12.92	18.9	Based on 12 x 6100 radiator

Table 7-9 Total heat cost per day for stand-alone radiator system

From Figure 7-10, it can be seen that a stand-alone systems offers significant cost saving and benefit in installation for single room which could be an extension or conversion. The major advantage of the stand-alone system in such application is initial cost of the system, installation cost and maintenance cost. For a single room, a stand-alone system has a total heat cost per day of £1.58 compared to £4.16 for a gas central heating based system offering 62% benefit.

It can also be seen that as the economies of scale for the central heating system improve the cost benefit of the stand-alone system reduces with the cost benefit of stand-alone system being only 37% for a studio apartment where it still offers ease of installation, flexibility to move and even optimise the location of the radiator to maximise thermal comfort in a room. Finally when the size of the built space increases, stand-alone system is not competitive.

Although it may offer flexibility and zero maintenance the total heat cost/day is nearly 200% more than the gas central heating system.

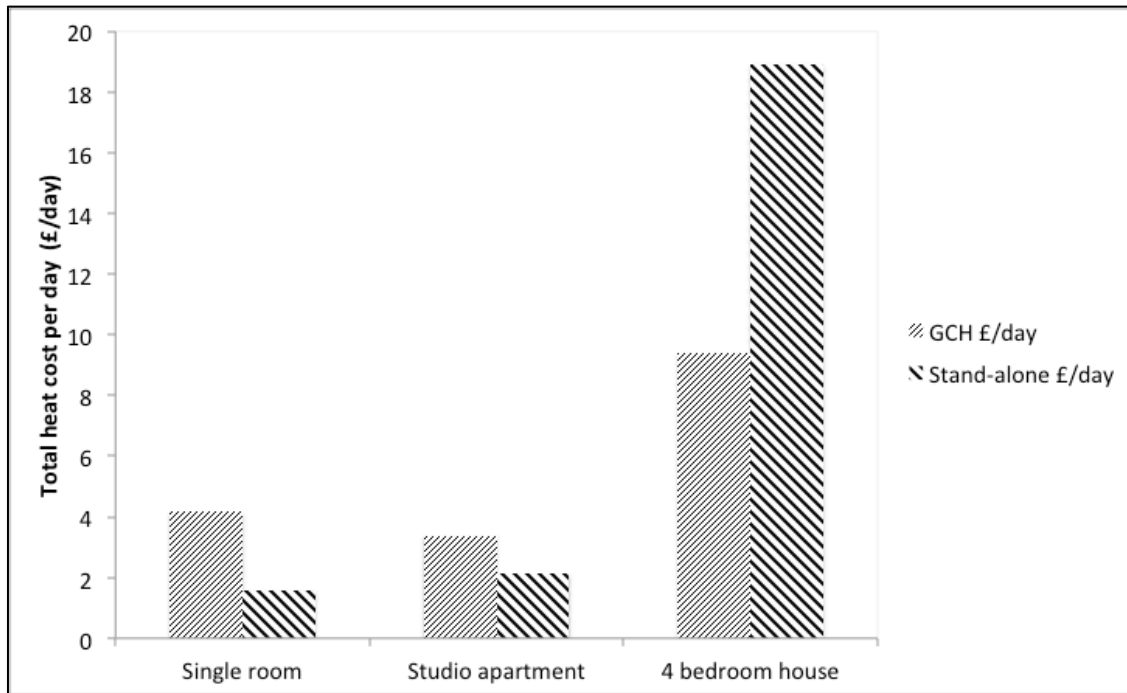


Figure 7-10 Total heat cost per day comparison (GCH to Stand-alone) for various built environment

7.13 Summary

A detailed investigation of the various costs involved in heating a room using a stand-alone radiator system have been has revealed the following results:

- A radiator sizing and cost estimation process has been developed for stand-alone radiators.
- Increase in the radiator size increases the manufacturing cost of the heating system.
- Increase in the heater size also increases operating cost of the radiator
- Loss co-efficient reduces with the increase in geometric factor of the radiator.
- The ratio of power input to power output reduces with the increase in the radiator size.
- Total cost of heating varies with geometric factor with the least cost of heating is observed with radiators with geometric factor of 0.16.

Hence, a complete investment cost and operation cost prediction has been presented in this chapter, which is based on the product developed in Chapters 4, and results presented in Chapter 5 and 6 regarding the experimental and CFD based analysis of the flow in stand-alone radiators.

Optimal radiator size for delivering the heating requirements for a room is by using multiple small radiators rather than a large radiator as it offers benefit on cost of operation and heat distribution in the room. A comparative study to central heating system has shown for smaller areas, extensions or conversions a stand-alone system can be very economical compared to a gas central heating system. The cost benefit reduces compared to gas central heating as the size of the built environment increases. Further investigation may be required to ascertain if selecting smaller radiators could offer a comparable cost to central heating system even in larger built environment.

8 CONCLUSION

From the results obtained in the previous chapters regarding the effect of geometric parameters on the pressure drop and distribution in a radiator, its impact on temperature distribution, cost model and optimisation approach for radiators, detailed conclusions have been drawn in this chapter. The major achievements and contributions of the study to the existing knowledge base are summarised and referenced back to initial aims of the research. Finally, the research works carried out in this study are evaluated and requirements for the future work in the area to stand-alone water filled radiator system are defined.

8.1 Research Problem Synopsis

To meet challenging targets of limiting carbon emission from domestic heating, major developments and innovations in improving thermal efficiency of buildings have taken place in the last two decades. There have also been developments in the heating systems, which have become efficient but it was found necessary to review currently used central heating systems. A systematic study of the effectiveness and limitations of these systems is required to identify new heating system to reduce energy consumption and improve effectiveness of the heating systems.

From a comprehensive review of the published literature on central heating systems, a number of limitations have been found out which are concerned with losses and lack of control, the proposed methods to reduce losses in the system are expensive, require regulatory changes and last but not the least central heating system does not offer flexibility for extensions and modifications. A unique development process is required to design and develop a robust stand-alone radiator system. In order to develop a radiator and to accurately predict the flow behaviour in radiators a set of aims and objectives have been formulated which define the scope of this research study. A summary of the primary aims of the thesis is provided in the following sections of this chapter along with the major achievements and contributions. For reference, the detailed objectives within each of these aims are given in Chapter 2.

8.2 Aim and main achievements

The main objectives of the thesis defined from an extensive literature review in this area are as follows:

Research Objective # 1: New product development process and development of a state of the art stand-alone water filled radiator

Achievement # 1: A new product development process customised for stand-alone radiators has been developed. The process enabled development of a product in a short period of time and incorporated quality assurance process to deliver a robust and reliable product. The stand-alone water filled radiator that has been developed offers the benefit of a central heating radiator system without the complexity of plumbing, installation and maintenance. In the new product development process, both mechanical and hydraulic considerations have been accounted for to ensure a safe, robust and commercially viable product is developed. Although the product has been tested according to standard and found to be very efficient, there is scope to improve the effectiveness of the stand-alone system.

Research Objective # 2: Critical performance analyses of stand-alone water filled radiators

Achievement # 2: Detailed experimental evaluation of radiators under different flow configurations and flow rates for two radiator sizes have been discussed. The results obtained from the investigation have been quantified and graphically represented. Two key parameters to quantify pressure loss and pressure variations in a radiator have been developed. The resulting equations have been critiqued and compared back to experimental results to validate the accuracy of the equations.

- Relationship of pressure drop to flow velocity has been developed
- Non dimensional parameter, loss co-efficient K has been developed as a function of effective Reynolds number
- Individual equations for each size and configuration has been developed
- We have investigated the effect of flow velocity on the pressure variation in a radiator – which gives us valuable information to study flow and temperature distribution.

Research Objective # 3: CFD based quantitative flow analysis in a stand-alone water filled radiator

Achievement # 3: Detailed analysis to quantify the effect of radiator size and inlet diameter under different flow configurations and flow rates have been discussed. The results obtained from the investigation have been quantified and graphically represented. Detailed flow analysis in different radiator sizes and radiators with different port diameters has revealed the following.

- Loss co-efficient K is independent of flow velocity
- Loss co-efficient K is a function of radiator size
- An equation for loss co-efficient as a function of radiator length and height has been developed
- Pressure distribution ratio co-efficient K_p is independent of size
- Pressure distribution ratio co-efficient K_p is dependent on flow velocity
- Flow velocity in the central channels of the radiator is limited.
- Port diameter has a significant impact on loss co-efficient of the radiator.
- 12 mm port diameter also has high pressure distribution ratio co-efficient suggesting uniform flow distribution.

Research Objective # 4: Cost model and optimal design for a stand-alone water filled radiator

Achievement # 4: A detailed investigation of the various costs involved in heating a room using a stand-alone radiator system have been has revealed the following results:

- A radiator sizing and cost estimation process has been developed for stand-alone radiators.
- Increase in the radiator size increases the manufacturing cost of the heating system.
- Increase in the heater size also increases operating cost of the radiator
- Loss co-efficient reduces with the increase in geometric factor of the radiator.
- The ratio of power input to power output reduces with the increase in the radiator size.
- Total cost of heating varies with geometric factor with the least cost of heating is observed with radiators with geometric factor of 0.16.

8.3 Thesis Conclusions

Research sub-objective # 1: Develop bespoke product development process for stand-alone water filled radiators

A bespoke new product development approach that combines approach of existing staged product development process and commercial demands to the organisation to industrialise novel water filled stand-alone radiator. This approach details multiple simultaneous stages compared to a stage-block NPD approach. The approach highlights the organic nature of new product development required for a stand-alone radiator system, where some of the supporting activities are interlinked and influence the outcome of the following activity. This bespoke process has been deployed to design and development of the product and manufacturing process. The process has introduced benefits of reconfigurable modularity and quality assurance process in product development. Last but not the least the process has also introduced an activity to critically evaluate the product design and identify opportunities to optimise the cost of ownership.

Research sub-objective # 2: Identify product design specifications for a new stand-alone water filled radiators

Review of central heating and existing stand-alone products has given a good foundation to generate system requirements, ideation and innovation, which have been compared against customer, needs and market demands. Product definition has been used to develop concepts, which enabled us to create a DFMEA (Design Failure Mode Effect and Analysis) to do early assessment of concept. System architecture has been developed based on validated concepts, which were assessed for product cost and project investment estimates. The cost estimates enabled detailed business analysis and market feasibility for the product.

Research sub-objective # 3: Design and development of stand- alone water filled radiator

Based on robust concept development, hydraulic and mechanical design development has been undertaken to ensure the new stand-water filed radiator system complies to BS EN ISO 9001:2000 for quality control [57], BS 7593 [58] for corrosion mitigation, BS EN 442 [13] for manufacturing and testing standards and not exceed 8 bar of pressure during operation. Detailed component level design has been completed to ensure the components and the final assembly delivers the product specification detailed in the concept phase. A bespoke DFMA (design for manufacture and assembly) and DFMEA (design failure mode effect and analysis) process has been developed to deliver a robust stand-alone radiator design.

Research sub-objective # 4: Performance evaluation of stand-alone water filled radiators

Performance evaluation for domestic heating systems has been carried out in accordance with British standards. All the guidelines detailed in BS EN 442-1 and BS EN 442-2 for test setup and accuracy of measurement have been followed. Using the equations in the BS EN 442 [13] a standard characteristic equation is generated for the radiator. Results of the test conducted according to EN 442-1 and EN 442-2 to quantify the thermal output of the radiators are given in Table 8-1.

	3100	6100
Heater size in radiator	900 w	2000 w
Thermal Output	770.36 W	1537.029 W
Efficiency	98.76%	97.4%

Table 8-1 Thermal output of stand-alone radiators as per BS EN 442 test

The results indicate that the stand-alone radiators are over 97% efficient for the largest radiator and 98.76% for a small radiator.

Research sub-objective # 5: To analyse temperature distribution in a stand-alone water filled radiator

The effect of point of entry of fluid in a stand-alone radiator system has been analysed both qualitatively and quantitatively. Both double and single panel radiators have been analysed to quantify the difference between the two radiators. The study has given a clear indication of the flow path of hot water in each of the cases. It has been observed that the flow path is unique for each of the cases. This indicates that the flow rate and flow configuration along with the buoyancy effect of the hot water plays a significant role in the temperature distribution on the panel. Thermal investigation has shown that the flow rate and flow configurations have a significant impact on the temperature distribution and temperature drop across the radiator. Operating temperature of the water also contributes towards the flow distribution and in turn performance of radiators.

Research sub-objective # 6: To analyse the effect of point of entry and flow rate on pressure drop in a stand-alone water filled radiator

Experimental investigation has been carried to analyse pressure drop within a stand-alone radiator. The study was carried out on a radiator with BBOE and BTOE configuration at various flow rates. Pressure drop across the radiator has been measured in 300 mm x 600 mm and 600 mm x 1000 mm radiators. Loss co-efficient has been developed. Relationships between loss coefficient and Reynolds number have been quantified, which shows similar trend for both configurations, and shows the loss coefficient decreases as the velocity increases. Relationship between loss coefficients as a function of Reynolds number has also been developed in this study for both BBOE and BTOE configurations.

Research sub-objective # 7: To analyse the effect of point of entry and flow rate on pressure distribution in a stand-alone water filled radiator

Experimental investigation has been carried to analyse pressure distribution within a stand-alone radiator. The study was carried out on a radiator with BBOE and BTOE configuration at various flow rates. Pressure distribution across the radiator has been measured in 300 mm x 600 mm and 600 mm x 1000 mm radiators. Pressure distribution coefficient has been developed. Relationships between pressure distribution coefficient and flow velocity have been quantified, which shows similar trend for both configurations, and shows the pressure distribution coefficient decreases as the velocity increases. Relationship has also been developed in this study for both BBOE and BTOE configurations.

Research sub-objective # 8: To formulate the effect of radiator size on pressure drop and pressure distribution in a stand-alone water filled radiator

In both BBOE and BTOE configurations loss co-efficient varies with radiator size. Geometric parameters of the radiator have been reviewed to establish a correlation between loss-coefficient and a non-dimensional geometric parameter.

$$G_f = \frac{\ln\left(\frac{L \times 1000}{16.66}\right) \times \left(L \times \left[1.81 + \frac{(h - 0.3) \times 0.43}{0.1}\right]\right) \times 0.001}{(L \times h) \times \sqrt[2]{L^2 + h^2}}$$

Loss co-efficient is independent of flow rate but changes with size in both flow configuration. The length of the complex flow path in the radiator effectively increases with the increase in size. The geometric factor reduces as the radiator size increases. Loss co-efficient can be expressed as a function of geometric factor as

$$K = -24.595 \times \left[\frac{\ln\left(\frac{L \times 1000}{16.66}\right) \times \left(L \times \left[1.81 + \frac{(h - 0.3) \times 0.43}{0.1}\right]\right) \times 0.001}{(L \times h) \times \sqrt[2]{L^2 + h^2}} \right] + 7.1613$$

A pressure distribution ratio co-efficient has been developed that is independent of radiator size and flow configuration. Over the range of flow velocities, comparing the calculated pressure distribution ratios co-efficient and size independent pressure distribution ratio co-efficient it can be seen that a good co-relation exists. Further comparing the pressure distribution ratio co-efficient from CFD results for the three radiators with the calculated pressure distribution ratio co-efficient a good co-relation is observed with an average deviation of only 1.66%. Unlike the loss co-efficient both flow velocity and the radiator size influence the pressure distribution in the radiator. To achieve an even distribution and low losses a smaller radiator at lower flow velocity is recommended for a BBOE configuration.

Research sub-objective #9: To formulate the effect port diameter on pressure drop and pressure distribution in a stand-alone water filled radiator

Loss co-efficient radiator is compared for three different port diameters over a range of Reynolds number in BBOE configuration. Loss co-efficient is constant for a given radiator and it has been observed that that the loss co-efficient is constant for a port diameter within the radiator. However the value of K does change with change in port diameter. Loss co-efficient increases with increase in port diameter. Radiator with 8 mm port diameter has higher K values compared to a radiator with 6 mm port diameters by an average of 214%. Port diameter of 12 mm has significantly higher K values compared to a 6 mm port diameter radiator by 481%. K values vary by 85% between a radiator with 8 mm and 12 mm port diameter. Pressure variation in a radiator with 12 mm port diameter is independent of flow rate and flow configuration. 12 mm port diameter also has significantly better flow distribution, which will provide uniform temperature distribution.

Research sub-objective # 10: Development of robust cost model for stand-alone water filled radiators

A complete investment cost, operation cost and total heat cost prediction methodology has been developed and presented, which is based on the unique stand-alone radiator that has been developed and evaluated.

The manufacturing cost can be calculated using

$$C_{Manufacturing} = C_1 \cdot \left(L \times \left[8.53 + \frac{(h - 0.3) \times 2.91}{0.1} \right] \right) + (C_2 \cdot Q_{heater}) + C_3 + C_4$$

The operation cost can be calculated using

$$C_{Operation} = C_5 \cdot \left[\frac{\dot{m} \times \Delta P_{Total}}{\eta_{pump}} \right] \cdot \tau_{pump} + C_6 \cdot \left[\frac{I^2 \times R}{\eta_{heater}} \right] \cdot \tau_{heater}$$

Total heating cost can be calculated using

$$C_{heating/day} = \frac{[C_1 \cdot (L \times [8.53 + \frac{(h - 0.3) \times 2.91}{0.1}]) + (C_2 \cdot Q_{heater}) + C_3 + C_4] \cdot C_7}{5 \times 365} + 5 \times C_6 \cdot \left[\frac{I^2 \times R}{\eta_{heater}} \right] \cdot \tau_{heater}$$

Furthermore, design example has been used to validate the principle of the cost model.

Research sub-objective # 11: Optimisation of radiator cost and comparative study of stand-alone water filled radiator to a central heating system

Optimisation based on least cost principle has been developed. It can be seen that an optimal radiator size for delivering the heating requirements for a room is by using multiple small radiators rather than a large radiator as it offers benefit on cost of operation and heat distribution in the room. A comparative study to central heating system has shown for smaller areas, extensions or conversions a stand-alone system can be very economical compared to a gas central heating system. The cost benefit reduces compared to gas central heating as the size of the built environment increases.

8.4 Thesis Contributions

The major contributions of this research study are summarized below in which novelties of this research are described:

Contribution 1

A bespoke product development process has been developed for stand-alone water filled radiators. Using this, an innovative heating product has been developed which consolidated the existing range and optimised the manufacturing process. Similar product does not exist in the market. The product is safe and accredited by Nemko. New stand-alone radiators are over 97% efficient. Product has been successfully launched in the market with the projected sales increase of 70%.

Contribution 2

Detailed experimental evaluation of stand-alone water filled radiators under different flow configurations and flow rates for two radiator sizes have been conducted to develop a novel relationship of pressure drop to flow velocity. Further a non-dimensional parameter, loss co-efficient K has been developed as a function of effective Reynolds number to quantify pressure losses in radiator. Individual equations for each size and configuration has been developed which can used to develop parametric models for system losses. Effect of flow velocity on the pressure variation in a radiator has been investigated to develop a pressure distribution co-efficient – which gives us valuable information to study flow and temperature distribution in a radiator.

Contribution 3

Geometry of the radiator has significant influence on radiator performance. Unfortunately very limited information is available on the internal flow field within the radiators. Numerical investigation on flow through radiators is a major contribution of this study. Detailed analysis to quantify the effect of radiator size and inlet diameter under different flow configurations and flow rates have been discussed. The results obtained from the investigation have been quantified and graphically represented. Numerical analysis has also given a novel insight into pressure and velocity distribution in a radiator, which has not been done previously. A non-dimensional geometric factor has been developed to account for radiator size. A unique relationship has been established between loss co-efficient and port diameter that has been primarily developed to quantify the influence of inlet and out port diameter.

Contribution 4

Heating cost for a built environment is a significant percentage of domestic expenditure. The net cost of space heating should account for initial investment cost for the heating system, installation cost, maintenance cost and operation cost. Although there are several surveys conducted and reports generated by department of energy, CIBSE and other government organisations to measure the cost of heating to the end customer using central heating, there is limited information available on methodology to compute total cost of heating per day for stand-alone systems that includes all the factors. Additionally there is limited comparative study between a central heating and stand-alone system that accounts for all aspects of ownership and operation. A methodological approach to predict cost for water filled stand-alone system has been developed which accounts for manufacturing cost and operation cost. A cost comparative study of central heating system and a stand-alone has been conducted to objectively quantify benefit of one system to the other.

8.5 Recommendations for future Work

The design, operation and optimization of stand-alone radiators have been presented in the present study such that gaps identified in literature could be bridged. In light of the concluded remarks provided in the previous sections, a vast potential for further research in this particular area of stand-alone heating has been unlocked. The main areas identified for further work are described below which are associated to further performance-related analysis, design and optimization of stand-alone radiators.

Recommendation 1

More advanced modelling techniques have now become available such as fluid structure interface and workbench. Using such models, the flow of hot water in the radiator and its interaction with the metal body of the radiator can be analysed with much better accuracy. In these techniques, the metallic radiator body accounts for thermal expansion, which in turn changes the volume in which the fluid flows. Pressure drop under such circumstances can be very interesting to investigate. These advanced models do not require any inputs in terms of volume change or pressure resulting from fluid expansion. The hydrodynamic forces acting on the radiator panel are enumerated on the fly and necessary modifications are carried out for the flow path, velocity and pressure in the radiator. The recommended advanced modelling techniques are computationally very expensive and require massive computational power.

Recommendation 2

Different shapes and channel configurations of the radiator can be analysed using CFD, and the results compared with the one presented in this study for optimisation purposes. Although rust inhibitors are added to the system, there is a high likely hood of particulate formation due to electrochemical reaction in a closed circuit with different materials. Wear and tear analysis can be conducted on the various radiator components to develop a prognostic tool for stand-alone radiators. In addition to possible component failure, any particulate matter can form sludge, which can affect the thermal output of the radiator resulting in performance drop. An estimation of the wear and tear can have significant effect on the design and optimisation of such stand-alone systems.

Recommendation 3

Current work has physically measured internal pressure only at 6 points in the radiator, which have been used to validate the numerical work. Experimental work can be performed using PIV or LDV and compared to the numerical studies for flow visualisation inside the radiator. PIV especially can be very suitable to ascertain flow path and velocity distribution. If coupled with heat, buoyancy effect can also be visualised. In such a scenario, the operating temperature will have a significant impact on the pressure drop considerations in the radiator. Although significant literature is available on external airflow on the radiator, further studies can be conducted on a stand –alone radiator system with forced convection. Addition of a fan will marginally increase the power consumption but may significantly improve the heat output from the stand-alone system.

Recommendation 4

In recent years, there have been many thermal applications where addition of micro/nano fluids has significantly improved the heat transfer capability of the system. As a stand-alone system is self contained and sealed, there is a huge potential to improve the effectiveness of the radiator by increasing the specific heat capacity of the operating fluid. With the pump being magnetic and the need to minimise the cost of ownership, there are significant challenges that have to be researched.

Recommendation 5

The product development process developed can be further tuned and enhanced to incorporate further developments in reconfigurable manufacturing systems. Also to conduct a thorough design for assembly (DFA) in conjunction with the new product development process.

9 REFERENCES

1. Met Office (2012). *Annual average in United Kingdom*. Retrieved from <http://www.metoffice.gov.uk/public/weather/climate> Accessed 21st April 2017
2. Haines, R. W., & Myers, M. E., & Leed, A. P. (2010). *HVAC Systems Design Handbook* (5th ed.). (pp. 459). McGraw-Hill
3. Huebner, G. M., & McMichael, M., & Shipworth, D., & Shipworth, M., Durand-Daubin, M., & Summerfield, A., (2013). Heating patterns in English homes: Comparing results from a national survey against common model assumptions. *Building and Environment*, (70) 298-305.
4. Department of Energy and Climate Change. (2008) *Climate change act 2008*. London: Department of Energy and Climate Change The Stationary Office.
5. Department of Energy and Climate Change. (2009) *The UK low carbon transition plan: national strategy for climate and energy*. London: Department of Energy and Climate Change The Stationary Office.
6. Palmer, J., & Cooper, I. (2012). *United Kingdom energy housing factfile*. Department of Energy and Climate Change, London. Retrieved from: https://www.gov.uk/government/uploads/system/uploads/attachment_data/file/201167/uk_housing_fact_file_2012.pdf.
7. Garlo (2006) *Wikimedia, UKHomePerformanceRatingChartsVertical.png*. *Wikimedia Commons, the free media repository*. Retrieved from <https://commons.wikimedia.org/w/index.php?title=File:UKHomePerformanceRatingChartsVertical.png&oldid=178951938>.
8. Knauff (2011). *Think Insulation: Knauff Insulation* Retrieved from "[How much insulation do I need?](#)".
9. Mitchell, P. (2008). *Central Heating- Installation, Maintenance and Repair EPC*”, Brailsford Press.
10. British Standard Institution. (2008). *BS EN ISO 13790:2008 Energy performance of buildings. Calculation of energy use for space heating and cooling*. London: BSI.
11. British Standard Institution. (2008). *BS EN 15316-4-2:2008 Heating systems in buildings. Method for calculation of system energy requirements and system efficiencies. Space heating generation systems, heat pump systems*. London: BSI.

12. Institute of Domestic Heating & Environmental Engineers (2017). *Energy related products*. Retrieved from: <https://idhee.org.uk>
13. British Standard Institution. (2014). *BS EN 442-2:2014 Radiators and convectors. Test methods and rating*. London: BSI.
14. Jaga Homes (2017). *Roman heating systems*. Retrieved from: https://www.jagahomeheating.co.uk/Assets/User/1150-399-Heating_2.png
15. Energy Saving Trust (1996). *The economic thickness of insulation for hot pipes*. Fuel Efficiency Booklet
16. Bakos, G. C., & Spirou, A., & Tsagas, N. F. (1999). Energy management method for fuel saving in central heating installations. *Energy and Buildings* (29) 35-139.
17. Liao, Z., & Sawinsons, M., & Dexter, A. L. (2005). On the control of heating systems in the UK. *Building and Environment* (40) 343-351. License No:- 4136090393888 to use image
18. Ahern, C., & Norton, B. (2015). Energy savings across EU domestic building stock by optimizing hydraulic distribution in domestic space heating systems. *Energy and Buildings* (91) 199-209 licence no 4136340261594 to use image
19. Beck, S. M. B., & Grinsted, S. C., & Blackey, S. G., & Worden, K. (2004). A novel design for panel radiators. *Applied Thermal Engineering* (24) 1291-1301.
20. Beck, S. M. B., & Blackey, S. G., & Chung, M. C. (2001). The effect of wall emissivity on radiator heat output. *Building Service Engineering Research and technology* (22.3) 185-194.
21. Harper, R. D., & Dickson, W. A. (1995). Reducing the burn risk to elderly persons living in residential care. *Burns* (21.3) 205-208.
22. Harper, R. D., & Dickson, W. A. (1996). Domestic central heating radiators: a cause for concern in all age groups. *Burns* (22.3) 217-220.
23. Veryzer, R. W. (1998). Discontinuous innovation and the New Product Development Process. *Journal of Product Innovation Management* (15) 304-321.
24. Ulrich, K. T., & Eppinger, S. D. (2012). *Product Design and Development* (5th ed). New York: McGraw-Hill Irwin ISBN 978-0-07-3400477-6
25. Ohio University. (2009). *Principles of Marketing: New-Product Development and Product Life-Cycle Strategies*. Retrieved from www.ohio.edu/people/gupta/MKT202Kotler/Chapter%2009.ppt dated Oct 2015

26. Azzi, A., & Battini, D., & Faccio, M., & Persona, A. (2011). Variability-oriented assembly system design: a case study in the construction industry. *Assem Autom* 31(4) 348–357.
27. Saliba, M., & Zarb, A., & Borg, J. (2010). A modular, reconfigurable end effector for the plastics industry. *Assem Autom* 30(2) 147–154
28. Lateef-Ur, R., & Ateekh-Ur, R. (2013). Manufacturing configuration selection using multicriteria decision tool. *Int J Adv Manuf Tech* 65(5–8) 625–639.
29. Newman, W., & Podgurski, A., & Quinn, R., & Merat, F., & Branicky, M., Barendt, N., & Causey, G., & Haaser, E., Yoohwan, K., & Swaminathan, J., & Velasco, V. (2000). Design lessons for building agile manufacturing systems. *IEEE T Robot Autom* 16(3) 228–238.
30. Mourtzis, D., & Doukas, M., & Psarommatis, F. (2013). Design and operation of manufacturing networks for mass customization. *CIRP Ann Manuf Tech* 62(1) 467–470.
31. Daaboul, J., & Bernard, A., Laroche, F. (2012). Extended value network modelling and simulation for mass customization implementation. *J Intelligent Manuf* 23(6) 2427–2439.
32. Feng, Y., & Zheng, B., & Tan, J., & Wei, Z. (2009). An exploratory study of the general requirement representation model for product configuration in mass customization mode. *Int J Adv Manuf Tech* 40(7–8) 785–796.
33. Felfering, A., & Friedrich, G., & Jannarch, D. (2001). Conceptual modelling for configuration of mass-customizable products. *Artif Intell Eng* 15 165–176.
34. Mesa, J., & Maury, H., & Turizo, J., & Bula, A. (2014). A methodology to define reconfigurable system architecture for a compact heat exchanger assembly machine. *Int J Adv Manuf Technol* (70) 2199-2210.
35. Peach, J. (1972). Radiators and other Convectors. *Environmental science and technology*. (39) 239-253.
36. Walters, K., & Fine, R. H. (1973). The Performance of Radiators and Convectors Using Medium Temperature Hot Water Laboratory report. *Heating and ventilation research association*.
37. McIntyre, D. A. (1986). Output of radiators at reduced flow rate. *Building Services Engineering Research and Technology*. 7(2) 92-95.
38. Ward, I. C. (1991). Domestic Radiators: Performance at lower mass flow rates and lower temperature differentials than those specified in standard performance

- test. *Building service engineering research and technology* (12) pp 87-94. - permission granted from rightslink
39. Giesecke, F. E, & Kratz, A. P. (1945). Heat emissions and friction heads of hot water radiators and convectors. *University of Illinois Urbana*
 40. Etemad, S. Gh., & Bakhtiari, F. (1999). General equation for fully developed fluid flow and heat transfer characteristics in complex geometries. *Int. Comm Heat Mass Transfer* (26.2) 229-238.
 41. Dehdakhel, A. A., & Rahimi, M., & Alsairafi, A. A. (2010). CFD modeling of flow and heat transfer in a thermo-syphon. *International Communications in Heat and Mass Transfer* (37) 312 – 318.
 42. Sato, A. I., & Scalon, V. L., & Padilha, A. (2012). Numerical analysis of a modified evacuated tubes solar condenser. *International Conference on Renewable Energies and Power Quality*. 28 – 30 March, Spain
 43. Subramanian, J., & Kumar, S., & Kozhndu, T., & Selvam, T. (2012). Experimental Studies on Variable Header Solar Water Heating System. *International Conference on Mechanical, Production and Automobile Engineering*. 28 – 29 April, Singapore
 44. Iordanou, G., & Tsirigotis, G. (2012). Computational Fluid Dynamics (CFD) Investigations of the Effect of Placing a Metallic Mesh in the Channels of a Passive Solar Condenser Model. *Electronics & Electrical Engineering*. (121) 69.
 45. Freegah, B., & Asim, T. & Mishra, R. (2013). Computational Fluid Dynamics based Analysis of a Closed Thermo-Siphon Hot Water Solar System. *26th International Congress of Condition Monitoring and Diagnostic Engineering Management*
 46. Freegah, B., & Asim, T., & Mishra, R. (2013). Effects of condenser volume on the performance of a solar thermo-syphon. *Annual Researchers Conference Computing and Engineering 2013 (CEARC'13)*. December 2013, University of Huddersfield, Huddersfield, UK, 140-145
 47. S. El-Din, H. S. (2005). Heat transfer characteristics of an inclined single-phase toroidal thermosyphon. *Alexandria Engineering Journal*, 44(2)157-171.
 48. Freegah, B., & Asim, T., & Albarzenji, D., & Pradhan, S., & Mishra, R. (2014). Effect of the shape of connecting pipes on the performance output of a closed-loop hot water solar Thermo-syphon. *3rd International Workshop and Congress on e-Maintenance*

49. Freegah, B., & Asim, T., & Mishra, R. (2015). Effect of Solar Heat Flux and Thermal Loading on the Flow Distribution within the Riser Pipes of a Closed-Loop Thermo-syphon Solar Water Heater System. *28th International Congress of Condition Monitoring and Diagnostic Engineering Management*
50. Erdogmus, A. B. (2011). *Simulation of the heater test room defined by EN 442 standard and virtual testing of different type of heaters* Doctoral Thesis submitted at Izmir Institute of Technology.
51. Shah, R.K., & London, A. L. (1974). Thermal Boundary Conditions and Some Solutions for Laminar Duct Flow Forced Convection. *ASME J. Heat Transfer* (96) 159-165.
52. Akin, D. (2007). Computer aided design of thermal systems. *Izmir*
53. Versteeg, H.K., & Malalasekera, W. (2007) *An introduction to computational fluid dynamics: the finite volume method*. London:Pearson Education.
54. Schlichting, H., & Gersten, K. (2004). *Boundary layer Theory*. (8th ed.) Springer-Verlag.
55. ANSYS 13.0.0 (2014). *User Guide* Retrieved from http://www1.ansys.com/customer/content/documentation/130/wb2_help.pdf
56. Chrysler LLC, Ford Motor Company, General Motors Corporation. (2008). *Potential Failure Mode and Effects Analysis (FMEA): Reference Manual*. (4th ed.) Chrysler LLC, Ford Motor Company, General Motors Corporation
57. British Standard Institution. (2000). *BS EN ISO 9001:2000 Quality management systems. Requirements* (A5 Laminated). London: BSI.
58. British Standard Institution. (2006) *BS 7593:2006 Code of practice for treatment of water in domestic hot water central heating systems*. London: BSI.
59. Pillutla, G., & Mishra, R., & Barrans, S. M., & Barrans, J. (2009). Experimental Investigation of Effect of Point of Fluid Entry in Standalone Domestic Heating Radiator. *Fluid Mechanics and Fluid Power conference Pune*
60. Quinn Radiators (2010). *Q22604CW-Warmastyle datasheet and Dimensions - Quinn radiators brochure*.
61. Kell, G. S. (1975). Density, thermal expansivity, and compressibility of liquid water from 0° to 150 °C: Correlations and tables for atmospheric pressure and saturation reviewed and expressed on 1968 temperature scale. *J. Chem. Eng. Data* 20(1) 97-105.

62. British Standard Institution (2013). *BS IEC 60529:1992+A2:2013 Degrees of protection provided by enclosures (IP code)*. London: BSI.
63. British Standard Institution (2009). *BS EN 60335-2-30, Household and similar electrical appliances- Safety Part2-30: particular requirements for room heaters*". (4th ed) 2002-2009. London : BSI.
64. Termoteknik radiators (2010). *Radiator catalogue, TT_RGK_2017_01_soft.pdf*.
65. & Jewett, J. W. (2012). *Principles of physics : Calculus based Text*. (5th ed.). Cengage Learning
66. Serway, R. A., & Vuille, C. (2012). *College Physics*. (11th ed.) Vol.2 Cengage Learning ISBN 978-1-305-96552-2
67. Wilson, I. O., (1981). Magnesium oxide as high temperature insulation. *IEE PROC* (128 Pt A) 159-164
68. Laing pumps : *Specification sheet* Retrieved from <http://urpravo2.ru/laing-circulation-pump/>
69. Grundfos pumps: *Specification sheet* Retrieved from <http://uk.grundfos.com/products/find-product/alpha21.html>
70. Fernox Website: *Alphi-11 specifications*. Retrieved from <https://www.fernox.com/inhibitors-protectors/alphi-11-antifreeze-protector-5l>
71. Fernox Website: *AF-10 Biocide specifications*. Retrieved from <https://www.fernox.com/bacterial-control/af10-biocide-500ml>
72. Heat-Electric UK: *Product images*. Retrieved from <http://www.heatelectric-uk.com>
73. NEMKO: *Product testing and certification*. Retrieved from <https://www.nemko.com/product-testing/emc-testing/emc-marks>
74. Kowlski, J. (1995). Triple objective optimum design of a two-column radiator of central heating. *International communications in Heat and Mass transfer* (22.3) 401-409.
75. Bojic, M., & Trifunovic, N. (1998). Linear programming optimization of heat distribution in a district- heating system by valve adjustment and substation retrofit. *Building and Enviornment* (35) 151-159.
76. Arslanturk, C., & Ozguc, A. F. (2006). Optimization of a central- heating radiator. *Applied Energy* (83) 1190-1197.
77. T Asim (Feb 2013) "Computational Fluid Dynamics Based Diagnostics and Optimal Design of Hydraulic Capsule Pipelines" PhD thesis submitted at University of Huddersfield. Discussion with the author.

78. Briault, T. Arup Energy Consulting. CIBSE Symposium (17th April 2015) *The price of heat* Retrieved from <http://www.cibse.org/knowledge/knowledge-items/detail?id=a0q20000008I6yb>
79. Department for Business, Energy and Industry Strategy (31st march 2016). *Annual domestic energy price.* Retrieved from <https://www.gov.uk/government/statistical-data-sets/annual-domestic-energy-price-statistics#history>
80. FLIR Data sheet A655sc High resolution science grade LWIR camera Retrieved from http://www.flirmedia.com/MMC/THG/Brochures/RND_011/RND_011_US.pdf

10 APPENDIX I

10.1 Flow sensor data sheets

	Unit 6 Mercury House, Calleva Park Aldermaston, Berkshire, RG7 8PN Tel: +44 (0)118 981 7980 Fax: +44 (0)118 981 7990 e-mail: sales@impress-sensors.co.uk Website: www.impress-sensors.co.uk	<h2 style="margin: 0;">DATA SHEET</h2>																																																																															
Pressure - Temperature - Level - Distance - Control - Indication - Data logging																																																																																	
<p>VFS 1-20 Vortex flow sensor, 1-20 l/min</p>  <p style="text-align: center;">Fig. 1 VFS 1-20 sensor</p> <p>Technical overview West Direct Sensors™, type VFS, are a series of combined flow- and temperature sensors (two-in-one) based on the principle of vortex shedding behind a bluff body. The VFS sensors are designed for high-volume production and are fully compatible with wet, aggressive media. The VFS sensor utilises MEMS sensing technology in combination with a novel packaging concept using corrosion-resistant coating on the MEMS sensor element. This makes the VFS sensor very robust and ideal for high-volume OEM applications. VFS sensors are available for flow ranges of 1.3-20, 2-40, 5-100 and 10-200 l/min.</p> <p>Applications</p> <ul style="list-style-type: none"> • Burner control in domestic gas boilers • Thermal management in solar heating systems • Industrial process flow control • Flow rate detection for pump controls • Monitoring of pumps, valves and filters • Cooling and temperature control • Domestic hot-water stations. <p>Features</p> <ul style="list-style-type: none"> • Flow ranges: 1.3-20, 2-40, 5-100 and 10-200 l/min. • Designed for harsh environments • Based on vortex shedding • Voltage output (ratiometric, ideal for use with micro-processor and PLC) • Compact and well-proven design • MEMS sensing technology • Approved for potable water: WRAS, NSF, KTW, W270, ACS. 	<p>Benefits</p> <ul style="list-style-type: none"> • No moving parts • Flow and temperature sensor in one package (two-in-one sensor) • Fast temperature response (direct media contact) • Compatible with wet, aggressive media • Cost-effective and robust construction. <p>Specifications</p> <table border="1" style="width: 100%; border-collapse: collapse;"> <tr><td colspan="2">Pressure</td></tr> <tr><td>Range</td><td>1.3 to 20 l/min</td></tr> <tr><td>Accuracy (±1σ, 0 to 100°C)</td><td>±1.5 %FS</td></tr> <tr><td>Response time (83.2%)</td><td>< 1.5 s</td></tr> <tr><td>Resolution</td><td>0.05 l/min</td></tr> <tr><td colspan="2">Temperature</td></tr> <tr><td>Range</td><td>0 to 100°C</td></tr> <tr><td>Accuracy (±1σ, 25 to 80°C)</td><td>±1°C</td></tr> <tr><td>Accuracy (±1σ, 0 to 100°C)</td><td>±2°C</td></tr> <tr><td>Response time (83.2% at 50%FS flow)</td><td>< 1.5s</td></tr> <tr><td>Resolution</td><td>0.5°C</td></tr> <tr><td colspan="2">Media and environment</td></tr> <tr><td>Media types</td><td>Liquids. The sensor is compatible with aggressive media.</td></tr> <tr><td>Media temperature (operation)</td><td>0 to 100°C</td></tr> <tr><td>Media temperature (peak)</td><td>-25 to 120°C</td></tr> <tr><td>Ambient air temp. (operation)</td><td>-25 to 60°C</td></tr> <tr><td>Ambient air temp. (peak)</td><td>-55 to 90°C</td></tr> <tr><td>Humidity</td><td>0 - 95 % (relative), non-condensing</td></tr> <tr><td>Burst pressure</td><td>> 16 bar</td></tr> <tr><td colspan="2">Electrical data</td></tr> <tr><td>Power supply</td><td>5 V DC (±5%). Grounding of the sensor supply is recommended</td></tr> <tr><td>Output signals</td><td>Ratiometric</td></tr> <tr><td>Flow signal</td><td>0.35 - 3.5 V</td></tr> <tr><td>Temperature signal</td><td>0.5 - 3.5 V</td></tr> <tr><td>Power consumption</td><td>< 50 mW</td></tr> <tr><td>Load impedance</td><td>> 10 kΩ</td></tr> <tr><td colspan="2">Sensor materials</td></tr> <tr><td>Sensor element</td><td>Silicon-based MEMS sensor</td></tr> <tr><td>Seal (sensor to housing)</td><td>EPDM rubber</td></tr> <tr><td>Housing</td><td>Composites (PPS, PA66)</td></tr> <tr><td>Flow pipe</td><td>PPA 40-GF</td></tr> <tr><td>Wetted materials</td><td>Corrosion-resistant coating EPDM, PPS, PPA 40-GF</td></tr> <tr><td colspan="2">Environmental standards</td></tr> <tr><td>Enclosure class</td><td>IP44</td></tr> <tr><td>Temperature cycling</td><td>IEC 68-2-14</td></tr> <tr><td>Vibration (non-destructive)</td><td>20 - 2000 Hz, 10G, 4h</td></tr> <tr><td>Electromagnetic compatibility</td><td>EN 61326-1</td></tr> <tr><td colspan="2">Dimensions</td></tr> <tr><td>Sensor element</td><td>47*40*25 mm</td></tr> <tr><td>Flow pipe</td><td>82*39*25 mm</td></tr> </table>	Pressure		Range	1.3 to 20 l/min	Accuracy (±1σ, 0 to 100°C)	±1.5 %FS	Response time (83.2%)	< 1.5 s	Resolution	0.05 l/min	Temperature		Range	0 to 100°C	Accuracy (±1σ, 25 to 80°C)	±1°C	Accuracy (±1σ, 0 to 100°C)	±2°C	Response time (83.2% at 50%FS flow)	< 1.5s	Resolution	0.5°C	Media and environment		Media types	Liquids. The sensor is compatible with aggressive media.	Media temperature (operation)	0 to 100°C	Media temperature (peak)	-25 to 120°C	Ambient air temp. (operation)	-25 to 60°C	Ambient air temp. (peak)	-55 to 90°C	Humidity	0 - 95 % (relative), non-condensing	Burst pressure	> 16 bar	Electrical data		Power supply	5 V DC (±5%). Grounding of the sensor supply is recommended	Output signals	Ratiometric	Flow signal	0.35 - 3.5 V	Temperature signal	0.5 - 3.5 V	Power consumption	< 50 mW	Load impedance	> 10 kΩ	Sensor materials		Sensor element	Silicon-based MEMS sensor	Seal (sensor to housing)	EPDM rubber	Housing	Composites (PPS, PA66)	Flow pipe	PPA 40-GF	Wetted materials	Corrosion-resistant coating EPDM, PPS, PPA 40-GF	Environmental standards		Enclosure class	IP44	Temperature cycling	IEC 68-2-14	Vibration (non-destructive)	20 - 2000 Hz, 10G, 4h	Electromagnetic compatibility	EN 61326-1	Dimensions		Sensor element	47*40*25 mm	Flow pipe	82*39*25 mm
Pressure																																																																																	
Range	1.3 to 20 l/min																																																																																
Accuracy (±1σ, 0 to 100°C)	±1.5 %FS																																																																																
Response time (83.2%)	< 1.5 s																																																																																
Resolution	0.05 l/min																																																																																
Temperature																																																																																	
Range	0 to 100°C																																																																																
Accuracy (±1σ, 25 to 80°C)	±1°C																																																																																
Accuracy (±1σ, 0 to 100°C)	±2°C																																																																																
Response time (83.2% at 50%FS flow)	< 1.5s																																																																																
Resolution	0.5°C																																																																																
Media and environment																																																																																	
Media types	Liquids. The sensor is compatible with aggressive media.																																																																																
Media temperature (operation)	0 to 100°C																																																																																
Media temperature (peak)	-25 to 120°C																																																																																
Ambient air temp. (operation)	-25 to 60°C																																																																																
Ambient air temp. (peak)	-55 to 90°C																																																																																
Humidity	0 - 95 % (relative), non-condensing																																																																																
Burst pressure	> 16 bar																																																																																
Electrical data																																																																																	
Power supply	5 V DC (±5%). Grounding of the sensor supply is recommended																																																																																
Output signals	Ratiometric																																																																																
Flow signal	0.35 - 3.5 V																																																																																
Temperature signal	0.5 - 3.5 V																																																																																
Power consumption	< 50 mW																																																																																
Load impedance	> 10 kΩ																																																																																
Sensor materials																																																																																	
Sensor element	Silicon-based MEMS sensor																																																																																
Seal (sensor to housing)	EPDM rubber																																																																																
Housing	Composites (PPS, PA66)																																																																																
Flow pipe	PPA 40-GF																																																																																
Wetted materials	Corrosion-resistant coating EPDM, PPS, PPA 40-GF																																																																																
Environmental standards																																																																																	
Enclosure class	IP44																																																																																
Temperature cycling	IEC 68-2-14																																																																																
Vibration (non-destructive)	20 - 2000 Hz, 10G, 4h																																																																																
Electromagnetic compatibility	EN 61326-1																																																																																
Dimensions																																																																																	
Sensor element	47*40*25 mm																																																																																
Flow pipe	82*39*25 mm																																																																																

Dimensions (in mm)

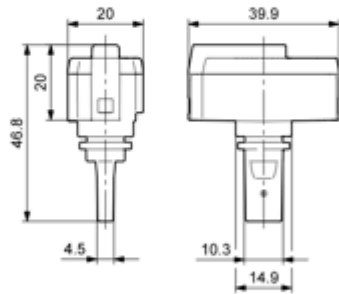


Fig. 2 Dimensional sketches of sensor element

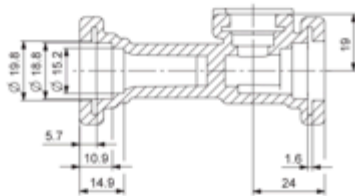


Fig. 3 Dimensional sketch of flow pipe

Type key

The VFS sensor is labelled with a type designation.

	96577493	- XX	- XXX	XXXXX
Product number				
Revision				
Production year and week				
Consecutive number				

96702082	0207	GB
----------	------	-----------

Electrical connections

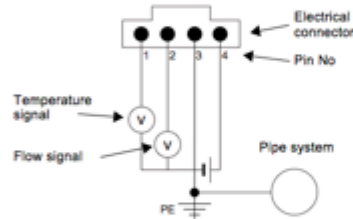


Fig. 4 Electrical connections

Pin configuration

- | | |
|---|--|
| 1 | Temperature signal (0.5 to 3.5V relative to pin 3) |
| 2 | Flow signal (0.35 to 3.5V relative to pin 3) |
| 3 | GND (0V) |
| 4 | Voltage supply (+5V DC), PELV |

Sensor output signals

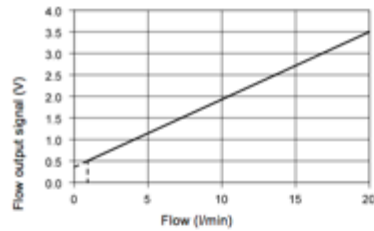


Fig. 5 Flow response

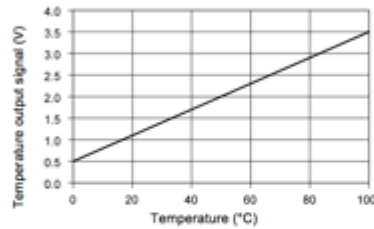


Fig. 6 Temperature response

Subject to alterations.

Visit the website: www.impress-sensors.co.uk

10.2 Pressure sensor data sheet



IMPRESS
SENSORS & SYSTEMS

Unit 6 Mercury House, Calleva Park
Aldermaston, Berkshire, RG7 8PN
Tel: +44 (0)118 981 7980
Fax: +44 (0)118 981 7990
e-mail: sales@impress-sensors.co.uk
Website: www.impress-sensors.co.uk

Pressure - Temperature - Level - Distance - Control - Indication - Data logging



IMP

Industrial Pressure Transmitter

- Thick film ceramic sensor
- Accuracy: $\pm 0.25\% \text{ FS BFSL}$ (0.1% optional)
- Pressure ranges from 0.5 to 700 bar
- Gauge, Sealed Gauge or Absolute reference
- Variety of Outputs including mV, Volts and mA

The industrial pressure transmitter, IMP, has a piezo-resistive ceramic pressure sensor giving it excellent media compatibility. The housing is made from stainless steel with a choice of internal O ring seals to select to ensure the product is suitable for a wide range of applications. Every device is temperature compensated and calibrated and supplied with a traceable serial number and calibration certificate. The electronics incorporate a microprocessor based amplifier, this means there are no adjusting pots and therefore the electronics are very stable, especially in high vibration / shock applications.

There are many options available on the IMP pressure transmitter. These include the following :

- Pressure range and engineering units
- Pressure reference (G, SG or Abs)
- Output
- Accuracy (Non-linearity & hysteresis)
- Thermal accuracy
- Electrical connection
- Process connection
- Process connection material
- O ring seal material

Suitable for the following applications:

- Hydraulics
- Pneumatics
- Autoclave & Sterilisation
- Agricultural machinery
- Laboratory testing
- Mechanical engineering
- Environmental engineering
- Automotive testing
- Tank gauging
- Pumps & compressors
- HVAC

IMP Industrial Pressure Transmitter



IMP Industrial Pressure Transmitter

Visit the website: www.impress-sensors.co.uk

Company Reg. No.: 4346738, VAT No.: 788 6596 54, Reg Address: Impress Sensors & Systems Ltd, Unit 6 Mercury House, Calleva Park, Aldermaston, Berkshire, RG7 8PN

IMP

Industrial Pressure Transmitter

Technical Datasheet

Input Pressure Range

Nominal pressure, Gauge	Bar	0.5	1	2	5	10	20	50	100	250	400	600	700
Nominal pressure, Absolute & SG	Bar	0.5	1	2	5	10	20	50	100	250	400	600	700
Compound Range	Bar	-	-1...0 ⁽¹⁾	-1...2 ⁽¹⁾	-1...5	-1...9	-1...19	-1...29	-	-	-	-	-
Permissible Overpressure	Bar	1	2	4	10	20	40	100	200	400	650	880	880
Burst Pressure	Bar	2	4	5	12	25	50	120	250	500	650	880	880

⁽¹⁾ $\pm 0.2\%$ / FS (BFSL) accuracy not possible in this range

Output Signal & Supply Voltage

Wire system	Output	Supply Voltage
2-wire	4 - 20mA	9 - 32V dc
	0 - 5V dc	9 - 32V dc
	0 - 10V dc	13 - 32V dc
	1 - 5V dc	9 - 32V dc
	1 - 10V dc	13 - 32V dc
3-wire	1 - 6V dc	9 - 32V dc
	0 - 6V dc	9 - 32V dc
	0.5 to 4.5V dc	5V dc
	Passive mV/V (un-rationalised)	2 - 30V dc
	2mV/V (rationalised)	2 - 30V dc
4-wire	10mV/V (amplified)	3 - 12V dc

Performance

Accuracy (Non-linearity & hysteresis)	$< \pm 0.25\%$ / FS (BFSL) $< \pm 0.1\%$ / FS (BFSL) optional	
Setting Errors (offsets)	2-wire 3-wire 4-wire	Zero & Full Scale, $< \pm 0.5\%$ / FS Zero & Full Scale, $< \pm 0.5\%$ / FS see table below
Permissible Load	2-wire 3-wire 4-wire	$R_{max} = [(V_S - V_S \text{ min}) / 0.02] \Omega$ $R_{min} = 10 \text{ k} \Omega$ $R_{min} = 11 \text{ k} \Omega$
Influence Effects	Supply Load	mV/V & 0.5 to 4.5V - Ratiometric, other outputs - $< 0.005\%$ FS / 1V 0.05% FSO / k Ω

Permissible Temperatures & Thermal Effects

Media temperature	-20°C to +135°C (150°C with integrated cooling element)
Ambient temperature	-20° to +80°C
Storage temperature	-40°C to +125°C
Compensated temperature range	+20°C to +80°C
Thermal Zero Shift (TZS)	$< \pm 0.04\%$ / FS / °C (option code 4) $< \pm 0.02\%$ / FS / °C (option code 2) $< \pm 0.01\%$ / FS / °C (option code 1)
Thermal Span Shift (TSS)	$< -0.015\%$ / °C

Electrical Protection

Supply reverse polarity protection	No damage but also no function
Electromagnetic compatibility	CE Compliant

Mechanical Stability

Shock	100 g / 11 ms
Vibration	10 g RMS (20 ... 2000 Hz)

Materials

Housing & process connection	303 Stainless Steel 316L Stainless Steel (optional) High Grade DUPLEX Stainless Steel UNS31803 (optional)
'O' ring seals	Viton NBR, Nitrile (optional) EPDM (optional) Chemraz (optional)
Diaphragm	Ceramic Al ₂ O ₃ 96 %
Media wetted parts	Housing and process connection, 'O' ring seal, diaphragm

Miscellaneous

Current consumption	2-wire, 3-wire & 4-wire	Limits at 25mA, Typ. 6mA, Typ.2 – 5mA
Weight	Approx. 100g	
Installation position	Any	
Operation Life	> 100 x 10 ⁶ cycles	
Insulation Resistance	>500M Ω at 50V dc	

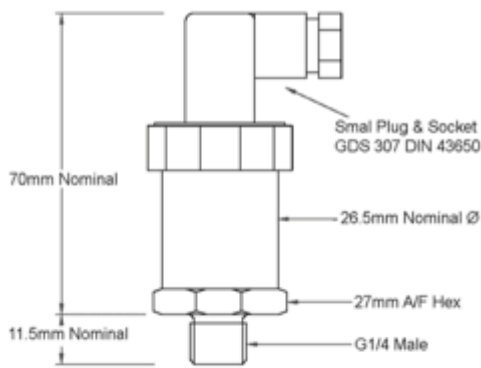
Typical Passive mV/V Outputs

Nominal pressure	Bar	1	2	5	10	20	50	100	250	400	600	700
Output	mV/V	2.0..3.5	2.0..4.0	2.4..4.5	3.6..6.0	2.5..4.0	4.0..6.5	3.1..4.8	3.1..4.8	3.1..4.8	3.7..5.7	4.3..6.7
Zero Setting Error	mV/V	0.1	0.1	0.1	0.1	0.1	0.1	0.1	0.1	0.1	0.1	0.1
Span Setting Error	%	30	30	30	30	30	30	30	30	30	30	30

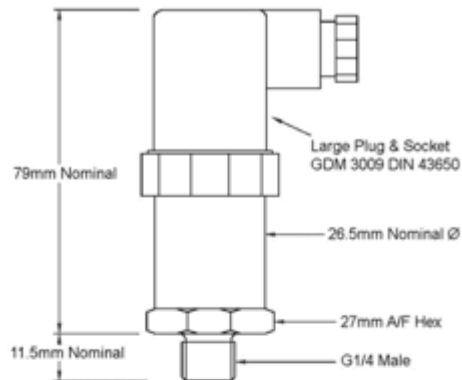
Wiring Designation

		Small Plug & Socket (Code A)	Large Plug & Socket (Code B)	IP66 Cable (Code C)	AMP 6-pin Bayonet (Code D)	IP68 Vented Cable (Code E)	Binder 6-pin connector (Code F)	M12x1, 4-pin connector (Code G)
2-wire	+ve Supply	Pin 1	Pin 1	Red	Pin 1	Red	Pin 1	Pin 1
	-ve Supply	Pin 2	Pin 2	Blue	Pin 2	Blue	Pin 2	Pin 2
	Ground	Earth Pin	Earth Pin	Green	Earth Pin	White	Pin 3	Pin 3
3-wire	+ve Supply	Pin 1	Pin 1	Red	Pin 1	Red	Pin 1	Pin 1
	-ve Supply	Pin 2	Pin 2	Blue	Pin 2	Blue	Pin 2	Pin 2
	+ve Output	Pin 3	Pin 3	Green	Pin 3	White	Pin 3	Pin 3
	Ground	Earth Pin	Earth Pin	Yellow	Earth Pin	Yellow	Pin 4	Pin 4
4-wire	+ve Supply	Pin 1	Pin 1	Red	Pin 1	Red	Pin 1	Pin 1
	-ve Supply	Pin 2	Pin 2	Blue	Pin 2	Blue	Pin 2	Pin 2
	+ve Output	Pin 3	Pin 3	Green	Pin 3	White	Pin 3	Pin 3
	-ve Output	Earth Pin	Earth Pin	Yellow	Pin 4	Yellow	Pin 4	Pin 4

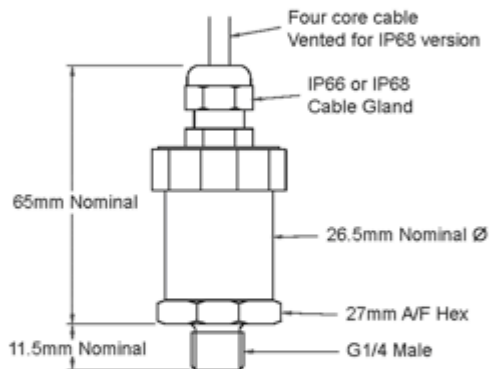
Electrical Connections



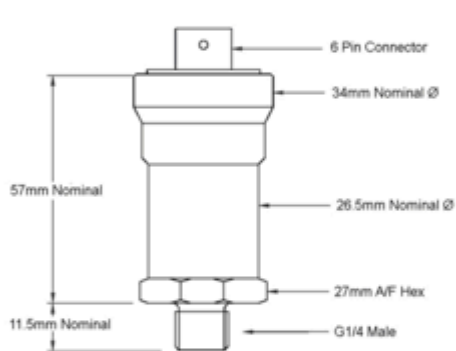
Small Plug & Socket
IP65, GDS 307 DIN 43650



Large Plug & Socket
IP65, GDM 3009 DIN 43650



Cable Gland Assembly
IP65 gland, screened PVC industrial cable



Amphenol Connector
6 pin, IP67, IP54 on gauge versions

Suggested Accessories



PA 430
In head display and switching device



SPS-24
Din rail power supply



dTrans
Signal conditioner and switching device

Visit the website: www.impress-sensors.co.uk

Company Reg. No.: 4346738, VAT No.: 786 6596 54, Reg Address: Impress Sensors & Systems Ltd, Unit 6 Mercury House, Calleva Park, Aldermaston, Berkshire, RG7 8PN

DSN002 Issue: 06 Ref: 090609A

Datasheet is subject to change without notice.

10.3 Data logger data sheet

Functional Details

This chapter contains detailed information on all of the features available from the board, including:

- a diagram and explanations of physical board components
- a functional block diagram
- information on how to use the signals generated by the board
- diagrams of signals using default or conventional board settings

USB-1616HS components

These USB-1616HS components are shown in Figure 4.

- Six removable screw terminal blocks
- One USB port
- One external power connector
- One 25-pin expansion connector
- Two LED indicators ("Active" and "Power")

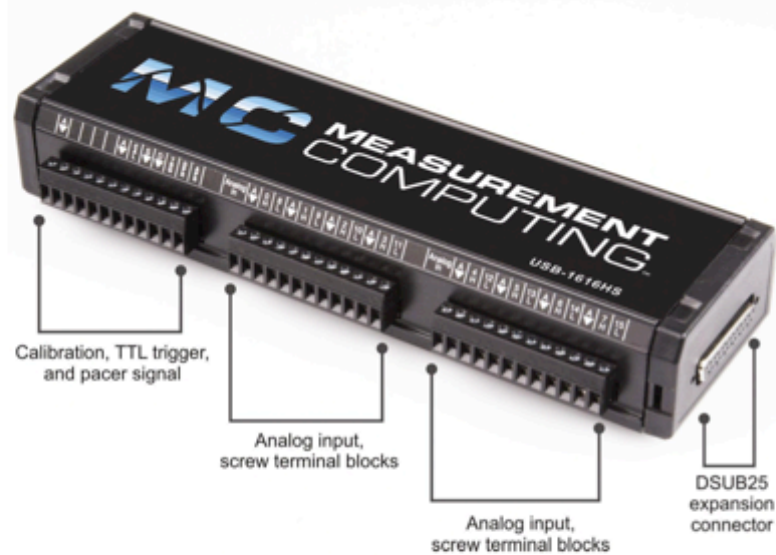


Figure 4. USB-1616HS components – front view

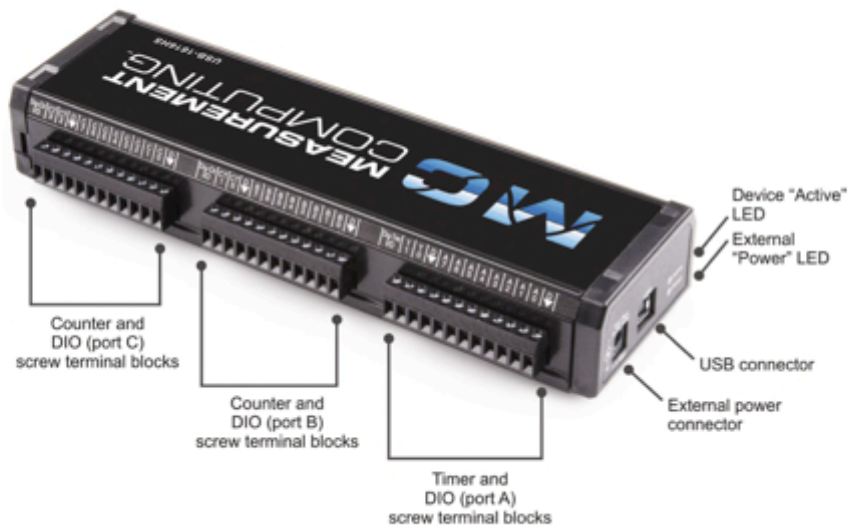


Figure 5. USB-1616HS components – rear view

External power connector

Although the USB-1616HS is powered by a USB port on a host PC, an external power connector may also be required to provide sufficient power for the USB-1616HS.

Connect the optional TR-2U power supply to the external power supply connector. This power supply provides 9 VDC, 1 A power to the USB-1616HS.

USB-1616HS block diagram

Figure 6 shows a simplified block diagram of the USB-1616HS. This board provides all of the functional elements shown in the figure.

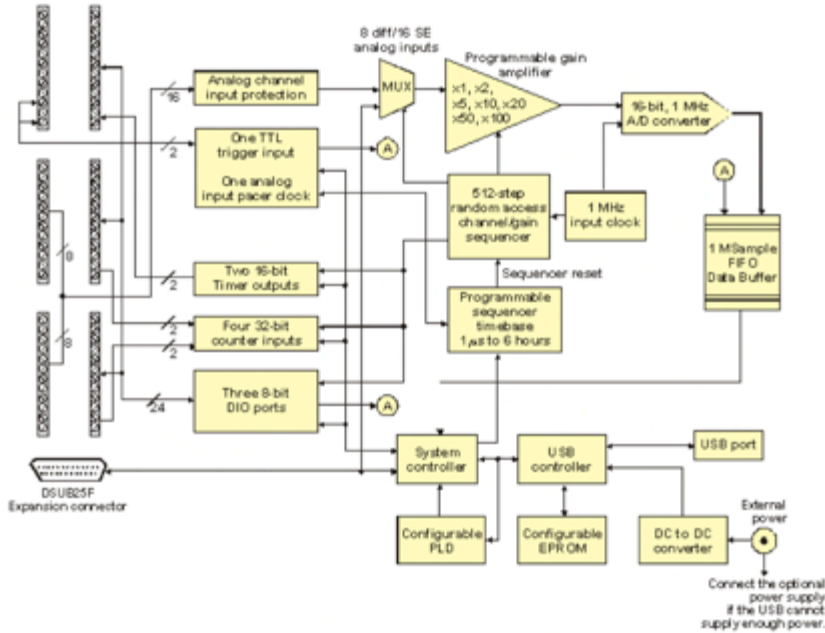


Figure 6. USB-1616HS functional block diagram

Synchronous I/O – mixing analog, digital, and counter scanning

The USB-1616HS can read analog, digital, and counter inputs, while generating two digital pattern outputs at the same time. Digital and counter inputs do not affect the overall A/D rate because these inputs use no time slot in the scanning sequencer.

For example, one analog input channel can be scanned at the full 1 MHz A/D rate along with digital and counter input channels. Each analog channel can have a different gain, and counter and digital channels do not need additional scanning bandwidth as long as there is at least one analog channel in the scan group.

Digital input channel sampling is not done during the "dead time" of the scan period where no analog sampling is being done either.

Analog input

The USB-1616HS has a 16-bit, 1-MHz A/D coupled with 16 single-ended, or eight differential analog inputs. Seven software programmable ranges provide inputs from ±10 V to ±100 mV full scale.

Screw terminal pin outs

USB-1616HS screw terminal pin out – single-ended connections

Analog Out	Analog common (A▼)	Port A	Digital common (D▼)	DIG-Tmr I/O
	NC		FIRSTPORTA Bit 0 (A0)	
	NC		FIRSTPORTA Bit 1 (A1)	
	NC		FIRSTPORTA Bit 2 (A2)	
	NC		FIRSTPORTA Bit 3 (A3)	
	Analog common (A▼)		FIRSTPORTA Bit 4 (A4)	
	CAL (Reserved for self-calibration)		FIRSTPORTA Bit 5 (A5)	
	Signal ground (S▼)		FIRSTPORTA Bit 6 (A6)	
	Digital common (D▼)		FIRSTPORTA Bit 7 (A7)	
	TTL trigger (TRG)		Digital common (D▼)	
	Output scan clock I/O (DPR)		Timer 0 (T0)	
	Input scan clock I/O (APR)		Timer 1 (T1)	
Analog In	Analog common (A▼)	Port B	Digital common (D▼)	Dig-Ctr I/O
	CH 0 (0H)		FIRSTPORTB Bit 0 (B0)	
	CH 8 (8L)		FIRSTPORTB Bit 1 (B1)	
	Analog common (A▼)		FIRSTPORTB Bit 2 (B2)	
	CH 1 (1H)		FIRSTPORTB Bit 3 (B3)	
	CH 9 (9L)		FIRSTPORTB Bit 4 (B4)	
	Analog common (A▼)		FIRSTPORTB Bit 5 (B5)	
	CH 2 (2H)		FIRSTPORTB Bit 6 (B6)	
	CH 10 (10L)		FIRSTPORTB Bit 7 (B7)	
	Analog common (A▼)		Digital common (D▼)	
	CH 3 (3H)		Counter 0 (CT0)	
	CH 11 (11L)		Counter 1 (CT1)	
Analog In	Analog common (A▼)	Port C	Digital common (D▼)	Dig-Ctr I/O
	CH 4 (4H)		FIRSTPORTC Bit 0 (C0)	
	CH 12 (12L)		FIRSTPORTC Bit 1 (C1)	
	Analog common (A▼)		FIRSTPORTC Bit 2 (C2)	
	CH 5 (5H)		FIRSTPORTC Bit 3 (C3)	
	CH 13 (13L)		FIRSTPORTC Bit 4 (C4)	
	Analog common (A▼)		FIRSTPORTC Bit 5 (C5)	
	CH 6 (6H)		FIRSTPORTC Bit 6 (C6)	
	CH 14 (14L)		FIRSTPORTC Bit 7 (C7)	
	Analog common (A▼)		Digital common (D▼)	
	CH 7 (7H)		Counter 2 (CT2)	
	CH 15 (15L)		Counter 3 (CT3)	

USB-1616HS screw terminal pin out – differential connections

Analog Out	Analog common (A↕)	Port A	Digital common (D↕)	DIG-Tmr I/O
	NC		FIRSTPORTA Bit 0 (A0)	
	NC		FIRSTPORTA Bit 1 (A1)	
	NC		FIRSTPORTA Bit 2 (A2)	
	NC		FIRSTPORTA Bit 3 (A3)	
	NC		FIRSTPORTA Bit 4 (A4)	
	Analog common (A↕)		FIRSTPORTA Bit 5 (A5)	
	CAL (Reserved for self-calibration)		FIRSTPORTA Bit 6 (A6)	
	Signal ground (S↕)		FIRSTPORTA Bit 7 (A7)	
	Digital common (D↕)		Digital common (D↕)	
	TTL trigger (TRG)		Timer 0 (T0)	
	Output scan clock I/O (DPR)		Timer 1 (T1)	
	Input scan clock I/O (APR)			
Analog In	Analog common (A↕)	Port B	Digital common (D↕)	Dig-Ctr I/O
	CH 0 HI (0H)		FIRSTPORTB Bit 0 (B0)	
	CH 0 LO (0L)		FIRSTPORTB Bit 1 (B1)	
	Analog common (A↕)		FIRSTPORTB Bit 2 (B2)	
	CH 1 HI (1H)		FIRSTPORTB Bit 3 (B3)	
	CH 1 LO (1L)		FIRSTPORTB Bit 4 (B4)	
	Analog common (A↕)		FIRSTPORTB Bit 5 (B5)	
	CH 2 HI (2H)		FIRSTPORTB Bit 6 (B6)	
	CH 2 LO (2L)		FIRSTPORTB Bit 7 (B7)	
	Analog common (A↕)		Digital common (D↕)	
	CH 3 HI (3H)		Counter 0 (CT0)	
	CH 3 LO (3L)		Counter 1 (CT1)	
	Analog In		Analog common (A↕)	
CH 4 HI (4H)		FIRSTPORTC Bit 0 (C0)		
CH 4 LO (4L)		FIRSTPORTC Bit 1 (C1)		
Analog common (A↕)		FIRSTPORTC Bit 2 (C2)		
CH 5 HI (5H)		FIRSTPORTC Bit 3 (C3)		
CH 5 LO (5L)		FIRSTPORTC Bit 4 (C4)		
Analog common (A↕)		FIRSTPORTC Bit 5 (C5)		
CH 6 HI (6H)		FIRSTPORTC Bit 6 (C6)		
CH 6 LO (6L)		FIRSTPORTC Bit 7 (C7)		
Analog common (A↕)		Digital common (D↕)		
CH 7 HI (7H)		Counter 2 (CT2)		
CH 7 LO (7L)		Counter 3 (CT3)		

DSUB25F expansion connector

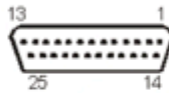


Figure 2. DSUB25F expansion connector pin out

10.4 Thermal camera datasheet



**FLIR
SYSTEMS**

The Global Leader in Infrared Cameras

ThermaCAM® S65HSV

INFRARED CAMERA



The ThermaCAM® S65HSV is a highly refined infrared research system. Its powerful new features and conveniences enable the professional thermographer to work with unprecedented efficiency and productivity. Working in concert with ThermaCAM Researcher reporting and database software, the S65HSV fully automates the process of collecting, reporting, and archiving infrared images and thermal data.



- Bluetooth® Voice Recording Technology
- Burst & AVI Recording
- Radiometric FireWire®
- Radiometric JPEG Image Storage

- Auto-focus/Auto-hot-spot Tracker
- Detachable Remote Control/LCD Handle
- Built-in Ram/CompactFlash® Card
- Built-in Laser LocatIR™ Target Pointer

Features both thermal and visual camera capabilities – at the touch of a button!

Extraordinary Thermal Sensitivity and Imaging Quality

Thermal sensitivity of 0.05°C coupled with a 76,000 pixel display provides extremely accurate, high-resolution 14-bit thermal images in real time. Plus, the state-of-the-art 320 x 240 uncooled microbolometer detector means the S65 is ready to go in seconds. The built-in external 4-inch LCD screen displays digital images of corresponding thermal images captured by the IR system.

Easy to Operate

Ergonomic, intuitive controls make operation seamless and efficient. A user-friendly joystick, familiar menus, and soft programmable buttons (allowing feature customization) on both the camera body and detachable handle provide for easy one-handed operation. The built-in Laser LocatIR™ provides point-and-shoot accuracy.

Rugged and Lightweight

The S65HSV was designed for use in harsh environments. It has an IP54 environmental encapsulation, and a robust industrial shock rating. At under 4.4 lbs., it is the lightest full-featured infrared camera available.

Flexible Viewing Options

The built-in color viewfinder is ideal for outdoor applications, while the detachable 4-inch color LCD on the camera's handle adjusts to any viewing angle, and may be used to operate the camera via redundant controls – for optimal use in hard-to-reach areas – indoors and out.

Flexible Image Storage

Images can be stored in Windows-friendly JPEG format, removable CompactFlash® memory card, or internal flash RAM. The camera may be set up to automatically capture images at preset intervals.

Burst and AVI Recording

Powerful burst recording captures moving targets for sequences up to 16 minutes long. Sequences may be played back on the camera or transferred to a PC for further analysis. Nonradiometric moving images may be optionally recorded in AVI file format for convenient report playback using industry-standard players.

Store User Profiles

Personal camera settings may be stored on the S65HSV, for several users, a time-saving feature.

Special Features Boost Your Efficiency

A brilliant LED target light automatically turns on when visual image mode is selected. Powerful auto-focus and auto-hot-spot features save time and effort. The S65HSV can automatically indicate the temperature and position of the hottest spot in the image and instantly calculate the difference between different measurement points. Sound and color alarms warn when targets exceed temperature maximums set by the user.

Voice Recording with Bluetooth Technology...and More

The S65HSV can record up to 30 seconds of voice comment with each image. A cordless Bluetooth earpiece eliminates all cable connections, increasing operator safety. In addition, text comments for each image can be entered manually or preloaded from a PC with optional ThermaCAM Reporter software.

Wide Range of Accessories

Optional optics include: microscopic, wide-angle and telescopic to address diverse application requirements. Infrared heads-up displays (IRHUD) are available, to augment situational awareness. Power options include lightweight, rechargeable, long-life Li-Ion batteries, and the ability to operate the S65HSV from external power sources.

Optional Software Does the Work for You!

ThermaCAM Researcher reporting and analysis software analyzes your data in real time. ThermaCAM Database software enables you to trend, archive, and organize inspection data and reports quickly and easily. ThermaCAM Image Builder knits multiple IR images together to create a single radiometric composite.

ThermaCAM® S65HSV Technical Specifications

Imaging Performance	
Thermal	
Field of view/min focus distance	20° x 15° / 0.3 m
Spatial resolution (IFOV)	1.1 mrad
Electronic zoom function	2, 4, 8, Interpolating
Focus	Automatic or manual
Digital image enhancement, on/off	Normal and enhanced
Detector type	Focal plane array (FPA) uncooled microbolometer; 320 x 240 pixels
Spectral range	7.5 to 13 µm
Thermal sensitivity	50 mK at 30° C (86° F)
Visual	
Built-in Visual Camera	640 x 480 pixels, full color
Image Presentation	
Viewfinder	Built-in high-resolution color LCD (TFT)
Video output	RS170 EIA/NTSC or CCIR/PAL
External display	Built-in high-resolution color LCD (TFT) 4" LCD with integrated remote control
Measurement	
Temperature ranges	-40° C to +120° C (-40° F to +248° F), Range 1 0° C to +250° C (+32° F to +482° F), Range 2 +100° C to +500° C (+212° F to +932° F), Range 3 +250° C to +1500° C (+482° F to +2732° F), Range 4
Accuracy (% of reading)	± 2° C or ± 2% (3.6° F)
Measurement modes	Up to 10 movable spots. Automatic temperature difference (Δ) and placement and reading of maximum and minimum temperatures. Up to 5 movable circle areas or boxes. Up to 2 Isotherms. Line profile.
Emissivity corrections	Variable from 0.1 to 1.0 or select from listings in pre-defined material list
Measurement features	Automatic corrections based on user input for reflected ambient temperature, distance, relative humidity, atmospheric transmission, and external optics
Optics transmission correction	Automatic, based on signals from internal sensors
Image Storage	
Type	Removable CompactFlash (256 MB) memory card; built-in Flash memory (30 images); built-in (128 MB) RAM memory for burst and AVI recording
File format - THERMAL	Standard .JPEG; 14 bit thermal measurement data included
File format - VISUAL	Standard .JPEG linked with corresponding thermal image
Voice annotation of images	Input via supplied Bluetooth® wireless headset up to 30 seconds of digital voice clip per image stored with image
Text annotation of images	Predefined by user and stored with image
System Status Indicator	
LCD display	Shows status of battery and storage media. Indication of power, communication and storage modes.
Power Source	
Battery type	Li-Ion, rechargeable, field-replaceable
Battery operating time	2 hours continuous operation
Charging system	In camera IAC adapter or 12V from car or 2 bay intelligent charger
External power operation	AC adapter 110/220 VAC, 50/60Hz or 12V from car (cable with standard plug optional)
Power saving	Automatic shutdown and sleep mode (user-selectable)
Environmental	
Operating temperature range	-15° C to +50° C (5° F to 122° F)
Storage temperature range	-40° C to +70° C (-40° F to 158° F)
Humidity	Operating and storage 10% to 95%, non-condensing IEC 359
Encapsulation	IP 54 IEC 529
Shock	Operational: 25G, IEC 68-2-29
Vibration	Operational: 2G, IEC 68-2-6
Physical Characteristics	
Weight	2.0 kg (4.4 lbs) w/battery and top handle (includes remote control, LCD, video camera and laser); 1.4 kg (3.1 lbs) excluding battery and handle
Size	100mm x 120mm x 220 mm (3.9" x 4.7" x 8.7") camera only
Tripod mounting	1/4" - 20

ThermaCAM S65HSV System Includes:	
IR camera with visual camera, Laser LocatIR, remote with LCD display	
High-output multi-LED target light	
Bluetooth wireless headset	
Carrying case, lens cap, shoulder strap, hand strap	
User manual (multilingual)	
Batteries (2)	
Power supply	
Battery charger	
FireWire® (IEEE 1394) cable	
Video cable with RCA plug	
USB cable	
256 MB CompactFlash card	
ThermaCAM QuickView™ software	
Lenses (optional)	
Field of view minimum focus distance	3X Telescope (5.6" x 4.294m) 2X Telescope (10" x 7.647m) 0.5X Wide angle (37" x 2890.1m) 0.3X Wide angle (68" x 5170.1m) 164 µm Close-up (52mm x 39mm/150mm) 88 µm Close-up (28mm x 21mm/80mm) 38.5 µm Close-up (12mm x 9mm/19mm)
Interfaces	
Firewire output (IEEE 1394)	Real-time digital transfer of radiometric thermal images or digital video (DV) out
USB / RS232	Image (thermal and visual), measurement data, voice and text transfer to PC
IrDA	Two-way data transfer from laptop, PDA
Remote control	Removable handle with redundant controls and LCD
Laser LocatIR™	
Classification type	Class 2 Semiconductor AlGaInP Diode Laser: 1 mW/635 nm (red)



The Global Leader in Infrared Cameras

1 800 613 0507
www.flir.ca

Specifications subject to change. © Copyright 2005, FLIR Systems, Inc. All rights reserved. 1061005PL

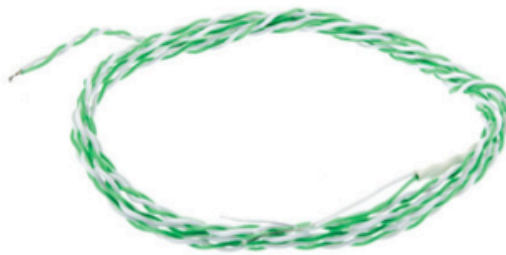
10.5 K-type thermocouple datasheet



Data sheet THERMOCOUPLE

ENGLISH

RS Stock No. 621-2158



TYPE K THERMOCOUPLE RS					
RANGE :					
<ul style="list-style-type: none"> 50 / 250°C 					
USE :					
<ul style="list-style-type: none"> 					
KEY POINT :					
<ul style="list-style-type: none"> 					
SPECIFICATIONS :					
<ul style="list-style-type: none"> Matter = PTFE Hot junction grouded 					
DIMENSIONS :					
<ul style="list-style-type: none"> Cable length = 1000 mm 					
METROLOGICAL DATA :					
<ul style="list-style-type: none"> As per IEC 584 Standard tolerance TC "K" class1: $-40^{\circ}\text{C} < t^{\circ} < 375^{\circ}\text{C} = \pm 1.5^{\circ}\text{C}$ $375^{\circ}\text{C} < t^{\circ} < 1000^{\circ}\text{C} = \pm 0.004 \text{ [t]}$ Time constant at 63% in water: 0.7 sec Output signal FEM(mV) as per curve of "K" type as per norme IEC 60584 					
Other type:					
	tolerance	J	K	N	T
Length					
	1000	621-2142	621-2158	621-2136	621-2164

RS, Professionally Approved Products, gives you professional quality parts across all products categories. Our range has been testified by engineers as giving comparable quality to that of the leading brands without paying a premium price.

10.6 Metrological report for radiator internal surface

10.6.1 Introduction

The Alicona Infinite Focus Microscope (IFM) was used to investigate the surface roughness of a radiator panel inner determine the corrosion invasion of the surface.

10.6.2 Methodology

The 20x objective was used on the IFM to take areal datasets with approximate dimensions of 2x2 in various locations along the sample as depicted below:

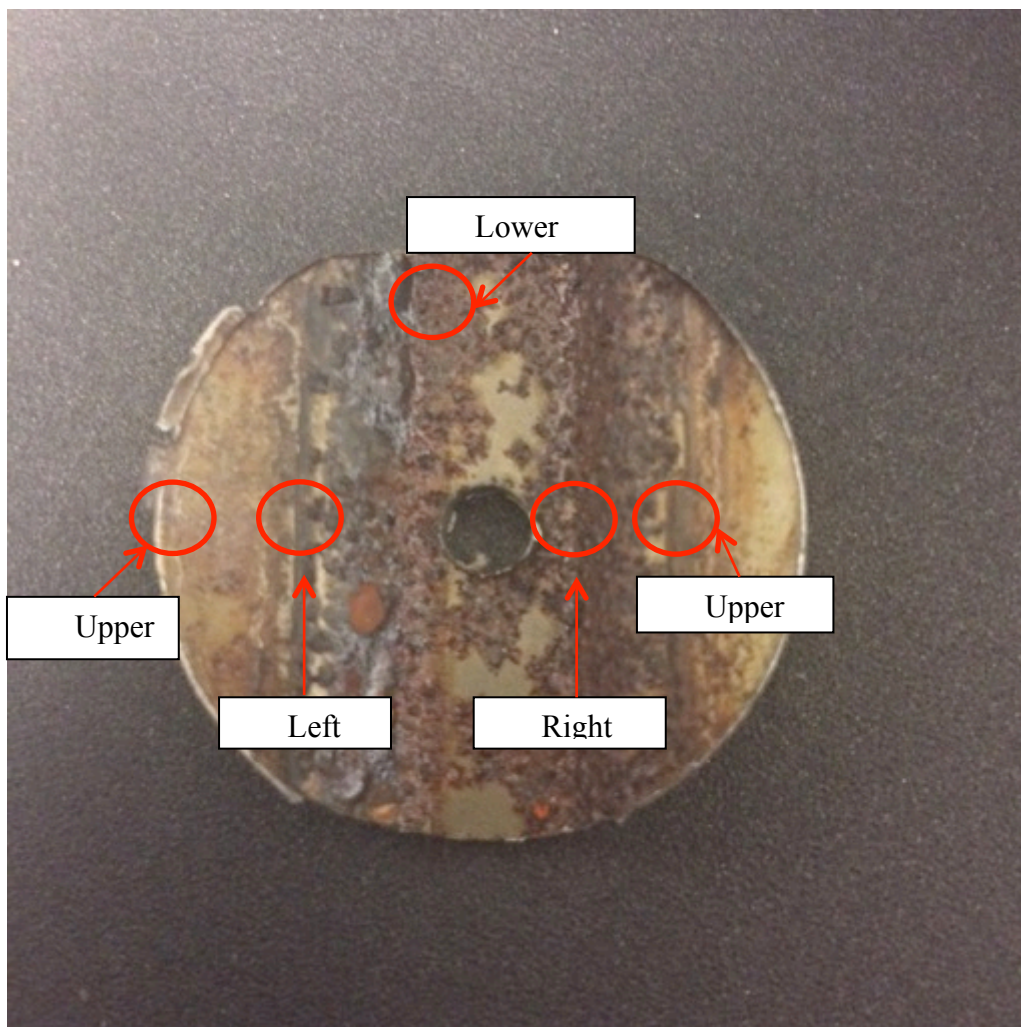


Fig.1 picture of radiator panel sample depicting measurement areas (red circles)

10.6.3 Results

Before the datasets were analysed, the form was removed from each dataset to give a more accurate representation of the roughness values. This was done using a Gaussian roughness filter in the Alicona software. The resulting Ra and Sa values are tabulated below:

Fig.2 table of roughness results:

Sample name	Ra (μm)	Sa (μm)
Left flank	7.53	9.33
Right flank	7.72	10.69
Lower surface	3.54	6.70
Upper left	1.54	1.79
Upper right	1.88	2.32

10.6.4 Screen Shot Images

Fig 3 Left Flank Colour Map and True Colour Images

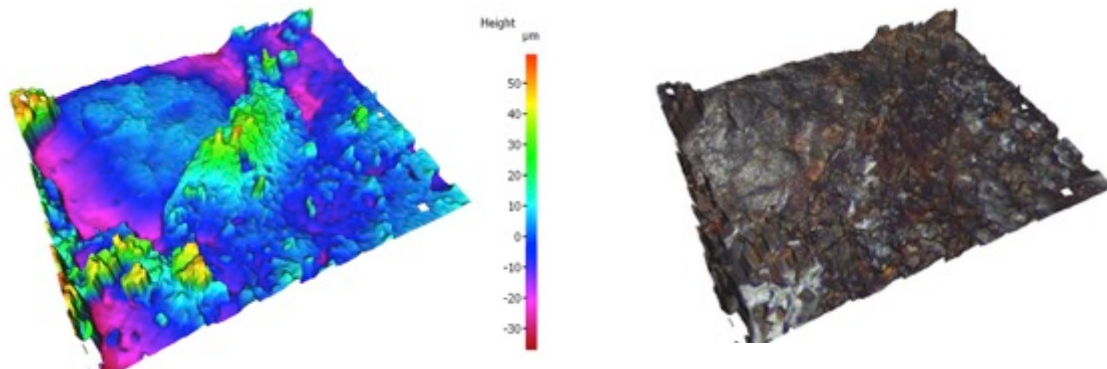


Fig 4 Right Flank colour Map and True colour Images

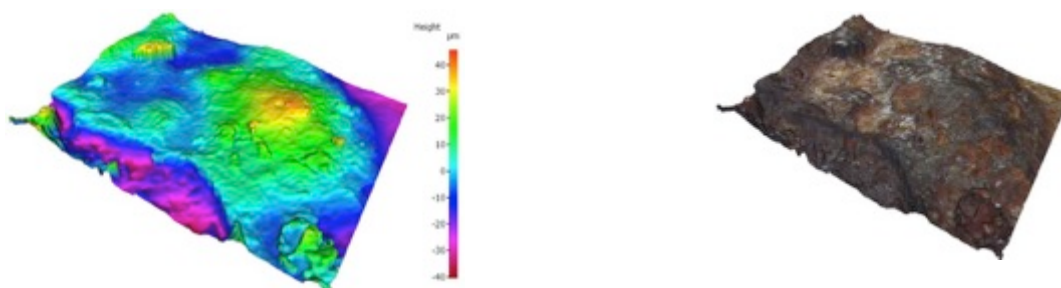


Fig 5 Lower Surface colour map and true colour Images

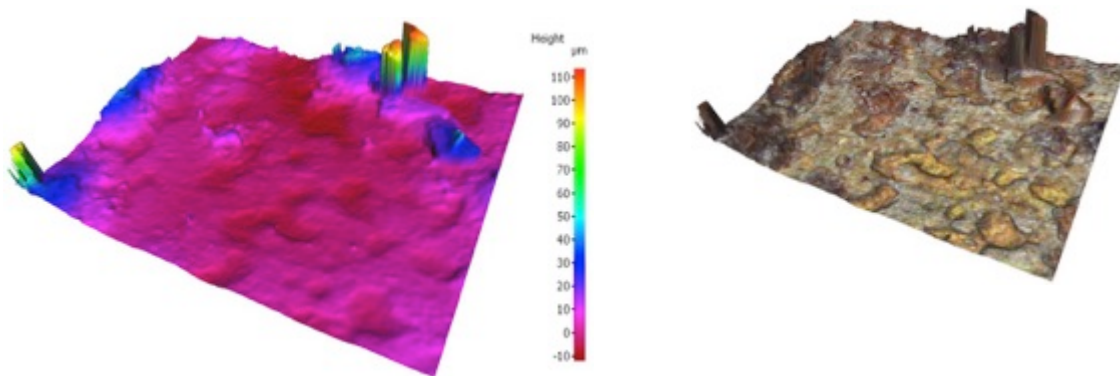


Fig 6 Upper Left colour map and true colour Images

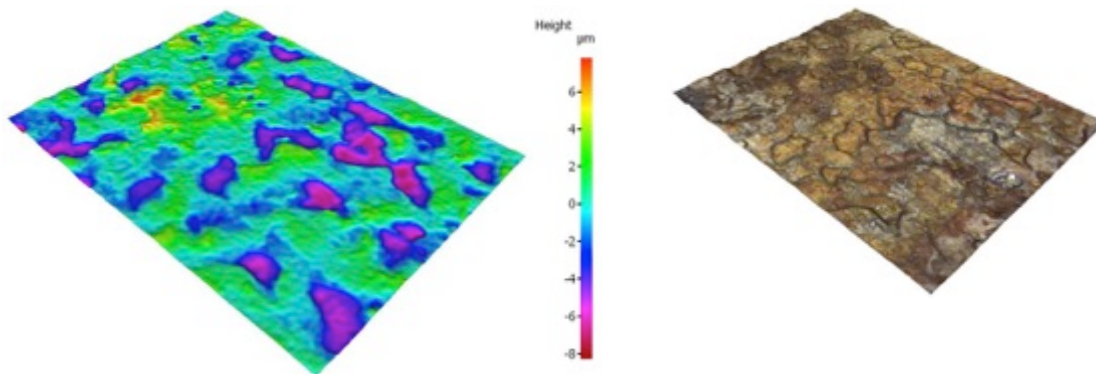
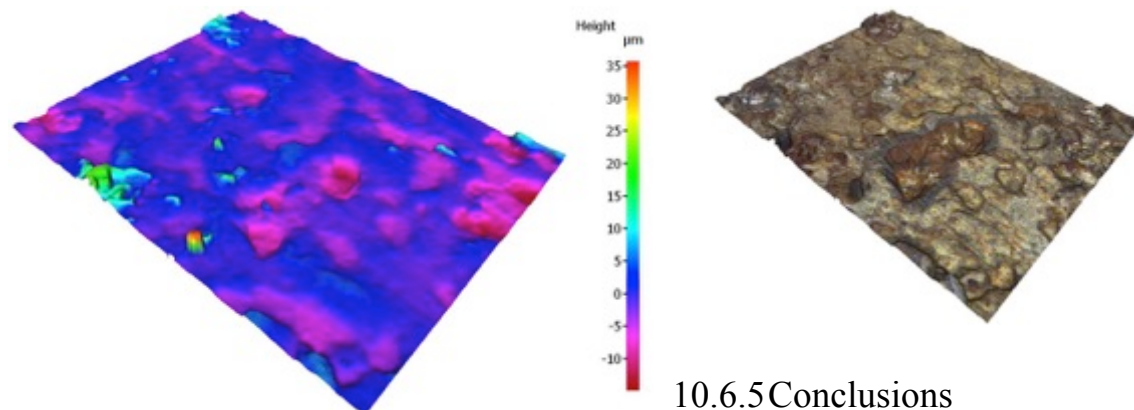


Fig 7 Upper right colour map and true colour images



10.6.5 Conclusions

It can be seen in the surface parameters that the areas with higher roughness are located on the flanks of the component. The lower surface has lower roughness, and the upper

surfaces have the lowest roughness values of all areas. Therefore, it can be shown that the most damage to the component has occurred in its flanks.